

**“Cytotoxicity and P-glycoprotein inhibition by  
cardiotonic steroids”**

**Dissertation  
zur Erlangung des Grades**

**“Doktor der Naturwissenschaften”**

**im Promotionsfach Pharmazie**

**am Fachbereich Chemie, Pharmazie und  
Geowissenschaften der Johannes Gutenberg-Universität in  
Mainz**

**vorgelegt von Maen Zeino  
geboren am 88.03.1988 in Damaskus, Syrien**

**Mainz, März 2015**

**Betreuer:**

Prof. Dr. [REDACTED]

**Gutachter der Arbeit:**

Prof. Dr. [REDACTED]

Prof. Dr. [REDACTED]

Prof. Dr. [REDACTED]

**Datum der mündlichen Prüfung:**

29.04.2015

**Prüfungskommission:**

Prof. Dr. [REDACTED]

Prof. Dr. [REDACTED]

Prof. Dr. [REDACTED]

PD Dr. [REDACTED]

Dr. [REDACTED] (Protokoll)

## Publications

### *Original publications as lead author*

- M. Zeino, M. Paulsen, M. Zehl, E. Urban, B. Kopp, T. Efferth, "Identification of New P-Glycoprotein Inhibitors Derived from Cardiotonic Steroids", *Biochemical Pharmacology*, 93(1), 11-24, 2015.
- M. Zeino, M. E. Saeed, O. Kadioglu, and T. Efferth, "The ability of molecular docking to unravel the controversy and challenges related to P-glycoprotein-a well-known, yet poorly understood drug transporter," *Invest New Drugs*, Apr 22 2014
- M. Zeino, Q. Zhao, T. Eichhorn, J. Hermann, and R. Müller, "Molecular docking studies of myxobacterial disorazoles and tubulysins to tubulin," *Journal of Bioscience and Medicine*, vol. 3, pp. 31-43, 2013

### *Original publications as co-author*

- V. Kuete, L. P. Sandjo, J. A. Seukep, M. Zeino, A. T. Mbaveng, B. Ngadjui, *et al.*, "Cytotoxic Compounds from the Fruits of *Uapaca togoensis* towards Multifactorial Drug-Resistant Cancer Cells," *Planta Med*, vol. 81, pp. 32-8, Jan 2015.
- Saeed, M., Zeino, M., Kadioglu, O., Volm, M., & Efferth, T, "Overcoming of P-glycoprotein-mediated multidrug resistance of tumors in vivo by drug combinations," *Synergy*, 1(1), 44-58, Sep 2014
- R. Hamm, M. Zeino, S. Frewert, and T. Efferth, "Up-regulation of cholesterol associated genes as novel resistance mechanism in glioblastoma cells in response to archazolid B," *Toxicol Appl Pharmacol*, vol. 281, pp. 78-86, Sep 2014.
- V. Kuete, L. P. Sandjo, D. E. Djeussi, M. Zeino, G. M. Kwamou, B. Ngadjui, *et al.*, "Cytotoxic flavonoids and isoflavonoids from *Erythrina sigmoidea* towards multifactorial drug resistant cancer cells," *Invest New Drugs*, vol. 32, pp. 1053-62, Dec 2014.
- R. Hamm, Y. R. Chen, E. J. Seo, M. Zeino, C. F. Wu, R. Müller, *et al.*, "Induction of cholesterol biosynthesis by archazolid B in T24 bladder cancer cells," *Biochem Pharmacol*, vol. 91, pp. 18-30, Sep 2014.
- C. Noysang, A. Mahringer, M. Zeino, M. Saeed, O. Luanratana, G. Fricker, *et al.*, "Cytotoxicity and inhibition of P-glycoprotein by selected medicinal plants from Thailand," *J Ethnopharmacol*, vol. 155, pp. 633-41, Aug 2014.
- C. Reiter, A. Capcı Karagöz, T. Fröhlich, V. Klein, M. Zeino, K. Viertel, *et al.*, "Synthesis and study of cytotoxic activity of 1,2,4-trioxane- and egonol-derived hybrid

molecules against *Plasmodium falciparum* and multidrug-resistant human leukemia cells," *Eur J Med Chem*, vol. 75, pp. 403-12, Mar 2014.

- T. AlSalim, M. E. Saeed, J. S. Hadi, M. Zeino, R. Gany, O. Kadioglu, et al., "Cytotoxicity of novel sulfanilamides towards sensitive and multidrug-resistant leukemia cells," *Curr Med Chem*, vol. 21, pp. 2715-25, 2014.
- A. Veerappan, T. Eichhorn, M. Zeino, T. Efferth, and D. Schneider, "Differential interactions of the broad spectrum drugs artemisinin, dihydroartemisinin and artesunate with serum albumin," *Phytomedicine*, vol. 20, pp. 969-74, Aug 2013.
- A. M. Saab, A. Guerrini, G. Sacchetti, S. Maietti, M. Zeino, J. Arend, et al., "Phytochemical analysis and cytotoxicity towards multidrug-resistant leukemia cells of essential oils derived from Lebanese medicinal plants," *Planta Med*, vol. 78, pp. 1927-31, Dec 2012.

*Submitted manuscripts (in revision: **meanwhile accepted**)*

- Zeino, M., Brenk, R., Gruber, L., Zehl, M., Urban, E., Kopp, B., & Efferth, T. (2015). Cytotoxicity of cardiotonic steroids in sensitive and multidrug-resistant leukemia cells and the link with Na<sup>+</sup>/K<sup>+</sup>-ATPase. *The Journal of steroid biochemistry and molecular biology*, 150, 97-111.

*Poster*

- M. Zeino, M. Paulsen, M. Zehl, E. Urban, B. Kopp, T. Efferth, "Identification of New P-Glycoprotein Inhibitors Derived from Cardiotonic Steroids", [Poster], 128<sup>th</sup> meeting of the Gesellschaft Deutscher Naturforscher und Ärzte (GDNÄ) "Vorbild Natur: Faszination Mensch und Technologie", Mainz, 2014.
- M. Zeino, M. E. Saeed, O. Kadioglu, and T. Efferth, "The ability of molecular docking to unravel the controversy and challenges related to P-glycoprotein-a well-known, yet poorly understood drug transporter," [Poster], 128<sup>th</sup> meeting of the Gesellschaft Deutscher Naturforscher und Ärzte (GDNÄ) "Vorbild Natur: Faszination Mensch und Technologie", Mainz, 2014.

## Erklärung

Hiermit erkläre ich an Eides statt, dass ich diese Arbeit selbständig verfasst und keine anderen als die angegebenen Quellen und Hilfsmittel verwendet habe.

Mainz, 04.05.15

Keine Unterschrift zwecks Datenschutz

---

---

Ort, Datum

Maen Zeino

## Acknowledgement

My journey into exploring and applying the theoretical knowledge I have gained during my studies has begun, as I received an acceptance letter from him to a PhD position in his department while applying for a DAAD scholarship. Starting with that moment, my life was filled with eagerness, challenges and enthusiasm to have the chance to practice science in a leading country as Germany. Through the great scientific and internationally diverse atmosphere at his lab, I was able to develop at both the personal and professional level. For that, my deepest gratitude goes to Prof. Dr. [REDACTED] with his great support and mentorship that made it possible to finalize this dissertation.

I would like to also thank Prof. Dr. [REDACTED], PD Dr. [REDACTED] and Prof. Dr. [REDACTED] for revising this scientific work and taking part in the examination process.

Many thanks to Dr. [REDACTED], who helped me walk the first footsteps in the field of flow cytometry and was always there when help was needed. I also thank the kind staff at the IMB, specifically [REDACTED], [REDACTED] and [REDACTED] for their technical and moral support, which made my time at the IMB most joyful.

I would like to also take the chance to thank Prof. Dr. [REDACTED], Dr. [REDACTED] and Prof. Dr. [REDACTED] for providing us with the substances and for their valuable advice whenever asked for.

I am also grateful for the group of Prof. Dr. [REDACTED] for the access to MOE software and their support in bioinformatics.

A special word has to go to the outstanding team at the Department of Pharmaceutical Biology. Thanks to [REDACTED] who showed me the various techniques in the cell culture lab with great patience and joy. It has been always a blast to work with you. Furthermore, your spiritual support along with that of [REDACTED] and Dr. [REDACTED] has always kept me going. Thank you all three for the fruitful and lovely conversations that always contributed to my personality. Many thanks to [REDACTED] and [REDACTED] for their permanent encouragement and strong belief in me. I also thank Dr. [REDACTED], [REDACTED] and [REDACTED] for their readiness to help and support. Thanks to [REDACTED], [REDACTED], for her help with university registration and office work. The last team member I would like to specially thank is [REDACTED], first for critically reading and revising this thesis and second, because she has become a true companion of my journey with all its ups and downs. An authentic, sincere friendship

has developed over the years, for which I can only be most grateful. Whenever in need, she was always there with her words and deeds. Thank you for the limitless support, introducing me to the German culture and showing me how a true friendship is.

Many thanks to the internship and diploma students [REDACTED], [REDACTED] and [REDACTED] [REDACTED], whom I had the chance to supervise at some point, for the support and good times in the lab.

Much gratitude is entitled to the German Academic Exchange Organization (DAAD) for the financial support throughout my PhD and to [REDACTED], my regional supervisor at DAAD for her careful and patient guidance.

I have to mention my Syrian friends, who managed to maintain an everlasting friendship despite the seas separating us. Their E-mails and voices via skype always added happiness to my life. Thank you [REDACTED], [REDACTED], [REDACTED], [REDACTED], [REDACTED] [REDACTED], [REDACTED], [REDACTED]. Thanks also to a newly sincerely developed friendship with [REDACTED].

With the beautiful words of the great scientist Albert Einstein “Rejoice with your family in the land of life”, I come to thank my parents [REDACTED] and [REDACTED] for their endless love, care and support. I hope I can live up to the morals and values you raised me upon. My parents, my brothers [REDACTED] and [REDACTED], and my sisters [REDACTED] and [REDACTED] [REDACTED]... There are no words to describe my gratitude to all of you. I am glad you are essential elements of my life.

Last but not least, I would like to thank that better half yet to come for a beautiful life yet to be lived together.

### ***Dedication***

*I dedicate this work to my country Syria. A country torn out by war, but with great hope, I am sure it will stand up on its feet and become more beautiful and safer than it already once was.*

## Abstract

Cardiotonic steroids, which are regularly used in the treatment of heart failure, are natural compounds encountered throughout the plant and animal kingdom and are considered to be promising chemotherapeutics.  $\text{Na}^+/\text{K}^+$ -ATPase has been established as the molecular target of cardiotonic steroids. Recently,  $\text{Na}^+/\text{K}^+$ -ATPase has been implicated in cancer biology affecting several signaling pathways. Classical multidrug resistance – mediated by P-glycoprotein – is responsible for chemotherapy failure in certain tumors by extruding many chemotherapeutics outside the cell. In this study, we evaluated cytotoxicity of 66 cardiotonic steroids and their derivatives in two sensitive and multidrug-resistant leukemia cell lines. Results revealed cytotoxicity of many of the compounds at various molar ranges but all with low resistance indices (i.e. similar  $\text{IC}_{50}$  values between sensitive and resistant cell lines). Data were subject to structure-activity relationship (SAR), quantitative structure-activity relationship (QSAR), and molecular docking on  $\text{Na}^+/\text{K}^+$ -ATPase, which first elaborated the role of chemical substitutions on cytotoxicity and second pointed out a possible differential expression of  $\text{Na}^+/\text{K}^+$ -ATPase of the two cell lines. By immunoblotting, a down-regulation of  $\text{Na}^+/\text{K}^+$ -ATPase in multidrug-resistant cells was confirmed, which was tracked down by next generation sequencing further unraveling deregulations of  $\text{Na}^+/\text{K}^+$ -ATPase signalosome in multidrug-resistant cells. Thereby, a link between  $\text{Na}^+/\text{K}^+$ -ATPase down-regulation and P-glycoprotein expression was established. We further tried to discover any inhibitors of P-glycoprotein by means of high throughput flow cytometry. Six cardiotonic steroids were able to inhibit P-glycoprotein-mediated efflux and partially restore the cytotoxic effect of doxorubicin – a substrate of P-glycoprotein – in multidrug-resistant cells. Separately, we evaluated the application of molecular docking in P-glycoprotein research by assessing its ability to first discriminate between different P-glycoprotein-interacting groups of molecules, and second to predict the binding site of a certain molecule. After thorough statistical analysis, we conclude, despite the various challenges, that molecular docking should not be underestimated as differences between the distinct groups were significant. Furthermore, the ability of molecular docking to define the binding site of a substance was explored.

## Zusammenfassung

Herzwirksame Glykoside sind in der Natur sowohl im Tier- als auch im Pflanzenreich zu finden und werden regelmäßig zur Therapie von Herzinsuffizienz eingesetzt. In letzter Zeit belegten viele Studien, dass herzwirksame Glykoside vielversprechende Substanzen für die Behandlung von Krebs darstellen. Ihr Wirkmechanismus basiert auf der Hemmung der  $\text{Na}^+/\text{K}^+$ -ATPase. Die  $\text{Na}^+/\text{K}^+$ -ATPase spielt neuerdings eine wichtige Rolle in der Krebsbiologie, da sie viele relevante Signalwege beeinflusst. Multiresistenzen gegen Arzneimittel sind oftmals verantwortlich für das Scheitern einer Chemotherapie. Bei multi-drug-resistenten Tumoren erfolgt ein Transport der Chemotherapeutika aus der Krebszelle hinaus durch das Membranprotein P-Glykoprotein. In der vorliegenden Arbeit wurde die Zytotoxizität von 66 herzwirksamen Glykosiden und ihren Derivaten in sensitiven und resistenten Leukämie-Zellen getestet. Die Ergebnisse zeigen, dass diese Naturstoffe die Zell-Linien in verschiedenen molaren Bereichen abtöten. Allerdings waren die Resistenz-Indizes niedrig (d. h. die  $\text{IC}_{50}$  Werte waren in beiden Zell-Linien ähnlich). Die untersuchten 66 Substanzen besitzen eine große Vielfalt an chemischen Substituenten. Die Wirkung dieser Substituenten auf die Zytotoxizität wurde daher durch Struktur-Aktivitäts-Beziehung (SAR) erforscht. Des Weiteren wiesen quantitative Struktur-Aktivitäts-Beziehung (QSAR) und molekulares Docking darauf hin, dass die  $\text{Na}^+/\text{K}^+$ -ATPase in sensitiven und resistenten Zellen unterschiedlich stark exprimiert wird. Eine Herunterregulation der  $\text{Na}^+/\text{K}^+$ -ATPase in multi-drug-resistenten Zellen wurde durch Western Blot bestätigt und die Wirkung dieser auf relevante Signalwege durch Next-Generation-Sequenzierung weiter verfolgt. Dadurch konnte eine Verbindung zwischen der Überexpression von P-Glykoprotein und der Herunterregulation der  $\text{Na}^+/\text{K}^+$ -ATPase hergestellt werden. Der zweite Aspekt der Arbeit war die Hemmung von P-Glykoprotein durch herzwirksame Glykoside, welche durch Hochdurchsatz-Durchflusszytometrie getestet wurde. Sechs wirksame Glykoside konnten den P-Glykoprotein-vermittelten Transport von Doxorubicin inhibieren. Zudem konnte die Zytotoxizität von Doxorubicin in multi-drug-resistenten Zellen teilweise wieder zurück erlangt werden. Unabhängig von herzwirksamen Glykosiden war die Bewertung der Anwendung von molekularem Docking in der P-Glykoprotein Forschung ein weiterer Aspekt der Arbeit. Es ließ sich schlussfolgern, dass molekulares Docking fähig ist, zwischen den verschiedenen Molekülen zu unterscheiden, die mit P-Glykoprotein interagieren. Die Anwendbarkeit von molekularem Docking in Bezug auf die Bestimmung der Bindestelle einer Substanz wurde ebenfalls untersucht.

---

**Table of contents**

<b>Acknowledgement .....</b>	<b>I</b>
<b>Abstract .....</b>	<b>III</b>
<b>Zusammenfassung .....</b>	<b>IV</b>
<b>Table of contents.....</b>	<b>V</b>
<b>List of Abbreviations.....</b>	<b>1</b>
<b>1 Introduction.....</b>	<b>4</b>
<b>1.1 Basic facts about cancer .....</b>	<b>4</b>
<b>1.2 Cancer treatment.....</b>	<b>5</b>
<b>1.3 Chemotherapy .....</b>	<b>6</b>
<b>1.4 Natural compounds in chemotherapy .....</b>	<b>7</b>
<b>1.5 Cardiotonic steroids .....</b>	<b>8</b>
1.5.1 Clinincal use throughout History .....	8
1.5.2 Chemistry .....	9
1.5.3 Mode of action .....	10
1.5.4 Na <sup>+</sup> /K <sup>+</sup> -ATPase as a molecular target .....	10
1.5.5 Application in cancer therapy.....	12
<b>1.6 Multidrug resistance .....</b>	<b>14</b>
<b>1.7 P-glycoprotein.....</b>	<b>17</b>
1.7.1 History and discovery.....	17
1.7.2 Human tissue distribution and physiology .....	17
1.7.3 Structure .....	18
1.7.4 Transport mechanism .....	19
1.7.5 Catalytic cycle .....	21
1.7.6 P-glycoprotein inhibition.....	22
1.7.6.1 Mechanisms of inhibition .....	22

---

1.7.6.2	P-glycoprotein inhibitors in three generations .....	24
1.7.6.3	Natural products as P-glycoprotein inhibitors .....	25
<b>1.8</b>	<b>Molecular docking and P-glycoprotein research .....</b>	<b>25</b>
<b>2</b>	<b>Aim of the thesis .....</b>	<b>27</b>
<b>3</b>	<b>Results .....</b>	<b>28</b>
<b>3.1</b>	<b>Cytotoxicity of cardiotonic steroids .....</b>	<b>28</b>
3.1.1	Cytotoxicity of cardiotonic steroids in sensitive and MDR leukemia cells .....	28
3.1.2	Cytotoxicity of cardiotonic steroids in non-tumor cells .....	32
3.1.3	Structure activity relationship (SAR) .....	33
3.1.4	Quantitative structure activity relationship (QSAR) .....	34
3.1.5	Molecular docking .....	36
3.1.6	Expression of Na <sup>+</sup> /K <sup>+</sup> -ATPase in sensitive and MDR cells .....	42
3.1.7	Next generation sequencing .....	43
3.1.8	Summary: Cytotoxicity of cardiotonic steroids .....	46
<b>3.2</b>	<b>Cardiotonic steroids and P-glycoprotein inhibition .....</b>	<b>47</b>
3.2.1	Model system .....	47
3.2.1.1	Expression of P-glycoprotein in sensitive and MDR leukemia cells .....	47
3.2.1.2	Uptake studies of doxorubicin over a time course .....	49
3.2.2	High throughput screening of cardiotonic steroids for P-glycoprotein inhibition .....	50
3.2.2.1	Identification of six P-glycoprotein-inhibiting cardiotonic steroids .....	51
3.2.2.2	P-glycoprotein inhibition by compound 15i at different concentrations .....	52
3.2.2.3	P-glycoprotein inhibition by compound 15i over a time course .....	52
3.2.3	Effect of six modulators on P-gp-ATPase activity .....	53
3.2.4	Molecular docking on P-glycoprotein .....	54
3.2.5	MDR reversal in MDR cells .....	58
3.2.6	Summary: Cardiotonic steroids and P-glycoprotein inhibition .....	61

---

<b>3.3</b>	<b>Utilization of molecular docking in P-glycoprotein research .....</b>	<b>62</b>
3.3.1	Molecular docking.....	62
3.3.2	Statistical analysis .....	69
3.3.3	Summary: Utilization of molecular docking in P-glycoprotein research .....	70
<b>4</b>	<b>Discussion.....</b>	<b>71</b>
<b>4.1</b>	<b>Cytotoxicity of cardiotonic steroids and the link with Na/K ATPase .....</b>	<b>71</b>
4.1.1	Cytotoxicity in sensitive and MDR leukemia cell lines .....	71
4.1.2	Structure activity relationship .....	72
4.1.3	Differential Na <sup>+</sup> /K <sup>+</sup> -ATPase expression in MDR cells through QSAR and molecular docking .....	72
4.1.4	Na <sup>+</sup> /K <sup>+</sup> -ATPase down-regulation in MDR cells.....	73
<b>4.2</b>	<b>Inhibition of P-glycoprotein by cardiotonic steroids.....</b>	<b>76</b>
4.2.1	P-gp expression in the model system .....	76
4.2.2	Interaction of six modulating cardiotonic steroids with P-glycoprotein.....	76
4.2.3	Potential of cardiotonic steroids in the clinic .....	80
<b>4.3</b>	<b>Molecular docking in P-glycoprotein research .....</b>	<b>81</b>
4.3.1	Estimation of binding affinities .....	81
4.3.2	Estimation of the binding mode .....	82
<b>5</b>	<b>Summary and conclusions.....</b>	<b>85</b>
<b>6</b>	<b>Material and Methods .....</b>	<b>87</b>
<b>6.1</b>	<b>Chemicals and equipment.....</b>	<b>87</b>
<b>6.2</b>	<b>Cell culture.....</b>	<b>97</b>
6.2.1	Leukemia cell lines.....	97
6.2.2	KB epidermal carcinoma cell lines.....	97
6.2.3	Non-tumor cells (human peripheral mononuclear cells PMNC) .....	98
<b>6.3</b>	<b>Cytotoxicity assay .....</b>	<b>98</b>
6.3.1	Cytotoxicity of cardiotonic steroids in sensitive and MDR leukemia cell lines .....	98

---

6.3.2	Reversal of doxorubicin resistance by cardiotonic steroids .....	99
<b>6.4</b>	<b>Quantitative structure activity relationship (QSAR) .....</b>	<b>99</b>
<b>6.5</b>	<b>Analysis of protein expression in sensitive and MDR leukemia cell lines .....</b>	<b>100</b>
6.5.1	Immunoblotting of P-glycoprotein and Na <sup>+</sup> /K <sup>+</sup> -ATPase .....	100
6.5.1.1	Protein extraction.....	100
6.5.1.2	SDS-PAGE and western blot.....	100
6.5.1.3	Gel and Buffer recipes .....	101
6.5.2	Analysis of P-glycoprotein expression by immunocytochemistry .....	101
6.5.3	Analysis of P-glycoprotein expression by flow cytometry.....	102
<b>6.6</b>	<b>Flow cytometry high throughput screening .....</b>	<b>102</b>
<b>6.7</b>	<b>P-glycoprotein-ATPase assay .....</b>	<b>103</b>
<b>6.8</b>	<b>Molecular docking.....</b>	<b>104</b>
6.8.1	Molecular docking of cardiotonic steroids into Na <sup>+</sup> /K <sup>+</sup> -ATPase.....	104
6.8.2	Utilization of molecular docking in P-glycoprotein research.....	104
6.8.2.1	Ligand selection and preparation.....	104
6.8.2.2	Homology modeling of human P-glycoprotein .....	105
6.8.2.3	Molecular docking.....	106
6.8.3	Molecular docking of P-glycoprotein-modulating cardiotonic steroids .....	106
<b>6.1</b>	<b>Next generation sequencing .....</b>	<b>107</b>
<b>7</b>	<b>References .....</b>	<b>108</b>
<b>8</b>	<b>Appendix.....</b>	<b>117</b>
<b>8.1</b>	<b>NMR and MS Data.....</b>	<b>117</b>
<b>8.2</b>	<b>Curriculum vitae .....</b>	<b>138</b>

## List of Abbreviations

Abbreviation	Connotation
AA	Amino acid
#AA_LBE	Number of ouabain-interacting amino acids in the lowest binding energy cluster
#AA_BE	Number of ouabain-interacting amino acids in the cluster with the highest number of conformations
#Conf_LBE	Number of conformations in the cluster with the lowest binding energy
#Conf_BE	Highest number of conformations
ABC	ATP binding cassette
ABCB1	ATP-binding cassette sub-family B member 1/P-glycoprotein/MDR1
ABCB4	ATP-binding cassette sub-family B member 4/MDR2/3
ADP	Adenosine diphosphate
AP-1	Activator protein-1
APS	Ammonium persulfate
Akt	Murine thymoma viral oncogene homolog
ATP	Adenosine triphosphate
BCL-2	B-cell CLL/lymphoma 2
BCRP	Breast cancer resistance protein
BD	Becton Dickinson
BE	Binding energy at the cluster with the highest number of conformations
BSA	Bovine serum albumin
Ca <sup>2+</sup> ATPase	Calcium adenosyltriphosphatase
CAS	Chemical Abstracts Service
DNA	Deoxyribonucleic acid
DMEM	Dulbecco's modified eagle medium
DMSO	Dimethyl sulfoxide
DPBS	Dulbecco's phosphate-buffered saline
EDTA	Ethylene diamine tetraacetic acid
EGFR	Epidermal growth factor receptor
EGTA	Ethylene glycol tetraacetic acid
Erk	Extracellular signal-regulated kinases
FA	Formic acid
FACS	Fluorescence-activated cell sorting
FBS	Fetal bovine serum
FITC	Fluorescein isothiocyanate
GIT	Gastrointestinal tract
H <sup>+</sup> /K <sup>+</sup> ATPase	Hydrogen-potassium adenosyltriphosphatase
HOMO	Highest occupied molecular orbital
HRP	Horseradish peroxidase

---

IC <sub>50</sub>	Half maximal inhibitory concentration
IP3R	Inositol 1,4,5-triphosphate receptor
LBE	Average binding energy in the lowest binding energy cluster
LOO	Leave-one-out
LUMO	Lowest unoccupied molecular orbital
MEK	Mitogen-activated protein kinase kinase
MDR	Multidrug resistance
MDR1	Multidrug resistance protein 1/ABCB1/P-glycoprotein
MDR2/3	Multidrug resistance protein 2/3/ABCB4
MFI	Mean fluorescence intensity
MTS	Methanethiosulfonate
mRNA	Messenger ribonucleic acid
MS	Mass spectrometry
MYC	Avian myelocytomatosis viral oncogene homolog
NAD <sup>+</sup>	Oxidized nicotinamide adenine dinucleotide
NADH	Reduced nicotinamide adenine dinucleotide
Na <sup>+</sup> /K <sup>+</sup> -ATPase	Sodium-potassium adenylyltriophosphatase
NBD	Nucleotide-binding domain
NCI	National cancer institute
NF-κB	Nuclear factor of kappa light polypeptide gene enhancer in B-cells
NMR	Nuclear magnetic resonance
P <sub>i</sub>	Inorganic phosphate
PARP1	Poly (ADP-ribose) polymerase 1
PDB	Protein data bank
P-gp	P-glycoprotein
PI3K	Phosphatidylinositol 3-kinase
PKC	Protein kinase C
PLC	Phospholipase C
PLS	Partial least square
PMNC	Human peripheral mononuclear cells
PVDF	Polyvinyl difluoride
QSAR	Quantitative structure-activity relationship
Raf	Rapidly accelerated fibrosarcoma proto-oncogene
Ras	Rat sarcoma viral oncogene homolog
RIPA	Radio-immunoprecipitation assay
RMSD	Root-mean-square deviation
RNA	Ribonucleic acid
ROS	Reactive oxygen species
RPMI 1640	Roswell Park Memorial Institute 1640
SAR	Structure-activity relationship
SEM	Standard error of mean

---

SDS	Sodium dodecyl sulfate
SDS-PAGE	Sodium dodecyl sulfate-polyacrilamide gel electrophoresis
Src	Sarcoma proto-oncogene tyrosine-protein kinase
TBS-T	Tris-buffered saline-Tween20
TEMED	Tetramethylenediamine
TM	Transmembrane
TMD	Transmembrane domain
TP53	Tumor protein 53
Tris	Tris (hydroxymethyl) aminomethane

---

# 1 Introduction

## 1.1 Basic facts about cancer

Cancer, first documented around 2500 B.C. in Egyptian papyri [1], is the first leading cause of death in developed countries and the second in developing ones [2] with 12.7 million new cases and 7.6 deaths to have occurred in 2008 worldwide [3]. Factors such as population growth, aging and cancer-associated lifestyle choices (e.g. smoking) have led to an increase in cancer burden overtime [2]. By definition, cancer is an abnormal cellular growth caused by imbalances between cell proliferation and death due to various changes in gene expression. The resulting cell population is tissue-invasive and able to metastasize to distant locations leading eventually to death if untreated [4]. To understand the biology of cancer, Hanahan and Weinberg have summarized the hallmarks of cancer in the following six biological capabilities of tumor cells [5]: 1) sustaining proliferative signaling that strictly regulates entrance of cells into growth-division cycle in normal tissues, thereby maintaining homeostasis of cell number and function, 2) evading growth suppressors that restrict cell proliferation known as tumor suppressors, 3) resisting cell death (apoptosis) via attenuation of apoptotic signals that would otherwise function as a barrier to cancer, 4) enabling replicative immortality, where tumor cells – after the deregulation of growth-division signaling in favor of proliferation – are able to replicate infinitely most likely by maintenance of telomeres, which protect the ends of chromosomes, 5) inducing angiogenesis to form new vasculature (a process normally occurring in adults only during wound healing and female reproductive cycling) in order to supply tumor cells with nutrients and remove their waste and 6) activating invasion into neighboring tissues and metastasis to distant places.

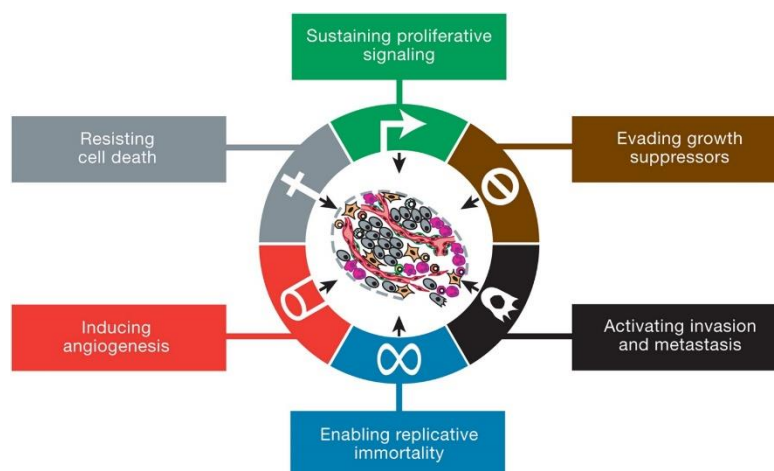


**Figure 1:** The hallmarks of cancer as suggested by Hanahan [5]. With permission from Elsevier; Copyright 2011

Two further hallmarks have emerged over the years to play an essential role in cancer biology. These are [5]: 1) deregulating cellular energetics by shifting energy metabolism to aerobic glycolysis – known as the Warburg effect – rather than the oxidative phosphorylation in the mitochondria, thereby favoring the formation of macromolecules needed for building new cells [6] and 2) evading the immune system, which is still an unresolved issue, as tumor cells are believed to attenuate components of the immune system that are triggered to fight against them. Acquisition of these hallmarks is facilitated by two enabling characteristics, which include [5]: 1) genome instability presented by mutant genotypes and further epigenetic mechanisms (i.e. mechanisms not involving the DNA sequence such as DNA methylation and histone modifications [7]) and 2) tumor-promoting inflammation, where the immune system – in an initial attempt to fight tumors – paradoxically supports tumor initiation and progression by secreting growth, survival and proangiogenic factors.

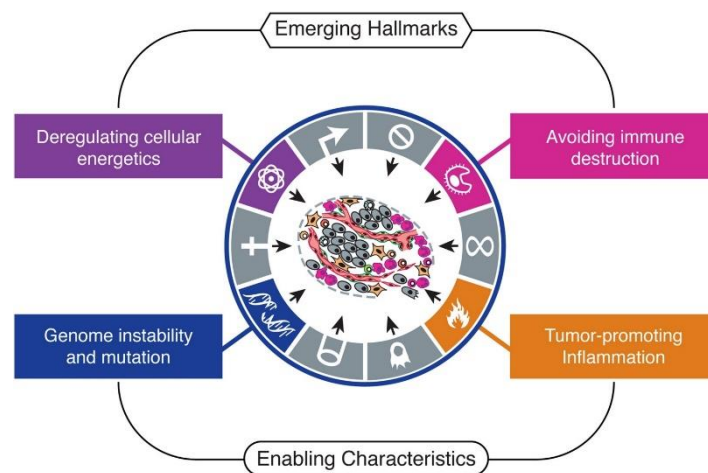


**Figure 2:** Two new cancer hallmarks and the enabling characteristic leading to cancer development [5]. With permission from Elsevier; Copyright 2011.

## 1.2 Cancer treatment

Currently, a collaboration of a multidisciplinary team of surgeons, radiotherapists and medical oncologists is essential in the treatment of cancer [8]. Surgery aims to remove an entire tumor – often accompanied by a portion of healthy tissues to eliminate any potential invasive residuals [9]. Therefore, it remains a cornerstone in the treatment of solid tumors either alone or followed by radiotherapy or chemotherapy [10]. Radiotherapy is based on inducing DNA damage (double-strand breaks and abnormal crosslinks) thereby causing cell death via interaction of photons with cellular molecules and water thereby liberating free radicals [9, 11]. Until 1950, cancer therapy remained mainly in the hands of surgeons and radiotherapy first emerged in 1960 [12]. However, both could not eradicate metastases since the treatment had to reach every

organ in the body [12]. Hence, focus on chemotherapy, which involves the use of drugs at some time point during the course of illness [8], has evolved [12] and will be discussed in more details in the next paragraph.

### 1.3 Chemotherapy

The term chemotherapy was first introduced in the early 1900s by the German scientist Paul Ehrlich, who defined it as the use of chemicals to treat disease [13]. In terms of cancer treatment, the first use of chemicals dates back to the post-World War II era, as mustard gases were reported to cause marked regression in lymphoma patients in 1943. This breakthrough set off the first major attempts to synthesize and test other alkylating agents, which brought chlorambucil and cyclophosphamide to life [13]. Since then, huge efforts have succeeded to introduce several other compounds (e.g. methotrexate, purine analogs, *Vinca* alkaloids and anthracyclines) [12, 13]. Current cancer chemotherapy is able to cure some disseminated tumors (e.g. testicular carcinoma and hairy cell leukemia) and is effective in decreasing tumor size, alleviating symptoms and prolonging life in other non-curable metastatic cancers [8, 14]. Chemotherapy (most often combined with radiotherapy) – in an approach called adjuvant chemotherapy – has been used after tumor resection especially in patients with high recurrence risk thereby increasing cure rate and prolonging survival [8, 14]. In neoadjuvant chemotherapy, cytotoxic drugs are applied prior to surgery or irradiation making resection possible in otherwise inoperable tumors [8, 15]. Taken together, chemotherapy has evolved over the years to play an essential role in cancer treatment.

Major classes of classical cytotoxic agents include alkylating agents (e.g. cyclophosphamide and nitrosoureas), agents acting as alkylating drugs (e.g. platinum analogs), antimetabolites (e.g. methotrexate, purine and pyrimidine antagonists), plant alkaloids (e.g. *Vinca* alkaloids and taxans), antitumor antibiotics (e.g. anthracyclines) [8, 14]. Because chemotherapy is basically aimed at killing rapidly dividing cells, normal cells – especially those undergoing rapid proliferation (e.g. buccal mucosa, bone marrow, gastrointestinal mucosa and hair) – often cannot be spared the damage [16]. Therefore, most chemotherapeutic agents have a narrow therapeutic index due to severe adverse effects often including (stomatitis, nausea and vomiting, infections and hair loss) [16, 17]. Other toxicities are confined with specific agents such as cardiotoxicity with doxorubicin and pulmonary fibrosis with bleomycin [16, 18]. Due to the lack of tumor specificity, a new approach – called targeted chemotherapy – has evolved over the past decades to identify medications (small-molecule drugs and monoclonal antibodies) that

specifically interfere with molecules involved in abnormal tumorous cellular events [19, 20]. Ever since, the search of effective and less toxic molecules for chemotherapy has been an ongoing task. Natural compounds provide a great source for identification of new compounds as will be discussed in full details in the next paragraphs.

#### 1.4 Natural compounds in chemotherapy

From the early dawn of ancient medicine, nature has been a generous source of various compounds to combat human diseases [21]. Throughout our evolution, natural products have played a central role in disease and injury treatment, beginning with our early ancestors, who chewed certain herbs to relieve pain or wrapped leaves around wounds to improve healing [22]. Accordingly, the use of natural products is suggested to date back 60,000 years, as Neanderthals in Mesopotamia seem to have been aware of the medicinal value of many plants [22]. In the context of cancer treatment, the contribution of nature can be traced back to American Indians, who used extracts from mayapple (*Podophyllum peltatum*) to treat skin cancers. The main constituent of this plant is podophyllotoxin, from which the known anticancer drugs etoposide and teniposide have emerged [23]. In modern chemotherapy, the *Vinca* alkaloids were the first anticancer agents discovered in 1958 from plant sources, even though the plant *Catharanthus roseus*, from which they are derived, had been used in folklore as a hypoglycemic agent in several parts of the world [23, 24]. Over 60% of the approved chemotherapeutic agents since 1940 can be linked to natural origins [25]. In fact, it is only until the last decades that natural compounds played a second role in drug discovery due to the emergence of combinatorial chemistry and molecular biology [22]. Even though combinatorial chemistry has been very successful in optimizing structures and many recently approved drugs – thereby leading to this move-away from natural products, it has been able to identify only one compound subsequently approved as a drug in a time frame of 30 years [26]. Some might even consider this shift responsible for the paucity of new candidates in the development pipeline [22, 26]. Only in the year 2010, seven antitumor drugs have been approved, of which one is a pure microbial natural product without any modification and four are derived from natural compounds [26]. Hence, natural products are coming back into vogue but with a different approach than empirical screening, in which natural extracts are first carefully screened against purified enzymes in molecularly defined assays and then distracting molecules are excluded thereby allowing the identification of compounds with genuine anticancer activity [23]. Nevertheless, the role of combinatorial chemistry should not be neglected as it still significantly contributes to this field by optimizing lead structures obtained from Mother Nature instead of synthesizing derivatives

from scratch [27]. With these approaches combined, the hope of identifying novel and effective anticancer agents with fewer side effects is far from fading away.

## 1.5 Cardiotonic steroids

Cardiotonic steroids (sometimes referred to as cardiac glycosides) are a group of therapeutics that have long been in clinical use for treatment of heart failure and arrhythmia [28, 29]. They occur in nature in both plant and animal kingdoms. They are found in several plants belonging to *Asclepiadaceae*, *Apocynaceae*, *Ranunculaceae*, *Scrophulariaceae* and *Asparagaceae* (subfamily *Scilloideae*) [28, 30]. In the animal kingdom, cardiotonic steroids are encountered in species of toads within the *Bufo* genera [28, 30]. Recently, they have emerged as potential candidates in cancer treatment due to retrospective studies that reported lower deaths from cancer in patients already receiving cardiotonic steroids [30]. Furthermore, their target  $\text{Na}^+/\text{K}^+$ -ATPase has been implicated in cancer biology and its expression profiles were different in some tumors as compared to normal tissues [30]. In the following paragraphs, chemistry, pharmacology and potential use of cardiotonic steroids in cancer therapy will be thoroughly discussed.

### 1.5.1 Clinical use throughout History

The use of cardiotonic steroids has been reported in ancient texts 1500 years ago, as they were used as arrow poisons (*Strophanthus* species used by natives in Africa [31]), abortifacients, emetics, diuretics and heart tonics [32]. The efficacy of plants containing cardiotonic steroids has been known by ancient Egyptians as well as ancient Romans and Syrians who used a plant called Squill (or sea onion), *Urginea maritima*, in heart disease [28, 31]. Also in the far-eastern part of the world, cardiotonic steroids have been introduced to clinical practice around 1000 years ago, as cardiotonic steroids-containing dried toad skins were used in the traditional Chinese preparation Ch'an Su to treat cardiac dysfunction [33]. In India, live toads were used in veterinary medicine to remove throat obstruction by rubbing them on the swollen areas in cattle's body [34]. In 1250, Welsh physicians collected different herbs, where the plant foxglove, *Digitalis Purpurea* was mentioned in their prescriptions [31]. However, it is only until the eighteenth century, as serious scientific medicinal application of cardiotonic steroids was reported by the British physician William Withering who detailed the beneficial and toxic effects of foxglove in the treatment of edema [31, 33, 35]. In 1875, the German chemist Oswald Schmiedeberg was the first to isolate a pure glycoside in crystal form, which he called digitoxin.

To date, *Digitalis* is still the cornerstone of treatment of heart failure and the accompanying arrhythmias making it probably the oldest drug continuously used by clinicians [29, 36].

### 1.5.2 Chemistry

Cardiotonic steroids – as the name implies – possess a steroidal core, which is believed to be an essential feature of the activity of the compounds [29, 37, 38]. Within this steroidal nucleus, substitutions at position 17 subcategorize cardiotonic steroids into two classes: cardenolides (having a five-membered butyrolactone) and bufadienolides (having a six-membered  $\alpha$ -pyrone) [29, 30, 38-40]. The core structures of both classes are shown in **Figure 3**.

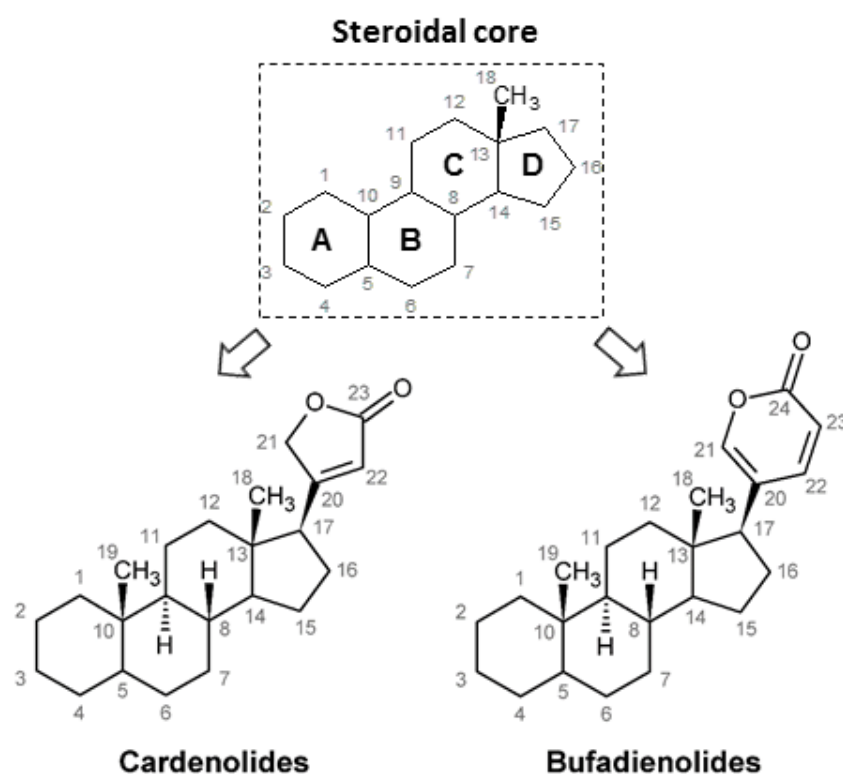


**Figure 3:** Steroidal core structures of cardenolides and bufadienolides with a butyrolactone and  $\alpha$ -pyrone ring at position 17, respectively.

In general, cardiotonic steroids have a unique configuration differing from other common steroid systems in that rings A/B and C/D are *cis* fused yielding a U-shaped aglycone [29, 30, 38]. Up to four various sugars can be attached at position 3; the most commonly encountered ones include L-rhamnose, D-glucose, D-digitoxose and D-digitalose [29, 30]. The variation between these sugars often influences the activity of the compound [40]. Furthermore, other substituents and their stereochemical configuration may vary widely giving a large diversity of naturally occurring compounds [30, 40]

### 1.5.3 Mode of action

In 1953, Na<sup>+</sup>/K<sup>+</sup>-ATPase was discovered – and over the years repeatedly confirmed – to be the molecular target inhibited by cardiotonic steroids [29, 41]. Years of intensive research has yielded probably the best so far established mode of action of a drug [29]. Na<sup>+</sup>/K<sup>+</sup>-ATPase is a membrane protein that actively transports sodium and potassium ions against their gradients across the plasma membrane. Via ATP hydrolysis, this pump gains energy required to extrude three sodium ions outside the cell in exchange for two potassium ions entering cytoplasm, thereby maintaining a low intracellular Na<sup>+</sup>/K<sup>+</sup> ratio. Maintenance of this electrochemical gradient is essential for vital cellular events [42]. When this process is disturbed by cardiotonic steroids, intracellular Na<sup>+</sup> increases [42]. To cope with that, cells try to restore Na<sup>+</sup> to its basal levels by stimulating the Na<sup>+</sup>/Ca<sup>2+</sup>-exchanger to expel Na<sup>+</sup> and in return, drive Ca<sup>2+</sup> into the cell [14, 42]. This calcium is then sequestered in the endoplasmic reticulum and later released facilitating the interaction of actin and myosin thereby causing an increase in cardiac contractility in a so-called positive inotropic effect [14, 35, 42]. Since the integrity of Na<sup>+</sup>/K<sup>+</sup>-ATPase's function is essential for ion homeostasis, disturbances affect the electrophysiology of the heart leading to antiarrhythmic effect at therapeutic concentrations (beneficial in atrial fibrillation) and to rhythm disturbances at higher toxic concentrations [14, 35, 36]. Another important physiological response upon *Digitalis* treatment is diuresis, which is due to impairment of renal Na<sup>+</sup>/K<sup>+</sup>-ATPase ultimately leading to inhibition of Na<sup>+</sup> reabsorption [35].

### 1.5.4 Na<sup>+</sup>/K<sup>+</sup>-ATPase as a molecular target

Na<sup>+</sup>/K<sup>+</sup>-ATPase is a member of the P-type ATPase family, which includes Ca<sup>2+</sup>-ATPase and H<sup>+</sup>/K<sup>+</sup>-ATPase among others and is expressed in all animal cells under strict regulations [43]. Structurally, it consists of three subunits: the  $\alpha$ -subunit forming the catalytic subunit and consisting of around 1000 residues, the heavily glycosylated  $\beta$ -subunit of about 300 residues and the regulatory subunit of 70-180 residues known as FXYD proteins [43]. The  $\alpha$ -subunit is the catalytic domain containing binding sites for Na<sup>+</sup>, K<sup>+</sup>, ATP and cardiotonic steroids [29, 33, 44]. It has in total four isoforms:  $\alpha 1$  is found ubiquitously,  $\alpha 2$  is found in skeletal muscles, heart, brain, adipocytes, vascular smooth muscle, eye and other tissues,  $\alpha 3$  is almost exclusively found in neurons and ovaries, but also found in white blood cells and heart of some species, and  $\alpha 4$  is expressed exclusively in sperm [45, 46]. The four isoforms are derived from separate genes with 92% for  $\alpha 1$  and  $\alpha 2$  and >96% homology for  $\alpha 3$  across species [47]. One major and controversial difference between the isoforms is their affinity to cardiotonic steroids, which is distinct among various species [47]. In humans, some reports revealed similar affinities to

ouabian among the distinct isoforms [48, 49]. Whereas others have reported that the affinity of  $\alpha 1$  to cardiotonic steroids is higher than that of other isoforms, leading to increased sensitivity [47, 50].

The  $\beta$ -subunit acts as a molecular chaperone important for maturation, insertion into the plasma membrane and conformational stability of the  $\alpha$ -subunit [43, 51, 52]. The FXYD proteins are a family of seven transmembrane proteins expressed in a tissue specific manner regulating the pump and its kinetic properties by adjusting affinities of  $\text{Na}^+$ ,  $\text{K}^+$  and ATP [52]. This structural complex is often found as dimeric and sometimes as tetrameric units [33, 53]. The binding site of cardiotonic steroids is highly conserved throughout evolution and is found on the extracellular surface (mainly on the first extracellular loop) of the  $\alpha$ -subunit and to a lesser extent on parts of the  $\beta$ -subunit [54].

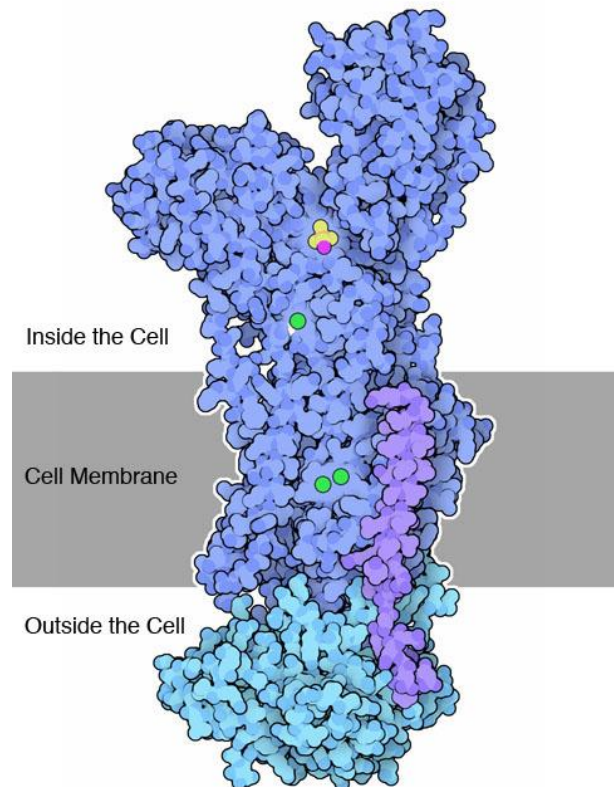


**Figure 4:** Structure of  $\text{Na}^+/\text{K}^+$ -ATPase: The  $\alpha$ -subunit is shown in blue. The  $\beta$ -subunit is shown in turquoise. The regulatory chain containing FXYD motifs is shown in purple. Image was retrieved with permission from David S. Goodsell and the RCSB PDB with slight modification [55].

### 1.5.5 Application in cancer therapy

Probably extending back to the 8<sup>th</sup> century, the use of plant extracts containing cardiotonic steroids has been introduced by Arab physicians to treat malignant diseases [32]. Chinese toad skins soaked in wine were also used to treat leukemia [56]. In China, since 1991, an injectable form of the Ch'an Su preparation (referred to as Hauchansu) has been approved in treatment regimens for cancer [32, 56]. In modern research, the potential use of cardiotonic steroids in cancer therapy was initially investigated *in vitro* around 40 years ago [57, 58] and was confirmed in several tumor cell lines including breast, prostate, leukemia, melanoma, pancreatic, lung, neuroblastoma and renal adenocarcinoma [29]. However, these findings were abandoned due to the toxicity of these compounds [32, 57]. It is only until recently that *Digitalis*-mediated apoptosis was found to be achievable at non-toxic concentrations, hence suggesting a promising use in cancer therapy [32]. The first clinical observation of possible antitumor activities of cardiotonic steroids was made in epidemiological studies by Stenkivist [59, 60] revealing that *Digitalis* treatment in women led to more benign characteristics in tumor cells and a lower recurrence rate of breast cancer [30, 32, 33, 42].

Recently, Na<sup>+</sup>/K<sup>+</sup>-ATPase emerged as an attractive molecular target in the battle against cancer in regards to diagnosis, prognosis, treatment and prevention [61, 62]. Over the past years, an important role of Na<sup>+</sup>/K<sup>+</sup>-ATPase in regulation of cellular growth and expression of various genes has been proposed, because altered activity and expression profiles of the pump were observed in some premalignant tissues and highly invasive tumors [32]. For example,  $\alpha 1$  subunits were found to be overexpressed in a significant amount of cases in melanomas, kidney cancers, non-small-cell lung cancers, and glioblastoma [39]. Additional to the pumping activity, there is a growing body of evidence that Na<sup>+</sup>/K<sup>+</sup>-ATPase, especially residing in the caveolae, is mainly involved in cellular signal transduction [33, 63, 64]. Binding of cardiotonic steroids to Na<sup>+</sup>/K<sup>+</sup>-ATPase – normally at concentrations less than those inhibiting the pumping activity [33, 65] – leads to a conformational change, which allows a specific interaction between Na<sup>+</sup>/K<sup>+</sup>-ATPase and Src thereby activating the latter. Active Src is then able to phosphorylate other proteins, among which is the endothelial growth factor receptor (EGFR) [33, 64, 66]. Furthermore, proper Na<sup>+</sup>/K<sup>+</sup>-ATPase signaling is linked to caveolins, which are enriched in the caveolae and are phosphorylated forming scaffolding proteins involved in various signaling pathways [64, 66]. Other proteins can be recruited such as PI3K and PLC thereby triggering complex downstream signaling events leading eventually to cell death via apoptosis or autophagy [32, 33, 67]. The downstream effects upon binding of cardiotonic steroids are

ubiquitous and involve for example, inhibition of Akt and NF- $\kappa$ B activation, which normally blocks apoptosis and has cytoprotective effects [32, 54, 68]. The increased intracellular calcium mediated by activation of PLC and the subsequent stimulation of (IP3R) – IP3-gated  $\text{Ca}^{+2}$  channels [69] – leads to decreased expression of transcription factors such as AP-1, which is important in cell survival as well as in apoptosis [32, 70-72]. The transactivation of EGFR via Src leads in turn to stimulation of the Ras/Raf/MEK/Erk cascade [64]. The activated Erk 1/2 proteins in turn lead to growth inhibition in some cancer cells [73, 74]. The  $\text{Na}^{+}/\text{K}^{+}$ -ATPase signalosome is shown in **Figure 5**.

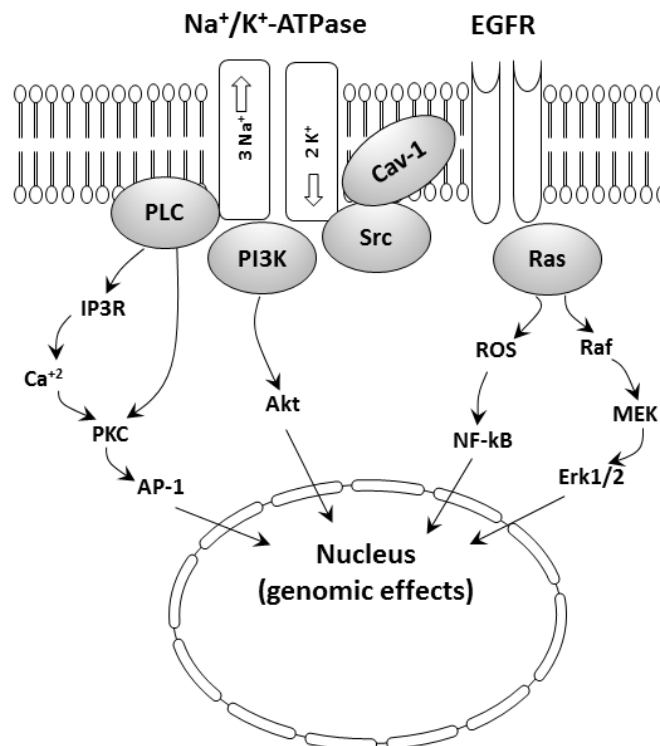


**Figure 5:** Signalosome of  $\text{Na}^{+}/\text{K}^{+}$ -ATPase. Binding of cardiotoxic steroids to  $\text{Na}^{+}/\text{K}^{+}$ -ATPase triggers a cascade of events starting with activation and phosphorylation of Src and caveolin-1, which leads to transactivation of EGFR. Other proteins are recruited such as: PLC, PI3K and Ras. The downstream effects are various and include inhibition of cytoprotective effects of NF- $\kappa$ B and Akt and activation of AP-1 and Erk1/2 leading eventually to cell death via apoptosis and autophagy. Copyright 2015 with permission from Elsevier; doi: 10.1016/j.jsbmb.2015.03.008; <http://www.sciencedirect.com/science/article/pii/S096007601500093X>.

Targeting  $\text{Na}^{+}/\text{K}^{+}$ -ATPase by cardiotoxic steroids as a chemotherapeutic approach seems to be especially promising, since they were shown to display strong anticancer activity in chemosensitive as well as multidrug-resistant (MDR) cell lines [75]. Pathways of evading the various resistance profiles include [61]: triggering apoptosis, expressional and post-translational regulation of proteins involved in MDR, down-regulation of growth factors (c-MYC and NF- $\kappa$ B), and depletion of intracellular ATP levels.

## 1.6 Multidrug resistance

One major obstacle facing chemotherapy is the development of drug resistance hindering total cure and increasing relapse. In general, resistance mechanisms can be attributed to: 1) host factors, where the pharmacokinetics (absorption, distribution, metabolism and excretion) of a drug limit the delivery to tumor cells or 2) pharmacodynamic factors within the tumor itself due to genetic and epigenetic alterations [76-78]. In the latter, various mechanisms have been tabulated for around 40 years and these include [8, 76-79]: 1) drug transport in and out of cancer cells, where influx of the drug is reduced or efflux is increased, 2) increased drug inactivation/detoxification (e.g. inactivation of alkylating agents and platinum drugs by increased thiol-glutathione or glutathion S transferase) or reduced drug activation (e.g. conversion of gapecitabine to the active form 5-fluorouracil by thymidine phosphorylase), 3) altered drug targets (e.g. up-regulation of thymidylate synthase and dihydrofolate reductase in cases of 5-fluorouracil and methotrexate, respectively) 4) increased DNA repair against agents that either directly induce DNA damage such as alkylating agents, platinum drugs or indirectly such as topoisomerase inhibitors 5) deregulation of apoptosis (e.g. mutations in the proapoptotic *TP53* and overexpression of members of anti-apoptotic BCL-2 family) 6) activation of pro-survival signaling e.g. via activation of the epidermal growth factor receptor (EGFR) as a resistance-promoting adaptive response and 7) the role of tumor microenvironment represented by autocrine, paracrine and endocrine activation of survival signaling pathways by cytokines and growth factors.

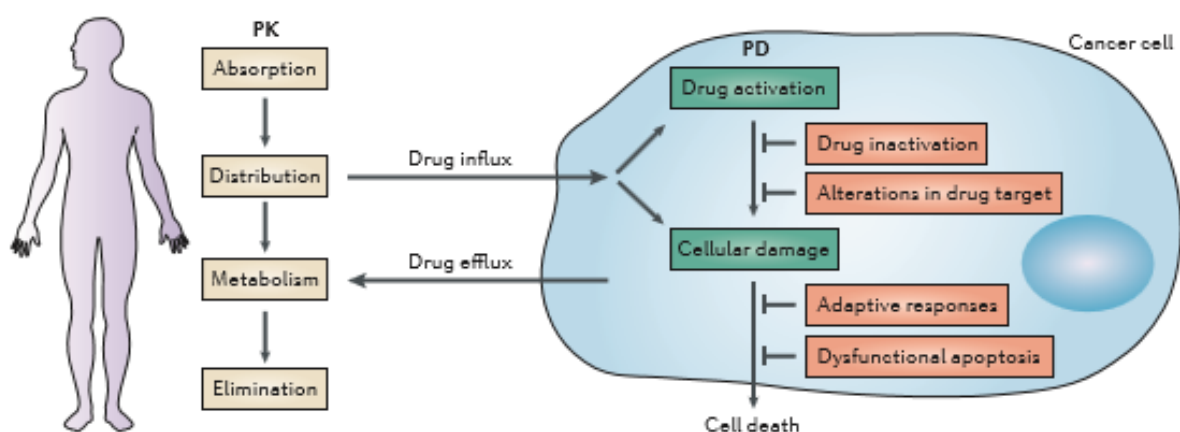


**Figure 6:** The principles of drug resistance in chemotherapy. Pharmacokinetic factors (absorption, distribution, metabolism and excretion) affect the delivery of drugs to tumors. Pharmacodynamic factors are processes that occur within the tumor cell and include effects on: drug influx/efflux, drug activation/inactivation, drug targets,

DNA repair and apoptosis and adaptive pro-survival responses. (Reprinted by permission from Macmillan Publishers Ltd: [Nat. Reviews] [77]; Copyright 2013; <http://www.nature.com>).

It is important to note that resistance mechanisms can either be intrinsic or acquired [76, 77, 80]. Whereas intrinsic mechanisms include those preexisting in the tumor bulk before initiation of treatment, acquired resistance develops during therapy generally via mutations and other adaptive responses (e.g. increased expression of drug target and activation of pro-survival signaling) [77].

The term multidrug resistance (MDR) describes the phenomenon, in which tumor cells develop resistance to structurally and mechanistically unrelated drugs [78]. Of the above mentioned general resistance mechanisms, the following can contribute to MDR: 1) reduced drug accumulation, 2) increased drug detoxification (e.g. by glutathione S transferase and cytochrome P450), 3) enhanced DNA repair capacity and 4) altered drug-induced apoptosis (e.g. BCL-2 pathway) [78, 80, 81]. A summary of these mechanisms is presented in **Figure 7**.

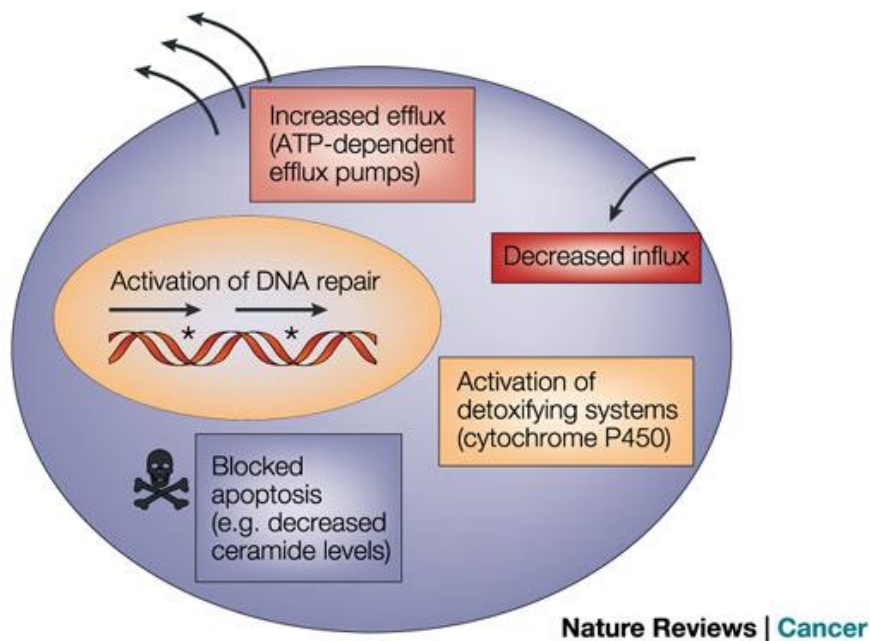


**Figure 7:** Cellular mechanisms of multidrug resistance (MDR). Tumor cells develop resistance to a variety of unrelated chemotherapeutics via several mechanisms: decreased drug influx, increased drug efflux, increased DNA repair, increased activity of detoxification systems and altered apoptosis responses. (Reprinted by permission from Macmillan Publishers Ltd: [Nat. Reviews] [78]; Copyright 2002; <http://www.nature.com>).

When MDR occurs via expression of efflux transporters, it is referred to as classical MDR [78, 80, 82]. This form is the most commonly encountered in laboratory and considered to be the principle mechanism of MDR [82-84]. Responsible for it are members of the so called ABC (ATP-binding cassette) transporter family. This family belongs to the larger family of membrane transport proteins that is comprised of three main families: 1) ion channels (transporting ions across plasma membranes down their electrochemical gradients), 2) transporters (facilitate the movement of a specific substrate with or against its gradient via a conformational change e.g. solute carriers (SLC)) and 3) aquaporins (transporting water molecules through the driving force of osmotic gradients) [85]. ABC transporter family contains more than 100 transporters existing in organisms as simple as prokaryotes and as complex as humans with 49 genes found in the latter and designated as subfamilies A-G [77, 79, 85]. As the name implies, ABC transporters contain an ATP-binding cassette, which is also referred to as the nucleotide-binding domain (NBD) [85]. All members of this family share a common protein fold of the nucleotide binding domain, which is distinct from other ATP-binding proteins [84]. The minimal functional core unit of ABC transporters consists of four domains: two transmembrane domains (TMDs) – comprising several  $\alpha$ -helices – and two NBDs [84, 85]. Some ABC transporters are transcribed as half transporters containing one TMD and one NBD that later form functional dimers (e.g. breast cancer resistant protein (BCRP)), whereas others readily exist as a full transporter (e.g. P-glycoprotein) [82, 84, 85]. In addition to their involvement in MDR, ABC transporters serve a wide range of physiological functions including [86]: 1) regulation of permeability at physiological barriers (e.g. blood brain barrier, blood testicles barrier and placenta), 2) excretion of toxins in gastrointestinal tract, liver and kidney, 3) transport of peptides to the endoplasmic reticulum which will later be identified as antigens by the immune system and 4) lipid transport and homeostasis. It has been established that 13 ABC transporters are implicated in MDR [83, 87]. However, recent studies suggest involvement of more than 20 members [83, 87]. P-glycoprotein represents the best characterized member of this family, since it is the first ABC transporter to be identified and is intensively implicated in MDR [84, 88]. Therefore, it will be discussed thoroughly in the next section.

## 1.7 P-glycoprotein

### 1.7.1 History and discovery

The discovery of P-glycoprotein by Victor Ling in 1976 marks a new era in MDR research [89]. This breakthrough has been preceded by several discoveries starting in the year 1968, as the uptake of daunomycin was assessed *in vitro* and *in vivo* in mouse leukemia tumors, leading to the first isolation of MDR cell lines [89, 90]. Later on, it was shown that MDR is caused by cytogenic abnormalities attributed to gene amplification [89]. In 1973, the role of drug efflux by a carrier-mediated extrusion mechanism and its inhibition in drug accumulation within tumor cells was demonstrated [89, 91]. In the following year, this efflux was proven to be energy-dependent [89, 92]. However, during this chronology of events, it was still difficult to imagine that all these processes accompanied by the highly pleiotropic nature of the MDR phenotype can be attributed to a classical drug-efflux transporter. At that time, a more global regulator of the cell membrane was thought of [89]. Nevertheless, in 1976 it was a defining moment, as investigations on permeability “membrane” mutant cells (with the recently developed technique at that time to label cell-surface carbohydrates) revealed a larger molecular weight peak found only in mutant cells – originally developed to obtain mutants in colchicine-binding protein (tubulin) that were surprisingly found to rather have reduced permeability of colchicine and other unrelated drugs [89]. Hence, the glycoprotein discovered was termed P-glycoprotein with the letter “P” referring to permeability.

### 1.7.2 Human tissue distribution and physiology

In humans, P-glycoprotein is encoded by a small gene family consisting of two adjacent genes *MDR1 (ABCB1)* and *MDR2/3 (ABCB4)* encoding class I (involved in MDR) and class II (involved in phosphatidylcholine transport) isoforms, respectively [80, 81, 93, 94]. P-glycoprotein is found in most tissues but is highly and functionally expressed in specific tissues including the luminal membranes of various segments of the gastrointestinal tract (GIT), the blood-brain barrier (BBB), blood-testis barrier, blood-inner ear barrier, placenta, and in excretory cells such as hepatocytes in the liver, adrenal gland epithelia and proximal tubule epithelia in the kidney [95-98].

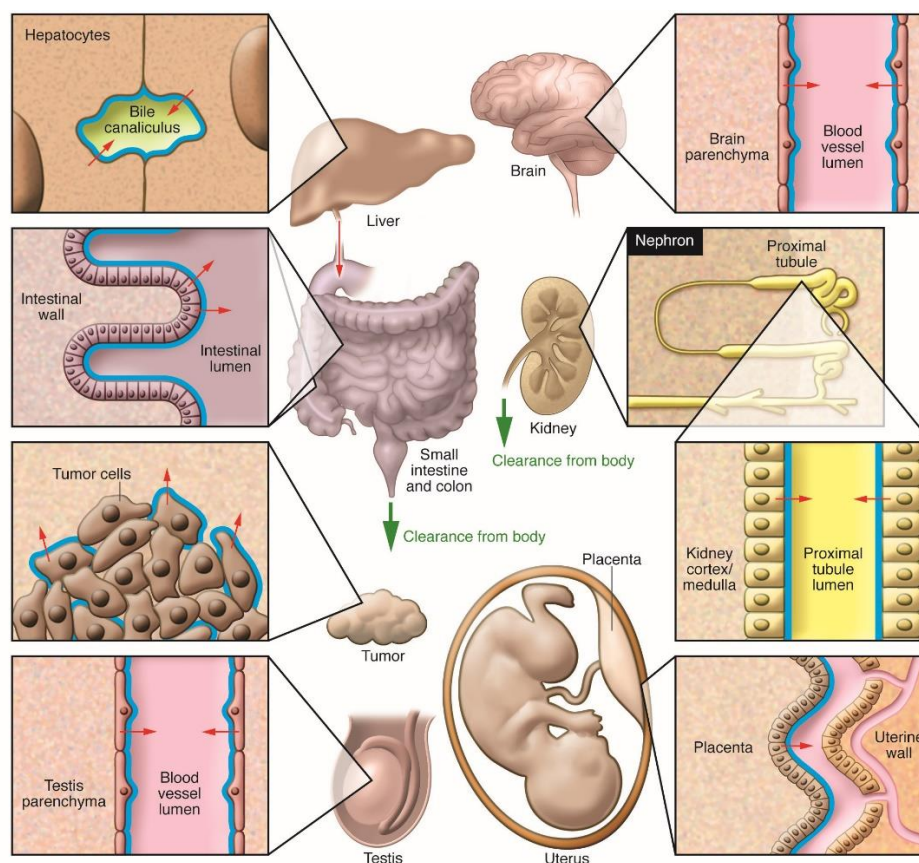


**Figure 8:** Functional expression of P-glycoprotein in various tissues. P-glycoprotein is at: blood-brain barrier, blood-testis barrier, gastrointestinal tract, liver, kidney and placenta. It is also expressed in some tumor cells, where it is responsible for classical MDR. (Republished with permission of American Society for Clinical Investigation, from [97]; permission conveyed through Copyright Clearance Center, Inc).

This tissue distribution suggests various physiological roles of P-glycoprotein including [98]: 1) protection of susceptible tissues such as the central nervous system, testis, ear and fetus from xenobiotics, 2) excretion of xenobiotics and metabolites into bile, urine and the lumen of the gastrointestinal tract and 3) transport of hormones from adrenal glands and uterine epithelium.

### 1.7.3 Structure

The membrane topology of P-glycoprotein was first elucidated by molecular biology techniques such as Cys-mutagenesis and later by electron microscopy revealing (like other ABC transporters) that it is comprised of two homologous halves each consisting of six transmembrane (TM) segments and a cytosolic nucleotide-binding domain (NBD) [88, 98, 99]. The NBD contains highly conserved motifs: 1) Walker A and B motifs that are found in other ATP-binding proteins and 2) Walker C (ABC signature), which is exclusive to the ABC superfamily [88]. Mutagenesis analysis has shown that the drug binding cavity is composed of TM segments of both halves, especially TMs 4, 5 and 6 in the N-terminal half and TMs 9, 10,



hydrophobic and amphiphilic nature. The early biological and biochemical knowledge suggested that hydrophobic ligands might interact with P-glycoprotein within the transmembrane domain, since modulation of anthracycline transport by chemosensitizers was proportional to their ability to partition in the lipid bilayer [104]. Therefore, the vacuum cleaner and flippase models were suggested. The vacuum cleaner model hypothesizes a direct extrusion from the lipid bilayer to the extracellular space, whereas in the flippase model, the substrate is first flipped (transported) from the inner leaflet of the membrane to the outer one and then expelled to the extracellular space [88, 102, 103]. Which model is the most reliable and the possibility of a combined model-system, where compounds gain access to the transporter via more than one route, remains controversial and needs further investigation [88, 103].

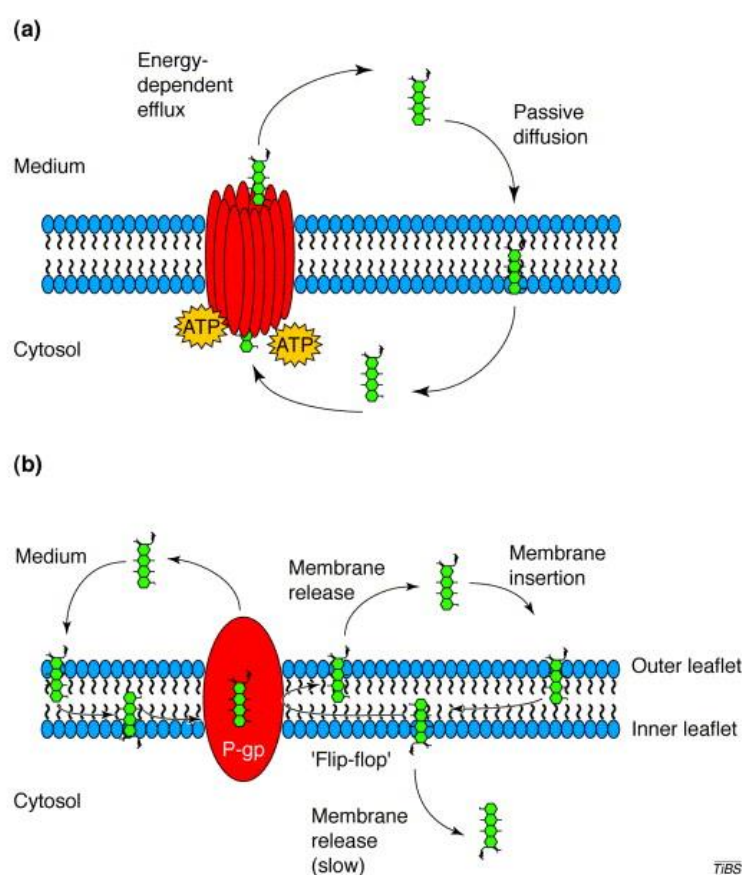


**Figure 10:** Three P-glycoprotein transport models. A: aqueous pore model. B: vacuum cleaner model and flippase model. For detailed description refer to text. (Retrieved from [105] with permission from Elsevier; Copyright 2000).

Several attempts have been made to clarify the ability of P-glycoprotein to interact with a wide diversity of compounds. In the late 1980's, it has been shown via photoaffinity labelling of P-glycoprotein with azidopine that P-glycoprotein confers two different binding sites for this drug [106]. In successive years, the results of several techniques including photoaffinity labelling,

site-directed antibodies and site-directed mutagenesis have been incorporated to determine the general binding domains and identify amino acids critical for the interaction of some agents with P-glycoprotein. In 1999, Shapiro *et al.* suggested the presence of three distinct binding sites: the H-site interacting with Hoechst 33342 and colchicine, R-site favoring rhodamine 123 and anthracyclines and a third binding site exerting allosteric interaction with the previous two [107]. The number of binding sites has increased over time to reach four and at a later point even seven [107]. The debate did not stop and the “substrate induced-fit” mechanism came to life hypothesized by Loo *et al.* proposing that a substrate, depending on its size and shape, is able to induce conformational changes in the transmembrane (TM) segments, allowing the substrate to accommodate within P-glycoprotein and be successively transported [108]. In other words, rather than the existence of multiple separate drug-binding sites, a large flexible binding pocket exists with residues quite mobile in the ligand-free state, but these become rigid upon ligand-binding via multiple Van der Waals and hydrophobic interaction that can be unique for each compound [88, 99].

### 1.7.5 Catalytic cycle

The drug transport by P-glycoprotein involves entry of the substrate to the drug-binding pocket, conformational change and then release of drug [99]. According to the alternating access and switch models, substrates enter the drug-binding cavity through the transmembrane domains (TMDs). When this happens, an ATP-driven closure of the NBD dimer occurs in a tweezers-like motion. This leads to a decrease in the distance between the intracellular segments of TMDs thereby shifting from the inward-facing to the outward-facing conformation with a concomitant switch from high to low drug-binding affinity thereby extruding drugs and solutes to the extracellular space [99, 109].

#### *Alternating sites:*

In the alternating sites mechanism, only one catalytic site can be in a transitional state at any instant and the two sites alternate in catalysis indicating asymmetry between the NBDs at some point during the catalytic cycle [99]. According to this model, the catalytic cycle proceeds as follows: 1) initial loose binding of ATP at both NBDs leads to the formation of a closed dimer. 2) One ATP molecule is tightly bound and committed to hydrolysis. 3) This ATP enters the transition state and the release of hydrolysis products (Pi and ADP) leads to dimer opening allowing another ATP binding to occur. In the next catalytic cycle, hydrolysis occurs at the opposite site, hence the name: alternating sites.

*Switch model:*

According to this model [109], the NBDs in the resting state are nucleotide-free forming an open dimer configuration. Then, binding of two ATPs leads to a closed dimer configuration. The two ATP molecules are hydrolyzed sequentially with the hydrolysis products remaining bound to the protein. This in turn leads to a sequential release of Pi and then ADP restores the protein to its basal configuration. Unlike the alternating sites model, hydrolysis of two ATP molecules is required to fulfil one catalytic cycle.

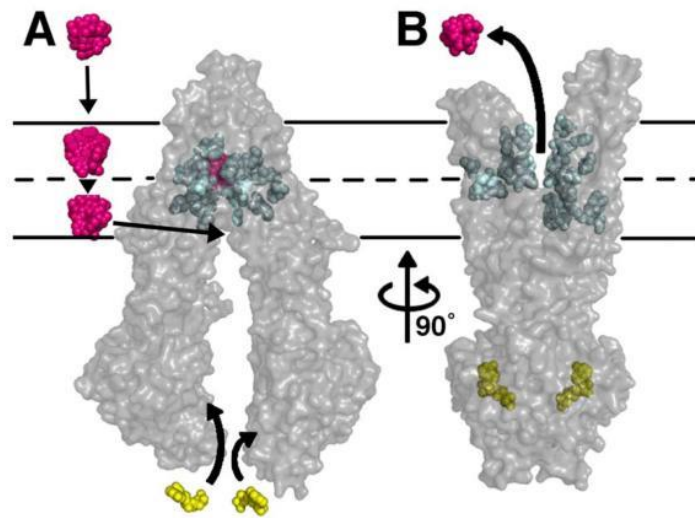


**Figure 11:** General scheme of P-glycoprotein efflux cycle. The substrate (magenta) partitions into the lipid bilayer from the outer leaflet to the inner leaflet. Then it gets trapped by the internal drug-binding cavity interacting with amino acids (cyan). ATP (yellow) binds to the NBDs leading to a conformational change extruding the ligand to the extracellular space. (Retrieved from [101] with permission from AAAS; Copyright 2009).

## 1.7.6 P-glycoprotein inhibition

### 1.7.6.1 Mechanisms of inhibition

Understanding the mechanism of inhibition of P-glycoprotein imposes another major challenge in this field of research. Despite the identification of numerous P-glycoprotein inhibitors, the exact mechanism of this inhibitory process remains to be fully elaborated. Some inhibitors have been described to act through competitive interactions with the substrate over a mutual binding site [110], while others may allosterically interact by binding to different sites than those occupied by substrates and thereby preventing the translocation and dissociation of the substrate [111]. Some agents interact with the nucleotide binding domain (NBD) causing an inhibition of the ATPase activity. Flavonoids represent a good example of such agents [112] and the amino acids that play a crucial role in the interaction with ATP were elucidated by sequence homology

and site-directed mutagenesis [113]. One model explaining P-glycoprotein inhibition is that the transporter may handle substrates and modulators in exactly the same way, however, the flip-flop rate across the membrane bilayers is the decisive step, where it is very fast in case of modulators. Therefore, P-glycoprotein cannot keep pace with the fast flip-flop rate of the modulators and is kept busy from transporting the slower substrates [88]. A further “indirect” mechanism of inhibition is the alteration of membrane fluidity. Some agents such as anesthetics (e.g. diethyl ether) and mild neutral detergents were reported to modulate multidrug resistance and cause concomitant increase of membrane fluidity, which may have a direct consequence on the “flippase” function of P-glycoprotein or cause an indirect effect via increasing the passive movement of the substrate within the membrane through alteration of the transmembrane microenvironment [114, 115]. Hence, compounds increasing the membrane fluidity lead in turn to increased flip-flop rates of substrates, which P-glycoprotein is not able to keep up with [88]. In **Figure 12**, we summarize these different mechanisms of P-glycoprotein inhibition via small molecules as well as the various interaction sites outlined throughout this introduction.

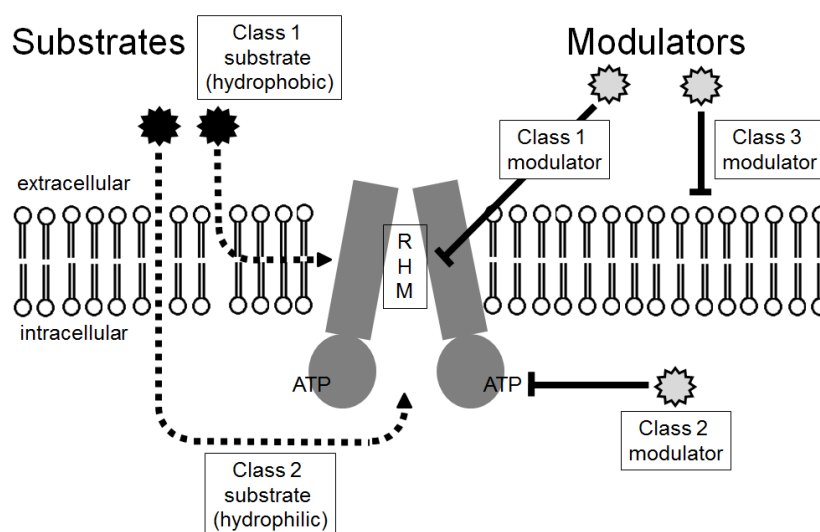


**Figure 12:** Schematic representation of the interaction of small molecules (substrates/modulators) with P-glycoprotein. Class 1 substrates are those of hydrophilic nature, which support the aqueous pore model. Class 2 represents the majority of P-glycoprotein substrates that fit to either the vacuum cleaner or the flippase model. Three classes of modulators are depicted: Class 1 consists of modulators competitively/allosterically interacting with the transmembrane region that is composed of R-, H- and M-sites (as suggested by Ferreira *et al.* [116]). Class 2 are modulators that interact with the nucleotide binding domain (NBD). Class 3 represents molecules that interfere with membrane fluidity and indirectly affect the function of P-glycoprotein. (Retrieved from [117] with kind permission from Springer Science + Business Media; Copyright 2014)

One approach to modulate the activity of P-glycoprotein is the use of monoclonal antibodies. MRK16 and UIC2 are monoclonal antibodies that bind to the extracellular domain of P-glycoprotein and both have shown to introduce inhibitory effects [118]. Epitopes of both antibodies have been mapped demonstrating the amino acids involved in this interaction [119, 120]. Another approach is targeting the expression of the protein by various mechanisms either via small molecules that lead to down-regulation of mRNA levels of the *MDR1* gene (e.g. tryptanthrine and trifluoperazine) or using RNA interference technology [121]. Furthermore, since *MDR1* expression requires the phosphorylation of the promoter by RNA helicase A, which is dependent on DNA-protein kinases, drugs that can inhibit this kinase activity can also be considered [121].

### 1.7.6.2 P-glycoprotein inhibitors in three generations

In the 1980s the discovery of Tsuruo *et al.* that verapamil – a calcium channel blocker – is able to inhibit P-glycoprotein has marked a major milestone in this field of research [122]. Ever since, the quest of finding further modulators of P-glycoprotein has never stopped and many compounds were able to exert inhibitory effects on P-glycoprotein.

First generation inhibitors are drugs already known on the market and clinically used to treat other conditions such as verapamil, cyclosporine, etc. These have unfortunately failed in clinical trials due to lack of potency and severe side effects at concentrations used to achieve this inhibition [123, 124]. Second generation inhibitors were developed to reduce the side effects observed with first generation drugs. However, clinical trials with second generation inhibitors such as valsopodar (PSC833) were also unsuccessful, since they have exerted significant pharmacokinetic interactions – i.e. the concomitant inhibition of cytochrome P450 monooxygenases – causing a necessary dose reduction of the chemotherapeutic agent administered in parallel and thereby insufficient plasma levels [123, 124]. Therefore, attempts to develop third generation inhibitors have been carried out, with the hope that these would have more specificity to P-glycoprotein and less cytotoxic effects [123]. In this context, compounds such as tariquidar and elacridar have been designed [123, 124]. Even though tariquidar showed promising results in preclinical and phase I studies, other studies were terminated due to complications [124]. Despite that, the National Cancer Institute (NCI) launched phase I/II trials that are as well ongoing [125]. Furthermore, it is noteworthy that clinical trials for verapamil and cyclosporine A from the first generation, valsopodar from second generation as well as tariquidar from the third generation are still ongoing [124].

### 1.7.6.3 Natural products as P-glycoprotein inhibitors

Due to the poor success of third generation inhibitors, many researchers have directed their focus to natural compounds to find new potential inhibitors. These are sometimes classified as fourth generation inhibitors [124]. The identified active components of food and plant extracts were used as lead compounds for chemical optimization to obtain selective P-glycoprotein inhibitors with high affinity [124]. In 1991, the interaction of grapefruit with several drugs gave the first hints to possible implications of herbal constituents in P-glycoprotein inhibition [121]. The return to natural compounds, especially those used in traditional medicine and dietary supplements has yielded various compounds capable of P-glycoprotein inhibition [126]. From a botanical point of view, since it is expected that many herbal constituents are P-glycoprotein substrates, it is plausible that inhibitors of P-glycoprotein may have co-developed in plants throughout evolution as a defense mechanism against plant-eating animals [126]. Several flavonoids, alkaloids, coumarins, steroids and terpenoids are only a few examples of natural constituents that inhibited P-glycoprotein *in vitro* [124, 126]. However, there is still a long road ahead to evaluate their efficiency in the clinic [121].

### 1.8 Molecular docking and P-glycoprotein research

Over the years, several *in vitro* assays have been developed to identify and investigate substrates and inhibitors of P-glycoprotein. These include cell-based transwell transport, use of fluorescent dyes followed by flow cytometry and fluorescent spectroscopy, and measurement of the ATPase activity of P-glycoprotein [127, 128]. However, these techniques are costly and require much time especially in terms of screening large compound libraries. Therefore, they are often used at later stages in the drug-development processes [128]. As a consequence, computational methods have emerged in the field of rational drug design and screening processes as fast and low-cost alternatives [128, 129]. These methods can be classified into ligand- and receptor-based: As ligand-based methodologies try to gain information from chemical features of the ligands to be screened (e.g. quantitative structure activity relationship; QSAR), receptor-based techniques take the crystal structure of the target into consideration (e.g. molecular docking) [130]. In some reports, ligand-based methodologies are fast and have proven able to differentiate between P-glycoprotein interacting and non-interacting molecules [129]. In others, obstacles were faced due to poor predictability or interpretability [130]. On the other hand, receptor-based approaches allow investigation of ligand-receptor interactions at the molecular level when crystal structures of the receptor are available [129, 130]. In the field of

P-glycoprotein research, receptor-based approaches have been limited due to the lack of reliable crystal structures of the protein [130, 131]. As previously mentioned, it is only until 2009 that the crystal structure of mouse P-glycoprotein has been elucidated by Aller *et al.* [101]. This discovery has revolutionized the knowledge of P-glycoprotein structure at the atomic level providing a good starting point to conduct molecular docking studies [129, 131]. Ever since, there have been several docking studies attempting to predict affinities of drugs and metabolites to P-glycoprotein. However, many of these have been confronted by various challenges including [116, 129, 131-133]: 1) the polyspecific nature of ligand-binding, 2) the huge chemical diversity of compounds transported by and/or inhibiting P-glycoprotein, 3) the discrepancies in literature regarding substrate/inhibitor-like interactions with P-glycoprotein, 4) the limitation in *in vitro* experiments represented by the inability to identify some P-glycoprotein substrates due to their fast flip-flop rate across the membrane, which masks their transport by P-glycoprotein 5) absence of co-crystallized substrates with P-glycoprotein preventing direct identification of binding sites, 6) low crystallographic resolution of structures and 7) the high flexibility of P-glycoprotein. Therefore, intensive efforts must continue to provide reliable *in silico* studies and wet lab experiments assessing the unresolved, complex field of P-glycoprotein research.

## 2 Aim of the thesis

With the developing trend of going back to nature to look for novel therapeutics, naturally occurring cardiotonic steroids represent promising compounds in cancer chemotherapy. Throughout literature, various hints have pointed to their antitumor activities *in vitro* and *in vivo*. Their established molecular target, Na<sup>+</sup>/K<sup>+</sup>-ATPase, has recently been implicated in cancer biology being a scaffold for many signaling pathways. Furthermore, cardiotonic steroids have been shown to evade multidrug resistance in many tumor cell lines. Multidrug resistance is the main cause of chemotherapy failure. A major transporter implicated in multidrug resistance is P-glycoprotein being the best characterized and most encountered ABC transporter in cancer chemotherapy. However, over 30 years of tedious research have failed to bring any P-glycoprotein inhibitor to the market. Therefore, it is of great necessity to search for novel inhibitors using high throughput techniques and other *in silico* methods. Provided with a chemical library of cardiotonic steroids and their derivatives, the research conducted and presented in this thesis has aimed at the following points:

- ***Analysis of cytotoxic effects of cardiotonic steroids in sensitive and multidrug-resistant, P-glycoprotein overexpressing leukemia cell lines:***

Results from this part were exploited first to gain more knowledge about relevant structural features by performing structure-activity relationship (SAR) analysis followed by development of quantitative structure activity relationship (QSAR) as an *in silico* model to predict cytotoxicity, second to analyze the link between cytotoxicity and Na<sup>+</sup>/K<sup>+</sup>-ATPase by means of molecular docking and third to obtain possible hints to an interaction with P-glycoprotein.

- ***Establishment of a high throughput platform to screen cardiotonic steroids for P-glycoprotein modulation:***

Cytotoxicity results and the inherent fluorescence of doxorubicin were incorporated to screen the entire library of cardiotonic steroids for P-glycoprotein inhibition by means of flow cytometry. Results were validated by various other techniques.

- ***Utilization of molecular docking in P-glycoprotein research:***

As a separate section and due to the emerging importance of *in silico* methods in drug development, we have tested the ability of molecular docking to predict interactions of small molecules with P-glycoprotein.

### 3 Results

#### 3.1 Cytotoxicity of cardiotonic steroids

As previously mentioned, various hints of potential use of cardiotonic steroids in cancer therapy and their advantage in evading multidrug resistance were already established. Being provided with a chemical library of 66 cardiotonic steroids and their derivatives, we aimed first at assessing their cytotoxic effects in sensitive and multidrug-resistant cell lines using resazurin reduction assay. The obtained results ( $IC_{50}$  values) then served as an initial platform to carry various investigations in many directions. First, structure activity relationship (SAR) analysis was conducted to elucidate the chemical substitutions that contribute to cytotoxicity. Later, a quantitative structure activity relationship (QSAR) model was developed in an attempt to predict cytotoxicity in both cell lines. Because  $Na^+/K^+$ -ATPase has been implicated in the cytotoxic effects of cardiotonic steroids, we conducted molecular docking of all compounds into  $Na^+/K^+$ -ATPase and then correlated the results with the  $IC_{50}$  values in both cell lines. Results from both QSAR and molecular docking pointed to a probable differential expression of  $Na^+/K^+$ -ATPase in sensitive and multidrug-resistant cell lines. This has been later confirmed via western blotting and next generation sequencing<sup>1</sup>.

##### 3.1.1 Cytotoxicity of cardiotonic steroids in sensitive and MDR leukemia cells

We tested a chemical library of 66 cardiotonic steroids and their derivatives for their cytotoxicity on drug-sensitive, parental CCRF-CEM and multidrug-resistant P-glycoprotein-expressing CEM/ADR5000 leukemia cell lines. Doxorubicin and verapamil were tested in parallel as control drugs. Digoxin and bufalin were tested as representatives of cardenolide and bufadienolide derivatives, respectively. The  $IC_{50}$  values are listed in **Tables 1** and **2**, with the compounds possessing  $IC_{50}$  values below 10  $\mu$ M (**Table 1**) being separated from those with  $IC_{50}$  values above (**Table 2**). The resistance indices were calculated for each compound by dividing the  $IC_{50}$  value in the resistant cell line by that in the sensitive one. Accordingly,

---

<sup>1</sup> The results of this section have been submitted to a peer-reviewed scientific journal: (**now accepted**) Zeino, M., Brenk, R., Gruber, L., Zehl, M., Urban, E., Kopp, B., & Efferth, T. (2015). Cytotoxicity of cardiotonic steroids in sensitive and multidrug-resistant leukemia cells and the link with  $Na^+/K^+$ -ATPase. *The Journal of steroid biochemistry and molecular biology*, 150, 97-111. Copyright 2015 with permission from Elsevier; doi: 10.1016/j.jsbmb.2015.03.008; <http://www.sciencedirect.com/science/article/pii/S096007601500093X>. All texts, figures and tables presented have been ultimately prepared by myself.

resistance indices above 1 indicated resistance, whereas below 1 sensitivity of the CEM/ADR5000 cells towards the tested compound compared to the parental cell line [134]. The resistance indices ranged from 0.30 to 3.33 for cardiotoxic steroids and derivatives. Doxorubicin and verapamil revealed resistance indices of 558 and 0.73, respectively. It is worth to note that compound 12B did not exert any cytotoxic effect on sensitive CCRF-CEM cells even at a maximum concentration of 100  $\mu\text{M}$ , but did so in CEM/ADR5000 cells, indicating a high degree of collateral sensitivity (hypersensitivity).

**Table 1:**  $\text{IC}_{50}$  values of cardiotoxic steroids exerting cytotoxic effects below 10  $\mu\text{M}$  on both leukemia cell lines. Mean values were calculated with the standard error of the mean (SEM). (\*\*\*) indicates three times repetition, whereas (\*\*) indicates two times repetition due to limited amounts of the substance. Resistance indices were obtained by dividing the  $\text{IC}_{50}$  values on the resistant cell line through that on the sensitive one.

Substance code	$\text{IC}_{50}$ ( $\mu\text{M}$ ) $\pm$ SEM		Resistance index
	CCRF-CEM	CEM/ADR5000	
2C***	0.022 $\pm$ 0.002	0.037 $\pm$ 0.002	1.68
2G**	0.0207 $\pm$ 0.0001	0.048 $\pm$ 0.004	2.32
2M***	0.012 $\pm$ 0.002	0.013 $\pm$ 0.003	1.08
2P***	0.0022 $\pm$ 0.0003	0.0029 $\pm$ 0.0004	1.32
2c**	0.026 $\pm$ 0.001	0.058 $\pm$ 0.003	2.23
3D**	1.63 $\pm$ 0.05	2.21 $\pm$ 0.02	1.36
6B**	0.009 $\pm$ 0.001	0.0172 $\pm$ 0.0001	1.91
7B**	0.77 $\pm$ 0.03	1.4 $\pm$ 0.2	1.82
7E**	0.15 $\pm$ 0.02	0.27 $\pm$ 0.04	1.80
10O***	0.007 $\pm$ 0.004	0.009 $\pm$ 0.002	1.29
10S***	0.15 $\pm$ 0.01	0.165 $\pm$ 0.009	1.10
15c**	2.1 $\pm$ 0.3	4.9 $\pm$ 0.6	2.33
15d**	0.09 $\pm$ 0.03	0.1144 $\pm$ 0.0002	1.27
16D***	2.4 $\pm$ 0.7	3 $\pm$ 1	1.25
21E**	0.018 $\pm$ 0.005	0.04 $\pm$ 0.01	2.22
22N**	0.018 $\pm$ 0.005	0.026 $\pm$ 0.003	1.44
23A***	0.25 $\pm$ 0.02	0.38 $\pm$ 0.01	1.52

23D***	2.0 ± 0.1	4.4 ± 0.2	2.20
23G**	4.6 ± 0.7	4 ± 1	0.87
27F***	0.23 ± 0.03	0.42 ± 0.07	1.83
32A***	0.018 ± 0.003	0.030 ± 0.006	1.67
35B***	2.9 ± 0.4	3.6 ± 0.6	1.24
44F**	3.90 ± 0.07	6.3 ± 0.2	1.62
53R**	0.57 ± 0.03	1.22 ± 0.04	2.14
54v**	8 ± 1	4.9 ± 0.6	0.61
62I**	4.4 ± 0.4	5.3 ± 0.5	1.20
bufalin***	0.0055 ± 0.0003	0.0062 ± 0.0007	1.13
digoxin***	0.031 ± 0.001	0.068 ± 0.009	2.19

**Table 2:** IC<sub>50</sub> values of the less active cardiotonic steroids, i.e. those that exert their cytotoxic effect only above 10 µM on one of the two leukemia cell lines. Mean values were calculated with the standard error of the mean (SEM). (\*\*\*) indicates three times repetition, whereas (\*\*) indicates two times repetition and (\*) indicates one repetition due to limited amounts of the substance. Resistance indices were obtained by dividing the IC<sub>50</sub> values on the resistant cell line through that on the sensitive one.

Substance code	IC <sub>50</sub> (µM) ± SEM		Resistance index
	CCRF-CEM	CEM/ADR5000	
4I	NA	NA	NA
4L	NA	NA	NA
10G	NA	NA	NA
10I***	22 ± 3	15 ± 2	0.68
10J	NA	NA	NA
11M**	12 ± 1	10 ± 1	0.83
12A**	16 ± 3	8.85 ± 0.04	0.55
12B**	NA	41 ± 6	NA
14D**	31 ± 1	26 ± 2	0.84
15S	NA	NA	NA
15h	NA	NA	NA

15i**	6 ± 1	20 ± 2	3.33
16G	NA	NA	NA
26K	NA	NA	NA
29C***	60 ± 10	18 ± 6	0.30
29b*	56 ± NA	35 ± NA	0.63
30M	NA	NA	NA
42C	NA	21 ± 5	NA
44G***	24 ± 5	24 ± 4	1.00
49d***	26 ± 3	28 ± 4	1.08
49h	NA	NA	NA
51D	NA	NA	NA
52I	NA	NA	NA
54C***	32 ± 6	21 ± 2	0.66
54E**	34 ± 5	36 ± 2	1.06
54T***	40 ± 18	15 ± 6	0.38
54r.***	20 ± 4	27 ± 6	1.35
54α**	23 ± 2	24 ± 3	1.04
54ε**	60 ± 19	60 ± 12	1.00
54ι	NA	NA	NA
54Eε**	72 ± 7	52 ± 6	0.72
55K**	27 ± 6	32 ± 1	1.19
62A	NA	NA	NA
62F*	NA	15 ± NA	NA
62J	NA	NA	NA
62N**	50 ± 16	70 ± 25	1.40
62P	NA	NA	NA
Doxorubicin*** <sup>2</sup>	0.043 ± 0.001	24 ± 4	558
Verapamil***	45 ± 7	33 ± 4	0.73

<sup>2</sup> IC<sub>50</sub> values for doxorubicin are also represented in and taken from section 3.2.5.

### 3.1.2 Cytotoxicity of cardiotonic steroids in non-tumor cells

In order to examine the potential side effects of cardiotonic steroids on normal cells, we selected the most active compounds with  $IC_{50}$  values below 10 nM and tested them on human peripheral mononuclear cells (PMNC) isolated from healthy donors. Dose response curves were generated and are presented alongside the curves of both leukemia cell lines in **Figure 13**.  $IC_{50}$  values were calculated from the corresponding dose response curve for each compound and are listed in **Table 3**. All four compounds exerted higher  $IC_{50}$  values on normal PMNC compared to sensitive and MDR leukemia cell lines.

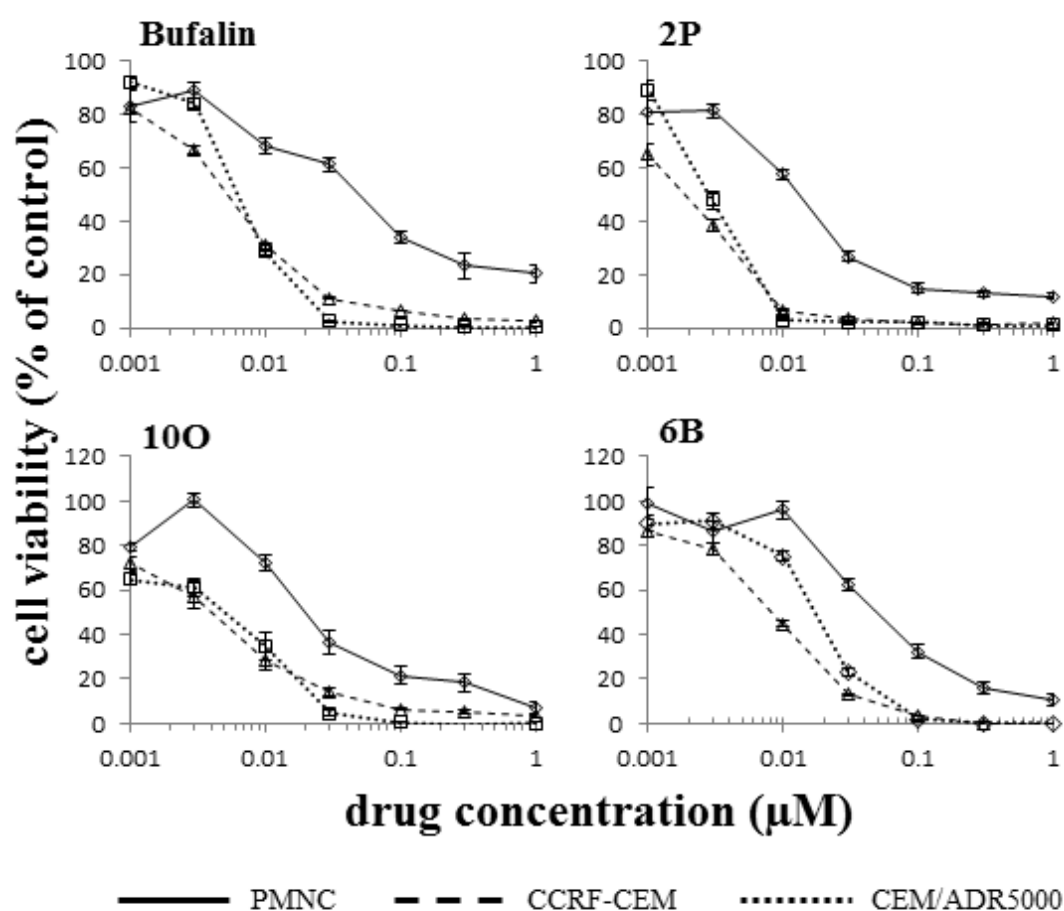


**Figure 13:** Dose response curves of the cytotoxicity of the four most cytotoxic cardiotonic steroids on healthy PMNC, sensitive CCRF-CEM, and multidrug-resistant CEM/ADR5000 leukemia cells. Each experiment was at least repeated twice. Each point in the curve represents mean  $\pm$  SEM.

**Table 3:** Comparison of IC<sub>50</sub> values of the four most potent cardiotoxic steroids on CCRF-CEM, CEM/ADR5000, and PMNC.

Compound	Cytotoxicity: IC <sub>50</sub> (μM) ± SEM		
	CCRF-CEM	CEM/ADR5000	PMNC
Bufalin	0.0055 ± 0.0003	0.0062 ± 0.0007	0.06 ± 0.01
2P	0.0022 ± 0.0003	0.0029 ± 0.0004	0.010 ± 0.001
10O	0.007 ± 0.004	0.009 ± 0.002	0.017 ± 0.006
6B	0.009 ± 0.001	0.0172 ± 0.0001	0.06 ± 0.03

### 3.1.3 Structure activity relationship (SAR)

The examined chemical library of cardiotoxic steroids and their derivatives is comprised of compounds possessing a common core structure with diverse chemical substitutions. Therefore, we aimed at gaining deeper insights into the effect of chemical substituents on cytotoxicity. Noteworthy is the influence of the nature of the lactone ring at position 17 (a butyrolactone in cardenolides and an  $\alpha$ -pyrone in bufadienolides). By comparing 3D to 4I, 10G to 10I, 10O to 11M, 53R to 54C, and 29C to 35B, we found out that the  $\alpha$ -pyrone was a particularly important substructure for the cytotoxic effect since replacing it by a methylcarboxy group strongly decreased the activity. The  $\alpha$ -pyrone was even more favorable than the butyrolactone (compare bufalin to compound 23G). The configuration of the methylcarboxy group at position 17 also affected activity because  $\beta$ -configuration strengthened the cytotoxic effect (compare compound 54C to 54E and 54 $\alpha$  to 54 $\epsilon$ ). Attaching a sugar moiety to a  $\beta$ -OH at position 3 dramatically increased the cytotoxic effect (compare compound 2P to 2M). However, having a  $\beta$ -configured acetyl group at this position did not alter the activity in some cases (compare 21E to 32A and 2C to 2G, who have almost identical IC<sub>50</sub> values) or increased the activity in other cases (compare 12A to 12B, 23A to 23G, and 26K to 29C). On the contrary, a ketone at position 3 reduced the cytotoxic effect by about 10-fold (compare 7E to 21E) and an azido group (N3) diminished the activity (compare 52I to 53R). Similar to position 3, a  $\beta$ -configured acetyl rather than a  $\beta$ -OH group at position 12 did not bring about any differences (compare 15c to 16D) considering the assumption that a  $\beta$ -configured acetyl group at position 3 had no effect. Substitutions at position 16 have been a matter of controversy [75]. We noticed that introducing

a  $\beta$ -configured acetyl group lowered the cytotoxicity (compare 10O to 21E). However, in cinobufagin derivatives that are characterized by a 14- $\beta$ ,15- $\beta$ -epoxy bridge, the  $\beta$ -configured acetyl group at C-16 may play a role [135]. Introducing an  $\alpha$ -OH at C-15 completely diminished the cytotoxic activity (compare 10O to 10J) and hydroxylation at position 12 led to a decrease in activity (compare 2M to 15d). Most of our findings were in accordance with previous studies [75, 135]. However, we can draw the following further conclusions: 1) Even though the essential role of the  $\alpha$ -pyrone ring at position 17 was addressed [75], a direct comparison with butyrolactone was not made. Here we show that the  $\alpha$ -pyrone is more favorable for the cytotoxic effect. 2) In case of replacement of the  $\alpha$ -pyrone ring by a methylcarboxy group, the  $\beta$ -configuration is preferred. 3) We found that a  $\beta$ -configured acetyl group at position 16 lowered cytotoxicity, contrary to what was previously reported [135]. 4) An azido group at position 3 was deleterious. A summary of the effects of different substituents is represented in **Figure 14**.

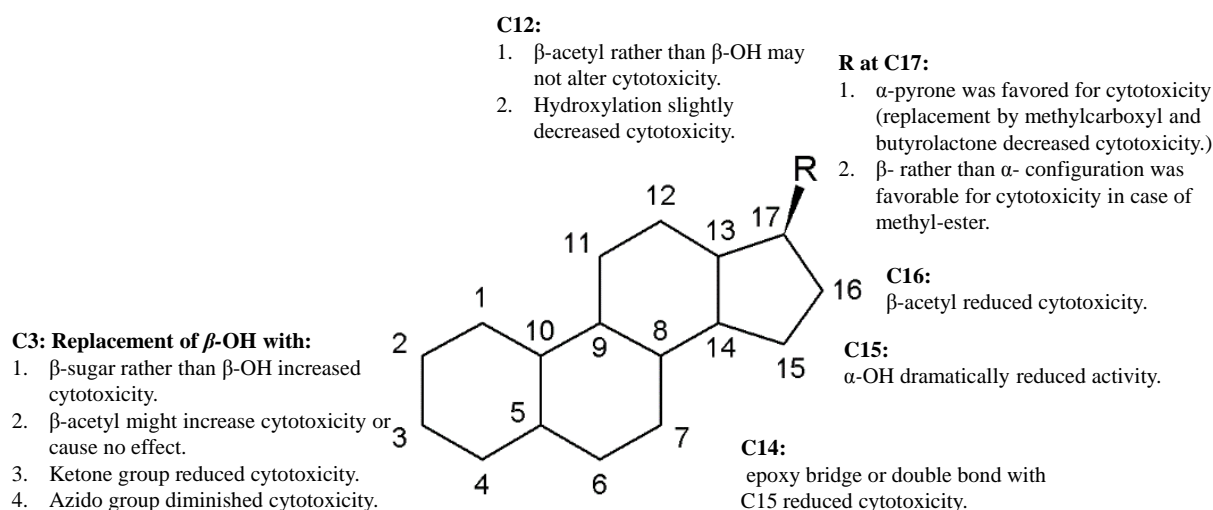


**Figure 14:** Summary of the effects of various functional groups on the cytotoxicity of cardiotonic steroids in leukemia cells.

### 3.1.4 Quantitative structure activity relationship (QSAR)

We further exploited the obtained  $IC_{50}$  values of the compound library to create a QSAR model and test its predictive ability. For this purpose, we divided the cytotoxicity data for each cell line into a training set to build the model and a test set to evaluate it. Correlation plots between experimental and predicted data with the respective Pearson correlation coefficients  $R$  and  $R^2$  were created and are presented in **Figure 15**. Correlations were observed in both cell lines with a slightly better correlation in CCRF-CEM than in CEM/ADR5000 cells ( $R^2$  training set: 0.62 and  $R^2$  test set: 0.61 for CCRF-CEM;  $R^2$  training set: 0.57 and  $R^2$  test set: 0.59 for CEM/ADR5000).

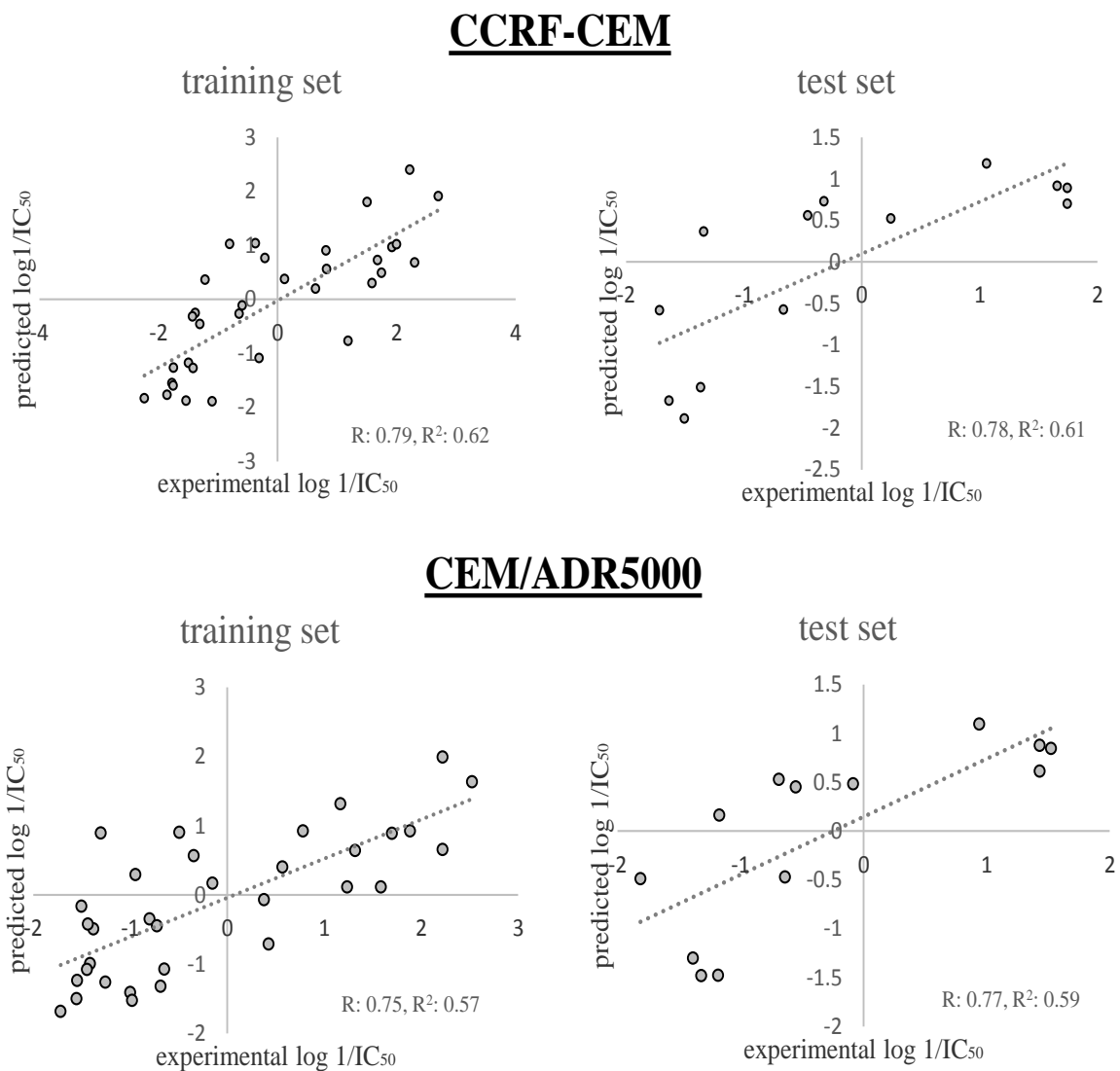


**Figure 15:** QSAR analysis of the cytotoxicity of cardiotonic steroids and derivatives in CCRF-CEM and CEM/ADR5000 cells. Experimental data are represented on the x-axis, predicted on the y-axis. Corresponding R and R<sup>2</sup> values are given below each scatter plot. The dotted line represents the trend line obtained by linear regression.

### 3.1.5 Molecular docking

Since previous studies gave hints of Na<sup>+</sup>/K<sup>+</sup>-ATPase involvement in the cytotoxic effect of cardiotonic steroids [32, 61, 75, 136, 137], we evaluated to which extent the tested compounds could potentially bind to this target *in silico*. Furthermore, correlations between molecular docking and resazurin reduction assay data were investigated. As a first step, we validated our docking approach in terms of reproducing the binding mode of the co-crystallized ligand ouabain. The RMSD value between the binding mode obtained by docking and the one found in the crystal structure was 0.67 Å indicating successful performance. An Overlay of the two binding modes is represented in **Figure 16** with the corresponding amino acids involved in ligand interactions.

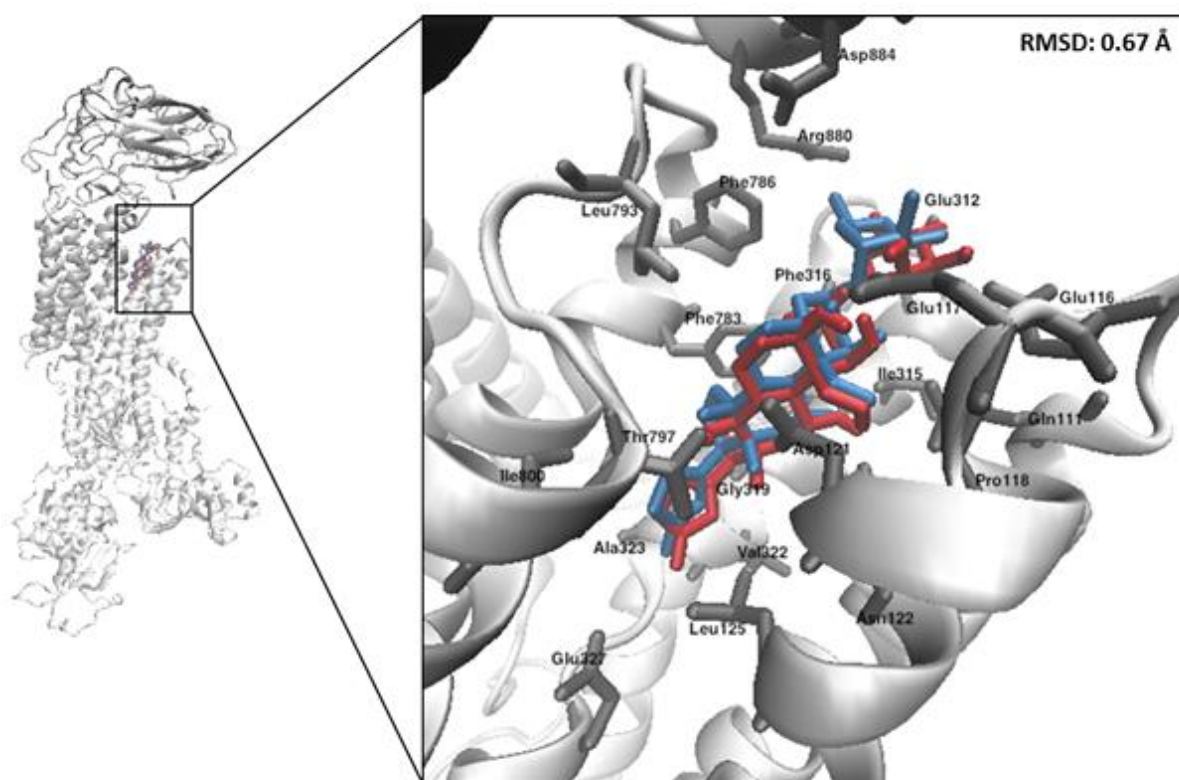


**Figure 16:** Molecular docking of ouabain to Na<sup>+</sup>/K<sup>+</sup>-ATPase. Left: Overall structure of porcine kidney Na<sup>+</sup>/K<sup>+</sup>-ATPase depicted in new cartoon style (gray) with the best docking solution of ouabain into the cardiotonic steroids binding site (red) and its crystallographically determined binding mode (blue). Right: detailed representation of the overlay of the mentioned structures with labeled interacting amino acids and calculated RMSD value between calculated and experimentally determined binding mode of ouabain.

Next, all compounds were docked into the binding site of Na<sup>+</sup>/K<sup>+</sup>-ATPase. Results are presented in **Table 4**, where several information for each compound are provided, including: 1) number of conformations in the lowest binding energy cluster and, if different, in the cluster with the highest number of conformations, 2) average binding energies in each respective cluster, 3) amino acids involved in hydrogen bond formations with the compounds, 4) total number of interacting amino acids displaying hydrophobic interactions and/or hydrogen bonds and 5) fraction of interacting amino acids that were in accordance with the amino acids found interacting with ouabain in the crystal structure of porcine kidney Na<sup>+</sup>/K<sup>+</sup>-ATPase [138].

**Table 4:** Analyses of the predicted interaction of 66 cardiotonic steroids and derivatives with porcine kidney Na<sup>+</sup>/K<sup>+</sup>-ATPase. For each compound, we report the number of conformations in the lowest binding energy cluster and, if different, in the cluster with the highest number of conformations, the average lowest binding energies in the respective clusters, the amino acids involved in H-bond formation, the total number of interacting amino acids, and the fraction of interacting amino acids in common with the known cardiotonic steroids binding site.

Compound	Number of conformations in cluster	Binding energy	Amino acids involved in H-bond formation with the compound	Number of interacting amino acids	Common interacting amino acids compound/ouabain
2C	195	-9.44	Gln111, Glu117, Thr797	10	0.80
2c	235	-9.35	Thr797	7	1.00
2G	162	-9.13	Thr797, Gln111	9	1.00
2M	239	-8.75	Thr797, Asn122	10	1.00
2P	222	-10.32	Thr797, Asn122, Glu116	11	0.91
3D	7	-10.1	Glu117	12	0.17
	148	-9.41	-	10	0.90
4I	9	-10.19	Glu117	9	0.22
	84	-8.79	-	8	0.88
4L	66	-9.85	-	14	0.86
6B	30	-8.63	Thr797, Asn122	10	1.00
	173	-8.58	Thr797, Asn122	10	1.00
7B	175	-10.01	Thr799	10	0.20
7E	175	-10.16	Thr797	11	0.82
10G	20	-9.37	-	10	0.20
	198	-8.92	Asp121	9	0.89
10I	8	-10.5	Glu117	10	0.20

---

	102	-8.98	-	11	0.91
10j	9	-9.3	Glu117	10	0.20
	173	-8.78	Thr797	8	1.00
10O	15	-9.63	Glu117	11	0.18
	215	-9.11	Thr797	7	1.00
10S	18	-8.91	Arg886, His912	11	0.27
	229	-8.83	Thr797	11	1.00
11M	17	-9.37	Glu117	9	0.22
	158	-7.93	-	7	0.86
12A	28	-9.51	Lys288	10	0.20
	107	-9.15	-	8	1.00
12B	229	-8.53	Ala323	8	1.00
14D	23	-9.81	Arg972	10	0.20
	89	-9.72	Gln111	11	0.91
15c	5	-10.04	Glu117	8	0.25
	58	-8.58	Thr797	10	1.00
15d	191	-8.41	Thr797	10	1.00
15h	19	-9.89	Thr799	10	0.20
	135	-8.94	Thr797	9	0.89
15i	124	-9.81	-	12	0.92
15S	4	-6.84	Gln111	10	1.00
	138	-6.55	Glu116	8	0.25
16D	198	-9.07	Glu117, Asn122, Thr979	9	1.00
16G	8	-10.10	Thr799, Arg886, Arg972	10	0.2
	105	-9.47	Asn122, Thr797	9	1.00
21E	9	-10.32	Glu117	12	0.17
	138	-10.1	Thr797	10	1.00
23A	18	-9.34	Glu117	10	0.20
	174	-8.65	Thr797	8	1.00
23D	231	-9.03	-	9	0.89
23G	88	-9.07	-	11	0.82
	154	-8.34	Thr797	10	1.00
26K	54	-7.85	Asn122, Gly796	10	0.50

---

27F	95	-9.44	-	9	0.78
29b	26	-9.07	Glu117	12	1.00
	59	-7.77		8	1.00
29C	27	-9.06	Thr799, Arg886, Tyr901	13	0.08
	117	-7.93	Asp121	12	0.92
30M	213	-8.89	Thr797	8	1.00
32A	199	-9.48	Thr797	11	0.82
35B	200	-9.25	Asp121	10	0.90
42C	9	-9.57	Glu117	11	0.18
	130	-8.84	Thr797	11	1.00
44F	19	-8.52	Glu117	10	0.90
	123	-8.39	Gln111	8	1.00
44G	18	-8.47	-	10	0.30
	232	-8.34	-	8	1.00
49d	100	-8.98	Asp121	10	0.30
49h	45	-7.67	Asn122	11	0.64
	72	-7.44	-	11	0.73
51D	36	-9.04	Gln111	6	1.00
	96	-8.19	-	10	0.80
52I	217	-7.99	-	9	1.00
53R	8	-9.29	Glu117, Arg886, Thr799	12	0.20
	235	-9.27	-	9	1.00
54C	25	-9.25	Thr799, Tyr901	12	0.17
	180	-8.24	-	9	1.00
54E	48	-9.26	Val798, Thr799	7	0.29
	126	-8.82	Gln111	9	0.89
54Ee	35	-8.94	Arg886, Thr799	10	0.20
54α	45	-9.66	Thr799, Arg886, Tyr901	9	0.22
54ε	44	-10.01	Thr799, Arg886	12	0.17
	133	-8.77	Gln11, Thr797	11	1.00
54r	15	-9.62	Thr799, Arg886	11	0.18
	128	-8.33	Asn122	12	0.75
54T	46	-9.6	Thr799, Arg886	10	0.20
	190	-9.09	Asn122	10	0.80

54t	35	-8.39	Asn122	10	0.70
	121	-8.18	-	10	1.00
54v	57	-9.21	Asn122	11	0.91
	144	-8.61	-	8	1.00
55K	69	-8.81	Thr797	14	0.71
62A	21	-8.32	Glu117	9	1.00
	72	-7.71	Gln111	9	0.89
62F	66	-7.61	Asp804, Asp121	11	0.82
62I	42	-8.41	Thr797	11	0.91
62J	2	-9.28	Glu117	14	0.21
	61	-7.49	Glu117	10	1.00
62N	10	-8.88	Phe783	15	0.67
	80	-8.29	Val798, Tyr901, His912	9	0.22
62P	11	-7.64	Asn122	9	0.67
	205	-7.49	-	7	0.29
ouabain	73	-9.97	Glu312, Glu116, Asn122, Thr797	14	1.00
digoxin	67	-10.48	Asp884	14	0.64
bufalin	250	-8.96	Thr797, Glu117	9	1.00

We then performed statistical analyses to correlate the  $IC_{50}$  values of cytotoxicity on CCRF-CEM and CEM/ADR5000 cell lines with each of the following parameters from molecular docking: 1) the average binding energy in the lowest binding energy cluster, 2) the average binding energy in the highest number of conformations cluster, 3) the number of conformations in the lowest binding energy cluster, 4) the number of conformations in the highest number of conformations cluster (if different from the latter), and 5) the fraction of the interacting amino acids obtained from molecular docking that are also described to be responsible for ouabain interaction. Afterwards, we carried out multiple correlation analyses to combine each two parameters from molecular docking and to see their relationship to the cytotoxic effect. The results are shown in **Table 5**.  $IC_{50}$  values on sensitive CCRF-CEM cells revealed a slightly stronger correlation with docking data than  $IC_{50}$  values in multidrug-resistant CEM/ADR5000 cells. The correlations with the binding energies were rather poor.  $IC_{50}$  values were better correlated with the number of conformations in the respective clusters. In multiple correlation analysis,  $IC_{50}$  values were best correlated when combining the binding energies at the highest

number of conformations cluster with the respective number of amino acids in common with the cardiotonic binding site.

**Table 5:** Pearson correlation coefficients between different outputs from molecular docking and IC<sub>50</sub> of CCRF-CEM and CEM/ADR5000 cells. LBE: average binding energy in the lowest binding energy cluster, #Conf\_LBE: number of conformations in the cluster with the lowest binding energy, #AA\_LBE: number of interacting amino acids in the lowest binding energy cluster that are also found in the previously described ouabain binding site, BE: average binding energy in the cluster with the highest number of conformations, #Conf\_BE: highest number of conformations and #AA\_BE: number of interacting amino acids in the cluster with the highest number of conformations that are also found in the previously described ouabain binding site.

Cell line	Parameter correlated with IC <sub>50</sub> values	Pearson coefficient	Parameters correlated with IC <sub>50</sub> values	Multiple correlation coefficient
CCRF-CEM	LBE	0.05	LBE and #Conf_LBE	0.44
	#Conf_LBE	-0.43	BE and #Conf_BE	0.45
	#AA_LBE	-0.39	LBE and #AA_LBE	0.45
	BE	0.26	BE and #AA_BE	0.49
	#Conf_BE	-0.43	#Conf_LBE and #AA_LBE	0.45
	#AA_BE	-0.35	#Conf_BE and #AA_BE	0.48
CEM/ADR5000	LBE	0.07	LBE and #Conf_LBE	0.28
	#Conf_LBE	-0.27	BE and #Conf_BE	0.36
	#AA_LBE	-0.19	LBE and #AA_LBE	0.25
	BE	0.17	BE and #AA_BE	0.40
	#Conf_BE	-0.35	#Conf_LBE and #AA_LBE	0.27
	#AA_BE	-0.32	#Conf_BE and #AA_BE	0.41

### 3.1.6 Expression of Na<sup>+</sup>/K<sup>+</sup>-ATPase in sensitive and MDR cells

Better correlations between the various outcomes of molecular docking with the cytotoxicity data for the CCRF-CEM cell line compared to the CEM/ADR5000 cell line were observed. This prompted us to investigate if differential expression of Na<sup>+</sup>/K<sup>+</sup>-ATPase in sensitive and MDR leukemia cells may account for this observation. Therefore, we performed western blot analyses (**Figure 17**).

Both cell lines revealed bands at ~100 kDa corresponding to the  $\alpha$ -subunit of Na<sup>+</sup>/K<sup>+</sup>-ATPase. However, CEM/ADR5000 cells expressed lower amounts of the protein compared to sensitive CCRF-CEM cells (almost half as much). Bands corresponding to  $\beta$ -actin at ~42 kDa showed equal protein loading on the gels. To further confirm the low expression levels of Na<sup>+</sup>/K<sup>+</sup>-ATPase in MDR cells, we tested another pair of sensitive (KB-3-1) and multidrug-resistant (KB-8-5) HeLa-derived cells. Indeed, Na<sup>+</sup>/K<sup>+</sup>-ATPase was down-regulated in KB-8-5 cells as well.

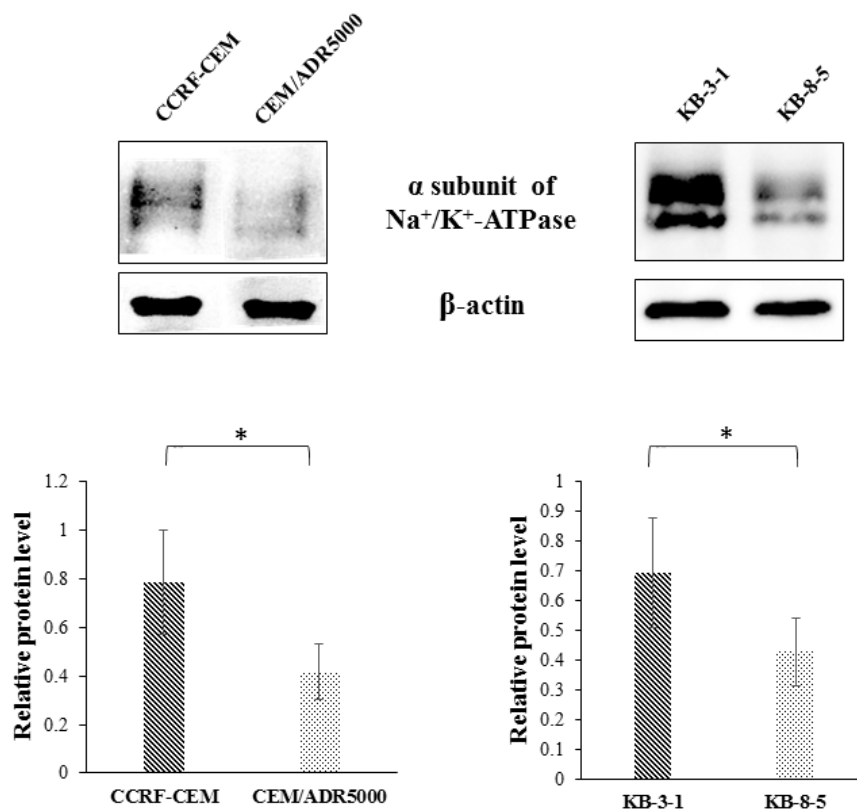


**Figure 17:** Expression of Na<sup>+</sup>/K<sup>+</sup>-ATPase  $\alpha$ -subunit in sensitive CCRF-CEM and multidrug-resistant CEM/ADR5000 cells. A. Western blot analysis of protein fractions isolated from both cell lines. Na<sup>+</sup>/K<sup>+</sup>-ATPase appeared at a molecular weight of ~100 kDa in both cell lines and the respective  $\beta$ -actin bands at ~42 kDa. B. Quantification of Na<sup>+</sup>/K<sup>+</sup>-ATPase in respect to  $\beta$ -actin (mean  $\pm$  SEM). Experiments were repeated three times. \*: p < 0.05; paired t-test.

### 3.1.7 Next generation sequencing

Using the powerful tool of whole genome next generation sequencing, profiling of gene expression by sequencing different mRNA species is now possible [139]. This technique has found various applications in molecular biology including, measurement of activity of thousand genes in parallel, detection of gene expression level between different cell lines or under different biological conditions, and investigation of cellular events and key signaling pathways [139]. Because western blot analysis revealed decreased Na<sup>+</sup>/K<sup>+</sup>-ATPase expression, we undertook an attempt to analyze the transcriptomes of both sensitive CCRF-CEM and multidrug-resistant CEM/ADR5000 cell lines with relevance to the above presented Na<sup>+</sup>/K<sup>+</sup>-ATPase signalosome (**Figure 5**). **Table 6** summarizes protein-coding RNA transcripts that are deregulated in MDR cells compared to sensitive cells. Noteworthy is the down-regulation of both  $\alpha 1$  and  $\alpha 3$  isoforms, which is consistent with western blot analysis.

**Table 6:** deregulations of protein-coding transcripts in multidrug-resistant cells. Next generation sequencing of both sensitive CCRF-CEM and CEM/ADR5000 was carried out and fold changes for each RNA transcript were calculated in CEM/ADR5000 in regards to CCRF-CEM. RNAs coding for proteins involved in the Na<sup>+</sup>/K<sup>+</sup>-ATPase signalosome are presented.

Fold change	Transcript ID	Gene name	Description
-2,470	ENST00000369496	ATP1A1	ATPase, Na <sup>+</sup> /K <sup>+</sup> transporting, alpha 1 polypeptide
-2,431	ENST00000302102	ATP1A3	ATPase, Na <sup>+</sup> /K <sup>+</sup> transporting, alpha 3 polypeptide
-1,714	ENST00000373567	SRC	SRC proto-oncogene, non-receptor tyrosine kinase
-2,214	ENST00000373558	SRC	SRC proto-oncogene, non-receptor tyrosine kinase
-2,923	ENST00000373578	SRC	SRC proto-oncogene, non-receptor tyrosine kinase
-5,000	ENST00000405348	CAV1	caveolin 1, caveolae protein, 22kDa
8,403	ENST00000339364	PIK3AP1	phosphoinositide-3-kinase adaptor protein 1
2,466	ENST00000265970	PIK3C2A	phosphatidylinositol-4-phosphate 3-kinase, catalytic subunit type 2 alpha
4,105	ENST00000424712	PIK3C2B	phosphatidylinositol-4-phosphate 3-kinase, catalytic subunit type 2 beta

---

2,019	ENST00000398870	PIK3C3	phosphatidylinositol 3-kinase, catalytic subunit type 3
1,643	ENST00000262039	PIK3C3	phosphatidylinositol 3-kinase, catalytic subunit type 3
-2,597	ENST00000263967	PIK3CA	phosphatidylinositol-4,5-bisphosphate 3-kinase, catalytic subunit alpha
2,624	ENST00000289153	PIK3CB	phosphatidylinositol-4,5-bisphosphate 3-kinase, catalytic subunit beta
2,100	ENST00000477593	PIK3CB	phosphatidylinositol-4,5-bisphosphate 3-kinase, catalytic subunit beta
-1,619	ENST00000496166	PIK3CG	phosphatidylinositol-4,5-bisphosphate 3-kinase, catalytic subunit gamma
5,265	ENST00000554848	AKT1	v-akt murine thymoma viral oncogene homolog 1
-1,923	ENST00000544168	AKT1	v-akt murine thymoma viral oncogene homolog 1
-2,567	ENST00000311278	AKT2	v-akt murine thymoma viral oncogene homolog 2
6,053	ENST00000366540	AKT3	v-akt murine thymoma viral oncogene homolog 3
2,571	ENST00000336199	AKT3	v-akt murine thymoma viral oncogene homolog 3
2,795	ENST00000357086	ITPR1	inositol 1,4,5-trisphosphate receptor, type 1
2,374	ENST00000443694	ITPR1	inositol 1,4,5-trisphosphate receptor, type 1
2,342	ENST00000456211	ITPR1	inositol 1,4,5-trisphosphate receptor, type 1
2,144	ENST00000354582	ITPR1	inositol 1,4,5-trisphosphate receptor, type 1
2,138	ENST00000302640	ITPR1	inositol 1,4,5-trisphosphate receptor, type 1
4,329	ENST00000381340	ITPR2	inositol 1,4,5-trisphosphate receptor, type 2
112,066	ENST00000413366	PRKCA	protein kinase C, alpha
-1,612	ENST00000303531	PRKCB	protein kinase C, beta
2,548	ENST00000306156	PRKCE	protein kinase C, epsilon
-1,535	ENST00000263125	PRKCQ	protein kinase C, theta
4,200	ENST00000461106	PRKCZ	protein kinase C, zeta

---

4,077	ENST00000400921	PRKCZ	protein kinase C, zeta
1,743	ENST00000601806	PRKD2	protein kinase D2
1,683	ENST00000433867	PRKD2	protein kinase D2
-2,119	ENST00000291281	PRKD2	protein kinase D2
-3,791	ENST00000595515	PRKD2	protein kinase D2
1,545	ENST00000307102	MAP2K1	mitogen-activated protein kinase kinase 1
-1,649	ENST00000395202	MAPK3	mitogen-activated protein kinase 3
-1,680	ENST00000484663	MAPK3	mitogen-activated protein kinase 3
-1,924	ENST00000322266	MAPK3	mitogen-activated protein kinase 3
-2,016	ENST00000395199	MAPK3	mitogen-activated protein kinase 3
9,258	ENST00000544786	MAPK1	mitogen-activated protein kinase 1
-1,563	ENST00000398822	MAPK1	mitogen-activated protein kinase 1
1,686	ENST00000256078	KRAS	Kirsten rat sarcoma viral oncogene homolog
1,695	ENST00000397594	HRAS	Harvey rat sarcoma viral oncogene homolog
-1,660	ENST00000417302	HRAS	Harvey rat sarcoma viral oncogene homolog
4,097	ENST00000394820	NFKB1	nuclear factor of kappa light polypeptide gene enhancer in B-cells 1
-2,072	ENST00000505458	NFKB1	nuclear factor of kappa light polypeptide gene enhancer in B-cells 1

---

### 3.1.8 Summary: Cytotoxicity of cardiotonic steroids

In the previous sections, cytotoxicity of cardiotonic steroids was analyzed in sensitive and multidrug-resistant leukemia cell lines. Results indicated that cardiotonic steroids have low resistance indices suggesting their potential in evading MDR. Structure-activity relationship was investigated revealing the effects of various chemical substitutions on the steroidal core in regards to cytotoxicity. With the hope to build a model capable of prediction of cytotoxicity of future novel cardiotonic steroids, QSAR analysis was conducted. Moderate correlations between experimental and predicted data were achieved with slightly better correlations in sensitive CCRF-CEM cells. Since  $\text{Na}^+/\text{K}^+$ -ATPase has been established as the molecular target of cardiotonic steroids throughout literature, molecular docking of our library to  $\text{Na}^+/\text{K}^+$ -ATPase was performed. Cytotoxicity data in both leukemia cells were linked with molecular docking data by means of statistical correlation analysis, which revealed lower correlations in MDR cells. This, in turn, provoked us to investigate the expression of  $\text{Na}^+/\text{K}^+$ -ATPase in sensitive and MDR cells and strikingly,  $\text{Na}^+/\text{K}^+$ -ATPase was indeed down-regulated in multidrug-resistant cells. Using the powerful tool of next generation sequencing, protein-coding RNA transcripts in both CCRF-CEM and CEM/ADR5000 were quantified and fold changes of proteins involved in the  $\text{Na}^+/\text{K}^+$ -ATPase signalosome were investigated in both cell lines. The down-regulation of  $\text{Na}^+/\text{K}^+$ -ATPase was confirmed on mRNA level and further deregulations of  $\text{Na}^+/\text{K}^+$ -ATPase signalosome were observed.

## 3.2 Cardiotoxic steroids and P-glycoprotein inhibition

After intensive analysis of cytotoxicity of cardiotoxic steroids in sensitive and multidrug-resistant leukemia cells, we were interested to screen them for P-glycoprotein inhibitory effects. Building on experiments carried out in our laboratory by [redacted] [140], we utilized the inherent fluorescence of doxorubicin – a known substrate of P-glycoprotein frequently used to identify modulators of drug resistance [141, 142] – to perform flow cytometry high throughput screening of the chemical library of cardiotoxic steroids and their derivatives. As an initial step, the expression of P-glycoprotein in both leukemia cell lines was checked by various techniques. The screen was conducted in a high throughput mode, and its outcome was validated using various methods including P-glycoprotein-ATPase assay, doxorubicin multidrug resistance reversal via resazurin reduction assay and molecular docking<sup>3</sup>.

### 3.2.1 Model system

Multidrug-resistant, P-glycoprotein overexpressing leukemia CEM/ADR5000 cells were used to conduct the screen for modulators of P-glycoprotein. Drug sensitive CCRF-CEM cells were used as control cells lacking P-glycoprotein expression. As mentioned in materials and methods, the multidrug-resistant phenotype was established by regular treatment of CEM/ADR5000 cells with doxorubicin to maintain the overexpression of P-glycoprotein. Before we conducted the high throughput screen, we checked the expression of P-glycoprotein in both cell lines and carried out uptake experiments of doxorubicin over a time course to choose the best time point for the screen.

#### 3.2.1.1 Expression of P-glycoprotein in sensitive and MDR leukemia cells

The overexpression of P-glycoprotein in CEM/ADR5000 cells has been validated by three independent methods: flow cytometry, immunoblotting and immunocytochemistry. Immunostaining with the FITC-coupled mouse anti-human P-glycoprotein antibody 17F9 displayed very high immunofluorescence signals in CEM/ADR5000 cells in flow cytometric analyses (**Figure 18 A**; solid line), indicating high P-glycoprotein expression. In contrast, both

---

<sup>3</sup> Results in this section have been published in a peer-reviewed scientific journal:

Text, figures and tables were prepared by myself and were reprinted (some with slight modifications to fit the thesis) from: M. Zeino, M. Paulsen, M. Zehl, E. Urban, B. Kopp, T. Efferth, “Identification of New P-Glycoprotein Inhibitors Derived from Cardiotoxic Steroids”, *Biochemical Pharmacology*, 93(1), 11-24, 2015. Copyright 2015 with permission from Elsevier; doi: 10.1016/j.bcp.2014; <http://www.sciencedirect.com/science/article/pii/S0006295214006273>.

stained (solid line) and non-stained parental CCRF-CEM cells (dashed line) showed similar low fluorescence signals. Immunoblotting using the monoclonal antibody C219 revealed similar results, where P-glycoprotein extracted from CEM/ADR5000 cells migrated in two intense thick bands between  $\sim 170$ - $220$  kDa (**Figure 18 B**; lane 1), whereas CCRF-CEM did not show any bands (**Figure 18 B**; lane 2). In immunocytochemistry, the membrane-bound localization of P-glycoprotein in CEM/ADR5000 cells has been observed using monoclonal antibody C219 (**Figure 18 C**; right side). The staining was intensive on the plasma membranes and occurred weakly in the cytoplasm. CCRF-CEM cells served as a negative control lacking any significant P-glycoprotein expression (**Figure 18 C**, left side).

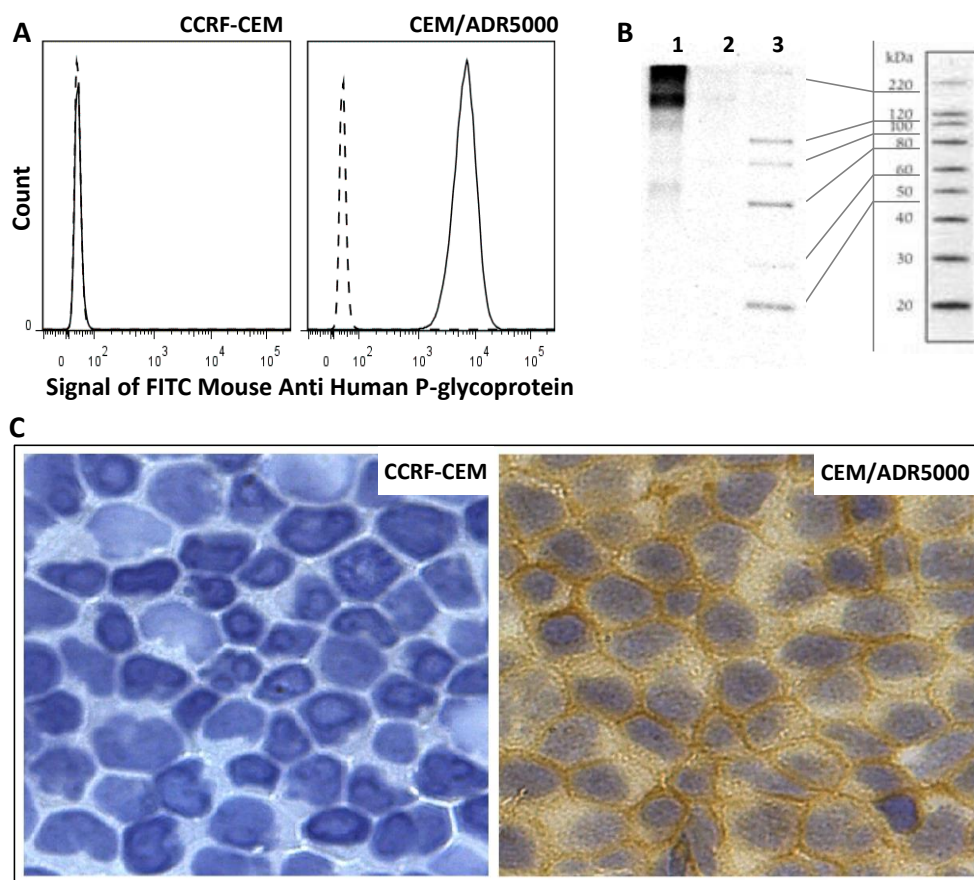


**Figure 18:** P-glycoprotein expression in CEM/ADR5000 cells in comparison to the parental sensitive cell line, CCRF-CEM. **A:** flow cytometric staining with FITC-labeled mouse anti-human P-glycoprotein antibody (clone 17F9). The unstained control is represented by dashed histograms, whereas stained by solid ones. **B:** Western blot analysis with CD243/P-glycoprotein antibody (clone C219) of proteins extracted from CEM/ADR5000 cells (lane 1) and from CCRF-CEM cells (lane 2). Lane 3 shows the molecular weight marker. **C:** Immunocytochemistry using the monoclonal antibody C219 with the aid of Ultravision Quanto Detection System HRP.

### 3.2.1.2 Uptake studies of doxorubicin over a time course

Initially, we selected a suitable time frame to perform the screening experiments. For this purpose, we conducted experiments with verapamil as positive control for the inhibition of P-glycoprotein-mediated doxorubicin efflux [143] after several incubation times on both CCRF-CEM and CEM/ADR5000 cells. **Figure 19** demonstrates the accumulation of doxorubicin in both cell lines over time with or without co-treatment of verapamil. It was clearly visible that doxorubicin piled up highly in CCRF-CEM cells, whereas its accumulation remained low in CEM/ADR5000 cells even after long incubation times up to 72 hours (**Figure 19 A**). Upon application of 20  $\mu\text{M}$  verapamil, the accumulation of doxorubicin in CEM/ADR5000 cells slightly increased after 3 h and dramatically after 24 h and remained at high levels after 48 h and 72 h (**Figure 19 B**). Therefore, 24 h was considered a suitable incubation time for carrying out the screening experiments.

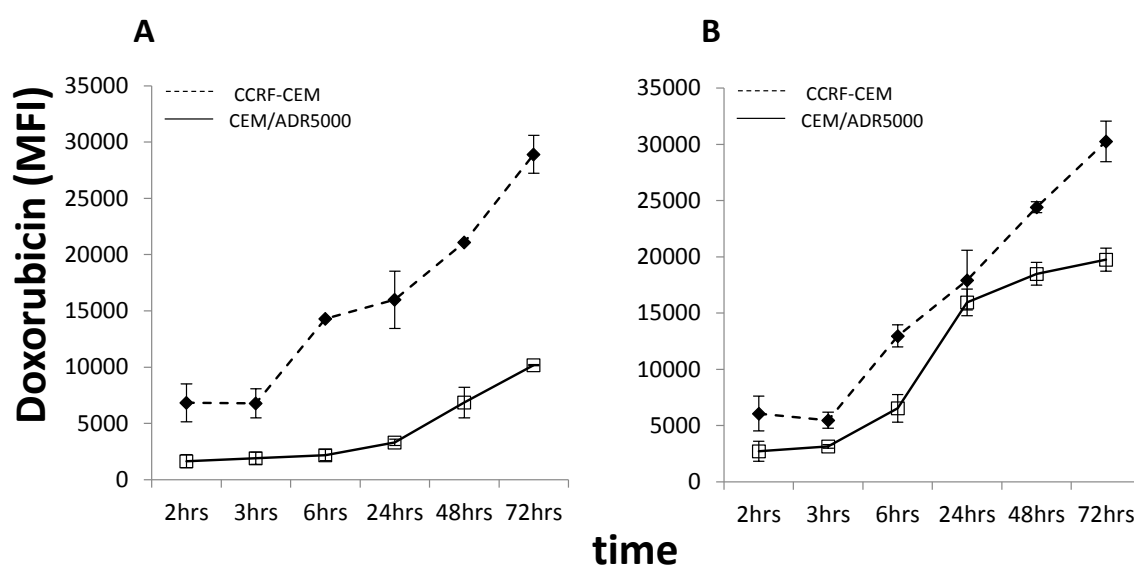


**Figure 19:** Setup experiments for high throughput screening of P-glycoprotein inhibitors. A: Time course of doxorubicin (20  $\mu\text{M}$ ) in CCRF-CEM (dashed line) and CEM/ADR5000 (solid line) after incubation for 2, 3, 6, 24, 48, and 72 hours. B: Effect of verapamil (20  $\mu\text{M}$ ) on doxorubicin (20  $\mu\text{M}$ ) uptake under the same conditions mentioned in A. Two independent experiments were carried out with 2 replicates each. Mean  $\pm$  SEM were calculated. MFI: mean fluorescence intensity.

To make sure that CEM/ADR5000 cells – with which the screen is to be carried out – were alive after treatment with doxorubicin for 24 hours, we conducted a resazurin reduction in the same conditions. As can be noticed from the dose-response curve in **Figure 20**. The percentage

of viable cells at a concentration of (20  $\mu\text{M}$ ) of doxorubicin – the concentration used later in the high throughput screen – was  $76.00 \pm 0.89 \%$ , indicating that most of the measured cells in flow cytometry were alive.

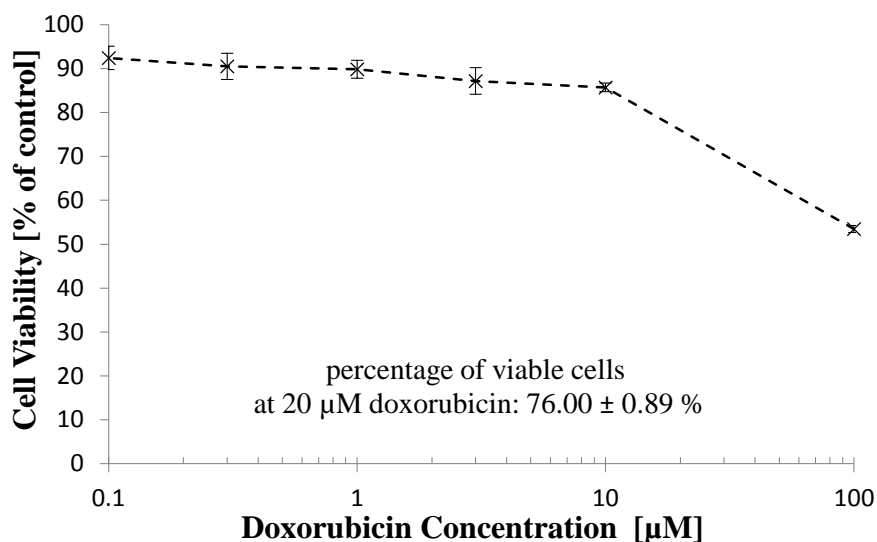


**Figure 20:** Dose-response curve of the doxorubicin's cytotoxic effect after 24 h on CEM/ADR5000 cells. The percentage of viable cells at a concentration of (20  $\mu\text{M}$ ) doxorubicin was  $76.00 \pm 0.89 \%$ . The experiment was repeated thrice, with each point representing mean  $\pm$  SEM.

### 3.2.2 High throughput screening of cardiotoxic steroids for P-glycoprotein inhibition

To save time and labor, it is of great importance to develop *in vitro* methods that can be applied in high throughput modes. Several approaches to assess the interaction with P-glycoprotein have been developed. ABC transporter activities can be determined by substrate efflux assays using either flow cytometry or fluorescence microplate readers. Both techniques can be implemented in a high throughput mode to screen large compound libraries [144]. However, microplate readers are less sensitive since they are designed for homogenous assays, where the output is a signal of the whole content of the well [144, 145]. In contrast, flow cytometry compiles individual measurements of thousands of single cells in the sample, thereby representing sample heterogeneity and enabling the exclusion of artifacts such as cell debris, dead cells and fluorescent precipitants [145]. Therefore, after the preliminary proof-of-principle experiments mentioned above, we implemented a high throughput setup for flow cytometry to identify potential cardiotoxic steroids capable of P-glycoprotein inhibition within the provided compound library tested in section 3.1.1.

### 3.2.2.1 Identification of six P-glycoprotein-inhibiting cardiotoxic steroids

Among the screened library of cardiotoxic steroids and their derivatives, six compounds caused increased doxorubicin retention in CEM/ADR5000 cells. The histograms in **Figure 21 A** show in details that co-incubation with the six cardiotoxic steroids elevated doxorubicin fluorescence compared to treatment of CEM/ADR5000 cells with doxorubicin alone, indicating higher intracellular doxorubicin accumulation due to P-glycoprotein inhibition. **Figure 21 B** depicts the fold change in doxorubicin fluorescence, if the respective compound has been added to the cells in the presence of doxorubicin. Verapamil was tested in parallel as a known inhibitor of P-glycoprotein. All test compounds have been applied in two concentrations based on their cytotoxic  $IC_{50}$  values ( $IC_{50}\times 5$  and  $IC_{50}/5$ ), which had been previously determined after 72 h incubation prior to flow cytometry (results are shown in section 3.1.1). The reason we chose these concentrations is to unify test conditions for all the compounds, since they exerted their cytotoxicity within various molar ranges. The six compounds exerted their P-glycoprotein-inhibitory effects only at the higher concentration ( $IC_{50}\times 5$ ), which are displayed in **Figure 21**.

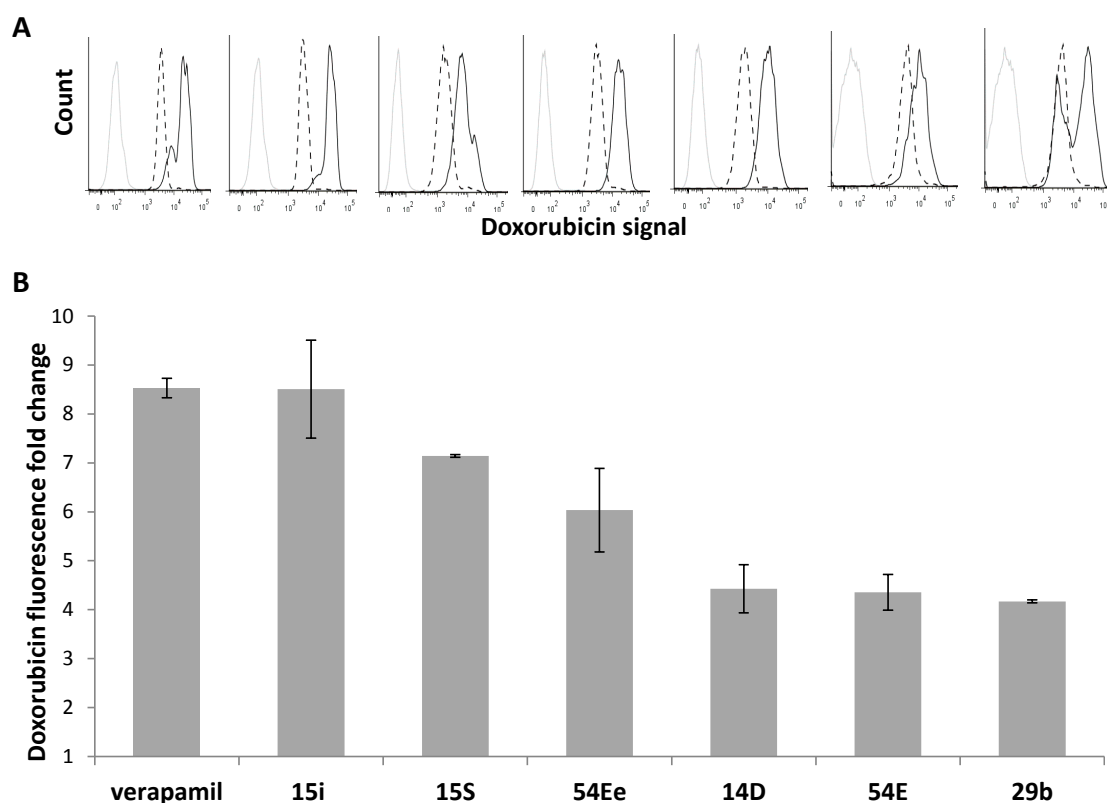


**Figure 21:** Discovery of novel inhibitors of P-glycoprotein by high throughput screening with flow cytometry. A: Histograms of the 24 hr treatment with the respective compounds ( $IC_{50}\times 5$ ) shown. For each compound, untreated cells are shown with gray histogram, doxorubicin treated cells in black dashed histogram and co-administration of

the respective modulators in black solid histogram. B: Effect of each compound ( $IC_{50} \times 5$ ) on the accumulation of doxorubicin within CEM/ADR5000 cells presented by fold change in doxorubicin fluorescence with co-administration of the respective compound compared to doxorubicin alone. Verapamil is shown on the left as a positive control for P-glycoprotein inhibition. Each bar represents: mean fold change  $\pm$  SEM for 2 independent measurements (with at least two replicates in one measurement).

### 3.2.2.2 P-glycoprotein inhibition by compound 15i at different concentrations

Interestingly, double peaks were noticed when some cardiotoxic steroids were combined with doxorubicin (e.g. 29b; **Figure 21 A**). We surmise that this effect is related to the modulator and its potency since after testing 15i – the first compound that appeared throughout the screen to inhibit the function of P-glycoprotein – at a dilution of concentrations ( $IC_{50} \times 5$ ,  $IC_{50} \times 2.5$ ,  $IC_{50}$ ,  $IC_{50}/2.5$  and  $IC_{50}/5$ ), double peaks were also observed at  $IC_{50}$  but not at  $IC_{50} \times 5$  and  $IC_{50} \times 2.5$  (**Figure 22**). This means that compound 15i is more potent than compound 29b at  $IC_{50} \times 5$ .

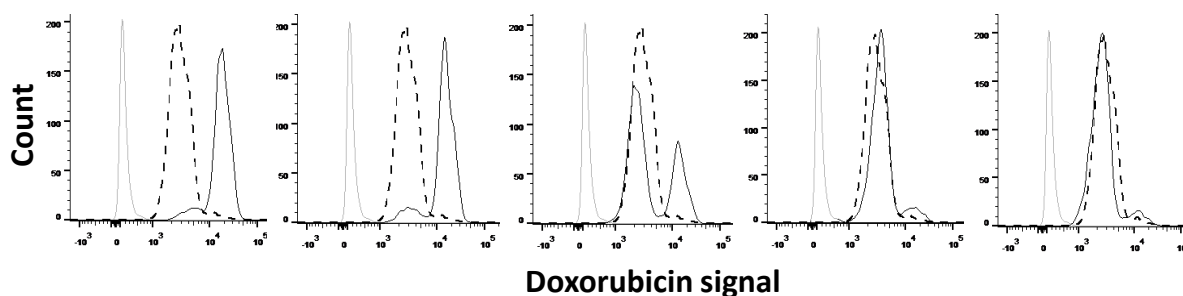


**Figure 22:** Effect of different concentrations of 15i (From left to right:  $IC_{50} \times 5$ ,  $IC_{50} \times 2.5$ ,  $IC_{50}$ ,  $IC_{50}/2.5$  and  $IC_{50}/5$ ) on doxorubicin (20  $\mu$ M) accumulation.

### 3.2.2.3 P-glycoprotein inhibition by compound 15i over a time course

We further tested compound 15i in the same manner reported earlier for verapamil. At a concentration of  $IC_{50} \times 5$ , compound 15i revealed a similar uptake profile as verapamil (**Figure 23 A**), where the dramatic increases of doxorubicin accumulation started to appear after 24 h. However, a concentration of  $IC_{50}/5$  did not alter the accumulation of doxorubicin significantly (**Figure 23 B**). This further strengthens the evidence that 15i, as a representative of this group of modulators, indeed interacts with P-glycoprotein probably in a manner close to that of verapamil.

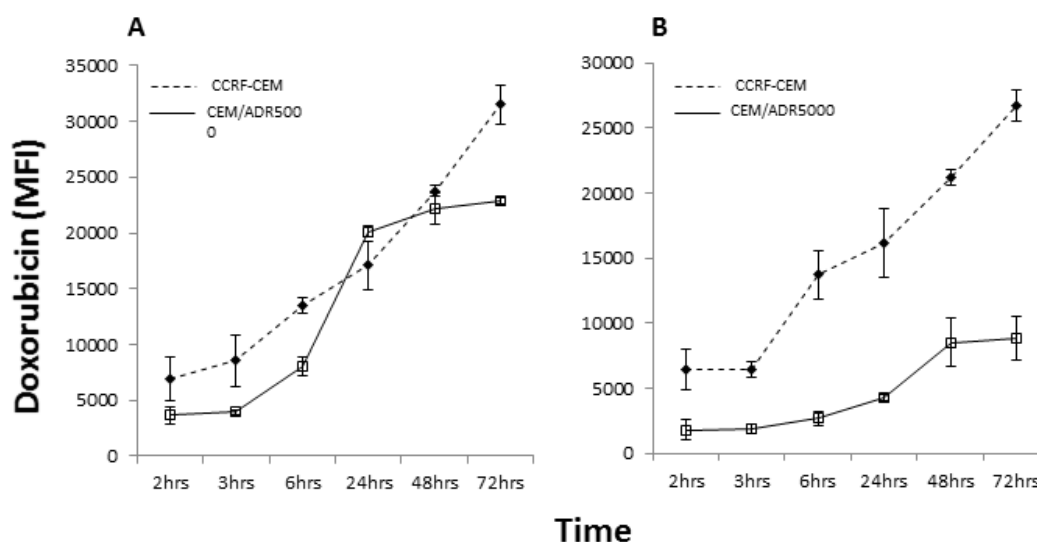


**Figure 23:** Time course of P-glycoprotein inhibitory effects of 15i on doxorubicin accumulation in CCRF-CEM (dashed line) and CEM/ADR5000 (solid line) after incubation for 2, 3, 6, 24, 48, and 72 h. A: IC<sub>50</sub>×5 B: IC<sub>50</sub>/5. MFI: mean fluorescence intensity. Experiments were repeated twice with at least two replicates in each experiment. Each point represents mean ± SEM.

### 3.2.3 Effect of six modulators on P-gp-ATPase activity

To further characterize the mode of action of the six cardiotonic steroids that increased doxorubicin accumulation in CEM/ADR5000 cells, we tested their effect on basal and verapamil-stimulated P-glycoprotein-ATPase activity in BD human P-glycoprotein expressing membranes (prepared from baculovirus infected insect cells). First, the expression of P-glycoprotein was checked in comparison to BD control membranes lacking P-glycoprotein via SDS-PAGE and immunoblotting (**Figure 24 A**). The effect of each compound on the respective activity (considered as 100%) was calculated as percentage of increase/decrease. Cyclosporine A was used as control inhibitor of P-glycoprotein-ATPase activity [146]. Compounds 15S, 14D, 54E and 54Ee induced basal P-glycoprotein-ATPase activity in a comparable manner to verapamil, whereas compounds 29b and 15i did not affect it (**Figure 24 B**). In addition to basal P-glycoprotein-ATPase activity, we also investigated verapamil-stimulated P-glycoprotein-ATPase activity. Only compound 15S clearly increased verapamil-stimulated P-glycoprotein-ATPase activity, whereas compounds 54E and 54Ee did not affect it. Compounds 15i, 29b and 14D caused a slight decrease of verapamil-stimulated P-glycoprotein-ATPase activity in a fashion similar to cyclosporine A (most pronounced in the case of 15i).

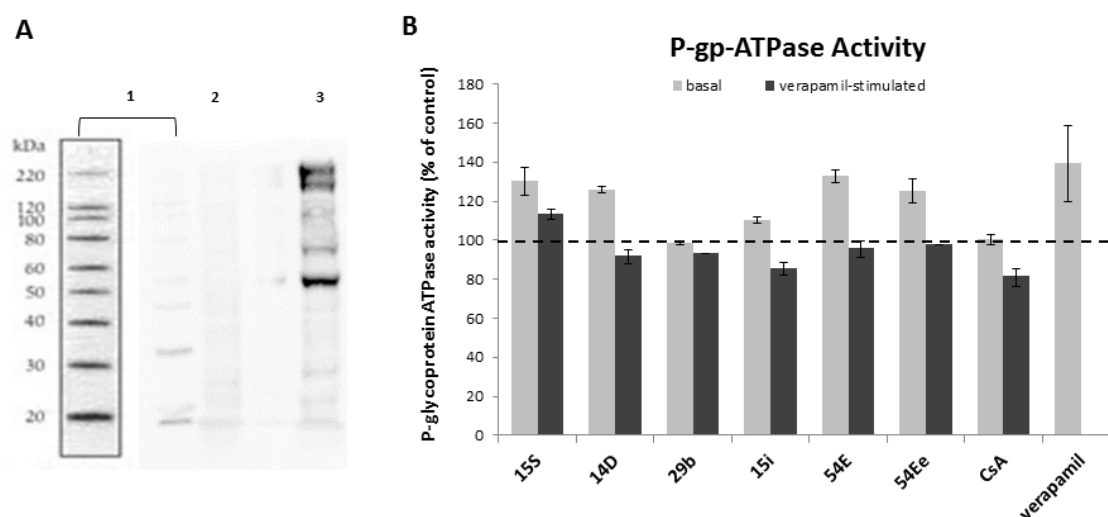


**Figure 24:** Effect of novel modulators on basal and verapamil-stimulated P-glycoprotein-ATPase activity. A: Western blot analysis with CD243/P-glycoprotein antibody (clone C219) (dilution 1:100). Lane 1 shows the molecular weight marker. Lane 2 control membrane preparation for ABC transporters (BD Biosciences). Lane 3 shows human P-glycoprotein-expressing membranes (BD Biosciences). B: Pgp-ATPase assay: Each compound was tested at (50  $\mu$ M). Verapamil was used at a concentration of (20  $\mu$ M). The percentage of modulation of P-glycoprotein-ATPase activity compared to the respective P-glycoprotein-ATPase activity without test compound was calculated for each compound (i.e. the data from the basal and verapamil-stimulated activities were set as 100% in the respective calculation for each compound). Each bar represents: mean percentage of modulation  $\pm$  SEM for two independent measurements.

### 3.2.4 Molecular docking on P-glycoprotein

We performed molecular docking to investigate the possible mode of binding of these six cardiotonic steroids at two predefined sites. The first site was the transmembrane domain (TMD), whose amino acids have been subcategorized into three drug binding sites: the H- (Hoechst 33342) site, the R-(rhodamine) site and the M-(modulator) site [116]. The second site was the nucleotide binding domain (NBD) covering amino acids responsible for the binding of ATP [113]. Calculations were run for doxorubicin as a control ligand binding to P-glycoprotein. **Tables 7 and 8** summarize the results for each compound providing information about the lowest binding energy cluster and, if different from that, the binding energy of the cluster with the highest number of conformations. The number of conformations in each of the previously mentioned clusters, the total number of interacting amino acids, the amino acids involved in hydrogen bonds and the distribution of the interacting amino acids at the respective sites are also displayed.

**Table 7:** Molecular docking of six P-glycoprotein-inhibiting cardiotonic steroids on homology-modeled human P-glycoprotein in the transmembrane domain. Stars indicate shared amino acids between the respective sites. AA: amino acids.

compound	binding energy (kcal/mol)	number of conformations in clusters	number of interacting AA	AA involved in H-bond	number of interacting AA in:		
					M-site	R-site	H-site
doxorubicin	-8.06	68	9	Gln132, Gln195, Gln347	-	1*	9*
14D	-10.16	40	11	Tyr 117	8*	1*	-
	-8.14	52	12	Thr837	2*	5*	-
15S	-10.29	64	10	-	6*	1*	-
	-8.43	99	10	Gln132, Cys137	-	1*	10*
15i	-9.94	65	10	-	6*	1*	-
29b	-8.94	2	14	Lys234	2	2	-
	-8.81	74	9	-	5*	1*	-
54E	-9.46	6	12	Ala342	2	1	-
	-9.10	96	10	-	6*	1*	-
54Ee	-10.26	1	11	Ala342	1	1	-
	-8.50	37	11	-	7*	1*	-

**Table 8:** Molecular docking of six P-glycoprotein-inhibiting cardiotoxic steroids on homology-modeled human P-glycoprotein at the nucleotide binding domain. AA: amino acids.

compound	binding energy (kcal/mol)	number of conformations in clusters	number of interacting AA	AA involved in H-bond	number of interacting AA in:
					NBD
doxorubicin	-8.68	1	14	Asn639, Ala640, Gly1073	7
	-7.54	18	13	Ala1275, His1232	1
14D	-9.77	1	10	Leu662, Gly1073, Gln1081	4
	-6.73	60	10	Ala640, Arg664	2
15S	-8.81	5	11	Lys665	-
	-7.78	25	9	Arg670, Arg659, Met628	1
15i	-9.52	4	13	Lys665, Arg673	-
	-7.18	40	9	Arg659, Gln1175	3
29b	-10.12	126	11	Ile663, Arg666, Arg669	-
54E	-9.99	103	10	Ile663, Arg666, Arg669	-
54Ee	-9.48	18	12	Ile663	1
	-6.40	40	10	Arg905	1

**Figure 25** demonstrates the binding modes of each cardiotoxic steroid within the lowest binding energy cluster with the respective interacting amino acids involved in hydrophobic interactions and hydrogen bonds at both regions. Binding modes of doxorubicin are also shown with its interacting amino acids respectively at both sites.

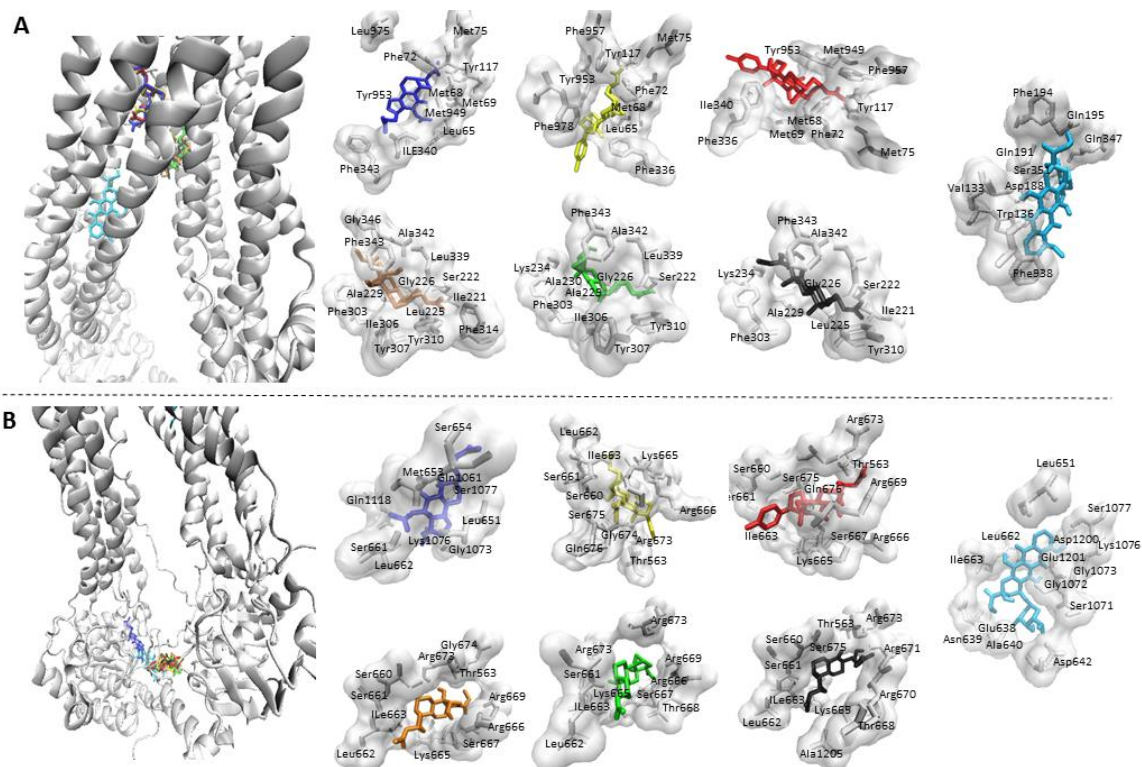


**Figure 25:** Molecular docking of the promising six P-glycoprotein inhibiting cardiotoxic steroids. A: at the transmembrane region. B: at the nucleotide binding domain (NBD). On the left, the backbone of P-glycoprotein at both regions is represented in new cartoon style in white. Cardiotoxic steroids are depicted in licorice in different colors: 14D: blue, 15i: yellow, 15S: red, 29b: orange, 54E: green and 54Ee: black. Doxorubicin (cyan) was docked as control drug. For each compound, the corresponding interacting amino acids are shown in licorice and in surface mode in white.

We used statistical analysis to differentiate between binding of the six ligands at the transmembrane region and at the cytoplasmic nucleotide domain. Using unpaired two tailed *t*-test, a significant difference ( $p$ -value < 0.05) between the affinities at both sites was observed only, if the binding mode with the highest number of conformations was considered – a characteristic claimed to be more trustworthy than looking only at the lowest binding energies [36]. The respective lower mean of binding energies (-8.60 kcal/mol) at TMD in comparison to NBD (-7.10 kcal/mol) may indicate a higher affinity exquisitely if binding within the transmembrane cavity takes place. In a similar manner, doxorubicin bound with higher affinities within TMD (-8.06 kcal/mol) than within NBD (-7.54 kcal/mol), when considering the cluster with the highest number of conformations.

### 3.2.5 MDR reversal in MDR cells

#### *Combination of doxorubicin with cardiotonic steroids in CEM/ADR5000 cells*

We carried out resazurin cell viability assays in P-glycoprotein overexpressing CEM/ADR5000 cells to assess the outcome of doxorubicin combination with the six P-glycoprotein modulating cardiotonic steroids and their ability to reverse multidrug resistance. We tested doxorubicin alone and in combination with verapamil as a control inhibitor of P-glycoprotein, followed by testing each cardiotonic steroid. Dose response curves demonstrating the respective combinations are represented in **Figure 26**. A higher cytotoxicity upon co-treatment with each modulator can be clearly noticed by an overall shift of the curve to the left.

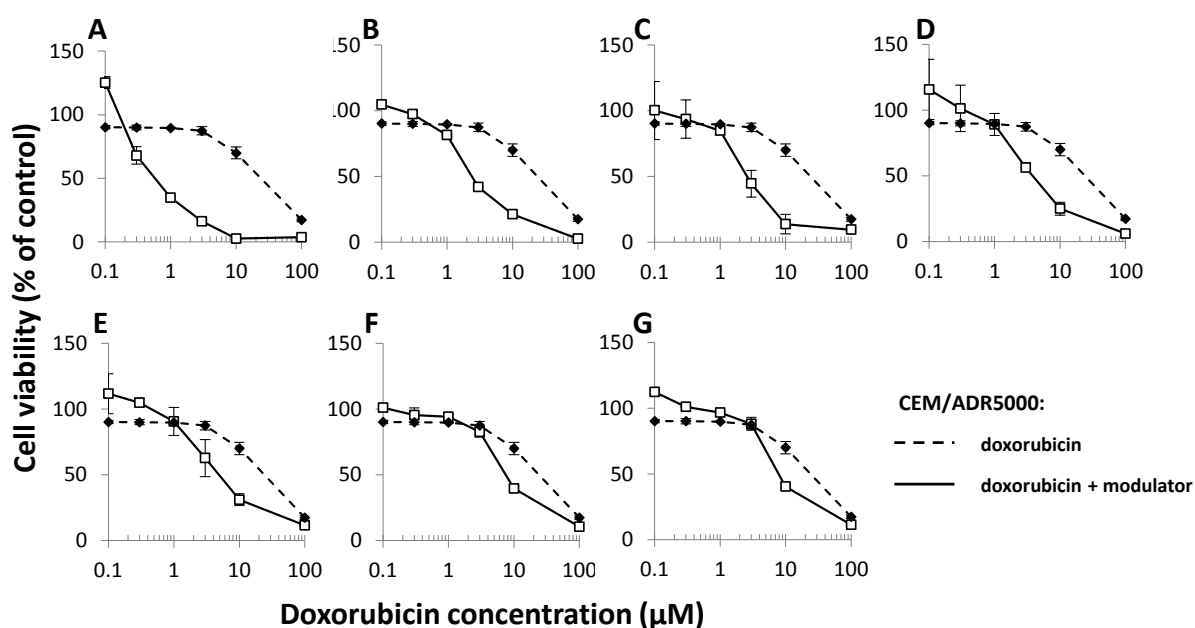


**Figure 26:** Effect of six cardiotonic steroids on the cytotoxicity of doxorubicin in P-glycoprotein overexpressing CEM-ADR5000 cells. A: Verapamil (20  $\mu\text{M}$ ), B: 15S, C: 54Ee, D: 14D, E: 15i, F: 54E and G: 29b. Each compound was tested at a single concentration ( $\text{IC}_{50}$ ) in combination with doxorubicin (0.1 to 100  $\mu\text{M}$ ). Experiments have been repeated at least twice and for each concentration at least in triplicates. Each point represents mean  $\pm$  SEM.

The  $\text{IC}_{50}$  values are shown in **Table 9**. Then, the degree of resistance reversal for each modulator was calculated by dividing the  $\text{IC}_{50}$  value of doxorubicin alone by the  $\text{IC}_{50}$  value of the respective combination. The combinations of doxorubicin with the six test compounds resulted in 3.06- to 10.03-fold reduced  $\text{IC}_{50}$  values compared to doxorubicin alone. The control drug, verapamil, accounted for the highest effect (42.74-fold decrease).

**Table 9:** Resazurin assay-derived IC<sub>50</sub> values of combination treatments of doxorubicin with verapamil and six P-glycoprotein inhibiting cardiotonic steroid derivatives and the respective calculated degree of resistance reversal in CEM/ADR5000 cells.

modulator	IC <sub>50</sub> combination with doxorubicin (Mean ± SEM μM)	Fold change in IC <sub>50</sub> (degree of resistance reversal)
-	24.07 ± 3.82	-
verapamil	0.56 ± 0.057	42.73
15S	2.40 ± 0.01	10.03
54Ee	2.82 ± 0.74	8.54
14D	3.76 ± 0.28	6.40
15i	4.27 ± 1.42	5.64
54E	7.46 ± 0.004	3.23
29b	7.87 ± 0.25	3.06

*Combination of doxorubicin with cardiotonic steroids in CCRF-CEM cells*

Same assays were conducted in drug sensitive CCRF-CEM cells as negative controls for the expression of P-glycoprotein. The corresponding dose-response curves are shown in **Figure 27**.

The effects of combining doxorubicin with the respective modulators in comparison to doxorubicin alone on cell viability were calculated as previously explained in CEM/ADR5000 cells and are shown in **Table 10**.

Compared to doxorubicin alone, verapamil and the six compounds caused only minor changes in the IC<sub>50</sub> values when each was combined with doxorubicin in CCRF-CEM cells (fold changes ranging between 0.86 and 1.59). This strengthens the evidence that the reversal of multidrug resistance observed in CEM/ADR5000 is related to P-glycoprotein.

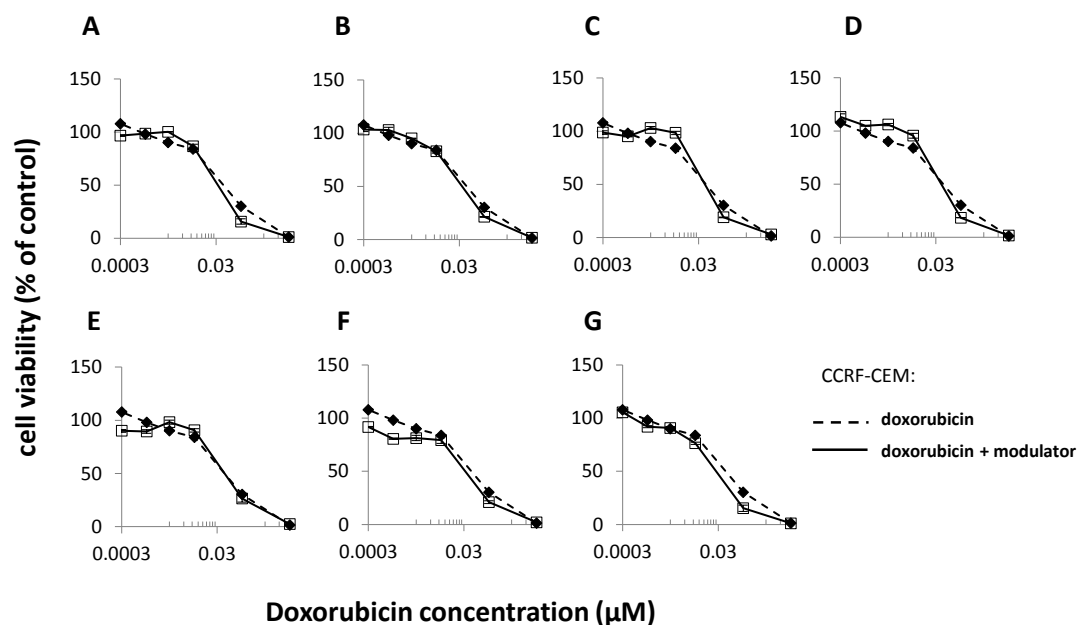


**Figure 27:** Effect of six cardiotoxic steroids on the cytotoxicity of doxorubicin in drug sensitive CCRF-CEM cells. A: Verapamil (20  $\mu\text{M}$ ), B: 15S, C: 54Ee, D: 14D, E: 15i, F: 54E and G: 29b. Each compound was tested at a single concentration ( $\text{IC}_{50}$ ) in combination with doxorubicin (0.0003 to 1  $\mu\text{M}$ ). Experiments have been repeated at least twice and for each concentration at least in triplicates. Each point represents mean  $\pm$  SEM.

**Table 10:** Resazurin assay-derived  $\text{IC}_{50}$  values of combination treatments of doxorubicin with verapamil and six P-glycoprotein inhibiting cardiotoxic steroid derivatives and the respective fold change in  $\text{IC}_{50}$  values compared to treatment of doxorubicin alone in CCRF-CEM cells.

modulator	$\text{IC}_{50}$ combination with doxorubicin (Mean $\pm$ SEM $\mu\text{M}$ )	Fold change in $\text{IC}_{50}$
-	0.043 $\pm$ 0.001	-
verapamil	0.035 $\pm$ 0.010	1.24
15S	0.034 $\pm$ 0.005	1.46
54Ee	0.041 $\pm$ 0.002	1.06
14D	0.038 $\pm$ 0.004	1.11
15i	0.050 $\pm$ 0.007	0.86
54E	0.032 $\pm$ 0.004	1.33
29b	0.027 $\pm$ 0.002	1.59

### 3.2.6 Summary: Cardiotonic steroids and P-glycoprotein inhibition

In the previous sections, we described a step-by-step workflow to identify potential inhibitors of P-glycoprotein. We set off with the establishment of the model system (sensitive CCRF-CEM and multidrug-resistant CEM/ADR5000 cells) by the evaluation of P-glycoprotein via three different methods (flow cytometry, western blot and immunocytochemistry). All techniques revealed overexpression of P-glycoprotein in CEM/ADR5000. Then, doxorubicin uptake was measured in both cell lines by means of flow cytometry taking advantage of the inherent fluorescence of the drug. Due to the overexpression of P-glycoprotein in CEM/ADR5000 cells, they exposed lower accumulation of doxorubicin when compared to CCRF-CEM cells. Subsequently, the chemical library of cardiotonic steroids was screened with flow cytometry in high throughput mode. Six cardiotonic steroids were capable of P-glycoprotein inhibition in a similar manner to verapamil. The interaction of these compounds with P-glycoprotein was further investigated via P-glycoprotein-ATPase assay and molecular docking. The six compounds had several effects on basal and drug-stimulated P-glycoprotein-ATPase activity causing either inhibition or induction. These effects along with analysis of binding modes by means of molecular docking characterize the interaction of these compounds with P-glycoprotein, which is fully discussed in section 4.2.2. Finally, the outcome of combining each of these six cardiotonic steroids with doxorubicin was assessed in both sensitive and multidrug-resistant cells. All compounds were able to significantly increase sensitivity of CEM/ADR5000 – but not CCRF-CEM – cells toward doxorubicin indicating inhibition of P-glycoprotein-mediated efflux of doxorubicin.

### 3.3 Utilization of molecular docking in P-glycoprotein research

Since *in silico* techniques have been playing an important role in drug development as previously discussed, we have assessed the usability of molecular docking in the field of P-glycoprotein research. P-glycoprotein poses a major challenge in molecular docking due to various factors mentioned in section 1.8. Therefore, we first attempted to differentiate between various groups of molecules interacting with P-glycoprotein. In order to do that, we assigned a set of compounds to three groups (substrates, modulators and non-substrates; presented in paragraph 6.8.2.1) and carried out molecular docking on both a crystal structure of mouse P-glycoprotein and on homology-modelled human P-glycoprotein derived from the same mouse crystal structure to cover most of the published data throughout literature. Binding energies and number of conformations in clusters were calculated and recorded to perform statistical analysis to see if there are significant differences between the various groups. We further evaluated the ability of molecular docking to predict the binding site of a ligand by analyzing interactions at the rhodamine (R)-site, Hoechst33342 (H)-site and Modulator (M)-site predefined by Ferreira *et al.* [116] as well as at the mapped nucleotide binding domain (NBD) [113] and the human monoclonal MRK16 epitope [119]<sup>4</sup>.

#### 3.3.1 Molecular docking

All docking results on human and mouse P-glycoprotein are respectively presented in **Tables 11 and 12** containing binding energies for each compound at the cluster with the lowest binding energy and that with the highest number of conformations in case different than the former one. Respective number of conformations at each cluster, number of interacting amino acids forming hydrophobic interactions and hydrogen bonds, names of amino acids involved in hydrogen bridges and the number of interacting amino acids found in each of the predefined sites are as well listed for each compound.

---

<sup>4</sup> Results in this section have been published in a peer-reviewed scientific journal:

Figures, texts and tables and paragraphs were ultimately prepared and written by myself and reprinted with kind permission from Springer Science + Business Media:

M. Zeino, M. E. M. Saeed, O. Kadioglu, T. Efferth, “The ability of molecular docking to unravel the controversy and challenges related to P-glycoprotein—a well-known, yet poorly understood drug transporter.”, *investigational new drugs*, 1-8, 2014; doi: 10.1007/s10637-014-0098-1; <http://link.springer.com/article/10.1007%2Fs10637-014-0098-1>

**Table 11:** Molecular docking results on human P-glycoprotein for substrates, modulators and non-substrates. For each ligand the lowest binding energy as well as the binding energy of the cluster with the highest number of conformations (in case different from the lowest binding energy one) is shown. Number of interacting amino acids, amino acids involved in hydrogen bonding, number of conformations in clusters and the distribution of the amino acids in the different sites have been shown. A star indicates a shared amino acid between the respective sites defined by Ferreira *et al.* [116].

compound	number of conformations in clusters	binding energy	AA involved in H-bond	number of interacting AA	number of interacting AA in:				
					M-site	R-site	H-site	NBD	MRK16 epitope
colchicin	14	-6.10	-	7	-	-	1	-	-
duanorubicin	1	-6.55	Glu875	10	-	2*	6*	-	-
	6	-4.62	Gly984	4	-	-	-	-	-
dexamethazone	1	-6.53	Gly674, Ser667	8	-	-	-	-	-
	7	-6.27	Ser931	7	-	-	5	-	-
digoxin	1	-6.21	-	8	1	6	-	-	-
	2	-5.19	Lys25	7	-	-	-	-	-
docetaxel	1	-3.80	-	6	-	-	-	-	-
doxorubicin	3	-5.22	Asp188	5	-	-	5	-	-
etoposide	6	-6.20	-	7	-	-	4	-	-
	9	-5.90	-	8	-	-	-	-	-
fexofenadine	2	-7.09	-	10	-	-	-	-	-
Hoechst 33342	14	-7.84	-	6	-	-	5	-	-
	23	-7.45	-	6	-	-	5	-	-
irinotecan	1	-8.61	-	9	1	3	-	-	-
	5	-	-	8	3**	2**	-	-	-
kaempferol	27	-5.90	Ser222	8	2	1	-	-	-
loperamide	2	-6.77	Ile306	8	2	2	-	-	-
	5	-5.85	-	7	2	3	-	-	-
mitomycin	1	-5.00	Glu636	7	-	-	-	1	-
	4	-4.13	Arg664	5	-	-	-	-	-
ondansetron	11	-7.12	Ser222	8	2	1	-	-	-
	24	-6.90	Tyr310	7	1	-	-	-	-
paclitaxel	1	-4.02	Thr199	7	-	-	-	-	-
procyanidin B2	1	-4.39	Ala987, Gln838, Ser993	8	-	-	-	-	-
	2	-4.21	-	-	-	-	-	-	-
rhodamine 123	2	-6.16	Tyr953	10	2	-	-	-	-
	8	-5.16	-	8	-	-	-	-	-
tenoposide	7	-6.62	-	9	-	-	-	-	-
topotecan	3	-6.08	-	8	1	1*	1*	-	-
	8	-5.25	-	6	-	-	-	-	-
vinblastine	3	-5.63	-	13	6**	5**	-	-	-
vincristine	1	-4.86	-	8	-	-	-	-	-
vinorelbine	4	-3.20	-	6	-	-	-	-	-
	3	-5.43	-	5	3	2	-	-	-

	4	-5.27	-	5	3	2	-	-	-
agosterol A	2	-5.95	Leu219	8	-	-	-	-	-
	3	-5.13	-	8	-	-	-	-	-
amiodarone	1	-7.02	-	9	-	-	-	2	-
	2	-6.02	Asn183	6	-	-	6	-	-
amorinin	1	-7.39	-	5	-	-	2	-	-
	3	-7.27	-	6	1	1	-	-	-
apigenin	11	-6.13	-	8	-	-	-	2	-
	31	-6.09	Ser222	6	1	1	-	-	-
biochanin A	4	-6.53	Arg670	9	-	-	-	1	-
	18	-5.56	-	5	-	-	-	-	-
biricodar	1	-7.44	-	11	2	3***	3***	-	-
	2	-6.15	-	5	-	-	5	-	-
catechin	6	-5.6	-	8	2	-	-	-	-
	13	-5.45	Ser222	7	1	1	-	-	-
cefoperazone	1	-6.24	Lys290	5	-	4	-	-	-
	2	-5.37	-	9	-	-	-	-	-
chrysin	12	-6.68	Lys665	12	-	-	-	3	-
	19	-6.18	Ala342	18	2	3*	1*	-	-
cyclosporine	1	-6.75	Lys 48 (2H)	11	-	-	-	-	-
	2	-6.21	-	10	1*	1*	-	-	-
diltiazem	3	-6.45	-	7	-	-	7	-	-
	4	-5.53	Ser1072(2H)	6	-	-	-	2	-
ginsenoside	1	-11.51	-	11	1	4*	1*	-	-
	4	-9.24	-	7	-	-	-	-	-
naringenin	12	-6.36	Arg609, Arg670, Lys665	7	-	-	-	2	-
	22	-6.18	Ser222	4	1	1	-	-	-
phloretin	1	-5.23	Gln1081	7	-	-	-	-	-
	5	-5.05	Ser222	7	1	-	-	-	-
quercetin	24	-6.04	Phe303, Ala342, Ser222	7	1	1	-	-	-
quinine	14	-6.91	-	9	2	1	-	-	-
rotenone	11	-7.27	-	6	1	3	-	-	-
	14	-7.01	-	7	-	2*	1*	-	-
sakuranetin	29	-6.70	Ser222	4	1	1	-	-	-
sesamin	5	-7.13	Gln118	6	-	-	-	2	-
	30	-6.94	-	6	-	-	1	-	-
sinensetin	9	-6.57	Ser222	7	1	1	-	-	-
stigmasterol	3	-8.78	-	6	-	-	-	-	-
	18	-8.15	-	6	-	-	-	-	-
syringaresinol	9	-5.54	Phe938, Val133, Cys137	7	-	-	2	-	-
tamoxifen	7	-5.5	-	8	6	-	-	-	-
tariquidar	2	-8.62	-	10	6	-	-	-	-
valsopodar	1	-8.32	-	13	1	2*	1*	-	-
	5	-6.38	-	6	-	-	-	-	-

verapamil	1	-4,76	-	9	8*	1*	-	-	-
	3	-4,34	-	9	-	2**	8**	-	-
5-fluorouracil	7	-3,66	Ser675, Ser661	4	-	-	-	-	-
	8	-3,44	-	6	-	-	-	-	-
6-mercaptopurine	4	-3,97	Pro447	6	-	-	-	1	-
	21	-3,76	Ser222	5	-	-	-	-	-
carmustine	3	-4,2	Ser222	3	-	-	-	-	-
	14	-4,1	His145, Ser931	6	-	-	-	-	-
chlorambucil	3	-5,64	-	5	-	4	-	-	-
	5	-4,45	-	6	-	-	6	-	-
cyclophosphamide	4	-4,52	-	7	4	-	-	-	-
	9	-3,78	Ser931	6	-	-	-	-	-
cytarabine	2	-3,4	Ser661	8	-	-	-	-	-
	4	-1,7	Glu184	3	-	-	3	-	-
decarbazine	1	-3,92	Asn639	2	-	-	-	-	-
	4	-3,89	Ser661	5	-	-	-	-	-
hydroxyurea			-						
lomustine	9	-5,37	-	6	-	-	-	-	-
	23	-5,11	-	8	1	1	-	-	-
melphalan	1	-4,4	Lys234	9	1	2*	1*	-	-
	3	-3,31	-	5	-	-	3	-	-
pentostatin	1	-4,3	Leu662	7	-	-	-	2	-
	9	-3,69	-	5	2	1	-	-	-
procarbazine	10	-5,38	-	8	2	2	-	-	-
	11	-4,91	-	8	-	1	-	-	-
temozolomide	6	-4,89	Gln537	7	-	-	-	-	-
	19	-4,7	Ser931, Glu889	7	-	-	-	-	-
	12	-4,7	-	6	-	-	-	5	-
thioguanine	47	-3,87	-	3	-	-	-	-	1
treosulfan	2	-3,7	-	5	2	2	-	-	-
	6	-2,6	-	3	-	1	-	-	-

**Table 12:** Molecular docking results on mouse P-glycoprotein for substrates, modulators and non-substrates. For each ligand the lowest binding energy as well as the binding energy of the cluster with the highest number of conformations (in case different from the lowest binding energy one) is shown. Number of interacting amino acids, amino acids involved in hydrogen bonding, number of conformations in clusters and the distribution of the amino acids in the different sites have been shown. A star indicates a shared amino acid between the respective sites defined by Ferreira *et al.* [116].

compound	number of conformations in clusters	binding energy	AA involved in H-bond	number of interacting AA	number of interacting AA in:			
					M-site	R-site	H-site	NBD
colchicin	2	-6.20	-	6	2	1	-	-
	12	-5.06	-	3	-	-	-	-
duanorubicin	5	-5.31	Ser 989	7	2*	2*	-	-
dexamethazone	6	-7.03	-	7	2	1	-	-
digoxin	2	-8.06	Gly296	11	2	3	-	-
docetaxel	1	-4.38	-	7	6**	2**	-	-
doxorubicin	1	-5.06	-	6	-	-	-	-
	3	-5.00	-	7	2*	2*	-	-
etoposide	18	-6.82	-	9	1	2*	1*	-
fexofenadine	1	-6.72	-	8	-	-	8	-
Hoechst 33342	2	-5.61	-	8	1	1	-	-
	3	-7.83	-	11	7*	4*	-	-
irinotecan	12	-6.97	-	9	1	2	-	-
	3	-8.94	-	9	2	3	-	-
kaempferol	10	-8.90	-	10	7**	4****	2**	-
	1	-5.60	-	6	6*	1*	-	-
loperamide	3	-5.36	-	7	7*	1*	-	-
	3	-6.9	-	7	2	3	-	-
mitomycin	5	-6.29	-	8	-	1*	1*	-
	1	-5.00	Glu636	7	-	-	-	1
ondansetron	4	-4.13	Arg664	5	-	-	-	-
	9	-7.15	-	9	2	2	-	-
paclitaxel	35	-6.9	-	7	1	1	-	-
	1	-5.84	Tyr303	11	8**	3**	-	-
procyanidin B2	2	-3.29	Phe299	6	-	-	-	-
	1	-4.83	-	8	-	-	-	-
rhodamine 123	3	-4.32	-	6	-	-	-	2
	2	-6.78	-	11	2	1	-	-
tenoposide	5	-5.72	Phe990	8	7	-	-	-
	4	-6.95	-	9	1	3**	2**	-
topotecan	4	-6.46	-	8	1	1*	1*	-
	9	-6.2	-	6	-	-	-	-
vinblastine	3	-4.85	-	10	2	1	-	-
vincristine	1	-4.76	-	5	-	-	-	-
vinorelbine	2	-3.56	Tyr1083, Asp801	8	-	-	-	-
	2	-5.15	Asn838	8	-	-	-	-

	4	-3.88		9	1	-	-	-
agosterol A	1	-5.92	-	10	1	2	-	-
	3	-5.41	Tyr949	9	6	1	-	-
amiodarone	2	-6.00	-	11	-	1*	1*	-
amorinin	18	-8.09	-	4	1	1	-	-
apigenin	5	-6.16	Gln721	7	7**	2**	-	-
	19	-5.29	-	8	2	1	-	-
biochanin A	28	-5.90	Ser218	7	2	1	-	-
biricodar	2	-7.56	-	7	1	-	-	-
catechin	4	-6.09	Tyr306, Leu971	8	7*	1*	-	-
	16	-5.23	-	7	1	2	-	-
cefoperazone	1	-5.49	-	7	-	1*	1*	-
chrysin	10	-6.58	-	5	6*	1*	-	-
	14	-5.62	-	6	1	1	-	-
diltiazem	1	-5.80	-	9	-	-	-	-
	2	-5.80	-	6	-	-	-	-
ginsenoside	11	-11.26	-	7	-	2	-	-
naringenin	2	-6.21	Tyr303	8	8**	2**	-	-
	19	-5.81	-	6	1	1	-	-
phloretin	1	-4.98	-	8	-	-	-	-
	10	-4.92	-	9	2	-	-	-
quercetin	3	-5.62	Tyr303	7	7*	1*	-	-
	20	-5.08	Phe299	8	-	2	-	-
quinine	14	-6.67	-	6	1	1	-	-
rotenone	22	-8.07	Ser975	9	9**	2**	-	-
	23	-7.30	-	7	1	-	-	-
sakuranetin	6	-6.76	-	8	8**	2**	-	-
	27	-5.86	-	6	-	-	-	-
sesamin	43	-7.18	-	9	2	2	-	-
sinensetin	13	-6.08	-	9	2	2	-	-
	14	-5.83	-	6	1			
stigmasterol	16	-8.99	-	6	1	1	-	-
syringaresinol	4	-5.52	-	6	1	1	-	-
tamoxifen	5	-6.59	-	7	1	1	-	-
	6	-4.65	-	7	2*	5*	-	-
tariquidar	1	-8.69	-	9	7	1	-	-
	2	-7.93	-	10	-	2*	1*	-
valsopodar	8	-7.74	-	12	-	1*	2*	-
verapamil	1	-5.26	-	11	2	1	-	-
5-fluorouracil	4	-3.89	-	6	-	-	-	-
	14	-3.34	-	4	-	2*	1*	-
6-mercaptopurine	5	-4.19	-	6	-	-	-	-
	9	-4.18	Ser725	4	-	-	-	4
carmustine	4	-4.32	-	7	7*	1*	-	-
	21	-4.04	-	5	5	-	-	-
chlorambucil	6	-5.52	Lys882	8	-	3	-	-
	7	-4.23	-	6	2	1	-	-

cyclophosphamide	7	-4.38	Gln795	7	-	-	-	-
	9	-2.97	-	6	-	-	-	-
cytarabine	6	-3.21	-	7	1	1	-	-
	7	-2.71	Gln795, Ser798	4	-	-	-	-
decarbazine	2	-3.64	-	5	-	-	-	-
	5	-2.97	-	5	1	-	-	-
Hydroxyurea			-					
			-					
lomustine	52	-5.76	-	4	1	1	-	-
melphalan	3	-3.39	-	5	-	-	-	-
pentostatin	2	-4.10	-	8	-	-	-	2
	10	-3.98	-	7	7	-	-	-
procarbazine	2	-5.71	-	7	6*	1*	-	-
	21	-5.2	-	8	1	1	-	-
temozolomide	1	-4.80	Glu1115	8	-	-	-	2
	19	-4.56	-	3	1	1	-	-
thioguanine	49	-4.02	Gln1219	2	-	-	-	-
treosulfan	1	-3.88	-	6	6	-	-	-
	5	-2.64	-	3	1	1	-	-

The means of lowest binding energies for substrates were -6.21 and -6.01 kcal/mol for human and mouse P-glycoprotein respectively – slightly higher than those of the modulators (-6.77 kcal/mol for human and -6.81 kcal/mol for mouse). Non-substrates notably received higher binding energies (-4.30 kcal/mol for human and -4.35 kcal/mol for mouse) (**Table 13**).

**Table 13:** Sample description and mean values of the lowest binding energies obtained by dockings on mouse and human P-glycoprotein.

sample	sample size (N)	mean (lowest binding energies)	
		Human (kcal/mol)	Mouse (kcal/mol)
substrates	22	-6.21	-6.01
modulators	27	-6.77	-6.81
non-substrates	15	-4.30	-4.35

In **Figure 28**, we have further displayed the results for interactions at three different sites on human P-glycoprotein: binding of a modulator to the M-site (verapamil), binding of substrate to the H-site (Hoechst 33342) and binding of a modulator to the nucleotide binding domain (apigenin). Both verapamil (8 amino acids out of all 9 interacting amino acids) and Hoechst 33342 (five amino acids out of all six interacting amino acids) were buried within the M- and H-site, respectively, in the transmembrane region, whereas in the case of apigenin, only two

amino acids out of total 8 interacting amino acids belonged to those involved in the interaction with ATP.

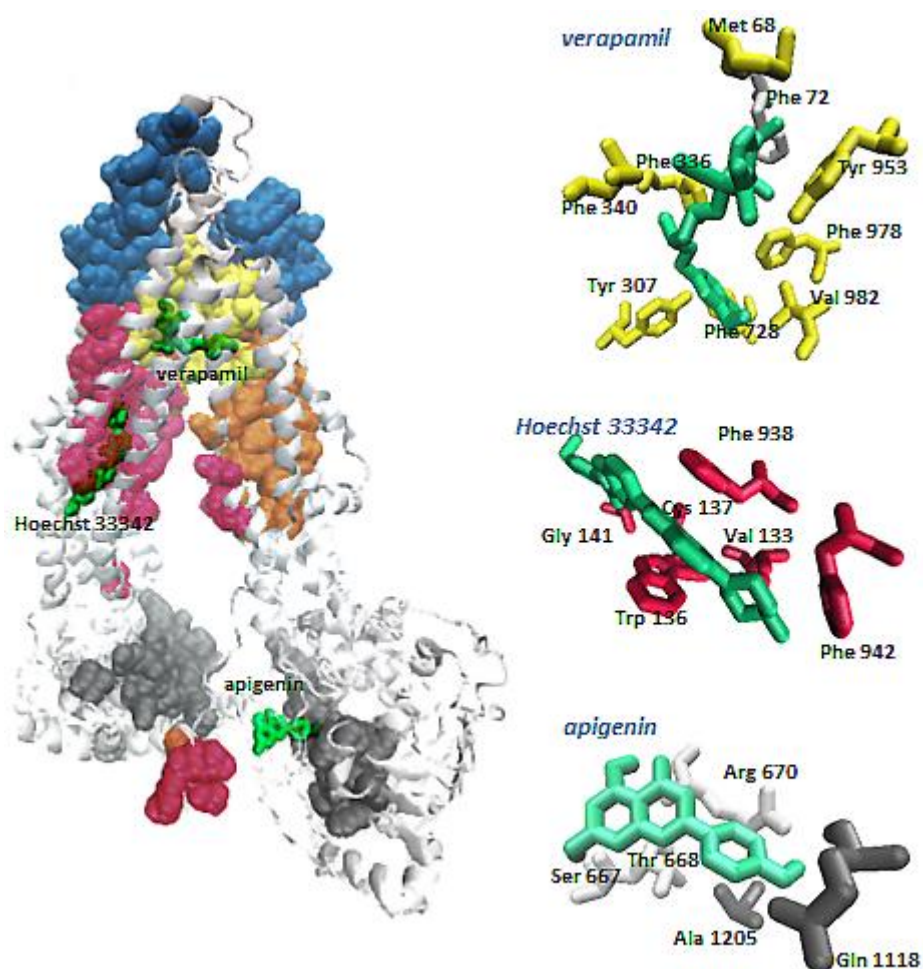


**Figure 28:** Interaction of ligands at several sites on human P-glycoprotein. On the left, we represent the homology modelled P-glycoprotein with the different interaction sites represented in CPK format: the transmembrane common drug binding pocket (DBP): yellow: M-site, red: H-site and orange: R-site; the amino acids involved in ATP binding within the cytoplasmic nucleotide binding domain (NBD): gray and the MRK16 epitope: blue. The rest of the P-glycoprotein molecule is represented in white new cartoon format. The three ligands (verapamil, Hoechst 33342 and apigenin) are represented in licorice in green. On the right, we show the ligands (green, licorice) with the respective interacting amino acids (colors depending on the interaction site, licorice)

### 3.3.2 Statistical analysis

As a starting point, the different samples i.e. substrates, modulators and non-substrates/modulators were first subjected to the Shapiro-Wilk test for normal distribution in order to choose the right test to perform the statistical analysis. When a sample tends to show

normal distributions, independent-sample *t*-test is recommended, whereas Mann Whitney U test is preferred in the case of non-normal distributions [30]. After performing the test on the three samples mentioned above taking the lowest binding energies as the dependent variable, a normal distribution was observed. Hence, the two independent-sample *t*-test was chosen in this case. However, when considering the number of conformations at the lowest binding energy cluster as the independent variable, the samples exerted *p*-values lower than 0.05 indicating a non-normal distribution. Therefore, we applied the Mann-Whitney U test in this case. Results of both *t*-test and Mann-Whitney U tests are presented in the **Table 14** presenting the level of significance for each comparison ( $p < 0.05$ : significant difference;  $p > 0.05$ : no significant difference)

**Table 14:** Statistical analysis using independent-sample *t*-test and Mann-Whitney U test. The statistical analysis was carried out on the basis of the two features of molecular docking, i.e. the lowest binding energies and number of conformations within, the lowest binding energy cluster.

dependent variable	comparison	<i>p</i> -value	
		human	mouse
lowest binding energies (independent-sample <i>t</i> -test)	substrates/modulators	< 0.05	> 0.05
	substrates/non-substrates	< 0.05	< 0.05
	modulators/non-substrates	< 0.05	< 0.05
number of conformation at lowest binding energy cluster (Mann-Whitney U test)	substrates/modulators	> 0.05	< 0.05
	substrates/non-substrates	> 0.05	> 0.05
	modulators/non-substrates	> 0.05	> 0.05

### 3.3.3 Summary: Utilization of molecular docking in P-glycoprotein research

In the previous sections we attempted to evaluate molecular docking in the context of P-glycoprotein research. In this study, we considered both features of molecular docking that are the estimation of binding affinities and prediction of the binding site. Via binding affinity estimations, molecular docking was able to differentiate between three groups interacting differently with P-glycoprotein (substrates, modulators and non-substrates). Furthermore, molecular docking was relatively able to assign compounds to their correct binding sites. However, this task is not easy, considering the fact that there are various reports throughout literature on the binding cavity of P-glycoprotein and its subsites (discussed thoroughly in section 4.3.2).

## 4 Discussion

### 4.1 Cytotoxicity of cardiotonic steroids and the link with Na/K ATPase

#### 4.1.1 Cytotoxicity in sensitive and MDR leukemia cell lines

Since cardiotonic steroids have recently been suggested as interesting compounds for cancer chemotherapy [7, 10], we tested the cytotoxic effect of a library of 66 cardiotonic steroids (mostly comprised of bufadienolides and their derivatives) towards CCRF-CEM leukemia cells and their multidrug-resistant, P-glycoprotein-overexpressing CEM/ADR5000 subline. The molar ranges of  $IC_{50}$  values on both cell lines were various as some compounds were cytotoxic in the nanomolar range and others in the micromolar range. Few compounds were found non-cytotoxic in both cell lines. Notable are the low resistance indices (not exceeding 2.5) for all compounds that exerted a cytotoxic effect. This is in accordance with previous studies, which tested cardiotonic steroids in drug-resistant cell lines and proved their ability to evade multidrug resistance [61, 136, 147]. For example, in the work of Johansson *et al.* [136], digoxin – a well-known P-glycoprotein substrate – displayed a very low resistance index (1.74) in P-glycoprotein associated multidrug-resistant cell lines. Furthermore, some of our compounds interestingly exerted higher cytotoxicity in resistant CEM/ADR5000 than in parental CCRF-CEM cells. This phenomenon is referred to as collateral sensitivity [134]. Verapamil – a well-known P-glycoprotein inhibitor – was also reported to confer collateral sensitivity to MDR cell lines [134, 148]. This has been directly linked to P-glycoprotein. The futile cycle model provides a seemingly legitimate explanation, in which verapamil is handled by P-glycoprotein in exactly the same way as non-modulating substrates with the only difference of flip-flop rates across the transmembrane bilayers. The rates are much faster in the case of verapamil and therefore render P-glycoprotein in a useless exhausted state [103, 134]. This futile cycle consumes high amounts of ATP, which has to be compensated through oxidative phosphorylation in turn generating higher amounts of reactive oxygen species (ROS) and leading eventually to apoptosis [134, 148]. Steroids such as prednisolone, dexamethasone, and progesterone were also found to confer collateral sensitivity to MDR cell lines [134]. This in turn is in support of our data that some steroidal compounds can cause collateral sensitivity. The exact mechanism of collateral sensitivity mediated by cardiotonic steroids and the involvement of P-glycoprotein in this process indeed requires further investigations.

Since one major obstacle in chemotherapy is the toxicity of chemotherapeutics in normal tissues leading to severe side effects [149], we further attempted to evaluate the effects of cardiotonic steroids in healthy tissues. Indeed, the four most efficacious compounds on leukemia cells were less cytotoxic in normal white blood cells (human peripheral mononuclear cells; PMNC), indicating at least partial tumor-specific effects.

#### 4.1.2 Structure activity relationship

With the importance of rational drug design and lead structure optimization, the chemical substitutions and their effect on cytotoxicity have been thoroughly analyzed and discussed in a structure-activity relationship report in section 3.1.3. Due to intensive reviews of structure-activity relationships of cardiotonic steroids-mediated cytotoxicity throughout literature [54, 75, 135], most of our findings have already been reported. However, we were still able to make new observations including: 1) the preferable existence of an  $\alpha$ -pyrone ring at position 17 over a butyrolactone, 2) the favored  $\beta$ -configuration of a methylcarboxy at position 17 in case the lactone was replaced, 3) the negative effect of a  $\beta$ -configured acetyl group at position 16 and 4) the deleterious effect of an azido group at position 3.

#### 4.1.3 Differential $\text{Na}^+/\text{K}^+$ -ATPase expression in MDR cells through QSAR and molecular docking

Subsequently, a QSAR model was built based on the  $\text{IC}_{50}$  values obtained for both cell lines. Through the process of choosing descriptors, we noticed that the number of hydrogen bonds and the number of hydrophobic interactions possibly play an essential role for cytotoxicity. This is in accordance with the fact that these two chemical features increase binding of cardiotonic steroids to  $\text{Na}^+/\text{K}^+$ -ATPase [137, 150]. Orbital molecular descriptors, namely highest occupied molecular orbital (HOMO) energy (PM3\_HOMO) and lowest unoccupied molecular orbital (LUMO) energy (PM3\_LUMO) were also used. These belong to quantum-chemical descriptors that characterize the shape, binding properties and reactivity of a molecule and its substituents [151]. They have the advantage that they can characterize molecules based on their molecular structure only and the proposed mechanism of action can be directly linked to the molecule's reactivity [151]. These descriptors have been successfully used in QSAR prediction in terms of cytotoxicity [152]. In our analysis, they were able to predict cytotoxicity in a much better manner than in a previous study, which only used a rather limited number of compounds [152]. Furthermore, orbital molecular calculations were also used in a QSAR analysis of cardiotonic steroids in their inhibition of  $\text{Na}^+/\text{K}^+$ -ATPase [153]. In the present analysis, moderate  $R^2$  values

were achieved for both cell lines and they were almost equal in both training and test sets, indicating a satisfactory ability to predict biological activities for compounds outside the training set.  $R^2$  values around 0.6 might indicate that the compounds have additional targets to  $\text{Na}^+/\text{K}^+$ -ATPase. In fact, QSAR application in cytotoxicity/toxicity prediction has always been a challenge owing to the fact that toxicity is often not well understood and involves various mechanisms and pathways [154]. However, QSAR accompanied with molecular docking has pointed to a possible differential expression of  $\text{Na}^+/\text{K}^+$ -ATPase between sensitive and multidrug-resistant cell lines, which will be thoroughly discussed below.

To further explore the mode of cytotoxic action of cardiotonic steroids, we performed molecular docking on  $\text{Na}^+/\text{K}^+$ -ATPase as possible molecular target involved in cytotoxicity. Subsequently, we correlated the  $\text{IC}_{50}$  values with several outcomes obtained from the docking analyses. It is noteworthy that  $\text{IC}_{50}$  values were best correlated with the number of conformations in the cluster with the highest number of conformations. This may be explained by the fact that the ability of molecular docking to predict the binding energy is less reliable than the prediction of the ligand's binding mode to the protein, which reveals the most reproducible docking configurations [117, 155]. The observation that a slightly better correlation was found in sensitive than in MDR cells might be explained by the fact that some compounds exerted collateral sensitivity as discussed above, which in turn adds up more complexity to the mode of cytotoxic action in MDR cells. The weaker correlation between  $\text{IC}_{50}$  values of cardiotonic steroids in CEM/ADR5000 cells and molecular docking data, which was also observed in QSAR analysis, inspired us to investigate a possible differential expression of  $\text{Na}^+/\text{K}^+$ -ATPase between sensitive and resistant cell lines.

#### **4.1.4 $\text{Na}^+/\text{K}^+$ -ATPase down-regulation in MDR cells**

Strikingly, the pump turned out to be less expressed in CEM/ADR5000 than in CCRF-CEM cells. To confirm these results, another pair of sensitive (KB-3-1) and multidrug-resistant (KB-8-5) cells was tested and also displayed a down-regulation of  $\text{Na}^+/\text{K}^+$ -ATPase in multidrug-resistant cells. Furthermore, the National Cancer Institute (NCI) database (<http://dtp.nci.nih.gov/>) revealed similar results via microarray analysis (experiment Id: 121768) in another pair of sensitive cancer (ovarian) cells and their multidrug-resistant counterparts, namely OVCAR-8 and NCI/ADR-RES, respectively. In support of our results,  $\text{Na}^+/\text{K}^+$ -ATPase was down-regulated almost by half in NCI/ADR-RES cells when compared to OVCAR-8 (RNA expression level: OVCAR-8: 980.6; NCI/ADR-RES: 572.7). Another noteworthy remark is that normal lymphocytes contained only traces of  $\text{Na}^+/\text{K}^+$ -ATPase when

tested via western blot (data not shown), which in turn supports the down-regulation of Na<sup>+</sup>/K<sup>+</sup>-ATPase in multidrug-resistant cells. Multidrug-resistant cells have been reported to resemble differentiated cells in some biochemical and functional properties and have a more normal, less tumorigenic phenotype than their sensitive counterparts [156, 157]. The down-regulation of Na<sup>+</sup>/K<sup>+</sup>-ATPase in multidrug-resistant cells might be one characteristic of this “normal” phenotype. Interestingly, the expression of Na<sup>+</sup>/K<sup>+</sup>-ATPase has also been reported to be elevated in mitogen-stimulated human lymphocytes transforming them from resting to proliferating state [158]. We further attempted to analyze the transcriptomes of both sensitive CCRF-CEM and multidrug-resistant CEM/ADR5000 cell lines with relevance to the above presented Na<sup>+</sup>/K<sup>+</sup>-ATPase signalosome in **Figure 5**. Both mRNA transcripts coding for  $\alpha 1$  and  $\alpha 3$  isoform subunits of Na<sup>+</sup>/K<sup>+</sup>-ATPase were down-regulated in CEM/ADR5000 cells. In regards to multidrug resistance, it is noteworthy that the expression of Na<sup>+</sup>/K<sup>+</sup>-ATPase was reported to be decreased in a cisplatin-resistant line and this reduced expression contributed to lower accumulation of cisplatin in resistant cells [159]. Remarkably, in this cell line, P-glycoprotein was overexpressed and accounted for resistance of paclitaxel [159]. This observation is in great accordance with our results providing evidence for a link between P-glycoprotein overexpression and Na<sup>+</sup>/K<sup>+</sup>-ATPase down-regulation. The observed overexpression of P-glycoprotein in the cisplatin-resistant cell line is believed to be a general cellular stress response as cisplatin does not interact with P-glycoprotein [159]. In the context of general resistance responses, reduced proliferation may be paradoxically crucial for the survival of some cancers [160], especially since cytotoxic drugs target fast proliferating cells [16]. Interestingly, it has been reported that the expression of  $\alpha 1$  subunit was correlated to the effects of ouabain on cell proliferation in a cell-specific manner: when ouabain induced expression of  $\alpha 1$  subunit, proliferation was stimulated in pig kidney epithelial cells, whereas an inhibition of proliferation of breast cancer and prostate cancer cells occurred and was accompanied by a down-regulation of  $\alpha 1$  subunit [161]. The correlation between the down-regulation of Na<sup>+</sup>/K<sup>+</sup>-ATPase and slower proliferation might represent a part of these multifactorial resistance mechanisms. The down-regulation of  $\alpha 3$  isoform has also been recently shown to be relevant to antiproliferative and apoptotic events of cardiotonic steroids in leukemia cells [162] and its knockdown led to increased cytotoxic IC<sub>50</sub> of bufalin in hepatocellular carcinoma cells [163].

The down-regulation of Src and caveolin-1 transcripts in CEM/ADR5000 cells is of great importance since activation of Src leads to phosphorylation of caveolin-1, which in turn down-

regulates P-glycoprotein activity [164]. It is plausible that these deregulations along with the lower expression of  $\text{Na}^+/\text{K}^+$ -ATPase are in favor of P-glycoprotein activity in MDR cells.

Worth to mention is the observed up-regulation of various phosphatidylinositol-4,5-bisphosphate 3-kinase (PI3K) subunits and some Akt transcripts. The activation of this signaling pathway has been reported to confer resistance to several tumor types [165] and its up-regulation has been recently observed in MDR cells [166]. Noteworthy are also the previous findings that intracellular  $\text{Ca}^{2+}$  levels are higher in MDR cells [167-169], which might be partly mediated by the observed up-regulation of transcripts of inositol 1,4,5-trisphosphate receptors (IP3R) that are  $\text{Ca}^{2+}$  release channels found in the endoplasmic reticulum [170]. Furthermore, it is remarkable that protein kinases C (PKCs) were deregulated. A dramatic up-regulation of PKC $\alpha$  (112 fold change) was found in CEM/ADR5000 cells. Prior reports have revealed that decreased  $\text{Na}^+/\text{K}^+$ -ATPase activity was accompanied by increased activities of PKCs in diabetic animal models [171] and that activation of PKC  $\alpha$  lead to a down-regulation of  $\text{Na}^+/\text{K}^+$ -ATPase activity [171-173].

In addition to the expression of P-glycoprotein, other mechanisms have been reported in multidrug-resistant cells. One example is the intracellular pH, which, in general, is higher in cancer cells than in normal cells [174]. The overexpression of P-glycoprotein has been linked to increased intracellular pH [105, 175]. Furthermore, increased  $\text{Na}^+/\text{H}^+$ -exchanger activity in MDR cell lines, partly via increased expression, has also been reported [176]. Therefore, it is very likely that differences in the expression of  $\text{Na}^+/\text{K}^+$ -ATPase between sensitive and MDR cell lines may also occur, especially considering the strong ties between pH and sodium homeostasis. In this context, cardiotonic steroids alter intracellular  $\text{Na}^+$  concentrations and thereby affect intracellular pH via the  $\text{Na}^+/\text{H}^+$ -exchanger leading to intracellular acidification that disfavors cancer growth [174].

The only moderate correlation between molecular docking results and cytotoxicity of cardiotonic steroids can be explained by several facts. Even though  $\text{Na}^+/\text{K}^+$ -ATPase has been frequently described as well-defined target of cardiotonic steroids [32, 61, 62, 75], additional mechanisms seem to be implicated in their mode of action [177]. Inhibition of DNA topoisomerases I and II [177], inhibition of poly (ADP-ribose) polymerase 1 (PARP1)[178], antagonism of estrogen [177] and inhibition of steroid receptor coactivators Src3 and Src1 [179] are all cellular events that have been associated with cardiotonic steroids and lead to apoptosis via ROS generation and caspase 3 activation [177, 180].

## 4.2 Inhibition of P-glycoprotein by cardiotonic steroids

After exploring the cytotoxic effect of cardiotonic steroids in sensitive and MDR cells, we were interested to search for potential modulators of P-glycoprotein. By means of flow cytometry in high throughput mode, we were able to identify six compounds capable of P-glycoprotein inhibition. The interaction of these compounds with P-glycoprotein was further evaluated via P-glycoprotein-ATPase assay and *in silico* molecular docking. Finally, we assessed the outcome of combining each of these compounds with doxorubicin on cell viability using resazurin reduction assays.

### 4.2.1 P-gp expression in the model system

As a first step, the expression of P-glycoprotein in multidrug-resistant CEM/ADR5000 leukemia cells has been verified by three independent methods including flow cytometry, western blot and immunocytochemistry. In flow cytometry, we used the 17F9 FITC-coupled mouse anti-human P-glycoprotein antibody, which has the advantage of simple application without further incubation with a secondary antibody thereby excluding possible cross reactivity and non-specific binding [181]. In immunoblotting, there are two observations worth mentioning: The first is that P-glycoprotein migrated in two intensive bands between ~ 170-220 kDa. This has already been reported [182] and is believed to be due to a different state of glycosylation, where P-glycoprotein is first manufactured in an immature form weighing 140 kDa and then being processed to the more mature and fully glycosylated forms (170 and 220 kDa). Another possible reason could be that membrane proteins are prone to aggregation after the standard denaturing thermal treatment before resolving the samples on SDS-PAGE gels [183-186]. The second observation is the appearance of a strong band at ~ 60 kDa and weaker bands at ~ 80 and 120 kDa in **Figure 24 A**. This has also previously been shown and is believed to be related to cleavage products of P-glycoprotein [187]. In immunocytochemistry, a noteworthy observation is the appearance of low amounts of P-glycoprotein in the cytoplasm in, which may indicate a redistribution of P-glycoprotein from the membrane to the Golgi apparatus and endoplasmic reticulum [188].

### 4.2.2 Interaction of six modulating cardiotonic steroids with P-glycoprotein

The high throughput screen yielded six cardiotonic steroids that were able to inhibit P-glycoprotein-mediated efflux of doxorubicin. To further investigate their interaction with P-glycoprotein, we applied P-glycoprotein-ATPase assay. It is generally accepted that P-

glycoprotein exhibits a basal ATPase activity, which is due to endogenous lipid transport [189]. Upon drug transport, P-glycoprotein-ATPase activity is usually enhanced and this is referred to as drug-stimulated P-glycoprotein-ATPase activity [189]. Both basal and drug-stimulated P-glycoprotein-ATPase activities are useful to determine the interaction of compounds with P-glycoprotein [190, 191]. In this regards, four scenarios can be encountered: 1) Compounds not interacting with P-glycoprotein do not affect basal P-glycoprotein-ATPase activity. 2) Compounds transported by P-glycoprotein stimulate P-glycoprotein-ATPase activity [192], although exceptions are known as in the case of cyclosporine A, which is discussed below. 3) Slowly transported compounds inhibit drug-stimulated P-glycoprotein-ATPase activity. 4) Non-competitive P-glycoprotein transport inhibitors inhibit both basal and drug-stimulated P-glycoprotein-ATPase activity. Therefore, we were interested in assessing the interaction of the six cardiotonic steroids in this regard.

The interaction of small molecules with P-glycoprotein-ATPase activity is quite complex as illustrated in the case of cyclosporine and its derivative PSC833 [146]: While cyclosporine A is transported by P-glycoprotein, PSC833 is no or only a poor substrate. However, both inhibit the P-glycoprotein-ATPase activity, suggesting that the mechanism of inhibition is transport-independent. Both compounds competitively inhibit verapamil-stimulated P-glycoprotein-ATPase activity. This indicates that those P-glycoprotein-ATPase inhibitors compete with stimulators by interacting or overlapping with the same binding sites. An interaction with P-glycoprotein does not necessarily mean that the interacting molecule is also being transported. The fact that some agents (e.g., verapamil and vinblastine) stimulate and others (e.g., cyclosporine A and analogues) inhibit P-glycoprotein-ATPase activity is still not completely understood [146]. It was suggested that P-glycoprotein confers a catalytic and an inhibitory site and depending on the affinity of the compound to either site, a stimulation or inhibition of P-glycoprotein-ATPase activity can be observed [146]. This assumption is further strengthened by the biphasic pattern of some compounds, in which stimulation at low concentrations is believed to occur due to binding to stimulatory sites and inhibition at high concentrations as a consequence of binding to inhibitory sites [99, 103]. Another explanation might be that cyclosporine A and analogues cause a conformational change leading in turn to disturbance of the ATP hydrolysis cycle [146].

Having this discussion in mind, our results on cardiotonic steroids may be explained as follows: Since compounds 15i and 29b did not affect basal ATPase activity but inhibited verapamil-stimulated P-glycoprotein-ATPase activity, they may be considered as transport-independent

inhibitors of P-glycoprotein in a manner similar to that of cyclosporine A and PSC833. This, however, does not exclude the possibility that they can still be transported. Compound 14D is a substrate of P-glycoprotein due to the stimulation of the basal P-glycoprotein-ATPase activity, but might be transported at slower rates than verapamil and, hence, a slight inhibition of stimulated P-glycoprotein-ATPase activity can be observed. Compounds 54E and 54Ee are both substrates but have no inhibitory effects on the catalytic cycle of P-glycoprotein, indicating that their transport rates are equal to that of verapamil. Since 15S is a P-glycoprotein substrate enhancing verapamil-stimulated P-glycoprotein-ATPase activity, it is most probably transported even faster than verapamil. Another way to gain hints if a compound is a substrate of P-glycoprotein is to examine cross-resistance in sensitive and multidrug-resistant P-glycoprotein-overexpressing cell lines. If a compound is cross-resistant, it is more likely to be a substrate of P-glycoprotein [134]. However, when we tested the 66 cardiotonic steroids in this approach, all of them revealed low resistance indices as thoroughly discussed in section 4.1.1.

*In silico* molecular docking was implemented to analyse the binding modes at the two possible interaction sites, transmembrane domain (TMD) and nucleotide binding domain (NBD). It is remarkable that the interacting amino acids were predominantly assigned to the M-(modulator) site classified by Ferreira *et al.* [116] (**Table 7**), which explains the P-glycoprotein inhibiting effects of the compounds. The interaction of digoxin-like compounds with P-glycoprotein has been intensively investigated by Gozalpour *et al.* [193]: Several amino acids were selected based on the amino acids identified to be responsible for drug binding in the crystalized structure of murine P-glycoprotein by Aller *et al.* [101]. Protein variants, where these amino acids were mutated, were further investigated to analyse their role in the interaction with digoxin-like compounds. Interestingly, amino acids Ile340 and Phe336 played a crucial role in the interaction with these cardiac glycosides. These two amino acids also appeared in our molecular docking analyses as interacting partners for compounds 14D, 15S, 15i, 29b, and 54Ee. It is noteworthy that these two amino acids belong to the M-(modulator) site, which is believed to exert modulatory effects on the function of P-glycoprotein. Worth mentioning is also the amino acid Phe343 belonging to the M-site and playing an important role for the binding of vinblastine, cyclosporine A and colchicine [193]. In a separate study, digoxin and vinblastine were found to bind at a mutual site [194]. In our docking results, this amino acid was also involved in the interaction with 14D, 29b, 54E and 54Ee, which is in agreement with the above mentioned literature [193, 194]

The reason why we carried out molecular docking on the NBD of P-glycoprotein was that some steroids interact with the cytosolic domain of P-glycoprotein in addition to affecting membrane transport and efflux as shown by Dayan *et al.* [195]. This newly identified site seems to be different, but in close proximity to the ATP binding site. Dayan *et al.* [195] suggested that domains between Walker motifs A and B could contribute to steroid binding. We have therefore analysed all amino acids predicted to be involved in the interaction of the six cardiotoxic steroid derivatives and visualized them in respect to the two Walker motifs. As shown in **Figure 29**, most interacting amino acids indeed accumulated between these two motifs.

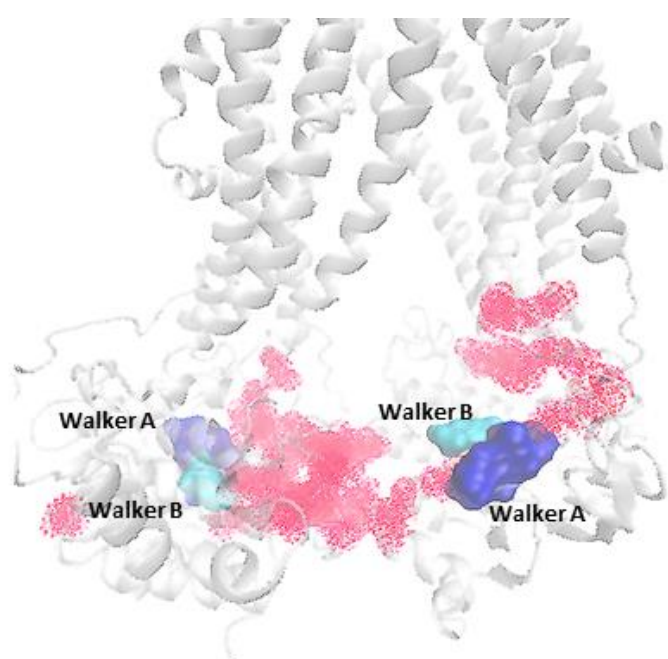


**Figure 29:** Amino acids implicated in the interaction of six cardiotoxic steroid derivatives by molecular docking on homology-modeled human P-glycoprotein at the NBD. The respective amino acids are shown dotted in red, whereas Walker motifs A (blue) and B (cyan) are represented in surface mode. The rest of the P-glycoprotein structure is shown in new cartoon mode in white. Reprinted from: [196]; Copyright 2015 with permission from Elsevier.

Dayan *et al.* [195] further showed that these steroids were of hydrophobic nature and exerted modulatory effects on P-glycoprotein, whereas steroids that are rather more hydrophilic and that are transported by P-glycoprotein did not seem to interact at that site. However, interaction of hydrophobic steroids at the TMD could not be excluded. It may be concluded that those cardiotoxic steroids interact with P-glycoprotein at both the TMD and NBD in a way comparable to flavonoids, which have been described to interact with both regions as well

[197]. The binding of doxorubicin was investigated in parallel as a control drug. At TMD, doxorubicin predominantly bound at the H-site with one amino acid shared with the R-site. In the work of Ferreira *et al.*, doxorubicin was reported to bind to R-site and also H-site at some poses [116]. In general, it has been presumed that anthracyclines bind to the R-site and have a positive effect at the H-site by increasing the efflux of Hoechst 33342 at low concentrations. However, at high concentrations, inhibition of Hoechst 33342 efflux indicated also possible binding of doxorubicin at H-site [116, 198]. Binding of doxorubicin at NBD has not been reported to our knowledge. Nevertheless, in site directed fluorescence labelling of P-glycoprotein at the NBD studies, doxorubicin caused fluorescence quenching, which was believed by the authors to be due to a conformational change preventing the label from binding to the NBD [199].

#### 4.2.3 Potential of cardiotonic steroids in the clinic

Finally, it is noteworthy that compound 15S possessed the highest activity in reversing doxorubicin resistance in CEM/ADR5000 cells. This nicely correlated with results from molecular docking at the TMD. Compound 15S showed the highest affinity to P-glycoprotein indicating a strong inhibitory effect. In the ATPase assay, it possessed strong substrate characteristics by inducing both basal and verapamil-induced P-glycoprotein-ATPase activity. This could be of great importance, as it may indicate that compound 15S is transported at higher rates than verapamil, which may render P-glycoprotein in a futile cycle – a mechanism proposed to explain the paradox of modulators being handled by the transporter in the same way as substrates and yet exerting inhibitory actions [103]. The reason why we now mention compound 15S is the fact that this compound was non-cytotoxic in our cell viability assays (Section 3.1.1). Therefore, adding it to chemotherapeutic regimes maybe of great potential, as it may lack side effects that were so far often responsible for failure of clinical trials [125]. In this context, clinical trials assessing the antitumor potential and tolerability of cardiotonic steroids have been carried out. In a pilot study at The University of Texas M. D. Anderson Cancer Center, the tolerability of Ch'an Su – a preparation containing cardiotonic steroids used in traditional Chinese medicine as local anesthetic, a cardiotonic, a diuretic and an antitumor agent in China – was assessed in a phase 1 clinical trial design [200]. No dose limiting toxicities were reported even at doses with 8 times the typical dose in China. Most importantly, cardiac toxicity was not observed. Cardiac toxicity is the major side effect, which prevented any clinical success with verapamil in terms of P-glycoprotein inhibition [118]. A clinical study reported that the combination of Ch'an Su with gemcitabine was well tolerated and effective in improving the

quality of life of gallbladder carcinoma patients [201]. A phase II clinical trial to evaluate the combination of Chansu with gemcitabine in the treatment of pancreatic cancer is recently completed (clinicaltrials.gov identifier: NCT00837239). Another phase I clinical trial reported the safe use of Nerium Oleander extract containing cardiotoxic steroids in refractory solid tumor patients but unfortunately evidence of antitumor activity was not reported [202].

### **4.3 Molecular docking in P-glycoprotein research**

To assess the value of molecular docking and its applicability in the complex field of P-glycoprotein, we addressed the question, whether or not molecular docking is first able to differentiate between three differently interacting groups with P-glycoprotein (substrates, modulators and non-substrates/modulators) and second predict the binding site of a certain ligand. Molecular docking was performed on the whole molecules of both mouse P-glycoprotein and the homology-modelled human P-glycoprotein in order to prevent any bias caused by prior definition of any binding site. We conducted statistical analysis using independent-sample *t*-test and Mann-Whitney U test based upon the lowest binding energies as well as the number of conformations within the lowest binding energy cluster respectively. We wanted to evaluate both features of molecular docking, namely: the estimation of binding affinities and the determination of the binding mode of the ligand to the protein [155].

#### **4.3.1 Estimation of binding affinities**

Almost all comparisons between the lowest binding energies of the several groups have revealed significant differences at a significant level of  $p < 0.05$ . Only in the case of comparing substrates to modulators docked to the mouse P-glycoprotein, no significant difference was observed ( $p > 0.05$ ). However, when taking the clustering function rather than the binding affinities into consideration, no significant difference ( $p > 0.05$ ) could be noticed except again the comparison between substrates and modulators ( $p < 0.05$ ). Considering both variables, we can conclude that molecular docking was able to differentiate between the distinct groups with significant differences. However, the estimation of binding energies seemed to be more reliable in this contest. Therefore, the claim that the ability of molecular docking to estimate binding energies is unsatisfying may have to be reconsidered. However, in this regards, it is worth mentioning that the classification of compounds into substrates and modulators of P-glycoprotein has not been an easy task due to several factors, among which are the large diversity of the interacting ligands and the existence of several binding sites on the protein [203]. Moreover, molecular docking trials with P-glycoprotein endure other several challenges

such as the fact that P-glycoprotein is a highly flexible protein and the absence of a high resolution crystal structure of the protein [132]. Nevertheless, the use of molecular docking must not be undervalued and combining the power of statistics with it might set a milestone on road to defining a borderline among those different classes.

#### 4.3.2 Estimation of the binding mode

We further went in depth to analyze the second feature of molecular docking, which is the ability to define the binding site of an interacting ligand. We showed that through the classification of the interacting amino acids at the various possible interaction sites on P-glycoprotein, a hint might be made about the possible binding site for the molecule. However, extreme care must be undertaken when interpreting the results considering the discrepancies found throughout literature in regards to determination of binding sites and interacting amino acids. Therefore, in the following text, we go over each presumed interaction site and discuss one example in full detail. Starting with the case of Hoechst 33342 and according to our dockings, five amino acids out of the whole interacting six were found in the H-binding site defined by Ferreira *et al.* [116] within both the lowest binding energy and highest number of conformation cluster. However, when docked upon mouse P-glycoprotein, Hoechst 33342 showed preference to the M- and R-site with the interacting amino acids distributed over both sites. The findings of Shapiro and Ling [198] that Hoechst 33342 and rhodamine 123 bound to two distinct cooperative sites were questioned in the work of Tang *et al.* [204]: First, the interaction, i.e. efflux stimulation, between both sites was considered as a possible artifact related to fluorescence quenching or direct displacement from the membrane, independent of the function of P-glycoprotein [204]. Second, they showed that the P-glycoprotein inhibitor GF-120918 inhibited the efflux of both rhodamine123 and Hoechst 33342 at identical IC<sub>50</sub> values, indicating either the binding of the inhibitor to both R- and H-site with the same affinity or the existence of one site binding both substrates at the same time [204]. This clearly poses the necessity of an extremely careful interpretation of data obtained from molecular docking on P-glycoprotein, since consensus even in the wet lab experiments could not be reached so far. However, we noticed that molecular docking was able to cover the controversy discussed above. Moving over to the R-site, our dockings showed that rhodamine 123 shared two amino acids with the amino acids embedded in the modulator (M-site) when docked on human P-glycoprotein and two amino acids and one amino acids within the M- and R-site respectively, when docked on mouse P-glycoprotein. When browsing literature to solve this mystery, we came across the work of Loo and Clarke [205], who used cysteine scanning mutagenesis to

identify the amino acids involved in the binding of rhodamine compounds. In their work, they used MTS-rhodamine, which inhibits the Cys-mutated P-glycoprotein, and rhodamine B, which protects from this inhibition to identify the amino acids that are within or close to the rhodamine drug binding site. They have identified 28 amino acids, whose inhibition by MTS-rhodamine was protected by rhodamine B. Of those, three amino acids, namely (Val981, Val982 and Ala985) were also identified in our docking for a possible interaction with rhodamine 123. In fact, mutants of two of those three amino acids (Val 981 and Val 982) were significantly protected by rhodamine B indicating a possible major role in this interaction. When comparing the amino acids identified with molecular docking by Ferreira *et al.* [116] to those identified by cysteine scanning mutagenesis by Loo and his colleagues [205], we could as well find three common amino acids (Gly300, Ile340 and Gly774), of which Ile340 seemed to be of significant relevance to the binding of rhodamine compounds to P-glycoprotein [205]. Taking our results and those of Ferreira *et al.* into consideration, we find a good agreement with the valuable site-directed mutagenesis data.

Using verapamil as a representative of a modulator binding to the M-site, we are able to assign 8 amino acids retrieved from our dockings at that site within the lowest binding energy cluster. Considering the cluster of the highest number of conformations, it bound with 8 amino acids to the H-site. Ferreira *et al.* have actually mapped the amino acid using molecular docking upon interaction with verapamil [116]. This is in turn in great agreement with our docking results. However, binding of verapamil preferentially to the H-site has also been described in the work of Shapiro and Ling [198]. In a similar set of cysteine scanning mutagenesis experiments, Loo and Clarke identified amino acids that might be involved in the interaction with verapamil [206]. Interestingly, mutants with the amino acid (Val982)–located in the M-site and the amino acid (Phe942)–located in the H-site were found to play a role in the interaction with verapamil [206]. Both amino acids were also identified in our dockings, which speaks for the credibility of this technique.

Another remark worth mentioning is in the case of some flavonoids. Going through the possible amino acids responsible for the binding of quercetin and kaempferol, a few amino acids were distributed among the M- and R-sites. One amino acid for biochanin A and two for apigenin (depicted in **Figure 28**) were found within the nucleotide binding domain (NBD). In literature, flavonoids have been described as a new set of compounds that bind to the nucleotide binding domain (NBD) [207]. Some have been also described to bind directly to the common P-glycoprotein substrate binding site [206]. In the special case of quercetin, it has been shown by

---

fluorescence quenching studies that it bound to the cytoplasmic domain of P-glycoprotein. However, Shapiro and Ling postulated the binding of quercetin to the H-site after they noticed that quercetin induced the transport of rhodamine 123 and partially inhibited that of Hoechst 33342 [206]. Again, we encounter the fact that binding of ligands to P-glycoprotein has been confronted with a lot of controversies throughout literature, but molecular docking seems to be able to cope with them through careful analysis.

## 5 Summary and conclusions

In this study, we dealt with the problematic of multidrug resistance (MDR) in three aspects. We established a link between two membrane proteins, namely P-glycoprotein – responsible for classical MDR – and  $\text{Na}^+/\text{K}^+$ -ATPase through the analysis of cytotoxicity of cardiotonic steroids on sensitive and multidrug-resistant leukemia cell lines. Then we have identified six cardiotonic steroids capable of P-glycoprotein inhibition. Finally, we assessed the value of molecular docking in P-glycoprotein research.

Cardiotonic steroids indeed represent an interesting group of compounds in the combat against multidrug-resistant cancers. After examining the cytotoxic effect of a chemical library of 66 cardiotonic steroids on drug-sensitive and multidrug-resistant leukemia cells, implementation of QSAR and molecular docking analyses indicated a differential expression of  $\text{Na}^+/\text{K}^+$ -ATPase, which considerably contributes to the mode of action of these compounds. We have observed a down-regulation of  $\text{Na}^+/\text{K}^+$ -ATPase in multidrug-resistant, P-glycoprotein-overexpressing cells. The downstream signaling pathways were as well deregulated. These deregulations in the  $\text{Na}^+/\text{K}^+$ -ATPase signalosome seem to be in favor of the multidrug-resistant phenotype. Cardiotonic steroids were able to evade multidrug resistance with their low resistance indices. However, these differences are still there and it is quite plausible that the down-regulation of  $\text{Na}^+/\text{K}^+$ -ATPase may account for them, either directly or indirectly by being a part of a multifactorial stress response alongside with the overexpression of P-glycoprotein. Not only were cardiotonic steroids able to evade multidrug resistance but some were also able to inhibit P-glycoprotein. This presents another potential use of cardiotonic steroids in chemotherapy regimens. Recently, clinical trials have revealed promising results considering the effectiveness and tolerability of cardiotonic steroids either alone or in combination with other chemotherapeutics.

Away from cardiotonic steroids and due to the growing importance of *in silico* studies, we assessed the value of molecular docking in P-glycoprotein research with all its challenges. Our work adds up to the many attempts carried out to try to look through the haze spread over the field of P-glycoprotein. We conclude that the power of molecular docking should not be undervalued in this area, as it was able to discriminate between distinct classes of drugs interacting differently with P-glycoprotein. Furthermore, despite the difficulties attached to using molecular docking with such a highly flexible protein, this technique might be useful in making a hint as to where a ligand might bind on the Protein. However, this must be carried out

---

with extreme care, since experimental data show great amount of controversy in some cases. In future, the combination of computational methods (e.g. molecular docking, molecular dynamics, QSAR, etc.), statistical analysis, and experimental data from competitive uptake assays to site-directed mutagenesis may provide a powerful tool to solve the riddles within the complex field of P-glycoprotein.

## 6 Material and Methods

### 6.1 Chemicals and equipment

#### *Cardiotonic steroids:*<sup>5</sup>

The library of cardiotonic steroids and derivatives (except for digoxin and bufalin) was obtained from Prof. [REDACTED] (Department of Pharmacognosy, University of Vienna, Austria) and their structures are clarified in **Table 15** and **Figure 30**. The majority of the chemical structures were confirmed or elucidated by NMR spectroscopy and mass spectrometry (MS) as described in more detail previously [75]. The NMR data of about half of the compounds in this library (2C, 2G, 2M, 2P, 2c, 3D, 4I, 4L, 6B, 7B, 7E, 10D, 10I, 10J, 10O, 10S, 12A, 12B, 14D, 15S, 15c, 15d, 15h, 16D, 16G, 21E, 27F, 29C, 32A, 35B, 42C, and 52I) have been made available in a recent study [75]. In addition, we have acquired the NMR and MS data, and thereby verified the structures, of all additional compounds that were either new (15i, 30M, 49h, 51D, 54E, 62A, 62F, 62I, and 62J) or known but also highly active (i.e. showed IC<sub>50</sub> values below 10 μM on both CCRF-CEM and CEM/ADR5000 leukemia cell lines) in the below described assay (22N, 23A, 23D, 23G, 44F, 53R, and 54v). These data can be found in the Appendix 8.1. All compounds were dissolved in DMSO and 100 μM or 50 μM stocks were prepared according to their solubility. For some compounds short ultrasonification in Sonorex RK 102 H Ultrasonic Cleaning Unit (Bandelin, Germany) was required for complete dissolution.

---

<sup>5</sup> Structure elucidation by means of NMR and MS were conducted by our collaboration partners at the Department of Pharmaceutical Chemistry at the University of Vienna

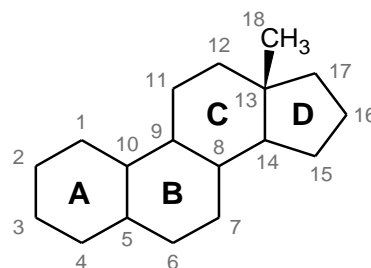


**Table 15:** Chemical structures of cardiotonic steroids presenting the various substitution at different positions

Compound	Substituent at position										CAS Reg. Nr.
	3	5	9	10	11	12	14	15	16	17	
2C	OH $\beta$	H $\alpha$	H $\alpha$	CHO $\beta$	H	H	OH $\beta$	H	H	<b>R</b> <sub>1</sub> $\beta$	468-18-8
2G	O-Ac $\beta$	H $\alpha$	H $\alpha$	CHO $\beta$	H	H	OH $\beta$	H	H	<b>R</b> <sub>1</sub> $\beta$	21857-75-0
2M	OH $\beta$	H $\beta$	H $\alpha$	CH <sub>3</sub> $\beta$	OH $\alpha$	H	OH $\beta$	H	H	<b>R</b> <sub>1</sub> $\beta$	465-11-2
2P	O-Rhamnosyl $\beta$	H $\beta$	H $\alpha$	CH <sub>3</sub> $\beta$	OH $\alpha$	H	OH $\beta$	H	H	<b>R</b> <sub>1</sub> $\beta$	85684-33-9
2c	=O	=C4	H $\alpha$	CH <sub>3</sub> $\beta$	H	H	OH $\beta$	H	H	<b>R</b> <sub>1</sub> $\beta$	545-28-8
3D	O-Ac $\beta$	H $\beta$	H $\alpha$	CH <sub>3</sub> $\beta$	O-Ac $\alpha$	=O	OH $\beta$	H	H	<b>R</b> <sub>1</sub> $\beta$	21853-56-5
4I	O-Ac $\beta$	H $\beta$	H $\alpha$	CH <sub>3</sub> $\beta$	O-Ac $\alpha$	=O	OH $\beta$	H	H	COOCH <sub>3</sub> $\beta$	17008-73-0
4L	O-Ac $\beta$	H $\beta$	H $\alpha$	CH <sub>3</sub> $\beta$	O-Ac $\alpha$	=O	O-CHO $\beta$	H	H	COOCH <sub>3</sub> $\beta$	1439307-15-9

6B	OH $\beta$	H $\beta$	=C11	CH <sub>3</sub> $\beta$	=C9 and OH	=O	OH $\beta$	H	H	<b>R</b> <sub>1</sub> $\beta$	4236-48-0
7B	O-Ac $\beta$	H $\beta$	H $\alpha$	CHO $\beta$	H	H	O-C15 $\beta$	O-C14 $\beta$	H	<b>R</b> <sub>1</sub> $\beta$	20987-25-1
7E	=O	H $\beta$	H $\alpha$	CH <sub>3</sub> $\beta$	H	H	OH $\beta$	H	O-Ac $\beta$	<b>R</b> <sub>1</sub> $\beta$	4266-46-0
10D	OH $\beta$	H $\alpha$	H $\alpha$	CH <sub>3</sub> $\beta$	H	H	OH $\beta$	H	H	<b>R</b> <sub>1</sub> $\beta$	33766-62-0
10G	O-Ac $\beta$	H $\beta$	H $\alpha$	CH <sub>3</sub> $\beta$	H	H	OH $\alpha$	=O	H	COOCH <sub>3</sub> $\beta$	115113-49-0
10I	O-Ac $\beta$	H $\beta$	H $\alpha$	CH <sub>3</sub> $\beta$	H	H	OH $\alpha$	=O	H	<b>R</b> <sub>1</sub> $\beta$	1439306-69-0
10J	O-Ac $\beta$	H $\beta$	H $\alpha$	CH <sub>3</sub> $\beta$	H	H	OH $\beta$	OH $\alpha$	H	<b>R</b> <sub>1</sub> $\beta$	4534-19-4
10O	O-Ac $\beta$	H $\beta$	H $\alpha$	CH <sub>3</sub> $\beta$	H	H	OH $\beta$	H	H	<b>R</b> <sub>1</sub> $\beta$	4029-66-7
10S	OH $\alpha$	H $\beta$	H $\alpha$	CH <sub>3</sub> $\beta$	H	H	OH $\beta$	H	H	<b>R</b> <sub>1</sub> $\beta$	465-20-3
11M	O-Ac $\beta$	H $\beta$	H $\alpha$	CH <sub>3</sub> $\beta$	H	H	OH $\beta$	H	H	COOCH <sub>3</sub> $\beta$	2900-98-3
12A	O-CHO $\beta$	H $\beta$	H $\alpha$	CH <sub>3</sub> $\beta$	H	H	O-C15 $\alpha$	O-C14 $\alpha$	H	<b>R</b> <sub>1</sub> $\beta$	1439306-78-1
12B	OH $\beta$	H $\beta$	H $\alpha$	CH <sub>3</sub> $\beta$	H	H	O-C15 $\alpha$	O-C14 $\alpha$	H	<b>R</b> <sub>1</sub> $\beta$	24183-15-1
14D	O-Ac $\beta$	H $\beta$	H $\alpha$	CH <sub>3</sub> $\beta$	=O	O-Ac $\beta$	H $\alpha$	H	H	CH <sub>2</sub> OAc $\beta$	17007-97-5
15S	O-Ac $\beta$	H $\beta$	H $\alpha$	CH <sub>3</sub> $\beta$	O-Ac $\alpha$	O-Ac $\beta$	OH $\beta$	H	H	COOCH <sub>3</sub> $\beta$	1439307-59-1
15c	O-Ac $\beta$	H $\beta$	H $\alpha$	CH <sub>3</sub> $\beta$	=O	O-Ac $\beta$	OH $\beta$	H	H	<b>R</b> <sub>1</sub> $\beta$	17008-66-1
15d	OH $\beta$	H $\beta$	H $\alpha$	CH <sub>3</sub> $\beta$	OH $\alpha$	OH $\beta$	OH $\beta$	H	H	<b>R</b> <sub>1</sub> $\beta$	51227-38-4

15h	O-Ac $\beta$	H $\beta$	H $\alpha$	CH <sub>3</sub> $\beta$	O-Ac $\alpha$	=O	OCO-C17 $\beta$	H	H	COO-C14 $\beta$	1439307-52-4
15i	O-Ac $\beta$	H $\beta$	H $\alpha$	CH <sub>3</sub> $\beta$	O-Ac $\alpha$	OH $\alpha$	OH $\beta$	H	H	<b>R<sub>1</sub></b> $\beta$	none
16D	OH $\beta$	H $\beta$	H $\alpha$	CH <sub>3</sub> $\beta$	=O	OH $\beta$	OH $\beta$	H	H	<b>R<sub>1</sub></b> $\beta$	17008-65-0
16G	O-Ac $\beta$	H $\beta$	H $\alpha$	CH <sub>3</sub> $\beta$	=O	O-Ac $\alpha$	OH $\beta$	H	H	<b>R<sub>1</sub></b> $\beta$	17008-70-7
21E	O-Ac $\beta$	H $\beta$	H $\alpha$	CH <sub>3</sub> $\beta$	H	H	OH $\beta$	H	O-Ac $\beta$	<b>R<sub>1</sub></b> $\beta$	4029-69-0
22N	<b>R<sub>2</sub></b> $\beta$	OH $\beta$	H $\alpha$	CH <sub>3</sub> $\beta$	H	H	OH $\beta$	H	H	<b>R<sub>1</sub></b> $\beta$	72093-20-0
23A	O-Ac $\beta$	H $\beta$	H $\alpha$	CH <sub>3</sub> $\beta$	H	H	OH $\beta$	H	H	<b>R<sub>3</sub></b> $\beta$	808-19-5
23D	O-Ac $\beta$	H $\beta$	H $\alpha$	CH <sub>3</sub> $\beta$	H	H	O-C15 $\beta$	O-C14 $\beta$	H	<b>R<sub>3</sub></b> $\beta$	4240-55-5
23G	OH $\beta$	H $\beta$	H $\alpha$	CH <sub>3</sub> $\beta$	H	H	OH $\beta$	H	H	<b>R<sub>3</sub></b> $\beta$	143-62-4
26K	OH $\beta$	H $\beta$	H $\alpha$	CH <sub>3</sub> $\beta$	H	H	O-C15 $\beta$	O-C14 $\beta$	OH $\beta$	COOCH <sub>3</sub> $\alpha$	113749-90-9
27F	NHCOCH <sub>3</sub> $\alpha$	H $\beta$	H $\alpha$	CH <sub>3</sub> $\beta$	H	H	O-C15 $\beta$	O-C14 $\beta$	O-Ac $\beta$	<b>R<sub>1</sub></b> $\beta$	1439306-07-6
29C	O-Ac $\beta$	H $\beta$	H $\alpha$	CH <sub>3</sub> $\beta$	H	H	O-C15 $\beta$	O-C14 $\beta$	OH $\beta$	COOCH <sub>3</sub> $\beta$	1439307-02-4
29b	O-Ac $\beta$	H $\beta$	H $\alpha$	CH <sub>3</sub> $\beta$	H	H	OH $\beta$	OH $\alpha$	=C17	COOCH <sub>3</sub>	113752-75-3
30M	OH $\beta$	H $\beta$	H $\alpha$	CH <sub>3</sub> $\beta$	H	H	H $\alpha$	=O	OH $\beta$	<b>R<sub>4</sub></b> $\beta$	none
32A	OH $\beta$	H $\beta$	H $\alpha$	CH <sub>3</sub> $\beta$	H	H	OH $\beta$	H	O-Ac $\beta$	<b>R<sub>1</sub></b> $\beta$	471-95-4
35B	O-Ac $\beta$	H $\beta$	H $\alpha$	CH <sub>3</sub> $\beta$	H	H	O-C15 $\beta$	O-C14 $\beta$	OH $\beta$	<b>R<sub>1</sub></b> $\beta$	4026-96-4

42C	O-Ac $\beta$	H $\beta$	H $\alpha$	CH <sub>3</sub> $\beta$	O-Ac $\alpha$	H	OH $\beta$	H	H	COOCH <sub>3</sub> $\beta$	115267-64-6
44F	OH $\beta$	H $\beta$	H $\alpha$	CH <sub>3</sub> $\beta$	H	H	=C8	H	H	<b>R</b> <sub>1</sub> $\beta$	7372-44-3
44G	OH $\beta$	H $\beta$	H $\alpha$	CH <sub>3</sub> $\beta$	H	H	=C15	=C14	H	<b>R</b> <sub>1</sub> $\beta$	7439-77-2
49d	OH $\beta$	OH $\beta$	H $\alpha$	CH <sub>3</sub> $\beta$	H	H	H $\alpha$	=O	H	COOCH <sub>3</sub> $\beta$	113749-87-4
49h	OH $\beta$	OH $\beta$	H $\alpha$	CH <sub>3</sub> $\beta$	H	H	O-C15 $\beta$	O-C14 $\beta$	H	COOH $\alpha$	none
51D	=O	H $\beta$	H $\alpha$	CH <sub>3</sub> $\beta$	H	H	O-C15 $\beta$	O-C14 $\beta$	H	COCH <sub>2</sub> OAc $\alpha$	none
52I	N <sub>3</sub> $\beta$	H $\beta$	H $\alpha$	CH <sub>3</sub> $\beta$	H	H	O-C15 $\beta$	O-C14 $\beta$	H	<b>R</b> <sub>1</sub> $\beta$	36121-81-0
53R	O-Ac $\beta$	H $\beta$	H $\alpha$	CH <sub>3</sub> $\beta$	H	H	O-C15 $\beta$	O-C14 $\beta$	H	<b>R</b> <sub>1</sub> $\beta$	4029-64-5
54C	O-Ac $\beta$	H $\beta$	H $\alpha$	CH <sub>3</sub> $\beta$	H	H	O-C15 $\beta$	O-C14 $\beta$	H	COOCH <sub>3</sub> $\beta$	23449-32-3
54E	O-Ac $\beta$	H $\beta$	H $\alpha$	CH <sub>3</sub> $\beta$	H	H	O-C15 $\beta$	O-C14 $\beta$	H	COOCH <sub>3</sub> $\alpha$	none
54T	O-Ac $\beta$	H $\beta$	H $\alpha$	CH <sub>3</sub> $\beta$	H	H	H $\alpha$	=O	H	COOCH <sub>3</sub> $\beta$	97905-88-9
54r	O-Ac $\beta$	H $\beta$	H $\alpha$	CH <sub>3</sub> $\beta$	H	H	H $\alpha$	<b>R</b> <sub>5</sub> $\beta$	H	COOCH <sub>3</sub> $\beta$	116027-85-1
54 $\alpha$	O-Ac $\beta$	H $\beta$	H $\alpha$	CH <sub>3</sub> $\beta$	H	H	H $\beta$	=O	H	COOCH <sub>3</sub> $\beta$	107596-72-5
54 $\epsilon$	O-Ac $\beta$	H $\beta$	H $\alpha$	CH <sub>3</sub> $\beta$	H	H	H $\beta$	=O	H	COOCH <sub>3</sub> $\alpha$	97905-89-0
54t	=O	H $\beta$	H $\alpha$	CH <sub>3</sub> $\beta$	H	H	H $\alpha$	=O	H	<b>R</b> <sub>1</sub> $\beta$	105984-49-4
54v	O-Ac $\beta$	H $\beta$	H $\alpha$	CH <sub>3</sub> $\beta$	H	H	H $\alpha$	O-Ac $\beta$	H	<b>R</b> <sub>1</sub> $\beta$	107204-41-1

---

54Ee						see Figure 30					119926-37-3
55K	<b>R<sub>6</sub></b> β	H β	H α	CH <sub>3</sub> β	H	H	OH β	H	H	<b>R<sub>3</sub></b> β	30219-07-9
62A	O-Ac β	=C6	H α	CH <sub>3</sub> β	H	H	H α	H	H	<b>R<sub>7</sub></b> β	none
62F	OH β	=C6	H α	CH <sub>3</sub> β	H	H	H α	H	H	<b>R<sub>8</sub></b> β	none
62I	O-Ac β	=C6	H α	CH <sub>3</sub> β	H	H	H α	H	H	<b>R<sub>9</sub></b> β	none
62J	O-Ac β	=C6	H α	CH <sub>3</sub> β	H	H	H α	H	H	<b>R<sub>8</sub></b> β	none
62N	OH β	=C6	H α	CH <sub>3</sub> β	H	H	H α	H	H	COCH <sub>2</sub> OCH <sub>3</sub> β	82995-02-6
62P	OH β	=C6	H α	CH <sub>3</sub> β	H	H	H α	H	H	COOH β	10325-79-8
Bufalin	OH β	H β	H α	CH <sub>3</sub> β	H	H	OH β	H	H	<b>R<sub>1</sub></b> β	465-21-4
Digoxin	O-[Digitoxose] <sub>3</sub>	H β	H α	CH <sub>3</sub> β	H	OH β	OH β	H	H	<b>R<sub>3</sub></b> β	20830-75-5

---

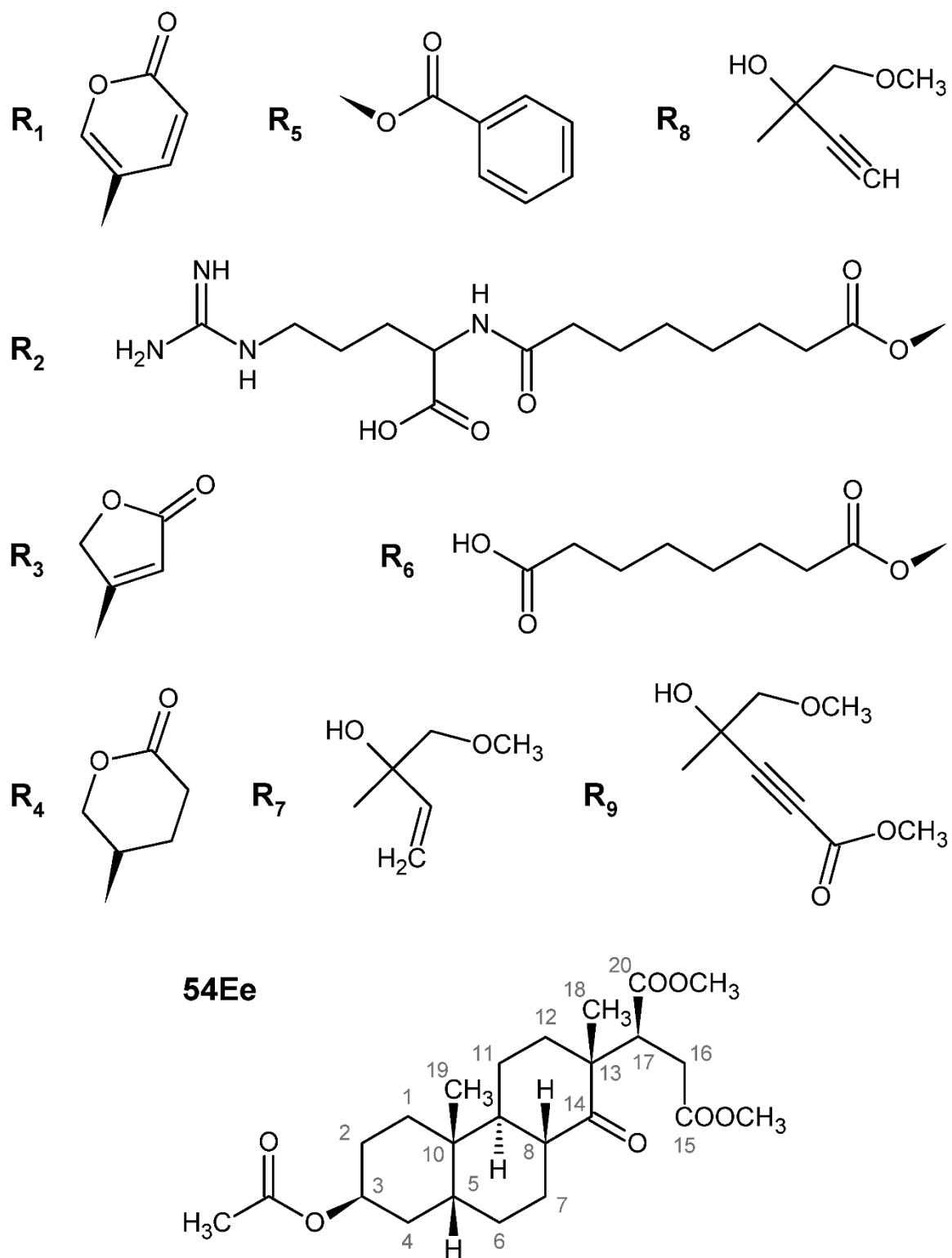


Figure 30: Structures of the bulky substituents (R<sub>1</sub>-R<sub>9</sub>) and of compound 54Ee listed in Table 15

*Verapamil, bufalin, and digoxin:*

These compounds were purchased from Sigma-Aldrich, Taufkirchen, Germany.

*Doxorubicin:*

Doxorubicin was kindly supplied from the Hospital Pharmacy, University of Mainz, Germany

*Cell culture media, reagents and disposable material***Table 16: Cell culture media, reagents and disposable material**

<b>Product</b>	<b>Supplier</b>
96-well, flat bottom cell culture microplate, clear, Nunclon®	Thermo Scientific, Germany
96 well, U-bottom tissue culture plates	Becton-Dickinson Biosciences, Germany
Cell culture flasks (25 cm <sup>2</sup> ), Nunclon®	Thermo Scientific, Germany
Cell culture flasks (75 cm <sup>2</sup> ), Nunclon®	Thermo Scientific, Germany
Centrifuge tube (15 ml)	Sarstedt, Germany
Centrifuge tube (50 ml)	Sarstedt, Germany
DPBS, no calcium, no magnesium	Life Technologies, Germany
FACS tubes	BD Biosciences, USA; Sarstedt, Germany
FACS tubes with cell strainer cap	BD Biosciences, USA
Fetal Bovine Serum (FBS)	Life Technologies, Germany
L-Glutamine	PAA Laboratories, Germany
Micro tubes (1.5 mL, 2.0 mL)	Sarstedt, Germany
Panserin 413	PAN-Biotech, Germany
Penicillin (10000 U/mL)/Streptomycin (10000 µg/mL)	Life Technologies, Germany
Phytohemagglutinin M form	Life Technologies, Germany
Pipette with tip (5 and 10 mL)	Greiner BIO-ONE, Germany
Pipette tip (10, 200 and 1250 µL)	Sarstedt, Germany
Roti® PVDF blot membrane (0.45 µm)	Roth, Germany
RPMI 1640	Life Technologies, Germany
RPMI 1640 without phenol red	PAA Laboratories, Germany
Trypsin-EDTA 0.25% (1×), phenol red	Life Technologies, Germany

*Chemicals, dyes, enzymes and kits***Table 17: Chemicals, dyes, antibodies, enzymes and kits**

<b>Product</b>	<b>Supplier</b>
30% acrylamide/bis solution 29:1	Bio-Rad, Germany
$\beta$ -Actin (13E5) rabbit mAb	Cell Signalling, Germany
Ammonium persulfate (APS)	Sigma-Aldrich, Germany
BD Gentest Human P-glycoprotein Membranes	Becton-Dickinson Biosciences, MA, USA
BD Control Membrane Preparation for ABC Transporters	Becton-Dickinson Biosciences, MA, USA
BD Gentest ATPase Assay Kit	Becton-Dickinson Biosciences, MA, USA
Bovine serum albumin (BSA)	Sigma-Aldrich, MO, USA
Bromophenol Blue	Merck, Germany
Bufalin	Sigma-Aldrich, Germany
Complete Mini Protease Inhibitor	Roche, Germany
CD243/P-glycoprotein mouse antibody C219	ThermoFischer Scientific, Germany
Digoxin	Sigma-Aldrich, Germany
Dimethyl sulfoxide (DMSO)	Sigma-Aldrich, Germany
Doxorubicin	JGU Medical Center, Germany
FITC-coupled anti-P-glycoprotein mouse antibody (17F9)	Becton-Dickinson Pharmingen, Germany
Glycine	AppliChem, Germany
Histopaque <sup>®</sup>	Sigma-Aldrich, Germany
HRP-linked anti-mouse IgG	Cell Signaling, Germany
HRP-linked anti-rabbit IgG	Cell Signaling, Germany
Hydrochloric Acid 37% (HCl)	AppliChem, Germany
Luminata <sup>TM</sup> Classico Western HRP substrate	Merck Millipore, Germany
MagicMark <sup>TM</sup> XP Western Standard	Life Technologies, CA, USA
Mayer's hemalum solution	Merk Millipore, Germany
Methanol	J. T. Baker, NJ, USA
Na <sup>+</sup> /K <sup>+</sup> -ATPase $\alpha$ 1 rabbit antibody	Cell Signaling, Germany
Radioimmunoprecipitation (RIPA) buffer	Sigma-Aldrich, Germany
Resazurin	Sigma-Aldrich, Germany
Sodium bicarbonate	Sigma-Aldrich, MO, USA
Sodium chloride	Grüssing, Germany
Sodium dodecyl sulfate (SDS)	J. T. Baker, NJ, USA
Tetramethylethylenediamine (TEMED)	AppliChem, Germany
Tris (hydroxymethyl) aminomethane (Tris)	AppliChem, Germany
Tween20	Sigma-Aldrich, Germany
$\beta$ -Mercaptoethanol	AppliChem, Germany
( $\pm$ )-verapamil hydrochloride	Sigma-Aldrich, Germany
Ultravision Quanto Detection System HRP	Thermo Scientific, Germany

*Technical equipment and software***Table 18: Technical equipment and software**

<b>Device</b>	<b>Supplier</b>
Adobe Photoshop CS5 v 12.0.0.2	Adobe Systems, USA
Alpha Innotech FluorChem Q system	Biozym, Germany
AutoDock 4.2 software	Molecular Graphics Laboratory, CA, USA
AutoDockTools 1.5.6rc3 software	Molecular Graphics Laboratory, CA, USA
AutoGrid 4.2 software	Molecular Graphics Laboratory, CA, USA
BD LSRFortessa cell analyzer	Becton-Dickinson Biosciences, CA, USA
BD High Throughput Sampler (HTS)	Becton-Dickinson Biosciences, CA, USA
BD FACSDiva software	Becton-Dickinson Biosciences, CA, USA
Centrifuge 5424	Eppendorf, Germany
ChemSketch	ACD, Canada
Coulter Counter Z1	Beckman Coulter, Germany
Eppendorf 8-channel electric pipette	Eppendorf, Germany
FlowJo software	FlowJo LLC, OR, USA
Forma Steri-Cult 3310 CO <sub>2</sub> -Incubator	Thermo Scientific, Germany
Heraeus Cytospin	Thermo Scientific, Germany
Heraeus Fresco 21 microcentrifuge	Thermo Scientific, Germany
Heraeus Labofuge 400 R centrifuge	Thermo Scientific, Germany
ImageJ 1.4.6	NIH, MD, USA
Infinite M2000 Pro™ plate reader	Tecan, Germany
Microsoft Office	Microsoft Corporation, WA, USA
Milli-Q ultrapure water purification system	Millipore, Germany
Mini-PROTEAN® Tetra Cell	Bio-Rad, Germany
MODELLER 9.11	University of California, CA, USA
Molecular Operating Environment (MOE) 2012.10	Chemical Computing Group Inc., Canada
NanoDrop 1000 Spectrophotometer	PEQLAB, Germany
Neubauer counting chamber	Marienfeld, Germany
Optika XDS-2 trinocular inverted microscope	Optika, Italy
PyMOL 1.3	Schroedinger LLC, USA
Precisa BJ2200C balance	Precisa Gravimetrics AG, Switzerland
REAX 2000 vortexer	Heidolph, Germany
Safe 2020 Biological Safety Cabinets	Thermo Scientific, Germany
Sartorius R 160 P balance	Sartorius, Germany
Sonorex RK 102 H Ultrasonic Cleaning Unit	Babdelin, Germany
Spectrafuge™ Mini Centrifuge	Labnet, Germany
SPSS Statistics version 22	IBM, NY, USA
SUB Aqua 26 waterbath	Grant Scientific, Germany
Thermomixer comfort	Eppendorf, Germany

Universal 32 R centrifuge  
VMD 1.9 software

Hettich, Germany  
University of Illinois at Urbana  
Champaign, IL, USA

---

## 6.2 Cell culture

Cells were grown in in a humidified, 5% CO<sub>2</sub>-containing incubator at 37°C. Passaging took place twice a week. Cells were counted using either Coulter Counter Z1 (Beckman Coulter) or a Neubauer counting chamber (Marienfeld). Experiments were carried out on cells in the logarithmic phase of growth.

### 6.2.1 Leukemia cell lines

CCRF-CEM and CEM/ADR5000 leukemia cell lines were generously provided by Prof. [REDACTED] (Department of Pediatrics, University of Jena, Jena, Germany). The parental CCRF-CEM cells are lymphoblastic leukemia cells, which were isolated from peripheral blood of a child with acute lymphoblastic leukemia [208]. Cells were maintained in RPMI 1640 medium (Life Technologies, Schwerte, Germany) containing phenol red and supplied with 10% fetal bovine serum (Life Technologies) and 1% penicillin [100 U/mL]-streptomycin [100 µg/mL] (Life Technologies). To ensure the multidrug-resistant phenotypes, the MDR1-expressing CEM/ADR5000 cells were treated with 5000 ng/mL doxorubicin on a weekly basis. Selection of multidrug sublines by certain cytostatics has been previously described [209]. The multidrug resistance profile of these cell lines has been reported [210]. For flow cytometry experiments, same conditions were applied, except for the use of culture medium lacking phenol red (PAA, Cölbe, Germany)

### 6.2.2 KB epidermal carcinoma cell lines

KB-3-1 are subclones of KB epidermal carcinoma cells that are derivatives of the HeLa cell line [211]. Multidrug-resistant KB-8-5 are generated by treatment with colchicine at 10 ng/mL [211]. Both cell lines were kindly provided by Prof. [REDACTED] (Hematology and Oncology Department, Medical Clinic at Munich Technical University, Munich, Germany). Cells were maintained in DMEM medium (Life Technologies) containing phenol red and supplied with 10% fetal bovine serum (Life Technologies) and 1% penicillin [100 U/mL]-streptomycin [100 µg/mL] (Life Technologies).

### 6.2.3 Non-tumor cells (human peripheral mononuclear cells PMNC)

Blood samples were collected from healthy donors at the University Hospital, Mainz, Germany. Subsequently, blood (6 mL) was directly layered over 6 mL Histopaque-1077 (Sigma-Aldrich) and centrifuged at  $400\times g$  for 30 min at room temperature. This centrifugation led to aggregation and sedimentation of erythrocytes. Lymphocytes and other mononuclear cells remained at the opaque plasma/Histopaque-1077 interface, which was collected and later washed by 20 mL Panserin 413 medium (PAN-Biotech, Germany) supplemented with 2% phytohemagglutinin M (Life technologies) and centrifugation at  $300\times g$  for 10 min. The supernatant, which contained platelets, was discarded and the cell pellet was resuspended with 10 mL culture medium. This step has been repeated and buffy coat cells were subsequently used for the resazurin viability assays described below.

### 6.3 Cytotoxicity assay

We used the resazurin reduction assay to detect cell viability. Only viable cells are able to reduce resazurin to the highly fluorescent resorufin via cellular oxidoreductases as can be seen in **Figure 31**. The fluorescence of resorufin can be measured simply by a microplate reader [212-214].

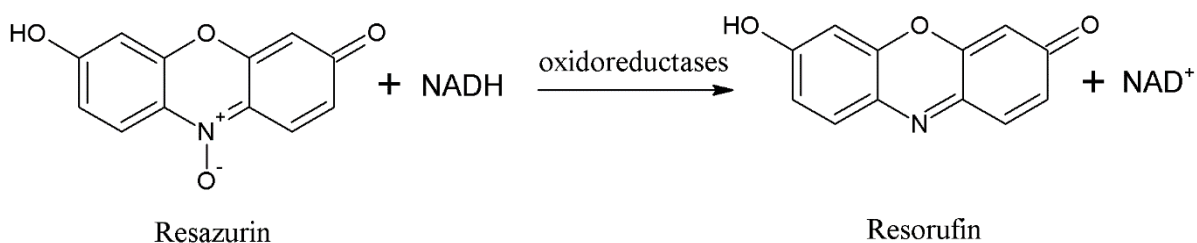


**Figure 31:** Reduction of resazurin to resorufin.

#### 6.3.1 Cytotoxicity of cardiotoxic steroids in sensitive and MDR leukemia cell lines

Both CCRF-CEM and CEM/ADR5000 cells were seeded in 96-well transparent flat-bottomed plates at a density of 20,000 cells/well with a final volume of 200  $\mu$ L. Compounds were tested in at least three independent experiments in two ranges each containing 10 concentrations (0.001, 0.003, 0.01, 0.03, 0.1, 0.3, 1, 3, 10, and 100  $\mu$ M) and (0.00003, 0.0001, 0.0003, 0.001, 0.003, 0.01, 0.03, 0.1, 0.3, and 1  $\mu$ M), respectively, to cover a wide concentration range. Doxorubicin and verapamil were used as control drugs. Each concentration was tested at least in triplicates within each single experiment. In all samples, the percentage of DMSO was kept at 1%. After an incubation of 72 h at 37°C and 5% CO<sub>2</sub>, 20  $\mu$ L of freshly prepared resazurin

0.01% (w/v) solution were added to each well. A further incubation for 4 h was applied and the plates were finally measured with a Tecan Reader Infinite m200 Pro (Crailsheim, Germany) at an excitation wavelength of 544 nm and an emission wavelength of 590 nm. Dose response curves were generated for each cardiotoxic steroids proportional to vehicle (DMSO in the case of cardiotoxic steroids and medium in the case of doxorubicin and verapamil)-treated cells as the 100% viability control.

### 6.3.2 Reversal of doxorubicin resistance by cardiotoxic steroids

CCRF-CEM and CEM/ADR5000 leukemia cells were seeded as described in the previous section. Doxorubicin was tested in six concentrations (0.1, 0.3, 1, 3, 10, and 100  $\mu\text{M}$ ) first alone and then in combination with the respective  $\text{IC}_{50}$  of each of the six cardiotoxic steroid derivatives. In the sensitive CCRF-CEM cells, concentrations of doxorubicin were (0.0003, 0.001, 0.003, 0.01, 0.1 and 1  $\mu\text{M}$ ). Same incubation and measurement conditions were applied as in the previous section. Experiments have been repeated at least twice each including three samples at each concentration. Dose response curves were generated for doxorubicin alone against untreated cells as 100% control and doxorubicin in combination with the respective cardiotoxic steroid derivatives against cells treated with the respective cardiotoxic steroid alone as 100% control.

## 6.4 Quantitative structure activity relationship (QSAR)

All compounds, for which  $\text{IC}_{50}$  values were obtained in both cell lines, were subjected to QSAR calculations. We separated the data into a training set of 33 compounds (bufalin, digoxin, 2G, 2M, 2P, 2c, 3D, 6B, 7B, 7E, 10O, 10S, 11M, 12A, 14D, 15i, 16D, 22N, 23A, 23D, 27F, 29b, 29C, 44F, 44G, 49d, 54E, 54Ee, 54e, 54r, 54v, 55K, and 62I) to build the model and a test set of 13 compounds (2C, 10I, 15c, 15d, 21E, 23G, 32A, 35B, 53R, 54C, 54T, 54 $\alpha$ , and 62N) to evaluate the model. MOE 2012.10 (Molecular Operating Environment, version: 2012.10, Chemical Computing Group Inc., Canada) was used to carry out the calculations. We chose six descriptors, in order to maintain the recommended training set chemicals:descriptors ratio of 5:1 [154]. These included number of H-bond acceptor atoms (a\_acc), number of rotatable bonds (b\_rotN), partition coefficient (logP (o/w)), total hydrophobic van der Waals surface area (PEOE\_VSA\_HYD), highest occupied molecular orbital (HOMO) energy (PM3\_HOMO), and lowest unoccupied molecular orbital (LUMO) energy (PM3\_LUMO). The correlation between experimental and predicted data was carried out using the partial least square (PLS) regression and the cross-validation using the leave-one-out (LOO) method.

## **6.5 Analysis of protein expression in sensitive and MDR leukemia cell lines**

### **6.5.1 Immunoblotting of P-glycoprotein and Na<sup>+</sup>/K<sup>+</sup>-ATPase**

#### **6.5.1.1 Protein extraction**

Proteins from CCRF-CEM, CEM/ADR5000, KB-3-1 and KB-8-5 cells were extracted by growing cells in 75 cm<sup>2</sup> tissue flasks for four days and then washing them with 20 mL DPBS. Afterwards, pellets were suspended in RIPA buffer (Sigma Aldrich) containing ½ tablet of complete Mini Protease Inhibitor (Roche, Mannheim, Germany). Cells were shaken 30 min at 4°C. Cell lysates were centrifuged at 14,000 × g for 15 min and supernatants were placed in new Eppendorf tubes. Concentrations of proteins were determined using NanoDrop1000 (PEQLAB, Erlangen, Germany).

#### **6.5.1.2 SDS-PAGE and western blot**

Proteins were separated on SDS-PAGE gels according to the method of Laemmli [215] using the Mini-PROTEAN® Tetra Cell system (Bio-Rad, Germany). In short, 30 µg protein were loaded in 6 × sample loading buffer (4 µL) and the volume was filled up to 24 µL with H<sub>2</sub>O. Before electrophoresis, samples were heated at 95°C for 10 min. Then, they were resolved on a 4% stacking gel atop the succeeding 10% running gel. The Magic Mark Western Blot Standard (Life Technologies) (3 µL) was run in parallel to estimate the protein size. Voltage was first set to 50 V through the stacking gel and then increased to 100 V till the end of electrophoresis. Proteins were then blotted onto a Roti®-PVDF membrane (Carl Roth, Karlsruhe, Germany) using the wet sandwich method. Blotting was performed at a 250 mA current for 1.5 h. The membrane was washed with Tris-buffered saline Tween 20 (TBS-T) thrice for 5 min and then blocked with 5% (w/v) bovine serum albumin (Sigma-Aldrich, Germany) for 1h. The membrane was again washed with TBS-T thrice for 5 min. For immunostaining, the following primary antibodies were used: rabbit Na<sup>+</sup>/K<sup>+</sup>-ATPase α1 antibody (Cell Signaling Technology, Frankfurt, Germany) at a dilution of 1:1000 (overnight incubation at 4°C) , mouse CD243/P-glycoprotein antibody C219 (ThermoFisher Scientific, Dreieich, Germany) at a dilution of 1:100 (overnight incubation at 4°C) and rabbit β-actin antibody (Cell Signaling Technology) at a dilution of 1:2000 (incubation at room temperature for 2 h). Secondary antibodies were HRP-linked anti-mouse and anti-rabbit IgG antibodies (Cell Signaling Technology), and were used accordingly at a dilution of 1:2000 for 1 h at room temperature. After incubations with primary and secondary antibodies, washing with TBS-T was applied. Finally, Luminata™ Classico Western HRP substrate (Merck Millipore,

Schwalbach, Germany) was added 5 min in the dark and pictures of the membrane were taken with an Alpha Innotech FluorChem Q system (Biozym, Oldendorf, Germany).

### 6.5.1.3 Gel and Buffer recipes

The above mentioned buffers were prepared using the following recipes:

**Table 19: Preparation of SDS-PAGE**

Stacking gel (4%)		Running gel (10%)	
H <sub>2</sub> O	3.075 mL	H <sub>2</sub> O	3.075 mL
0.5 M Tris-HCl (pH 6.8)	1.25 mL	1.5 M Tris-HCl (pH 8.8)	1.875 mL
20% SDS (w/v)	0.025 mL	20% SDS (w/v)	0.0375 mL
30% acrylamide/bis Solution, 29:1	0.67 mL	30% acrylamide/bis Solution, 29:1	2.475 mL
10% APS (w/v)	0.025 mL	10% APS (w/v)	0.0375 mL
TEMED	0.005 mL	TEMED	0.005 mL

**Table 20: Buffers for SDS-PAGE**

6 × sample loading buffer		Running buffer	
SDS	1.2 g	Tris-HCl	25 mM
Bromophenol Blue	0.006 g	Glycin	200 mM
Glycerol	4.7 mL	SDS (w/v)	0.1%
1 M Tris-HCl (pH 6.8)	0.6 mL	in H <sub>2</sub> O	
H <sub>2</sub> O	2.7 mL		
β-Mercaptoethanol (v/v)	5%		

**Table 21: Transfer buffer and washing buffer**

Transfer buffer (Towbin buffer)		Tris-buffered saline Tween 20 (TBS-T)	
Tris	25 mM	Tris-HCl (pH 7.5)	20 mM
Glycine	192 mM	NaCl	0.5 M
Methanol	20%	Tween 20 (w/v)	0.05%
in H <sub>2</sub> O		in H <sub>2</sub> O	

## 6.5.2 Analysis of P-glycoprotein expression by immunocytochemistry

Immunocytochemistry was performed with the aid of Ultravision Quanto Detection System HRP (Thermo Scientific). In brief, CCRF-CEM and CEM/ADR5000 cells were pelleted at 500×g for 10 min on a sterile slide with the help of Cytospin (Heraeus, Hanau, Germany). Cells were later fixed in 96% ethanol for 10 min and subsequently washed with phosphate buffered

saline. The slide was incubated 10 min with 0.3% hydrogen peroxide to prevent background staining that might occur via endogenous peroxidase. Ultra V block was applied for 5 min to inhibit unspecific binding. The primary antibody CD243/P-glycoprotein antibody C219 (ThermoFisher Scientific) was added at a dilution of 1:1000 and the slide was placed in a humidified chamber overnight. Washing with buffer succeeded after each of the three following steps. The slide was incubated with Primary Antibody Amplifier Quanto for 10 min. The HRP Polymer Quanto was added 10 min and then 30  $\mu$ L DAB Quanto Chromogen was added to 1 mL of DAB Quanto Substrate and incubated for 5 min. The slide was counterstained with Mayer's hemalum solution (Merck Millipore) to achieve nuclear staining. The slide was finally washed twice with buffer for five minutes and then rinsed with water, dehydrated and subjected to microscopy.

### **6.5.3 Analysis of P-glycoprotein expression by flow cytometry**

Both CCRF-CEM and CEM/ADR5000 cell lines were cultivated in a 75 cm<sup>2</sup> -flask until a cell density of about 10<sup>7</sup> cells/flask and then harvested and centrifuged at 1,200 rpm for 5 min. Cell pellets were washed twice with Staining Buffer (phosphate buffered saline with 5% fetal bovine serum). An aliquot of 20  $\mu$ L of the 17F9 FITC-coupled mouse anti-human P-glycoprotein antibody (Becton-Dickinson Pharmingen, Heidelberg, Germany), which binds to an external epitope and hence, no fixation of the cells required [216, 217], was directly added to 100  $\mu$ L of the cell suspension (10<sup>6</sup> cells) and the whole mix was incubated on ice for 20 min in the dark. Cells were washed twice with 500  $\mu$ L of the staining buffer. Non-stained cells of both cell lines were treated as controls. Cells were analyzed with an LSR-Fortessa FACS analyzer (Becton-Dickinson, Heidelberg, Germany). FITC fluorescence was measured with the blue laser at an excitation wavelength of 488 nm and emitted light was collected with a 530/30 nm bandpass filter. Dead cells were excluded by FSC/SSC gating. Cytographs and mean fluorescence values were analyzed with the help of FACSDiva software (Becton-Dickinson) and FlowJo software (Celeza, Olten, Switzerland).

### **6.6 Flow cytometry high throughput screening**

Doxorubicin (20  $\mu$ M) was used in all experiments as a substrate for P-glycoprotein and verapamil (20  $\mu$ M) as positive control for inhibition of P-glycoprotein mediated efflux [143]. To set up a desirable period of incubation for the screen, we have first tested verapamil at different time points (1, 2, 3, 6, 24, 48 and 72 h). Both CCRF-CEM and CEM/ADR5000 cells were seeded in complete RPMI 1640 culture medium lacking the indicator phenol red in 96

well, U-bottomed tissue culture plates (Becton-Dickinson) at a density of  $4 \times 10^4$  cells per well. Directly before each measurement, treatment medium was removed by centrifugation at 1200 rpm for 5 min and cell pellets were resuspended with the same medium mentioned above. Each compound has been tested on CEM/ADR5000 cells only at two concentrations based on the  $IC_{50}$  values from previous resazurin reduction assays: high concentration ( $IC_{50} \times 5$ ) and low concentration ( $IC_{50}/5$ ) (for compound 15S and others, which were found non-cytotoxic, we chose a concentration of (13  $\mu$ M) as a hypothetical  $IC_{50}$  value, based on calculating the mean  $IC_{50}$  value of all 66 compounds on CEM/ADR5000 cells. Measurements were carried out with a high throughput sampler (Becton-Dickenson) connected to an LSR-Fortessa FACS analyzer (Becton-Dickinson). Doxorubicin fluorescence was excited with the yellow green laser at a wavelength of 561 nm and emitted light was collected with a 610/20 nm bandpass filter. Dead cells and cell debris were excluded by FSC/SSC gating. All flow cytometry experiments were carried out in two independent experiments with at least two repetitions within the experiment. Cytographs and mean fluorescence values were analyzed with the help of FACSDiva software (Becton-Dickinson) and FlowJo software (Celeza).

### 6.7 P-glycoprotein-ATPase assay

Human P-glycoprotein expressing membranes prepared from baculovirus infected insect cells were purchased from (Beckton Dickenson Biosciences). First, the expression of P-glycoprotein was checked in comparison to BD control membranes lacking P-glycoprotein via SDS-PAGE and immunoblotting (**Figure 24 A**) following the same exact protocol mentioned in section 6.5.1.2. Then, P-glycoprotein-ATPase assay was carried with the aid of BD Gentest ATPase Assay kit. Briefly, a 60  $\mu$ L reaction mixture composed of 20  $\mu$ g membranes, the desired concentration of the drug (in the case of verapamil, the concentration was 20  $\mu$ M, whereas cardiotonic steroid derivatives were used at 50  $\mu$ M in order to obtain an observable effect), and 4 mM MgATP in assay buffer containing 50 mM Tris-MES, 2 mM ouabain, 2mM EGTA, 50 mM KCL, 2 mM dithiothreitol and 5 mM sodium azide was incubated for 20 min at 37°C. SDS 10% (30  $\mu$ L) was added to each well to stop the reaction. Afterwards a color reagent (35 mM ammonium molybdate in 15 mM zinc acetate: 10 % ascorbic acid (1:4)) was added to each well at a volume of 200  $\mu$ L. A further incubation of 20 min followed and at the end the absorption of liberated inorganic phosphate was measured using Tecan Reader Infinite m200 Pro. Nunc transparent flat-bottomed plates were used throughout the measurements.

## 6.8 Molecular docking

### 6.8.1 Molecular docking of cardiotonic steroids into Na<sup>+</sup>/K<sup>+</sup>-ATPase

Porcine Na<sup>+</sup>/K<sup>+</sup>-ATPase (Uniprot ID P05024) possesses a 98.3 % sequence identity to the human homologue (P05023). Since the crystal structure of the human protein has not yet been determined, the crystal structure of porcine Na<sup>+</sup>/K<sup>+</sup>-ATPase co-crystalized with ouabain (PDB ID: 4HYT, Protein Data Bank, <http://www.rcsb.org>) was used for docking. All non-protein atoms were deleted. Using AutodockTools-1.5.6rc3, the file was subsequently converted to the pdbqt format to perform molecular docking by Autodock4. All 2D structures of cardiotonic steroids were drawn and later energy-minimized into 3D structures using Corina Online Demo ([https://www.molecular-networks.com/online\\_demos/corina\\_demo](https://www.molecular-networks.com/online_demos/corina_demo)). A grid box in which the docking took place was constructed around the binding site of ouabain in a way that the ligand could freely move in the corresponding space (coordinates of the three dimensions [gridcenter]: X: -27.573, Y: 20.379 and Z: -71.529; number of grid points in the three dimensions [npts]: X: 90, Y: 80 and Z: 122; spacing: 0.375). The default docking parameters were kept except for changing the maximum number of energy evaluations [ga\_num\_evals] to 25,000,000 and the number of runs [ga\_run] to 250. The results were written in dlq files, which were later used to analyse the binding energies and the interacting amino acids for each ligand.

### 6.8.2 Utilization of molecular docking in P-glycoprotein research

#### 6.8.2.1 Ligand selection and preparation

The ligands to be docked were classified into three separate groups: substrates, modulators and non-substrates. This classification has been based on literature reviews [79, 203, 218]. Other ligands that are not found in those reviews, (e.g. some non-substrates) have been checked each for no interactions with P-glycoprotein. In this way, the substrates-, the modulators- and the non-interacting ligands- sets contained 22, 26 and 15 ligands respectively. When possible, 3D structures were directly downloaded from Pubchem (<https://pubchem.ncbi.nlm.nih.gov/>). Otherwise, the 2D structures were drawn and later energy-minimized into 3D structures using Corina Online Demo ([https://www.molecular-networks.com/online\\_demos/corina\\_demo](https://www.molecular-networks.com/online_demos/corina_demo)). All 3D structures were saved in PDB format ready to be docked. **Table 22** below shows the ligands classified in the respective groups.

**Table 22:** Classification of ligands into substrates, modulators and non-substrates of P-glycoprotein.

<b>substrates</b>	<b>Modulators</b>	<b>non-substrates</b>
colchicine	agosterol A	5-flurouracile
daunorubicin	Amiodarone	Carmustin
dexamethasone	Amorinin	Chlorambucil
digoxin	Apigenin	cyslophosphamide
docetaxel	biochanin A	Cytarabin
doxorubicin	Biricodar	Dacarbazine
etoposide	catechine	Hydroxyurea
fexfenadione	cefoperazone	Lomustine
Hoechst 33342	Chrysine	Melphalan
irinotecan	cyclosporine	mercaptopurine
kaempferol	Diltiazem	Pentostatin
loperamide	ginsenoside	procarbazine
mitomycin C	naringenin	temozolamide
ondanesterone	Phloretin	thioguanine
paclitaxel	Quercetin	Treosulfan
procyanidin B2	Quinine	
rhodamine 123	rotenone	
tenoposide	sakuranetin	
topotecan	Sesamin	
vinblastine	sinensetin	
vincristine	stigmasterol	
vinorelbine	syringaresinol	
	tamoxifen	
	tariquidar	
	valsopodar	
	verapamil	

### 6.8.2.2 Homology modeling of human P-glycoprotein<sup>6</sup>

The structure of human P-glycoprotein was previously constructed by us [219] using homology modelling with the x-ray crystallography-based structure of the mouse P-glycoprotein as a template structure. The latter was retrieved from the Protein Data Bank (www.pdb.org) (PDB

<sup>6</sup> The modeling of human P-glycoprotein was conducted by my colleague [REDACTED], Department of Pharmaceutical Biology, University of Mainz.

code: 3G60). Afterwards, both sequences were aligned using the EMBOSS needle ([http://www.ebi.ac.uk/Tools/psa/emboss\\_needle/](http://www.ebi.ac.uk/Tools/psa/emboss_needle/)) and subsequently homology models were created using the alignment file with the help of MODELLER 9.11 and Swiss MODEL alignment mode. The Swiss-MODEL structure assessment tool was then used to select the best homology model, which was then used to conduct the molecular docking studies.

### **6.8.2.3 Molecular docking**

Molecular docking was conducted following a protocol previously reported by us [220]. In brief, the X-ray crystallography-based structure of mouse P-glycoprotein and the homology modelled structure of human P-glycoprotein were set as the rigid receptor molecule. For the x-ray crystallography-based structures was first processed with AutodockTools-1.5.6rc3 [221] to toggle problems of incomplete structures due to missing atoms or waters and may include multimers or interaction partners of the receptor molecule. The output file after preparation was in PDBQT format, where information about atomic partial charges, torsion degrees of freedom and different atom types were added, e.g. aliphatic and aromatic carbon atoms or polar atoms forming hydrogen bonds.

A grid box was then constructed to define docking spaces. The dimensions of the grid box were set around the whole P-glycoprotein molecule as such that the ligand could freely move and rotate in the docking space (3D coordinates [gridcenter]: X: 29.265, Y: 82.480 and Z: 49.877). The grid box consisted of 126 grid points in all 3 dimensions (X,Y and Z) separated by a distance of 1 Å between each one.

Energies at each grid point were then evaluated for each atom type present in the ligand, and the values were then used to predict the energy of a particular ligand configuration. Docking parameters were set to 100 runs and 2,500,000 energy evaluations for each cycle. Docking was performed by Autodock4 [221] using the Lamarckian Algorithm. The corresponding binding energies and the number of conformations in each cluster were attained from the docking log files (dlg).

### **6.8.3 Molecular docking of P-glycoprotein-modulating cardiotonic steroids**

Molecular docking was carried out in a similar approach as in section 6.8.2.3. In short, the PDB file of the homology modelled human P-glycoprotein structure (built upon the crystal structure of mouse P-glycoprotein; PDB code: 3G60; section 6.8.2.2) was converted to PDBQT format using AutodockTools-1.5.6rc3 and was set as the macromolecule, upon which docking is to be

performed. 2D structures of the ligands were constructed and later converted to 3D structures using Corina Online Demo. A grid box was allocated to define docking spaces upon the macromolecule (3D coordinates at TMD [gridcenter]: X: 24.905, Y: 62.689 and Z: 31.320 with 120, 116 and 124 grid points in each coordinate respectively and 0.375 Å spacing; 3D coordinates at NBD [gridcenter]: X: 36.321, Y: 104.368 and Z: 70.408 with 120, 116 and 124 grid points in each coordinate respectively and 0.458 Å spacing). Energies for each atom type in the ligand were calculated at each grid point using Autogrid 4.2. These calculated energies were later used to predict binding energies for each ligand. Docking was carried out using Autodock 4.2 with 250 runs and 2.5 million evaluations for each cycle via the Lamarckian algorithm. Lowest binding energies were retrieved from the correspondent dlG file and amino acids were analyzed by AutodockTools. Images were created using Visual Molecular Dynamics VMD.

### **6.1 Next generation sequencing<sup>7</sup>**

Total RNA was isolated from CCRF-CEM and CEM/ADR5000 cells using Invitrap® Spin Universal RNA Mini Kit (STRATEC Molecular GmbH, Berlin, Germany). Both quality and quantity of total RNA were tested using an Agilent Bioanalyzer 2100 and Qubit Fluorometer (Life Technologies). To exclude rRNA and tRNA and consider only mRNA [222], Poly A+ RNA were isolated and fractionated. Afterwards, double stranded cDNA was synthesized using the TruSeq RNA sample prep v2 protocol (Illumina Inc., San Diego, CA). End-repaired, A-tailed and Adaptor-ligated cDNA was PCR-amplified via 10 cycles. The library was subject to sequencing in paired-end mode (2 x 100 bp) using 0.4 lane of an Illumina HiSeq 2000 flowcell. Transcripts were quantified using the reads per kilo base of exon model per million mapped reads (RPKM) measure [223]. Deregulations of transcripts in MDR cells were calculated by dividing RPKM values in CEM/ADR5000 cells by those in CCRF-CEM cells.

---

<sup>7</sup> Experimental procedures of next generation sequencing were carried out at GENterprise GENOMICS and the Institute of Molecular Genetics, Mainz, Germany

## 7 References

- [1] A. K. Tiwari and H. K. Roy, "Progress against cancer (1971-2011): how far have we come?," *J Intern Med*, vol. 271, pp. 392-9, Apr 2012.
- [2] A. Jemal, F. Bray, M. M. Center, J. Ferlay, E. Ward, and D. Forman, "Global cancer statistics," *CA Cancer J Clin*, vol. 61, pp. 69-90, 2011 Mar-Apr 2011.
- [3] J. Ferlay, H. R. Shin, F. Bray, D. Forman, C. Mathers, and D. M. Parkin, "Estimates of worldwide burden of cancer in 2008: GLOBOCAN 2008," *Int J Cancer*, vol. 127, pp. 2893-917, Dec 2010.
- [4] R. RW, *Cancer Biology*, 4th ed.: Oxford University Press, 2007.
- [5] D. Hanahan and R. A. Weinberg, "Hallmarks of cancer: the next generation," *Cell*, vol. 144, pp. 646-74, Mar 2011.
- [6] M. G. Vander Heiden, L. C. Cantley, and C. B. Thompson, "Understanding the Warburg effect: the metabolic requirements of cell proliferation," *Science*, vol. 324, pp. 1029-33, May 2009.
- [7] S. Sharma, T. K. Kelly, and P. A. Jones, "Epigenetics in cancer," *Carcinogenesis*, vol. 31, pp. 27-36, Jan 2010.
- [8] B. A. Chabner and D. L. Longo, *Cancer Chemotherapy and Biotherapy: Principles and Practice*, 5th ed.: Lippincott Williams & Wilkins, 2011.
- [9] R. Hickey, M. Vouche, D. Y. Sze, E. Hohlastos, J. Collins, T. Schirmang, *et al.*, "Cancer concepts and principles: primer for the interventional oncologist-part II," *J Vasc Interv Radiol*, vol. 24, pp. 1167-88, Aug 2013.
- [10] M. Reed, "Principles of cancer treatment by surgery," *Surgery (Oxford)*, vol. 27, pp. 178-181, 2009.
- [11] R. Baskar, K. A. Lee, R. Yeo, and K. W. Yeoh, "Cancer and radiation therapy: current advances and future directions," *Int J Med Sci*, vol. 9, pp. 193-9, 2012.
- [12] B. A. Chabner and T. G. Roberts, "Timeline: Chemotherapy and the war on cancer," *Nat Rev Cancer*, vol. 5, pp. 65-72, Jan 2005.
- [13] V. T. DeVita and E. Chu, "A history of cancer chemotherapy," *Cancer Res*, vol. 68, pp. 8643-53, Nov 2008.
- [14] B. G. Katzung, *Basic and Clinical Pharmacology*, 10th ed.: McGraw-Hill, 2007.
- [15] A. F. Schott and D. F. Hayes, "Defining the benefits of neoadjuvant chemotherapy for breast cancer," *J Clin Oncol*, vol. 30, pp. 1747-9, May 2012.
- [16] R. D. Howland and M. J. Mycek, *Lippincott's Illustrated Reviews: Pharmacology*, 3rd ed.: Lippincott Williams & Wilkins, 2006.
- [17] K. Lotfi-Jam, M. Carey, M. Jefford, P. Schofield, C. Charleson, and S. Aranda, "Nonpharmacologic strategies for managing common chemotherapy adverse effects: a systematic review," *J Clin Oncol*, vol. 26, pp. 5618-29, Dec 2008.
- [18] Y. Chen, P. Jungsuwadee, M. Vore, D. A. Butterfield, and D. K. St Clair, "Collateral damage in cancer chemotherapy: oxidative stress in nontargeted tissues," *Mol Interv*, vol. 7, pp. 147-56, Jun 2007.
- [19] R. V. Chari, "Targeted cancer therapy: conferring specificity to cytotoxic drugs," *Acc Chem Res*, vol. 41, pp. 98-107, Jan 2008.
- [20] M. Huang, A. Shen, J. Ding, and M. Geng, "Molecularly targeted cancer therapy: some lessons from the past decade," *Trends Pharmacol Sci*, vol. 35, pp. 41-50, Jan 2014.
- [21] S. Mondal, S. Bandyopadhyay, M. K. Ghosh, S. Mukhopadhyay, S. Roy, and C. Mandal, "Natural products: promising resources for cancer drug discovery," *Anticancer Agents Med Chem*, vol. 12, pp. 49-75, Jan 2012.
- [22] H. F. Ji, X. J. Li, and H. Y. Zhang, "Natural products and drug discovery. Can thousands of years of ancient medical knowledge lead us to new and powerful drug combinations in the fight against cancer and dementia?," *EMBO Rep*, vol. 10, pp. 194-200, Mar 2009.
- [23] J. Mann, "Natural products in cancer chemotherapy: past, present and future," *Nat Rev Cancer*, vol. 2, pp. 143-8, Feb 2002.
- [24] I. S. JOHNSON, J. G. ARMSTRONG, M. GORMAN, and J. P. BURNETT, "THE VINCA ALKALOIDS: A NEW CLASS OF ONCOLYTIC AGENTS," *Cancer Res*, vol. 23, pp. 1390-427, Sep 1963.
- [25] A. L. Demain and P. Vaishnav, "Natural products for cancer chemotherapy," *Microb Biotechnol*, vol. 4, pp. 687-99, Nov 2011.
- [26] D. J. Newman and G. M. Cragg, "Natural products as sources of new drugs over the 30 years from 1981 to 2010," *J Nat Prod*, vol. 75, pp. 311-35, Mar 2012.
- [27] D. J. Newman, "Natural products as leads to potential drugs: an old process or the new hope for drug discovery?," *J Med Chem*, vol. 51, pp. 2589-99, May 2008.
- [28] L. Krenn and B. Kopp, "Bufadienolides from animal and plant sources," *Phytochemistry*, vol. 48, pp. 1-29, May 1998.

- [29] I. Prassas and E. P. Diamandis, "Novel therapeutic applications of cardiac glycosides," *Nat Rev Drug Discov*, vol. 7, pp. 926-35, Nov 2008.
- [30] T. Mijatovic, E. Van Quaquebeke, B. Delest, O. Debeir, F. Darro, and R. Kiss, "Cardiotonic steroids on the road to anti-cancer therapy," *Biochim Biophys Acta*, vol. 1776, pp. 32-57, Sep 2007.
- [31] S. Norn and P. R. Kruse, "[Cardiac glycosides: From ancient history through Withering's foxglove to endogeneous cardiac glycosides]," *Dan Medicinhist Arbog*, pp. 119-32, 2004.
- [32] R. A. Newman, P. Yang, A. D. Pawlus, and K. I. Block, "Cardiac glycosides as novel cancer therapeutic agents," *Mol Interv*, vol. 8, pp. 36-49, Feb 2008.
- [33] A. Y. Bagrov, J. I. Shapiro, and O. V. Fedorova, "Endogenous cardiotonic steroids: physiology, pharmacology, and novel therapeutic targets," *Pharmacol Rev*, vol. 61, pp. 9-38, Mar 2009.
- [34] A. D. Garg, R. V. Hippargi, and A. N. Gandhare, "Toad skin-secretions: potent source of pharmacologically and therapeutically significant compounds," *Internet Journal of Pharmacology*, vol. 5(2), 2008.
- [35] S. H. Rahimtoola and T. Tak, "The use of digitalis in heart failure," *Curr Probl Cardiol*, vol. 21, pp. 781-853, Dec 1996.
- [36] R. J. Simpson, "Assessing the safety of drugs through observational research," *Heart*, vol. 94, pp. 129-30, Feb 2008.
- [37] W. Schönfeld, J. Weiland, C. Lindig, M. Masnyk, M. M. Kabat, A. Kurek, *et al.*, "The lead structure in cardiac glycosides is 5 beta, 14 beta-androstane-3 beta 14-diol," *Naunyn Schmiedeberts Arch Pharmacol*, vol. 329, pp. 414-26, Jun 1985.
- [38] A. A. Agrawal, G. Petschenka, R. A. Bingham, M. G. Weber, and S. Rasmann, "Toxic cardenolides: chemical ecology and coevolution of specialized plant-herbivore interactions," *New Phytol*, vol. 194, pp. 28-45, Apr 2012.
- [39] L. Moreno Y Banuls, A. Katz, W. Miklos, A. Cimmino, D. M. Tal, E. Ainbinder, *et al.*, "Hellebrin and its aglycone form hellebrigenin display similar in vitro growth inhibitory effects in cancer cells and binding profiles to the alpha subunits of the Na<sup>+</sup>/K<sup>+</sup>-ATPase," *Mol Cancer*, vol. 12, p. 33, 2013.
- [40] C. P. Melero, M. Medarde, and A. San Feliciano, "A Short Review on Cardiotonic Steroids and Their Aminoguanide Analogues," *Molecules*, vol. 5, pp. 51-81, 2000.
- [41] T. Clausen, "Acute stimulation of Na/K pump by cardiac glycosides in the nanomolar range," *J Gen Physiol*, vol. 119, pp. 295-6, Apr 2002.
- [42] H. A. Elbaz, T. A. Stueckle, W. Tse, Y. Rojanasakul, and C. Z. Dinu, "Digitoxin and its analogs as novel cancer therapeutics," *Exp Hematol Oncol*, vol. 1, p. 4, 2012.
- [43] C. Toyoshima, R. Kanai, and F. Cornelius, "First crystal structures of Na<sup>+</sup>,K<sup>+</sup>-ATPase: new light on the oldest ion pump," *Structure*, vol. 19, pp. 1732-8, Dec 2011.
- [44] G. Blanco and R. W. Mercer, "Isozymes of the Na-K-ATPase: heterogeneity in structure, diversity in function," *Am J Physiol*, vol. 275, pp. F633-50, Nov 1998.
- [45] I. Dostanic-Larson, J. N. Lorenz, J. W. Van Huysse, J. C. Neumann, A. E. Moseley, and J. B. Lingrel, "Physiological role of the alpha1- and alpha2-isoforms of the Na<sup>+</sup>-K<sup>+</sup>-ATPase and biological significance of their cardiac glycoside binding site," *Am J Physiol Regul Integr Comp Physiol*, vol. 290, pp. R524-8, Mar 2006.
- [46] J. B. Lingrel, M. T. Williams, C. V. Vorhees, and A. E. Moseley, "Na,K-ATPase and the role of alpha isoforms in behavior," *J Bioenerg Biomembr*, vol. 39, pp. 385-9, Dec 2007.
- [47] P. Yang, D. G. Menter, C. Cartwright, D. Chan, S. Dixon, M. Suraokar, *et al.*, "Oleandrin-mediated inhibition of human tumor cell proliferation: importance of Na,K-ATPase alpha subunits as drug targets," *Mol Cancer Ther*, vol. 8, pp. 2319-28, Aug 2009.
- [48] J. Wang, J. B. Velotta, A. A. McDonough, and R. A. Farley, "All human Na<sup>(+)</sup>-K<sup>(+)</sup>-ATPase alpha-subunit isoforms have a similar affinity for cardiac glycosides," *Am J Physiol Cell Physiol*, vol. 281, pp. C1336-43, Oct 2001.
- [49] J. Müller-Ehmsen, P. Juvvadi, C. B. Thompson, L. Tumyan, M. Croyle, J. B. Lingrel, *et al.*, "Ouabain and substrate affinities of human Na<sup>(+)</sup>-K<sup>(+)</sup>-ATPase alpha(1)beta(1), alpha(2)beta(1), and alpha(3)beta(1) when expressed separately in yeast cells," *Am J Physiol Cell Physiol*, vol. 281, pp. C1355-64, Oct 2001.
- [50] O. I. Shamraj, I. L. Grupp, G. Grupp, D. Melvin, N. Gradoux, W. Kremers, *et al.*, "Characterisation of Na/K-ATPase, its isoforms, and the inotropic response to ouabain in isolated failing human hearts," *Cardiovasc Res*, vol. 27, pp. 2229-37, Dec 1993.
- [51] L. Yatime, M. Laursen, J. P. Morth, M. Esmann, P. Nissen, and N. U. Fedosova, "Structural insights into the high affinity binding of cardiotonic steroids to the Na<sup>+</sup>,K<sup>+</sup>-ATPase," *J Struct Biol*, vol. 174, pp. 296-306, May 2011.
- [52] O. Vagin, L. A. Dada, E. Tokhtaeva, and G. Sachs, "The Na-K-ATPase  $\alpha_1\beta_1$  heterodimer as a cell adhesion molecule in epithelia," *Am J Physiol Cell Physiol*, vol. 302, pp. C1271-81, May 2012.
- [53] L. D. Faller, "Mechanistic studies of sodium pump," *Arch Biochem Biophys*, vol. 476, pp. 12-21, Aug 2008.

- [54] T. Mijatovic, F. Dufrasne, and R. Kiss, "Cardiotonic steroids-mediated targeting of the Na(+)/K(+)-ATPase to combat chemoresistant cancers," *Curr Med Chem*, vol. 19, pp. 627-46, 2012.
- [55] D. Goodsell, "Molecule of the Month: Sodium-Potassium Pump," in *Protein Data Bank (PDB)*, ed, 2009.
- [56] A. Gomes, P. Bhattacharjee, R. Mishra, A. K. Biswas, S. C. Dasgupta, and B. Giri, "Anticancer potential of animal venoms and toxins," *Indian J Exp Biol*, vol. 48, pp. 93-103, Feb 2010.
- [57] M. Slingerland, C. Cerella, H. J. Guchelaar, M. Diederich, and H. Gelderblom, "Cardiac glycosides in cancer therapy: from preclinical investigations towards clinical trials," *Invest New Drugs*, vol. 31, pp. 1087-94, Aug 2013.
- [58] O. Shiratori, "Growth inhibitory effect of cardiac glycosides and aglycones on neoplastic cells: in vitro and in vivo studies," *Gan*, vol. 58, pp. 521-8, Dec 1967.
- [59] B. Stenkvist, E. Bengtsson, O. Eriksson, J. Holmquist, B. Nordin, and S. Westman-Naeser, "Cardiac glycosides and breast cancer," *Lancet*, vol. 1, p. 563, Mar 1979.
- [60] B. Stenkvist, E. Bengtsson, G. Eklund, O. Eriksson, J. Holmquist, B. Nordin, *et al.*, "Evidence of a modifying influence of heart glucosides on the development of breast cancer," *Anal Quant Cytol*, vol. 2, pp. 49-54, 1980 Mar-Apr 1980.
- [61] T. Mijatovic and R. Kiss, "Cardiotonic Steroids-Mediated Na+/K+-ATPase Targeting Could Circumvent Various Chemoresistance Pathways," *Planta Med*, vol. 79, pp. 189-198, Mar 2013.
- [62] C. D. Simpson, I. A. Mawji, K. Anyiwe, M. A. Williams, X. Wang, A. L. Venugopal, *et al.*, "Inhibition of the sodium potassium adenosine triphosphatase pump sensitizes cancer cells to anoikis and prevents distant tumor formation," *Cancer Res*, vol. 69, pp. 2739-47, Apr 2009.
- [63] M. Liang, J. Tian, L. Liu, S. Pierre, J. Liu, J. Shapiro, *et al.*, "Identification of a pool of non-pumping Na/K-ATPase," *J Biol Chem*, vol. 282, pp. 10585-93, Apr 2007.
- [64] H. Wang, M. Haas, M. Liang, T. Cai, J. Tian, S. Li, *et al.*, "Ouabain assembles signaling cascades through the caveolar Na+/K+-ATPase," *J Biol Chem*, vol. 279, pp. 17250-9, Apr 2004.
- [65] J. Liu, J. Tian, M. Haas, J. I. Shapiro, A. Askari, and Z. Xie, "Ouabain interaction with cardiac Na+/K+-ATPase initiates signal cascades independent of changes in intracellular Na+ and Ca2+ concentrations," *J Biol Chem*, vol. 275, pp. 27838-44, Sep 2000.
- [66] A. N. Nguyen, K. Jansson, G. Sánchez, M. Sharma, G. A. Reif, D. P. Wallace, *et al.*, "Ouabain activates the Na-K-ATPase signalosome to induce autosomal dominant polycystic kidney disease cell proliferation," *Am J Physiol Renal Physiol*, vol. 301, pp. F897-906, Oct 2011.
- [67] D. Li, X. Qu, K. Hou, Y. Zhang, Q. Dong, Y. Teng, *et al.*, "PI3K/Akt is involved in bufalin-induced apoptosis in gastric cancer cells," *Anticancer Drugs*, vol. 20, pp. 59-64, Jan 2009.
- [68] T. Mijatovic, A. Op De Beeck, E. Van Quaquebeke, J. Dewelle, F. Darro, Y. de Launoit, *et al.*, "The cardenolide UNBS1450 is able to deactivate nuclear factor kappaB-mediated cytoprotective effects in human non-small cell lung cancer cells," *Mol Cancer Ther*, vol. 5, pp. 391-9, Feb 2006.
- [69] Z. Yuan, T. Cai, J. Tian, A. V. Ivanov, D. R. Giovannucci, and Z. Xie, "Na/K-ATPase tethers phospholipase C and IP3 receptor into a calcium-regulatory complex," *Mol Biol Cell*, vol. 16, pp. 4034-45, Sep 2005.
- [70] S. V. Pierre and Z. Xie, "The Na,K-ATPase receptor complex: its organization and membership," *Cell Biochem Biophys*, vol. 46, pp. 303-16, 2006.
- [71] M. Ameyar, M. Wisniewska, and J. B. Weitzman, "A role for AP-1 in apoptosis: the case for and against," *Biochimie*, vol. 85, pp. 747-52, Aug 2003.
- [72] K. Takeuchi, Y. Motoda, and F. Ito, "Role of transcription factor activator protein 1 (AP1) in epidermal growth factor-mediated protection against apoptosis induced by a DNA-damaging agent," *FEBS J*, vol. 273, pp. 3743-55, Aug 2006.
- [73] J. Liu and Z. J. Xie, "The sodium pump and cardiotonic steroids-induced signal transduction protein kinases and calcium-signaling microdomain in regulation of transporter trafficking," *Biochim Biophys Acta*, vol. 1802, pp. 1237-45, Dec 2010.
- [74] P. Kometiani, L. Liu, and A. Askari, "Digitalis-induced signaling by Na+/K+-ATPase in human breast cancer cells," *Mol Pharmacol*, vol. 67, pp. 929-36, Mar 2005.
- [75] L. Moreno Y Banuls, E. Urban, M. Gelbcke, F. Dufrasne, B. Kopp, R. Kiss, *et al.*, "Structure-activity relationship analysis of bufadienolide-induced in vitro growth inhibitory effects on mouse and human cancer cells," *J Nat Prod*, vol. 76, pp. 1078-84, Jun 2013.
- [76] M. M. Gottesman, "Mechanisms of cancer drug resistance," *Annu Rev Med*, vol. 53, pp. 615-27, 2002.
- [77] C. Holohan, S. Van Schaeybroeck, D. B. Longley, and P. G. Johnston, "Cancer drug resistance: an evolving paradigm," *Nat Rev Cancer*, vol. 13, pp. 714-26, Oct 2013.
- [78] M. M. Gottesman, T. Fojo, and S. E. Bates, "Multidrug resistance in cancer: role of ATP-dependent transporters," *Nat Rev Cancer*, vol. 2, pp. 48-58, Jan 2002.
- [79] C. H. Choi, "ABC transporters as multidrug resistance mechanisms and the development of chemosensitizers for their reversal," *Cancer Cell Int*, vol. 5, p. 30, Oct 2005.

- [80] R. Krishna and L. D. Mayer, "Multidrug resistance (MDR) in cancer. Mechanisms, reversal using modulators of MDR and the role of MDR modulators in influencing the pharmacokinetics of anticancer drugs," *Eur J Pharm Sci*, vol. 11, pp. 265-83, Oct 2000.
- [81] V. Ling, "Multidrug resistance: molecular mechanisms and clinical relevance," *Cancer Chemother Pharmacol*, vol. 40 Suppl, pp. S3-8, 1997.
- [82] G. Szakács, J. K. Paterson, J. A. Ludwig, C. Booth-Genthe, and M. M. Gottesman, "Targeting multidrug resistance in cancer," *Nat Rev Drug Discov*, vol. 5, pp. 219-34, Mar 2006.
- [83] G. Szakács, M. D. Hall, M. M. Gottesman, A. Boumendjel, R. Kachadourian, B. J. Day, *et al.*, "Targeting the Achilles heel of multidrug-resistant cancer by exploiting the fitness cost of resistance," *Chem Rev*, vol. 114, pp. 5753-74, Jun 2014.
- [84] C. F. Higgins, "Multiple molecular mechanisms for multidrug resistance transporters," *Nature*, vol. 446, pp. 749-57, Apr 2007.
- [85] V. Vasiliou, K. Vasiliou, and D. W. Nebert, "Human ATP-binding cassette (ABC) transporter family," *Hum Genomics*, vol. 3, pp. 281-90, Apr 2009.
- [86] J. P. Gillet, T. Efferth, and J. Remacle, "Chemotherapy-induced resistance by ATP-binding cassette transporter genes," *Biochim Biophys Acta*, vol. 1775, pp. 237-62, Jun 2007.
- [87] J. P. Gillet and M. M. Gottesman, "Advances in the molecular detection of ABC transporters involved in multidrug resistance in cancer," *Curr Pharm Biotechnol*, vol. 12, pp. 686-92, Apr 2011.
- [88] F. J. Sharom, "Complex Interplay between the P-Glycoprotein Multidrug Efflux Pump and the Membrane: Its Role in Modulating Protein Function," *Front Oncol*, vol. 4, p. 41, 2014.
- [89] M. M. Gottesman and V. Ling, "The molecular basis of multidrug resistance in cancer: the early years of P-glycoprotein research," *FEBS Lett*, vol. 580, pp. 998-1009, Feb 2006.
- [90] D. Kessel, V. Botterill, and I. Wodinsky, "Uptake and retention of daunomycin by mouse leukemic cells as factors in drug response," *Cancer Res*, vol. 28, pp. 938-41, May 1968.
- [91] K. Dano, "Active outward transport of daunomycin in resistant Ehrlich ascites tumor cells," *Biochim Biophys Acta*, vol. 323, pp. 466-83, Oct 1973.
- [92] Y. P. See, S. A. Carlsen, J. E. Till, and V. Ling, "Increased drug permeability in Chinese hamster ovary cells in the presence of cyanide," *Biochim Biophys Acta*, vol. 373, pp. 242-52, Dec 1974.
- [93] M. L. Amin, "P-glycoprotein Inhibition for Optimal Drug Delivery," *Drug Target Insights*, vol. 7, pp. 27-34, 2013.
- [94] F. J. Sharom, "The P-glycoprotein multidrug transporter," *Essays Biochem*, vol. 50, pp. 161-78, Sep 2011.
- [95] J. D. Wessler, L. T. Grip, J. Mendell, and R. P. Giugliano, "The P-glycoprotein transport system and cardiovascular drugs," *J Am Coll Cardiol*, vol. 61, pp. 2495-502, Jun 2013.
- [96] L. Kagan, T. Dreifinger, D. E. Mager, and A. Hoffman, "Role of p-glycoprotein in region-specific gastrointestinal absorption of talinolol in rats," *Drug Metab Dispos*, vol. 38, pp. 1560-6, Sep 2010.
- [97] P. Borst and A. H. Schinkel, "P-glycoprotein ABCB1: a major player in drug handling by mammals," *J Clin Invest*, vol. 123, pp. 4131-3, Oct 2013.
- [98] A. T. Clay and F. J. Sharom, "Multidrug Resistance Protein: P-glycoprotein," in *Drug Transporters: Molecular Characterization and Role in Drug Disposition*, G. You and M. E. Morris, Eds., 2nd ed, 2014, p. 141.
- [99] F. J. Sharom, "Shedding light on drug transport: structure and function of the P-glycoprotein multidrug transporter (ABCB1)," *Biochem Cell Biol*, vol. 84, pp. 979-92, Dec 2006.
- [100] T. W. Loo and D. M. Clarke, "Recent progress in understanding the mechanism of P-glycoprotein-mediated drug efflux," *J Membr Biol*, vol. 206, pp. 173-85, Aug 2005.
- [101] S. G. Aller, J. Yu, A. Ward, Y. Weng, S. Chittaboina, R. Zhuo, *et al.*, "Structure of P-glycoprotein reveals a molecular basis for poly-specific drug binding," *Science*, vol. 323, pp. 1718-22, Mar 2009.
- [102] C. J. Matheny, M. W. Lamb, K. R. Brouwer, and G. M. Pollack, "Pharmacokinetic and pharmacodynamic implications of P-glycoprotein modulation," *Pharmacotherapy*, vol. 21, pp. 778-96, Jul 2001.
- [103] F. J. Sharom, "The P-glycoprotein efflux pump: how does it transport drugs?," *J Membr Biol*, vol. 160, pp. 161-75, Dec 1997.
- [104] D. A. Gutmann, A. Ward, I. L. Urbatsch, G. Chang, and H. W. van Veen, "Understanding polyspecificity of multidrug ABC transporters: closing in on the gaps in ABCB1," *Trends Biochem Sci*, vol. 35, pp. 36-42, Jan 2010.
- [105] R. W. Johnstone, A. A. Ruefli, and M. J. Smyth, "Multiple physiological functions for multidrug transporter P-glycoprotein?," *Trends Biochem Sci*, vol. 25, pp. 1-6, Jan 2000.
- [106] E. P. Bruggemann, U. A. Germann, M. M. Gottesman, and I. Pastan, "Two different regions of P-glycoprotein [corrected] are photoaffinity-labeled by azidopine," *J Biol Chem*, vol. 264, pp. 15483-8, Sep 1989.
- [107] A. R. Safa, "Identification and characterization of the binding sites of P-glycoprotein for multidrug resistance-related drugs and modulators," *Curr Med Chem Anticancer Agents*, vol. 4, pp. 1-17, Jan 2004.

- [108] T. W. Loo, M. C. Bartlett, and D. M. Clarke, "Substrate-induced conformational changes in the transmembrane segments of human P-glycoprotein. Direct evidence for the substrate-induced fit mechanism for drug binding," *J Biol Chem*, vol. 278, pp. 13603-6, Apr 2003.
- [109] P. M. Jones, M. L. O'Mara, and A. M. George, "ABC transporters: a riddle wrapped in a mystery inside an enigma," *Trends Biochem Sci*, vol. 34, pp. 520-31, Oct 2009.
- [110] C. Globisch, I. K. Pajeva, and M. Wiese, "Identification of putative binding sites of P-glycoprotein based on its homology model," *ChemMedChem*, vol. 3, pp. 280-95, Feb 2008.
- [111] N. Maki, P. Hafkemeyer, and S. Dey, "Allosteric modulation of human P-glycoprotein. Inhibition of transport by preventing substrate translocation and dissociation," *J Biol Chem*, vol. 278, pp. 18132-9, May 2003.
- [112] R. Badhan and J. Penny, "In silico modelling of the interaction of flavonoids with human P-glycoprotein nucleotide-binding domain," *Eur J Med Chem*, vol. 41, pp. 285-95, Mar 2006.
- [113] S. V. Ambudkar, I. W. Kim, D. Xia, and Z. E. Sauna, "The A-loop, a novel conserved aromatic acid subdomain upstream of the Walker A motif in ABC transporters, is critical for ATP binding," *FEBS Lett*, vol. 580, pp. 1049-55, Feb 2006.
- [114] R. Regev, Y. G. Assaraf, and G. D. Eytan, "Membrane fluidization by ether, other anesthetics, and certain agents abolishes P-glycoprotein ATPase activity and modulates efflux from multidrug-resistant cells," *Eur J Biochem*, vol. 259, pp. 18-24, Jan 1999.
- [115] C. Cai, H. Zhu, and J. Chen, "Overexpression of caveolin-1 increases plasma membrane fluidity and reduces P-glycoprotein function in Hs578T/Dox," *Biochem Biophys Res Commun*, vol. 320, pp. 868-74, Jul 2004.
- [116] R. J. Ferreira, M. J. Ferreira, and D. J. dos Santos, "Molecular docking characterizes substrate-binding sites and efflux modulation mechanisms within P-glycoprotein," *J Chem Inf Model*, vol. 53, pp. 1747-60, Jul 2013.
- [117] M. Zeino, M. E. Saeed, O. Kadioglu, and T. Efferth, "The ability of molecular docking to unravel the controversy and challenges related to P-glycoprotein-a well-known, yet poorly understood drug transporter," *Invest New Drugs*, Apr 22 2014.
- [118] E. B. Mechetner and I. B. Roninson, "Efficient inhibition of P-glycoprotein-mediated multidrug resistance with a monoclonal antibody," *Proc Natl Acad Sci U S A*, vol. 89, pp. 5824-8, Jul 1 1992.
- [119] E. Georges, T. Tsuruo, and V. Ling, "Topology of P-glycoprotein as determined by epitope mapping of MRK-16 monoclonal antibody," *J Biol Chem*, vol. 268, pp. 1792-8, Jan 1993.
- [120] H. Nagy, K. Goda, R. Arceci, M. Cianfriglia, E. Mechetner, and G. Szabó, "P-Glycoprotein conformational changes detected by antibody competition," *Eur J Biochem*, vol. 268, pp. 2416-20, Apr 2001.
- [121] K. M. R. srivalli and P. K. Lakshami, "Overview of P-glycoprotein inhibitors: a rational outlook," *Brazilian Journal of Pharmaceutical Sciences*, vol. 48, pp. 353-367, 2012.
- [122] T. Tsuruo, H. Iida, S. Tsukagoshi, and Y. Sakurai, "Overcoming of vincristine resistance in P388 leukemia in vivo and in vitro through enhanced cytotoxicity of vincristine and vinblastine by verapamil," *Cancer Res*, vol. 41, pp. 1967-72, May 1981.
- [123] T. Ozben, "Mechanisms and strategies to overcome multiple drug resistance in cancer," *FEBS Lett*, vol. 580, pp. 2903-9, May 2006.
- [124] A. Palmeira, E. Sousa, M. H. Vasconcelos, and M. M. Pinto, "Three decades of P-gp inhibitors: skimming through several generations and scaffolds," *Curr Med Chem*, vol. 19, pp. 1946-2025, 2012.
- [125] H. M. Coley, "Overcoming multidrug resistance in cancer: clinical studies of p-glycoprotein inhibitors," *Methods Mol Biol*, vol. 596, pp. 341-58, 2010.
- [126] T. Eichhorn and T. Efferth, "P-glycoprotein and its inhibition in tumors by phytochemicals derived from Chinese herbs," *J Ethnopharmacol*, vol. 141, pp. 557-70, Jun 2012.
- [127] A. Garrigues, J. Nugier, S. Orłowski, and E. Ezan, "A high-throughput screening microplate test for the interaction of drugs with P-glycoprotein," *Anal Biochem*, vol. 305, pp. 106-14, Jun 2002.
- [128] S. Shityakov and C. Förster, "In silico structure-based screening of versatile P-glycoprotein inhibitors using polynomial empirical scoring functions," *Adv Appl Bioinform Chem*, vol. 7, pp. 1-9, 2014.
- [129] P. H. Palestro, L. Gavernet, G. L. Estiu, and L. E. Bruno Blanch, "Docking applied to the prediction of the affinity of compounds to P-glycoprotein," *Biomed Res Int*, vol. 2014, p. 358425, 2014.
- [130] W. Tan, H. Mei, L. Chao, T. Liu, X. Pan, M. Shu, *et al.*, "Combined QSAR and molecule docking studies on predicting P-glycoprotein inhibitors," *J Comput Aided Mol Des*, vol. 27, pp. 1067-73, Dec 2013.
- [131] L. Chen, Y. Li, H. Yu, L. Zhang, and T. Hou, "Computational models for predicting substrates or inhibitors of P-glycoprotein," *Drug Discov Today*, vol. 17, pp. 343-51, Apr 2012.
- [132] F. Klepsch, P. Chiba, and G. F. Ecker, "Exhaustive sampling of docking poses reveals binding hypotheses for propafenone type inhibitors of P-glycoprotein," *PLoS Comput Biol*, vol. 7, p. e1002036, May 2011.
- [133] E. Dolgih, C. Bryant, A. R. Renslo, and M. P. Jacobson, "Predicting binding to p-glycoprotein by flexible receptor docking," *PLoS Comput Biol*, vol. 7, p. e1002083, Jun 2011.

- [134] M. D. Hall, M. D. Handley, and M. M. Gottesman, "Is resistance useless? Multidrug resistance and collateral sensitivity," *Trends Pharmacol Sci*, vol. 30, pp. 546-56, Oct 2009.
- [135] M. Ye, G. Qu, H. Guo, and D. Guo, "Novel cytotoxic bufadienolides derived from bufalin by microbial hydroxylation and their structure-activity relationships," *J Steroid Biochem Mol Biol*, vol. 91, pp. 87-98, Jun 2004.
- [136] S. Johansson, P. Lindholm, J. Gullbo, R. Larsson, L. Bohlin, and P. Claeson, "Cytotoxicity of digitoxin and related cardiac glycosides in human tumor cells," *Anticancer Drugs*, vol. 12, pp. 475-83, Jun 2001.
- [137] R. J. Chen, T. Y. Chung, F. Y. Li, W. H. Yang, T. R. Jinn, and J. T. Tzen, "Steroid-like compounds in Chinese medicines promote blood circulation via inhibition of Na<sup>+</sup>/K<sup>+</sup> -ATPase," *Acta Pharmacol Sin*, vol. 31, pp. 696-702, Jun 2010.
- [138] M. Laursen, L. Yatime, P. Nissen, and N. U. Fedosova, "Crystal structure of the high-affinity Na<sup>+</sup>/K<sup>+</sup>-ATPase-ouabain complex with Mg<sup>2+</sup> bound in the cation binding site," *Proc Natl Acad Sci U S A*, vol. 110, pp. 10958-63, Jul 2013.
- [139] K. O. Mutz, A. Heilkenbrinker, M. Lönne, J. G. Walter, and F. Stahl, "Transcriptome analysis using next-generation sequencing," *Curr Opin Biotechnol*, vol. 24, pp. 22-30, Feb 2013.
- [140] B. Wiench, T. Eichhorn, B. Korn, M. Paulsen, and T. Efferth, "Utilizing inherent fluorescence of therapeutics to analyze real-time uptake and multi-parametric effector kinetics," *Methods*, vol. 57, pp. 376-82, Jul 2012.
- [141] I. C. van der Sandt, M. C. Blom-Roosemalen, A. G. de Boer, and D. D. Breimer, "Specificity of doxorubicin versus rhodamine-123 in assessing P-glycoprotein functionality in the LLC-PK1, LLC-PK1:MDR1 and Caco-2 cell lines," *Eur J Pharm Sci*, vol. 11, pp. 207-14, Sep 2000.
- [142] A. Krishan and R. M. Hamelik, "Flow cytometric monitoring of fluorescent drug retention and efflux," *Methods Mol Med*, vol. 111, pp. 149-66, 2005.
- [143] J. Weiss, S. M. Dormann, M. Martin-Facklam, C. J. Kerpen, N. Ketabi-Kiyanvash, and W. E. Haefeli, "Inhibition of P-glycoprotein by newer antidepressants," *J Pharmacol Exp Ther*, vol. 305, pp. 197-204, Apr 2003.
- [144] M. R. Ansbro, S. Shukla, S. V. Ambudkar, S. H. Yuspa, and L. Li, "Screening compounds with a novel high-throughput ABCB1-mediated efflux assay identifies drugs with known therapeutic targets at risk for multidrug resistance interference," *PLoS One*, vol. 8, p. e60334, 2013.
- [145] P. J. Bushway, M. Mercola, and J. H. Price, "A comparative analysis of standard microtiter plate reading versus imaging in cellular assays," *Assay Drug Dev Technol*, vol. 6, pp. 557-67, Aug 2008.
- [146] T. Watanabe, N. Kokubu, S. B. Charnick, M. Naito, T. Tsuruo, and D. Cohen, "Interaction of cyclosporin derivatives with the ATPase activity of human P-glycoprotein," *Br J Pharmacol*, vol. 122, pp. 241-8, Sep 1997.
- [147] A. Mahringer, S. Karamustafa, D. Klotz, S. Kahl, V. B. Konkimalla, Y. Wang, *et al.*, "Inhibition of P-glycoprotein at the blood-brain barrier by phytochemicals derived from traditional Chinese medicine," *Cancer Genomics Proteomics*, vol. 7, pp. 191-205, 2010 Jul-Aug 2010.
- [148] R. M. Laberge, R. Ambadipudi, and E. Georges, "P-glycoprotein (ABCB1) modulates collateral sensitivity of a multidrug resistant cell line to verapamil," *Arch Biochem Biophys*, vol. 491, pp. 53-60, Nov 2009.
- [149] X. Chen, M. Lowe, T. Herliczek, M. J. Hall, C. Danes, D. A. Lawrence, *et al.*, "Protection of normal proliferating cells against chemotherapy by staurosporine-mediated, selective, and reversible G(1) arrest," *J Natl Cancer Inst*, vol. 92, pp. 1999-2008, Dec 2000.
- [150] Y. Kamano, A. Yamashita, T. Nogawa, H. Morita, K. Takeya, H. Itokawa, *et al.*, "QSAR evaluation of the Ch'an Su and related bufadienolides against the colchicine-resistant primary liver carcinoma cell line PLC/PRF/5(1)," *Journal of Medicinal Chemistry*, vol. 45, pp. 5440-7, Dec 5 2002.
- [151] M. Karelson, V. S. Lobanov, and A. R. Katritzky, "Quantum-Chemical Descriptors in QSAR/QSPR Studies," *Chem Rev*, vol. 96, pp. 1027-1044, May 1996.
- [152] M. Ishihara, H. Wakabayashi, N. Motohashi, and H. Sakagami, "Estimation of relationship between the structure of trihaloacetylazulene derivatives determined by a semiempirical molecular-orbital method (PM5) and their cytotoxicity," *Anticancer Res*, vol. 30, pp. 837-41, Mar 2010.
- [153] M. Bohl, K. Ponsold, and G. Reck, "Quantitative structure-activity relationships of cardiotonic steroids using empirical molecular electrostatic potentials and semiempirical molecular orbital calculations," *J Steroid Biochem*, vol. 21, pp. 373-9, Oct 1984.
- [154] A. Cherkasov, E. N. Muratov, D. Fourches, A. Varnek, I. I. Baskin, M. Cronin, *et al.*, "QSAR modeling: where have you been? Where are you going to?," *J Med Chem*, vol. 57, pp. 4977-5010, Jun 2014.
- [155] J. G. Wise, "Catalytic transitions in the human MDR1 P-glycoprotein drug binding sites," *Biochemistry*, vol. 51, pp. 5125-41, Jun 26 2012.
- [156] W. T. Beck, M. C. Cirtain, R. A. Ashmun, and J. Mirro, "Differentiation and the multiple drug resistance phenotype in human leukemic cells," *Cancer Res*, vol. 46, pp. 4571-5, Sep 1986.

- [157] J. L. Biedler, H. Riehm, R. H. Peterson, and B. A. Spengler, "Membrane-mediated drug resistance and phenotypic reversion to normal growth behavior of Chinese hamster cells," *J Natl Cancer Inst*, vol. 55, pp. 671-80, Sep 1975.
- [158] I. Karitskaya, N. Aksenov, I. Vassilieva, V. Zenin, and I. Marakhova, "Long-term regulation of Na,K-ATPase pump during T-cell proliferation," *Pflugers Arch*, vol. 460, pp. 777-89, Sep 2010.
- [159] B. Stordal, M. Hamon, V. McEneaney, S. Roche, J. P. Gillet, J. J. O'Leary, *et al.*, "Resistance to paclitaxel in a cisplatin-resistant ovarian cancer cell line is mediated by P-glycoprotein," *PLoS One*, vol. 7, p. e40717, 2012.
- [160] V. Evdokimova, C. Tognon, T. Ng, and P. H. Sorensen, "Reduced proliferation and enhanced migration: two sides of the same coin? Molecular mechanisms of metastatic progression by YB-1," *Cell Cycle*, vol. 8, pp. 2901-6, Sep 2009.
- [161] J. Tian, X. Li, M. Liang, L. Liu, J. X. Xie, Q. Ye, *et al.*, "Changes in sodium pump expression dictate the effects of ouabain on cell growth," *J Biol Chem*, vol. 284, pp. 14921-9, May 2009.
- [162] S. H. Chan, W. J. Leu, L. C. Hsu, H. S. Chang, T. L. Hwang, I. S. Chen, *et al.*, "Reevesioside F induces potent and efficient anti-proliferative and apoptotic activities through Na<sup>+</sup>/K<sup>+</sup>-ATPase  $\alpha$ 3 subunit-involved mitochondrial stress and amplification of caspase cascades," *Biochem Pharmacol*, vol. 86, pp. 1564-75, Dec 2013.
- [163] H. Li, P. Wang, Y. Gao, X. Zhu, L. Liu, L. Cohen, *et al.*, "Na<sup>+</sup>/K<sup>+</sup>-ATPase  $\alpha$ 3 mediates sensitivity of hepatocellular carcinoma cells to bufalin," *Oncol Rep*, vol. 25, pp. 825-30, Mar 2011.
- [164] B. T. Hawkins, D. B. Sykes, and D. S. Miller, "Rapid, reversible modulation of blood-brain barrier P-glycoprotein transport activity by vascular endothelial growth factor," *J Neurosci*, vol. 30, pp. 1417-25, Jan 27 2010.
- [165] F. Lefranc and R. Kiss, "The sodium pump alpha1 subunit as a potential target to combat apoptosis-resistant glioblastomas," *Neoplasia*, vol. 10, pp. 198-206, Mar 2008.
- [166] Z. Liu, G. Zhu, R. H. Getzenberg, and R. W. Veltri, "The upregulation of PI3K/Akt and MAP kinase pathways is associated with resistance of microtubule-targeting drugs in prostate cancer," *J Cell Biochem*, Jan 2015.
- [167] M. Seres, E. Polakova, O. Krizanova, S. Hudecova, S. V. Klymenko, A. Breier, *et al.*, "Overexpression of P-glycoprotein in L1210/VCR cells is associated with changes in several endoplasmic reticulum proteins that may be partially responsible for the lack of thapsigargin sensitivity," *Gen Physiol Biophys*, vol. 27, pp. 211-21, Sep 2008.
- [168] N. Mestdagh, B. Vandewalle, L. Hornez, and J. P. Hélichart, "Comparative study of intracellular calcium and adenosine 3',5'-cyclic monophosphate levels in human breast carcinoma cells sensitive or resistant to Adriamycin: contribution to reversion of chemoresistance," *Biochem Pharmacol*, vol. 48, pp. 709-16, Aug 1994.
- [169] T. Tsuruo, H. Iida, H. Kawabata, S. Tsukagoshi, and Y. Sakurai, "High calcium content of pleiotropic drug-resistant P388 and K562 leukemia and Chinese hamster ovary cells," *Cancer Res*, vol. 44, pp. 5095-9, Nov 1984.
- [170] J. K. Foskett, C. White, K. H. Cheung, and D. O. Mak, "Inositol trisphosphate receptor Ca<sup>2+</sup> release channels," *Physiol Rev*, vol. 87, pp. 593-658, Apr 2007.
- [171] D. Galuska, S. Pirkmajer, R. Barrès, K. Ekberg, J. Wahren, and A. V. Chibalin, "C-peptide increases Na,K-ATPase expression via PKC- and MAP kinase-dependent activation of transcription factor ZEB in human renal tubular cells," *PLoS One*, vol. 6, p. e28294, 2011.
- [172] M. Liang and F. G. Knox, "Nitric oxide activates PKC $\alpha$  and inhibits Na<sup>+</sup>-K<sup>+</sup>-ATPase in opossum kidney cells," *Am J Physiol*, vol. 277, pp. F859-65, Dec 1999.
- [173] A. V. Chibalin, C. H. Pedemonte, A. I. Katz, E. Féraillé, P. O. Berggren, and A. M. Bertorello, "Phosphorylation of the catalytic alpha-subunit constitutes a triggering signal for Na<sup>+</sup>,K<sup>+</sup>-ATPase endocytosis," *J Biol Chem*, vol. 273, pp. 8814-9, Apr 1998.
- [174] C. Cerella, M. Dicato, and M. Diederich, "Assembling the puzzle of anti-cancer mechanisms triggered by cardiac glycosides," *Mitochondrion*, vol. 13, pp. 225-34, May 2013.
- [175] G. Young, L. Reuss, and G. A. Altenberg, "Altered intracellular pH regulation in cells with high levels of P-glycoprotein expression," *Int J Biochem Mol Biol*, vol. 2, pp. 219-27, 2011.
- [176] D. Boscoboinik, R. S. Gupta, and R. M. Epan, "Investigation of the relationship between altered intracellular pH and multidrug resistance in mammalian cells," *Br J Cancer*, vol. 61, pp. 568-72, Apr 1990.
- [177] K. Winnicka, K. Bielawski, A. Bielawska, and A. Surazynski, "Antiproliferative activity of derivatives of ouabain, digoxin and proscillaridin A in human MCF-7 and MDA-MB-231 breast cancer cells," *Biol Pharm Bull*, vol. 31, pp. 1131-40, Jun 2008.
- [178] H. Huang, Y. Cao, W. Wei, W. Liu, S. Y. Lu, Y. B. Chen, *et al.*, "Targeting poly (ADP-ribose) polymerase partially contributes to bufalin-induced cell death in multiple myeloma cells," *PLoS One*, vol. 8, p. e66130, 2013.

- [179] Y. Wang, D. M. Lonard, Y. Yu, D. C. Chow, T. G. Palzkill, J. Wang, *et al.*, "Bufalin is a potent small-molecule inhibitor of the steroid receptor coactivators SRC-3 and SRC-1," *Cancer Res*, vol. 74, pp. 1506-17, Mar 1 2014.
- [180] L. Sun, T. Chen, X. Wang, Y. Chen, and X. Wei, "Bufalin Induces Reactive Oxygen Species Dependent Bax Translocation and Apoptosis in ASTC-a-1 Cells," *Evid Based Complement Alternat Med*, vol. 2011, p. 249090, 2011.
- [181] D. A. Veal, D. Deere, B. Ferrari, J. Piper, and P. V. Atfield, "Fluorescence staining and flow cytometry for monitoring microbial cells," *J Immunol Methods*, vol. 243, pp. 191-210, Sep 21 2000.
- [182] M. S. Poruchynsky and V. Ling, "Detection of Oligomeric and Monomeric Forms of P-Glycoprotein in Multidrug-Resistant Cells (Vol 33, Pg 4163, 1994)," *Biochemistry*, vol. 33, pp. 9032-9032, Aug 2 1994.
- [183] C. Sagne, M. F. Isambert, J. P. Henry, and B. Gasnier, "SDS-resistant aggregation of membrane proteins: application to the purification of the vesicular monoamine transporter," *Biochem J*, vol. 316 ( Pt 3), pp. 825-31, Jun 15 1996.
- [184] Y. Zhao, J. Hu, G. Miao, L. Qu, Z. Wang, G. Li, *et al.*, "Transmembrane protein 208: a novel ER-localized protein that regulates autophagy and ER stress," *PLoS One*, vol. 8, p. e64228, 2013.
- [185] Y. N. Lee, L. K. Chen, H. C. Ma, H. H. Yang, H. P. Li, and S. Y. Lo, "Thermal aggregation of SARS-CoV membrane protein," *J Virol Methods*, vol. 129, pp. 152-61, Nov 2005.
- [186] M. W. McLane, G. Hatzidimitriou, J. Yuan, U. McCann, and G. Ricaurte, "Heating induces aggregation and decreases detection of serotonin transporter protein on western blots," *Synapse*, vol. 61, pp. 875-6, Oct 2007.
- [187] S. L. Nuti and U. S. Rao, "Proteolytic Cleavage of the Linker Region of the Human P-glycoprotein Modulates Its ATPase Function," *J Biol Chem*, vol. 277, pp. 29417-23, Aug 16 2002.
- [188] M. R. Abbaszadegan, A. E. Cress, B. W. Futscher, W. T. Bellamy, and W. S. Dalton, "Evidence for cytoplasmic P-glycoprotein location associated with increased multidrug resistance and resistance to chemosensitizers," *Cancer Res*, vol. 56, pp. 5435-5442, Dec 1 1996.
- [189] A. E. Senior, M. K. AlShawi, and I. L. Urbatsch, "The catalytic cycle of P-glycoprotein," *Febs Letters*, vol. 377, pp. 285-289, Dec 27 1995.
- [190] S. V. Ambudkar, S. Dey, C. A. Hrycyna, M. Ramachandra, I. Pastan, and M. M. Gottesman, "Biochemical, cellular, and pharmacological aspects of the multidrug transporter," *Annu Rev Pharmacol Toxicol*, vol. 39, pp. 361-98, 1999.
- [191] M. Dongping, "Identify P-glycoprotein substrates and inhibitors with the rapid, HTS P-glycoprotein-glo™ assay system," *Promega Notes*, vol. 96, pp. 11-14, 2007.
- [192] D. Schwab, H. Fischer, A. Tabatabaei, S. Poli, and J. Huwyler, "Comparison of in vitro P-glycoprotein screening assays: Recommendations for their use in drug discovery," *Journal of Medicinal Chemistry*, vol. 46, pp. 1716-1725, Apr 24 2003.
- [193] E. Gozalpour, H. G. Wittgen, J. J. van den Heuvel, R. Greupink, F. G. Russel, and J. B. Koenderink, "Interaction of digitalis-like compounds with p-glycoprotein," *Toxicol Sci*, vol. 131, pp. 502-11, Feb 2013.
- [194] M. E. Taub, L. Podila, D. Ely, and I. Almeida, "Functional assessment of multiple P-glycoprotein (P-gp) probe substrates: influence of cell line and modulator concentration on P-gp activity," *Drug Metab Dispos*, vol. 33, pp. 1679-87, Nov 2005.
- [195] G. Dayan, J. M. Jault, H. Baubichon-Cortay, L. G. Baggetto, J. M. Renoir, E. E. Baulieu, *et al.*, "Binding of steroid modulators to recombinant cytosolic domain from mouse P-glycoprotein in close proximity to the ATP site," *Biochemistry*, vol. 36, pp. 15208-15, Dec 9 1997.
- [196] M. Zeino, M. S. Paulsen, M. Zehl, E. Urban, B. Kopp, and T. Efferth, "Identification of new P-glycoprotein inhibitors derived from cardiotonic steroids," *Biochem Pharmacol*, vol. 93, pp. 11-24, Jan 2015.
- [197] T. Bansal, M. Jaggi, R. K. Khar, and S. Talegaonkar, "Emerging Significance of Flavonoids as P-Glycoprotein Inhibitors in Cancer Chemotherapy," *Journal of Pharmacy and Pharmaceutical Sciences*, vol. 12, pp. 46-78, 2009.
- [198] A. B. Shapiro and V. Ling, "Positively cooperative sites for drug transport by P-glycoprotein with distinct drug specificities," *Eur J Biochem*, vol. 250, pp. 130-7, Nov 1997.
- [199] R. Liu and F. J. Sharom, "Site-directed fluorescence labeling of P-glycoprotein on cysteine residues in the nucleotide binding domains," *Biochemistry*, vol. 35, pp. 11865-73, Sep 10 1996.
- [200] Z. Meng, P. Yang, Y. Shen, W. Bei, Y. Zhang, Y. Ge, *et al.*, "Pilot study of huachansu in patients with hepatocellular carcinoma, nonsmall-cell lung cancer, or pancreatic cancer," *Cancer*, vol. 115, pp. 5309-18, Nov 15 2009.
- [201] T. J. Qin, X. H. Zhao, J. Yun, L. X. Zhang, Z. P. Ruan, and B. R. Pan, "Efficacy and safety of gemcitabine-oxaliplatin combined with huachansu in patients with advanced gallbladder carcinoma," *World J Gastroenterol*, vol. 14, pp. 5210-6, Sep 7 2008.
- [202] T. Mekhail, H. Kaur, R. Ganapathi, G. T. Budd, P. Elson, and R. M. Bukowski, "Phase I trial of Anvirzel in patients with refractory solid tumors," *Invest New Drugs*, vol. 24, pp. 423-7, Sep 2006.

- [203] Y. H. Wang, Y. Li, S. L. Yang, and L. Yang, "Classification of substrates and inhibitors of P-glycoprotein using unsupervised machine learning approach," *J Chem Inf Model*, vol. 45, pp. 750-7, 2005 May-Jun 2005.
- [204] F. Tang, H. Ouyang, J. Z. Yang, and R. T. Borchardt, "Bidirectional transport of rhodamine 123 and Hoechst 33342, fluorescence probes of the binding sites on P-glycoprotein, across MDCK-MDR1 cell monolayers," *J Pharm Sci*, vol. 93, pp. 1185-94, May 2004.
- [205] T. W. Loo and D. M. Clarke, "Location of the rhodamine-binding site in the human multidrug resistance P-glycoprotein," *J Biol Chem*, vol. 277, pp. 44332-8, Nov 2002.
- [206] T. W. Loo and D. M. Clarke, "Defining the drug-binding site in the human multidrug resistance P-glycoprotein using a methanethiosulfonate analog of verapamil, MTS-verapamil," *J Biol Chem*, vol. 276, pp. 14972-9, May 2001.
- [207] G. Kothandan, C. G. Gadhe, T. Madhavan, C. H. Choi, and S. J. Cho, "Docking and 3D-QSAR (quantitative structure activity relationship) studies of flavones, the potent inhibitors of p-glycoprotein targeting the nucleotide binding domain," *Eur J Med Chem*, vol. 46, pp. 4078-88, Sep 2011.
- [208] G. E. FOLEY, H. LAZARUS, S. FARBER, B. G. UZMAN, B. A. BOONE, and R. E. MCCARTHY, "CONTINUOUS CULTURE OF HUMAN LYMPHOBLASTS FROM PERIPHERAL BLOOD OF A CHILD WITH ACUTE LEUKEMIA," *Cancer*, vol. 18, pp. 522-9, Apr 1965.
- [209] A. Kimmig, V. Gekeler, M. Neumann, G. Frese, R. Handgretinger, G. Kardos, *et al.*, "Susceptibility of multidrug-resistant human leukemia cell lines to human interleukin 2-activated killer cells," *Cancer Res*, vol. 50, pp. 6793-9, Nov 1990.
- [210] J. P. Gillet, T. Efferth, D. Steinbach, J. Hamels, F. de Longueville, V. Bertholet, *et al.*, "Microarray-based detection of multidrug resistance in human tumor cells by expression profiling of ATP-binding cassette transporter genes," *Cancer Res*, vol. 64, pp. 8987-93, Dec 2004.
- [211] S. Akiyama, A. Fojo, J. A. Hanover, I. Pastan, and M. M. Gottesman, "Isolation and genetic characterization of human KB cell lines resistant to multiple drugs," *Somat Cell Mol Genet*, vol. 11, pp. 117-26, Mar 1985.
- [212] D. A. Hudman and N. J. Sargentini, "Resazurin-based assay for screening bacteria for radiation sensitivity," *Springerplus*, vol. 2, p. 55, Dec 2013.
- [213] R. H. Batchelor and M. Zhou, "Use of cellular glucose-6-phosphate dehydrogenase for cell quantitation: applications in cytotoxicity and apoptosis assays," *Anal Biochem*, vol. 329, pp. 35-42, Jun 2004.
- [214] B. Wiench, T. Eichhorn, M. Paulsen, and T. Efferth, "Shikonin directly targets mitochondria and causes mitochondrial dysfunction in cancer cells," *Evid Based Complement Alternat Med*, vol. 2012, p. 726025, 2012.
- [215] U. K. Laemmli, "Cleavage of structural proteins during the assembly of the head of bacteriophage T4," *Nature*, vol. 227, pp. 680-5, Aug 1970.
- [216] F. Y. Zhang, G. J. Du, L. Zhang, C. L. Zhang, W. L. Lu, and W. Liang, "Naringenin enhances the anti-tumor effect of doxorubicin through selectively inhibiting the activity of multidrug resistance-associated proteins but not P-glycoprotein," *Pharm Res*, vol. 26, pp. 914-25, Apr 2009.
- [217] T. A. Bogush, E. A. Dudko, E. A. Bogush, and A. I. u. Baryshnikov, "[Parameters of specific antibody interaction with P-gp in T-cell leukemia Jurkat cells]," *Antibiot Khimioter*, vol. 54, pp. 3-9, 2009.
- [218] R. B. Kim, "Drugs as P-glycoprotein substrates, inhibitors, and inducers," *Drug Metab Rev*, vol. 34, pp. 47-54, 2002 Feb-May 2002.
- [219] Y. Tajima, H. Nakagawa, A. Tamura, O. Kadioglu, K. Satake, Y. Mitani, *et al.*, "Nitensidine A, a guanidine alkaloid from *Pterogyne nitens*, is a novel substrate for human ABC transporter ABCB1," *Phytomedicine*, vol. 21, pp. 323-32, Feb 2014.
- [220] M. Zeino, Q. Zhao, T. Eichhorn, J. Hermann, and R. Müller, "Molecular docking studies of myxobacterial disorazoles and tubulysins to tubulin," *Journal of Bioscience and Medicine*, vol. 3, pp. 31-43, 2013.
- [221] G. M. Morris, R. Huey, W. Lindstrom, M. F. Sanner, R. K. Belew, D. S.Goodsell, *et al.*, "AutoDock4 and AutoDockTools4: Automated docking with selective receptor flexibility," *J Comput Chem*, vol. 30, pp. 2785-91, Dec 2009.
- [222] R. E. Kingston, "Preparation of poly(A)<sup>+</sup> RNA," *Curr Protoc Mol Biol*, vol. Chapter 4, p. Unit4.5, May 2001.
- [223] A. Mortazavi, B. A. Williams, K. McCue, L. Schaeffer, and B. Wold, "Mapping and quantifying mammalian transcriptomes by RNA-Seq," *Nat Methods*, vol. 5, pp. 621-8, Jul 2008.

## 8 Appendix

### 8.1 NMR and MS Data

#### Experimental procedure:

NMR spectra were recorded on a Bruker Avance 500 NMR spectrometer (UltraShield) using a 5 mm switchable probe (PA BBO 500SB BBF-H-D-05-Z, 1H, BB = 19F and 31P - 15N) with z axis gradients and an automatic tuning and matching accessory (BrukerBioSpin, Rheinstetten, Germany). The resonance frequencies were 500.13 MHz and 125.75 MHz for  $^1\text{H}$  NMR and  $^{13}\text{C}$  NMR, respectively. All measurements were performed in solutions in fully deuterated chloroform or methanol at 298 K. Standard 1D and gradient-enhanced (ge) 2D experiments, such as double-quantum filtered (DQF) COSY, NOESY, HSQC, and HMBC, were performed according to the manufacturer's instructions. The chemical shifts are referenced internally to the residual, non-deuterated solvent signal ( $\delta$  7.26 ppm for chloroform  $^1\text{H}$  or  $\delta$  3.31 ppm for methanol  $^1\text{H}$ ) and to the carbon signal of the solvent ( $\delta$  77.00 ppm for chloroform  $^{13}\text{C}$  or  $\delta$  49.00 ppm for methanol  $^{13}\text{C}$ ).

ESIMS<sup>n</sup> spectra were obtained on a HCT 3D-ion trap mass spectrometer (Bruker Daltonics, Bremen, Germany), and HRESIMS spectra were recorded either on a micrOTOF-Q II or on a maXis HD ESI-Qq-TOF mass spectrometer (both from Bruker Daltonics) in the positive-ion mode by direct infusion.

#### ESIMS<sup>n</sup> and HRESIMS data of compounds

##### 15i, 22N, 23A, 23D, 26K, 29b, 30M, 51D, 54E, 54v, 54Ee, 55K, 62A, 62F, 62I, and 62J

**(3 $\beta$ ,5 $\beta$ ,11 $\alpha$ ,12 $\alpha$ ,14 $\beta$ ,17 $\beta$ )-3,11-Bis(acetyloxy)-12,14-dihydroxy-bufa-20,22-dienolide (15i):** ESIMS  $m/z$  503.3 [M+H]<sup>+</sup>; ESIMS<sup>2</sup> (503.3  $\rightarrow$ )  $m/z$  443.2 (100), 425.2 (19), 383.2 (49), 365.2 (43), 347.2 (32), 337.2 (13), 319.2 (12), 193.0 (10), 191.1 (27); ESIMS<sup>3</sup> (503.3  $\rightarrow$  383.2  $\rightarrow$ )  $m/z$  383.2 (10), 365.2 (100), 347.2 (29), 337.2 (17), 319.2 (13), 239.0 (10), 219.0 (12), 201.0 (17), 193.0 (13), 191.0 (23), 175.0 (10), 173.0 (16), 149.0 (30), 147.0 (14), 145.0 (13); ESIMS<sup>3</sup> (503.3  $\rightarrow$  347.2  $\rightarrow$ )  $m/z$  347.2 (21), 329.2 (65), 319.2 (100), 305.1 (33), 303.1 (11), 301.1 (35), 291.1 (34), 287.1 (30), 279.1 (13), 277.1 (19), 273.1 (14), 265.1 (39), 263.1 (16), 259.1 (11), 253.1 (29), 251.0 (53), 249.1 (18), 247.0 (12), 245.1 (11), 239.0 (43), 237.0 (59), 235.1 (16), 233.0 (10), 225.1 (53), 223.0 (24), 221.0 (15), 213.0 (11), 211.0 (29), 209.0 (22), 207.0 (10), 201.0 (13), 199.0 (28), 197.0 (30), 195.0 (17), 187.0 (11), 185.0 (20), 183.0 (17), 181.0 (13), 173.0 (13), 171.0 (19), 169.0 (16), 161.0 (11), 159.0 (29), 157.0 (17), 155.0 (14), 147.0 (24), 145.0 (22), 143.0 (16), 131.0 (12), 105.0 (12); HRESIMS  $m/z$  503.2676 [M+H]<sup>+</sup> (calcd for C<sub>28</sub>H<sub>39</sub>O<sub>8</sub><sup>+</sup>, 503.2639,  $\Delta$  = 7.3 ppm).

**(3 $\beta$ ,5 $\beta$ )-3-[[8-[[4-[(aminoiminomethyl)amino]-1-carboxybutyl]amino]-1,8-dioxooctyl]oxy]-5,14-dihydroxy-bufa-20,22-dienolide (22N):** ESIMS  $m/z$  715.5 [M+H]<sup>+</sup>; ESIMS<sup>2</sup> (715.5  $\rightarrow$ )  $m/z$  697.5 (100), 679.4 (27), 331.2 (89), 278.1 (11); ESIMS<sup>3</sup> (715.5  $\rightarrow$  331.2  $\rightarrow$ )  $m/z$  314.2 (14), 313.2 (22), 278.1 (100), 271.1 (18), 268.1 (12), 260.1 (26), 253.1 (62), 250.1 (42), 175.1 (20), 158.0 (29), 156.1 (13), 139.0 (10); ESIMS<sup>3</sup> (715.5  $\rightarrow$  349.2  $\rightarrow$ )  $m/z$  349.2 (92), 332.2 (20), 331.2 (69), 321.2 (35), 314.2 (12), 313.2 (28), 307.2 (16), 304.2 (19), 303.2 (79), 294.1 (12), 293.2 (44), 290.1 (14), 289.2 (41), 283.2 (28), 281.1 (18), 279.1 (30), 275.1 (24), 269.1 (22), 268.1 (14), 267.1 (81), 265.2 (60), 263.2 (13), 261.1 (21), 255.1 (18), 254.1 (11), 253.1 (39), 251.1 (47), 250.1 (15), 249.1 (29), 247.1 (18), 241.1 (29), 239.1 (52), 237.1 (22), 235.1 (26), 233.1 (21), 227.1 (63), 225.1 (24), 223.1 (27), 221.1 (30), 215.1 (14), 214.1 (13), 213.1 (48), 211.1 (29), 209.1 (26), 207.0 (24), 205.1 (12), 203.0 (22), 201.0 (23), 199.1 (55), 197.1 (27), 195.1 (32), 193.0 (13), 189.0 (10), 187.0 (28), 185.1 (60), 183.0 (31), 181.0 (17), 175.0 (28), 173.1 (27), 171.1 (41), 169.0 (24), 167.0 (12), 161.0 (31), 160.1 (12), 159.1 (100), 157.0 (40), 155.0 (27), 149.0 (12), 147.1 (28), 145.0 (77), 143.1 (32), 142.1 (11), 135.0 (19), 133.1 (27), 131.1 (44), 129.0 (20), 128.0 (14), 123.0 (12), 119.1 (19), 117.1 (18), 105.1 (23).

**(3 $\beta$ ,5 $\beta$ )-3-(Acetyloxy)-14-hydroxy-card-20(22)-enolide (23A):** ESIMS  $m/z$  417.3 [M+H]<sup>+</sup>; ESIMS<sup>2</sup> (417.3  $\rightarrow$ )  $m/z$  357.2 (10), 339.2 (100); ESIMS<sup>3</sup> (417.3  $\rightarrow$  339.2  $\rightarrow$ )  $m/z$  339.2 (15), 321.2 (75), 303.2 (10), 293.2 (100),

283.1 (13), 279.2 (28), 257.1 (37), 243.1 (12), 231.1 (20), 229.1 (11), 215.1 (34), 213.1 (10), 211.1 (11), 201.1 (13), 199.1 (11), 189.1 (16), 187.1 (45), 185.1 (25), 161.1 (14), 135.1 (24), 131.0 (13), 121.1 (14).

**(3 $\beta$ ,5 $\beta$ ,15 $\beta$ )-3-(Acetyloxy)-14,15-epoxy-card-20(22)-enolide (23D):** ESIMS  $m/z$  415.2 [M+H]<sup>+</sup>; ESIMS<sup>2</sup> (415.2  $\rightarrow$ )  $m/z$  415.1 (16), 355.1 (100), 337.1 (29); ESIMS<sup>3</sup> (415.2  $\rightarrow$  337.1  $\rightarrow$ )  $m/z$  337.1 (12), 319.1 (100), 309.1 (18), 291.1 (49), 277.1 (34), 185.0 (10), 145.1 (11), 131.1 (12).

**(3 $\beta$ ,5 $\beta$ ,14 $\beta$ ,15 $\beta$ ,16 $\beta$ ,17 $\alpha$ )-14,15-Epoxy-3,16-dihydroxy-androstane-17-carboxylic acid methyl ester (26K):** ESIMS  $m/z$  382.3 [M+NH<sub>4</sub>]<sup>+</sup>; ESIMS<sup>2</sup> (382.3  $\rightarrow$ )  $m/z$  382.3 (12), 347.3 (61), 329.3 (100), 311.3 (19); ESIMS<sup>3</sup> (382.3  $\rightarrow$  329.3  $\rightarrow$ )  $m/z$  329.3 (17), 311.3 (100), 297.3 (54), 279.2 (10), 269.3 (66), 251.3 (51), 215.3 (69); ESIMS<sup>4</sup> (382.3  $\rightarrow$  329.3  $\rightarrow$  311.3  $\rightarrow$ )  $m/z$  279.2 (13), 251.3 (100); ESIMS<sup>4</sup> (382.3  $\rightarrow$  329.3  $\rightarrow$  251.3  $\rightarrow$ )  $m/z$  223.2 (18), 209.2 (50), 195.2 (100), 183.2 (15), 181.2 (31), 169.2 (49), 157.2 (18), 143.2 (87), 95.3 (13); ESIMS<sup>4</sup> (382.3  $\rightarrow$  329.3  $\rightarrow$  215.3  $\rightarrow$ )  $m/z$  215.3 (21), 187.2 (45), 173.2 (60), 159.2 (97), 147.2 (16), 145.2 (64), 135.3 (23), 133.3 (84), 131.2 (26), 121.3 (58), 119.3 (100), 109.3 (21), 107.3 (40), 105.3 (85), 95.3 (21), 93.4 (14), 81.4 (25).

**(3 $\beta$ ,5 $\beta$ ,14 $\beta$ ,15 $\alpha$ )-3-(Acetyloxy)-14,15-dihydroxy-androst-16-ene-17-carboxylic acid methyl ester (29b):** ESIMS  $m/z$  429.2 [M+Na]<sup>+</sup>, 389.2 [M-H<sub>2</sub>O+H]<sup>+</sup>; ESIMS<sup>2</sup> (389.2  $\rightarrow$ )  $m/z$  389.2 (12), 329.2 (100); ESIMS<sup>3</sup> (389.2  $\rightarrow$  329.2  $\rightarrow$ )  $m/z$  311.2 (100), 297.1 (29), 279.1 (14), 269.1 (25), 251.1 (51), 233.0 (15); ESIMS<sup>4</sup> (389.2  $\rightarrow$  329.2  $\rightarrow$  251.1  $\rightarrow$ )  $m/z$  251.1 (15), 236.1 (14), 223.1 (38), 209.0 (100), 195.0 (79), 183.0 (23), 181.0 (33), 171.0 (13), 169.0 (38), 159.0 (10), 157.0 (21), 155.0 (28), 145.0 (11), 143.0 (17).

**(3 $\beta$ ,5 $\beta$ ,14 $\alpha$ ,16 $\beta$ )-3,16-Dihydroxy-15-oxo-bufanolide (30M):** ESIMS  $m/z$  405.2 [M+H]<sup>+</sup>; ESIMS<sup>2</sup> (405.2  $\rightarrow$ )  $m/z$  405.2 (16), 387.2 (90), 369.2 (100), 351.2 (40); ESIMS<sup>3</sup> (405.2  $\rightarrow$  351.2  $\rightarrow$ )  $m/z$  351.2 (14), 333.2 (100), 323.2 (14), 315.2 (23), 305.2 (16), 291.2 (30), 269.1 (22), 251.1 (14), 237.1 (11), 209.1 (12); HRESIMS  $m/z$  405.2631 [M+H]<sup>+</sup> (calcd for C<sub>24</sub>H<sub>37</sub>O<sub>5</sub><sup>+</sup>, 405.2636,  $\Delta$  = -1.1 ppm).

**(5 $\beta$ ,14 $\beta$ ,15 $\beta$ ,17 $\alpha$ )-21-(Acetyloxy)-14,15-epoxy-pregnane-3,20-dione (51D):** ESIMS  $m/z$  389.2 [M+H]<sup>+</sup>, 371.2 [M-H<sub>2</sub>O+H]<sup>+</sup>; ESIMS<sup>2</sup> (389.2  $\rightarrow$ )  $m/z$  389.2 (12), 371.2 (100); ESIMS<sup>3</sup> (389.2  $\rightarrow$  371.2  $\rightarrow$ )  $m/z$  329.2 (93), 311.2 (100), 293.1 (16), 269.1 (22); ESIMS<sup>3</sup> (371.2  $\rightarrow$  311.2  $\rightarrow$ )  $m/z$  311.2 (14), 293.1 (31), 269.1 (100), 251.1 (28), 241.1 (16), 169.0 (13), 159.0 (13); ESIMS<sup>4</sup> (371.2  $\rightarrow$  311.2  $\rightarrow$  269.1  $\rightarrow$ )  $m/z$  251.1 (66), 211.1 (27), 209.0 (24), 199.1 (63), 195.0 (17), 169.0 (11), 159.0 (100), 145.0 (21); HRESIMS  $m/z$  389.2326 [M+H]<sup>+</sup> (calcd for C<sub>23</sub>H<sub>33</sub>O<sub>5</sub><sup>+</sup>, 389.2323,  $\Delta$  = 0.9 ppm).

**(3 $\beta$ ,5 $\beta$ ,14 $\beta$ ,15 $\beta$ ,17 $\alpha$ )-3-(Acetyloxy)-14,15-epoxy-androstane-17-carboxylic acid methyl ester (54E):** ESIMS  $m/z$  413.2 [M+Na]<sup>+</sup>, 391.2 [M+H]<sup>+</sup>, 331.2 [M-CH<sub>3</sub>COOH+H]<sup>+</sup>; ESIMS<sup>2</sup> (391.2  $\rightarrow$ )  $m/z$  391.2 (14), 331.2 (100); ESIMS<sup>2</sup> (331.2  $\rightarrow$ )  $m/z$  331.2 (18), 313.2 (90), 299.1 (100), 271.1 (21), 253.1 (32); ESIMS<sup>3</sup> (331.2  $\rightarrow$  299.1  $\rightarrow$ )  $m/z$  299.1 (17), 281.1 (60), 271.1 (52), 263.1 (13), 253.1 (100), 239.1 (21), 227.1 (18), 215.1 (94), 213.1 (40); ESIMS<sup>3</sup> (331.2  $\rightarrow$  253.1  $\rightarrow$ )  $m/z$  253.1 (22), 225.1 (25), 211.1 (58), 197.0 (98), 185.0 (27), 183.0 (47), 173.0 (11), 171.0 (79), 169.0 (19), 159.0 (37), 157.0 (95), 155.0 (14), 149.0 (49), 145.0 (33), 143.0 (100), 135.0 (27), 131.0 (30), 119.0 (15), 107.1 (11), 105.0 (22), 95.1 (11), 93.1 (11); HRESIMS  $m/z$  391.2521 [M+H]<sup>+</sup> (calcd for C<sub>23</sub>H<sub>35</sub>O<sub>5</sub><sup>+</sup>, 391.2479,  $\Delta$  = 10.8 ppm).

**(3 $\beta$ ,5 $\beta$ ,14 $\alpha$ ,15 $\beta$ )-3,15-Bis(acetyloxy)-bufa-20,22-dienolide (54v):** ESIMS  $m/z$  471.3 [M+H]<sup>+</sup>; ESIMS<sup>2</sup> (471.3  $\rightarrow$ )  $m/z$  471.2 (13), 411.2 (100), 351.2 (22); ESIMS<sup>3</sup> (471.3  $\rightarrow$  411.2  $\rightarrow$ )  $m/z$  351.2 (100); ESIMS<sup>4</sup> (471.3  $\rightarrow$  411.2  $\rightarrow$  351.2  $\rightarrow$ )  $m/z$  351.2 (69), 303.2 (11), 267.1 (21), 255.1 (19), 253.1 (25), 251.1 (11), 249.1 (15), 247.1 (10), 241.1 (40), 239.1 (42), 237.1 (13), 235.1 (18), 233.1 (12), 227.0 (11), 225.1 (21), 223.0 (28), 221.0 (23), 215.1 (10), 213.1 (25), 211.1 (36), 209.0 (29), 207.0 (22), 205.0 (14), 201.0 (28), 199.0 (28), 197.0 (49), 195.0 (54), 193.0 (22), 189.0 (21), 187.0 (61), 185.0 (30), 183.0 (55), 182.0 (13), 181.0 (35), 179.0 (22), 175.0 (16), 173.0 (18), 171.0 (55), 169.0 (68), 167.0 (35), 165.0 (23), 161.0 (24), 159.0 (62), 157.0 (70), 156.0 (11), 155.0 (64), 154.0 (12), 153.0 (24), 149.0 (19), 147.0 (34), 145.0 (88), 143.0 (93), 142.0 (25), 141.0 (50), 135.1 (19), 133.0 (46), 131.0 (100), 129.0 (59), 128.0 (62), 121.1 (22), 119.0 (99), 117.0 (73), 115.0 (51), 109.1 (11), 107.1 (45), 105.1 (91), 103.1 (16).

**2-[7-(Acetyloxy)tetradecahydro-2,4b-dimethyl-1-oxo-2-phenanthrenyl]-succinic acid dimethyl ester (54Ee):** ESIMS  $m/z$  437.3 [M+H]<sup>+</sup>; ESIMS<sup>2</sup> (437.3  $\rightarrow$ )  $m/z$  437.2 (12), 405.2 (100), 345.2 (74); ESIMS<sup>3</sup> (437.3  $\rightarrow$  405.2  $\rightarrow$ )  $m/z$  405.2 (11), 345.2 (100); ESIMS<sup>3</sup> (437.3  $\rightarrow$  345.2  $\rightarrow$ )  $m/z$  345.2 (13), 327.2 (43), 313.2 (23), 299.2 (16), 295.1 (12), 213.1 (100).

**(3 $\beta$ ,5 $\beta$ )-3-[(7-carboxy-1-oxoheptyl)oxy]-14-hydroxy-card-20(22)-enolide (55K):** ESIMS  $m/z$  531.2 [M+H]<sup>+</sup>, 513.2 [M-H<sub>2</sub>O+H]<sup>+</sup>; ESIMS<sup>2</sup> (531.2  $\rightarrow$ )  $m/z$  531.2 (100); ESIMS<sup>3</sup> (531.2  $\rightarrow$  513.2  $\rightarrow$ )  $m/z$  495.2 (11), 339.3 (100); ESIMS<sup>3</sup> (513.2  $\rightarrow$  339.3  $\rightarrow$ )  $m/z$  339.3 (15), 321.3 (48), 293.3 (73), 283.2 (21), 279.3 (31), 271.2 (13), 257.2 (100), 243.2 (27), 239.2 (12), 229.2 (11), 215.3 (74), 213.3 (12), 211.2 (16), 203.2 (13), 201.3 (19),

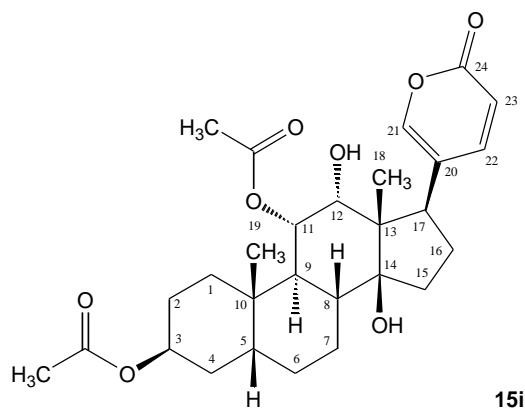
199.2 (11), 197.2 (14), 189.3 (37), 187.2 (18), 185.2 (16), 161.3 (40), 159.2 (17), 147.3 (30), 145.2 (17), 135.3 (30), 133.3 (24), 131.3 (13), 121.3 (21), 119.3 (14), 107.3 (11), 105.3 (14).

**(3 $\beta$ )-3-(Acetyloxy)-20-ethenyl-20-hydroxy-21-methoxy-pregn-5-en (62A):** ESIMS  $m/z$  434.3 [M+NH<sub>4</sub>]<sup>+</sup>; ESIMS<sup>2</sup> (434.3  $\rightarrow$ )  $m/z$  416.2 (100), 399.2 (97), 339.2 (14), 313.2 (16), 307.2 (14); ESIMS<sup>3</sup> (434.3  $\rightarrow$  399.2  $\rightarrow$ )  $m/z$  339.2 (29), 313.2 (54), 307.2 (100); ESIMS<sup>4</sup> (434.3  $\rightarrow$  399.2  $\rightarrow$  307.2  $\rightarrow$ )  $m/z$  307.2 (19), 279.2 (38), 265.1 (63), 251.1 (79), 241.1 (22), 239.1 (16), 237.1 (59), 227.1 (33), 225.1 (38), 223.0 (41), 215.1 (10), 213.1 (36), 211.1 (67), 209.0 (53), 203.1 (44), 201.1 (22), 199.0 (53), 197.0 (63), 195.0 (51), 189.1 (16), 187.0 (25), 185.0 (67), 183.0 (78), 181.0 (22), 177.1 (11), 175.0 (27), 173.0 (27), 171.0 (41), 169.0 (35), 163.1 (31), 161.0 (24), 159.0 (36), 157.0 (100), 155.0 (44), 149.0 (18), 147.0 (32), 145.0 (53), 143.0 (60), 142.0 (11), 141.0 (13), 135.0 (15), 133.0 (37), 131.0 (46), 129.0 (18), 123.1 (19), 121.0 (34), 119.0 (29), 117.0 (26), 109.1 (23), 107.1 (32), 105.0 (40), 95.1 (19), 93.1 (13), 91.1 (16); HRESIMS  $m/z$  439.2821 [M+Na]<sup>+</sup> (calcd for C<sub>26</sub>H<sub>40</sub>NaO<sub>4</sub><sup>+</sup>, 439.2819,  $\Delta$  = 0.6 ppm).

**(3 $\beta$ )-20-Ethinyl-3,20-dihydroxy-21-methoxy-pregn-5-en (62F):** ESIMS  $m/z$  390.3 [M+NH<sub>4</sub>]<sup>+</sup>; ESIMS<sup>2</sup> (390.3  $\rightarrow$ )  $m/z$  390.2 (11), 372.2 (22), 355.2 (100), 337.2 (24), 323.2 (32), 307.2 (15), 305.2 (51); ESIMS<sup>3</sup> (390.3  $\rightarrow$  355.2  $\rightarrow$ )  $m/z$  337.2 (22), 323.2 (25), 305.2 (100); ESIMS<sup>4</sup> (390.3  $\rightarrow$  355.2  $\rightarrow$  305.2  $\rightarrow$ )  $m/z$  305.2 (11), 290.2 (17), 277.1 (37), 263.1 (53), 249.1 (100), 237.1 (25), 235.1 (54), 225.1 (14), 223.1 (76), 221.0 (33), 211.1 (40), 209.0 (65), 207.0 (20), 199.1 (13), 197.0 (45), 195.0 (71), 193.0 (13), 185.0 (18), 183.0 (27), 181.0 (31), 175.1 (13), 173.0 (12), 171.0 (18), 169.0 (23), 167.0 (20), 161.0 (27), 159.0 (33), 157.0 (36), 155.0 (31), 147.0 (13), 145.0 (27), 143.0 (18), 133.0 (13), 131.0 (15), 119.0 (12), 105.1 (15); HRESIMS  $m/z$  390.3004 [M+NH<sub>4</sub>]<sup>+</sup> (calcd for C<sub>24</sub>H<sub>40</sub>NO<sub>3</sub><sup>+</sup>, 390.3003,  $\Delta$  = 0.4 ppm).

**(3 $\beta$ )-3-(Acetyloxy)-20-hydroxy-21-methoxy-chole-5-en-22-yn-24-oic acid methyl ester (62I):** ESIMS  $m/z$  490.3 [M+NH<sub>4</sub>]<sup>+</sup>; ESIMS<sup>2</sup> (490.3  $\rightarrow$ )  $m/z$  490.3 (10), 413.2 (100), 395.2 (32), 381.2 (11), 363.2 (100), 331.2 (26), 303.2 (28), 257.2 (16); ESIMS<sup>3</sup> (490.3  $\rightarrow$  413.2  $\rightarrow$ )  $m/z$  413.2 (11), 395.2 (43), 381.2 (23), 363.2 (100), 349.2 (13), 331.2 (22), 303.2 (25), 257.2 (35); ESIMS<sup>4</sup> (490.3  $\rightarrow$  363.2  $\rightarrow$ )  $m/z$  363.2 (14), 335.2 (15), 331.2 (91), 313.2 (11), 303.2 (100), 289.2 (16), 281.1 (15), 275.1 (17), 261.1 (11), 253.1 (20), 247.1 (12), 221.1 (14); ESIMS<sup>3</sup> (490.3  $\rightarrow$  303.2  $\rightarrow$ )  $m/z$  303.2 (23), 288.1 (50), 275.1 (84), 274.1 (31), 273.1 (16), 261.1 (82), 259.1 (20), 247.1 (100), 235.1 (30), 233.1 (38), 223.1 (13), 221.1 (51), 219.0 (16), 209.1 (27), 207.0 (30), 197.0 (12), 195.0 (17), 193.0 (25), 157.0 (10); HRESIMS  $m/z$  490.3164 [M+NH<sub>4</sub>]<sup>+</sup> (calcd for C<sub>28</sub>H<sub>44</sub>NO<sub>6</sub><sup>+</sup>, 490.3163,  $\Delta$  = 0.2 ppm).

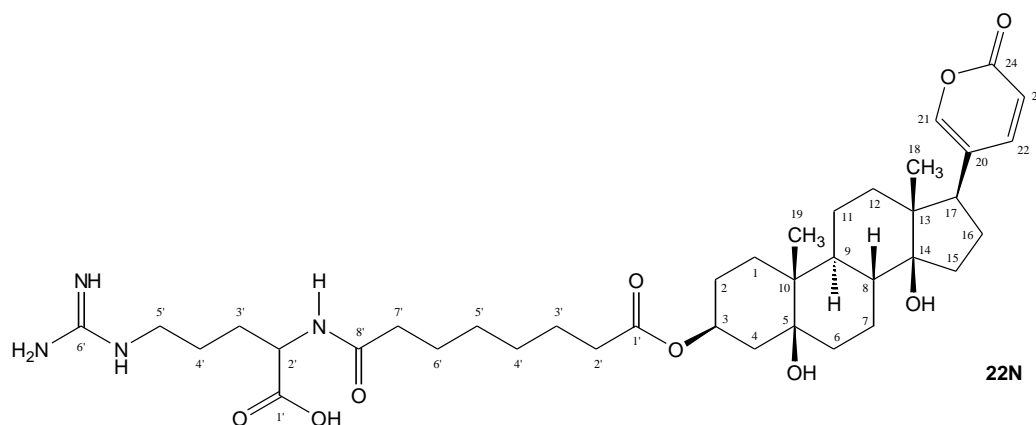
**(3 $\beta$ )-3-(Acetyloxy)-20-ethinyl-20-hydroxy-21-methoxy-pregn-5-en (62J):** ESIMS  $m/z$  432.3 [M+NH<sub>4</sub>]<sup>+</sup>; ESIMS<sup>2</sup> (432.3  $\rightarrow$ )  $m/z$  432.2 (17), 355.2 (100), 305.2 (32); ESIMS<sup>3</sup> (432.3  $\rightarrow$  355.2  $\rightarrow$ )  $m/z$  337.2 (17), 305.2 (100); ESIMS<sup>4</sup> (432.3  $\rightarrow$  355.2  $\rightarrow$  305.2  $\rightarrow$ )  $m/z$  305.2 (18), 290.2 (15), 277.1 (33), 263.1 (47), 249.1 (100), 237.1 (25), 235.1 (49), 225.1 (12), 223.1 (81), 221.1 (31), 211.1 (37), 209.1 (59), 207.0 (16), 199.1 (12), 197.1 (45), 195.0 (80), 193.0 (11), 185.1 (18), 183.0 (22), 181.0 (29), 175.1 (15), 171.0 (17), 169.0 (20), 167.0 (18), 161.1 (31), 159.0 (35), 157.0 (27), 155.0 (33), 147.0 (13), 145.0 (26), 143.0 (15), 133.0 (12), 131.0 (15), 105.1 (15); HRESIMS  $m/z$  432.3105 [M+NH<sub>4</sub>]<sup>+</sup> (calcd for C<sub>26</sub>H<sub>42</sub>NO<sub>4</sub><sup>+</sup>, 432.3108,  $\Delta$  = -0.8 ppm).

**$^1\text{H}$  NMR (500 MHz) and  $^{13}\text{C}$  NMR (125 MHz) data of compounds****15i, 22N, 23A, 23D, 26K, 29b, 30M, 51D, 54E, 54v, 54Ee, 55K, 62A, 62F, 62I, and 62J***(3 $\beta$ ,5 $\beta$ ,11 $\alpha$ ,12 $\alpha$ ,14 $\beta$ ,17 $\beta$ )-3,11-Bis(acetyloxy)-12,14-dihydroxy-bufa-20,22-dienolide, C<sub>28</sub>H<sub>38</sub>O<sub>8</sub>, CAS Registry Number: none*

<b>15i</b>		$^1\text{H}$	$^{13}\text{C}$
1	CH <sub>2</sub>	2.28/1.63	34.71
2	CH <sub>2</sub>	1.72/1.65	25.24
3	CH	5.10	70.23
4	CH <sub>2</sub>	1.93/1.47	30.43
5	CH	1.67	38.38
6	CH <sub>2</sub>	1.87/1.30	26.25
7	CH <sub>2</sub>	1.77/1.36	21.16
8	CH	1.63	41.16
9	CH	2.40	33.11
10	C	--	35.55
11	CH	5.15	73.81
12	CH	3.53	77.39
13	C	--	51.32
14	C	--	84.23
15	CH <sub>2</sub>	1.62/1.40	33.11
16	CH <sub>2</sub>	2.13/1.70	27.33
17	CH	3.25	45.18
18	CH <sub>3</sub>	0.78	17.11
19	CH <sub>3</sub>	1.01	23.50
20	C	--	121.64
21	CH	7.23	149.06

22	CH	7.76	146.96
23	CH	6.26	115.40
24	C	--	162.22
2x Ac COO	C	--	170.67
2x Ac CH <sub>3</sub>	CH <sub>3</sub>	2.05	21.55/21.48

(3 $\beta$ ,5 $\beta$ )-3-[[8-[[4-[(aminoiminomethyl)amino]-1-carboxybutyl]amino]-1,8-dioxooctyl]oxy]-5,14-dihydroxy-bufa-20,22-dienolide, Telocinobufatoxin, C<sub>38</sub>H<sub>58</sub>N<sub>4</sub>O<sub>9</sub>, **CAS Registry Number:** 72093-20-0

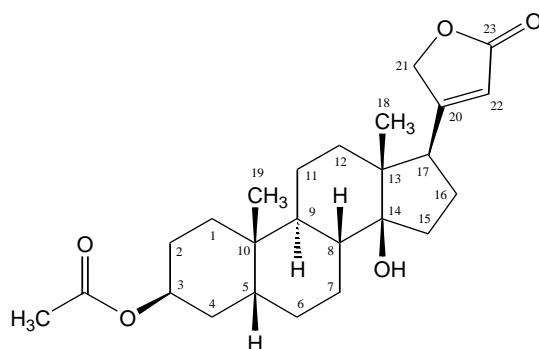


22N		<sup>1</sup> H	<sup>13</sup> C
1	CH <sub>2</sub>	1.76/1.39	26.63
2	CH <sub>2</sub>	1.75/1.60	25.47
3	CH	5.15	72.25
4	CH <sub>2</sub>	2.32/1.56	36.23
5	C	--	74.37
6	CH <sub>2</sub>	1.76/1.38	36.23
7	CH <sub>2</sub>	1.97/1.24	25.14
8	CH	1.66	41.93
9	CH	1.63	40.07
10	C	--	41.47
11	CH <sub>2</sub>	1.44/1.30	22.72
12	CH <sub>2</sub>	1.51/1.48	41.74
13	C	--	49.63
14	C	--	86.00
15	CH <sub>2</sub>	2.10/1.71	33.21
16	CH <sub>2</sub>	2.20/1.74	29.77
17	CH	2.56	52.09

18	CH <sub>3</sub>	0.71	17.21
19	CH <sub>3</sub>	0.96	17.15
20	C	--	125.00
21	CH	7.43	150.50
22	CH	8.00	149.33
23	CH	6.28	115.45
24	C	--	164.80
1'	C	--	175.46
2'	CH <sub>2</sub>	2.25	37.19
3'	CH <sub>2</sub>	1.63	26.82
4'	CH <sub>2</sub>	1.36	29.98
5'	CH <sub>2</sub>	1.36	29.88
6'	CH <sub>2</sub>	1.63	26.12
7'	CH <sub>2</sub>	2.35	35.41
8'	C	--	174.62
1"	C	--	178.36
2"	CH	4.28	55.11
3"	CH <sub>2</sub>	1.86/1.70	31.24
4"	CH <sub>2</sub>	1.64	25.92
5"	CH <sub>2</sub>	3.20	42.04
6"	C	--	159.19

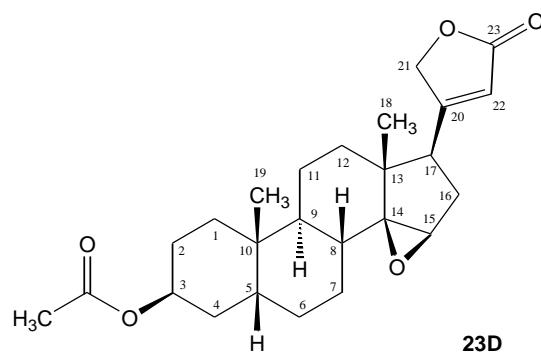
For comparison see: Chinese Chemical Letters 24 (2013) 731–733

(3 $\beta$ ,5 $\beta$ )-3-(Acetyloxy)-14-hydroxy-card-20(22)-enolide, 3-O-Acetyl-digitoxigenin, C<sub>25</sub>H<sub>36</sub>O<sub>5</sub>,  
**CAS Registry Number: 808-19-5**



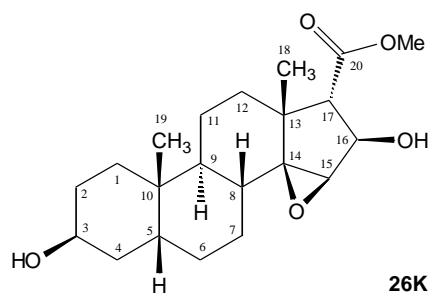
23A		<sup>1</sup> H	<sup>13</sup> C
1	CH <sub>2</sub>	1.45/1.36	30.38
2	CH <sub>2</sub>	1.63/1.53	24.99
3	CH	5.08	70.28
4	CH <sub>2</sub>	1.87/1.55	30.38
5	CH	1.68	36.74
6	CH <sub>2</sub>	1.87/1.28	26.27
7	CH <sub>2</sub>	1.69/1.22	21.49
8	CH	1.56	41.78
9	CH	1.59	35.60
10	C	--	35.12
11	CH <sub>2</sub>	1.42/1.22	21.11
12	CH <sub>2</sub>	1.51/1.39	39.93
13	C	--	49.53
14	C	--	85.53
15	CH <sub>2</sub>	2.13/1.69	33.16
16	CH <sub>2</sub>	2.15/1.87	26.82
17	CH	2.78	50.82
18	CH <sub>3</sub>	0.87	15.73
19	CH <sub>3</sub>	0.96	23.65
20	C	--	174.44
21	CH <sub>2</sub>	4.99/4.81	73.40
22	CH	5.88	117.71
23	C	--	174.44
Ac COO	C	--	170.71
Ac CH <sub>3</sub>	CH <sub>3</sub>	2.05	21.49

(3 $\beta$ ,5 $\beta$ ,15 $\beta$ )-3-(Acetyloxy)-14,15-epoxy-card-20(22)-enolide, C<sub>25</sub>H<sub>34</sub>O<sub>5</sub>, CAS Registry Number: 4240-55-5



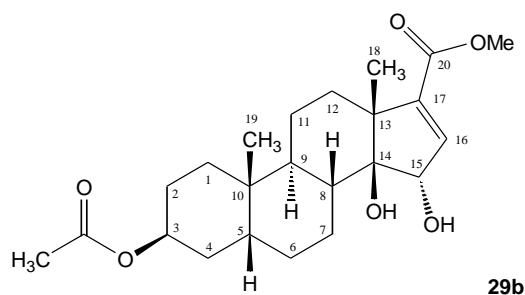
23D		<sup>1</sup> H	<sup>13</sup> C
1	CH <sub>2</sub>	1.54/1.36	30.28
2	CH <sub>2</sub>	1.62/1.50	24.96
3	CH	5.07	70.20
4	CH <sub>2</sub>	1.84/1.41	30.34
5	CH	1.67	36.71
6	CH <sub>2</sub>	1.84/1.19	25.51
7	CH <sub>2</sub>	1.51/1.35	20.77
8	CH	2.00	33.14
9	CH	1.55	39.44
10	C	--	35.22
11	CH <sub>2</sub>	1.46/0.88	20.60
12	CH <sub>2</sub>	1.62/1.37	38.11
13	C	--	45.31
14	C	--	73.92
15	CH	3.48	58.78
16	CH <sub>2</sub>	2.25/1.98	30.67
17	CH	2.78	46.84
18	CH <sub>3</sub>	0.93	15.81
19	CH <sub>3</sub>	1.00	23.69
20	C	--	173.01
21	CH <sub>2</sub>	4.88/4.70	73.71
22	CH	5.80	118.81
23	C	--	170.70
Ac COO	C	--	174.07
Ac CH <sub>3</sub>	CH <sub>3</sub>	2.05	21.48

(3 $\beta$ ,5 $\beta$ ,14 $\beta$ ,15 $\beta$ ,16 $\beta$ ,17 $\alpha$ )-14,15-Epoxy-3,16-dihydroxy-androstane-17-carboxylic acid methyl ester, C<sub>21</sub>H<sub>32</sub>O<sub>5</sub>, CAS Registry Number: 113749-90-9



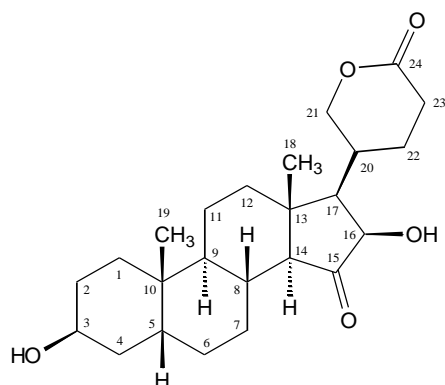
26K		<sup>1</sup> H	<sup>13</sup> C
1	CH <sub>2</sub>	1.48/1.46	29.40
2	CH <sub>2</sub>	1.51/1.49	27.77
3	CH	4.13	66.75
4	CH <sub>2</sub>	1.88/1.34	33.20
5	CH	1.76	35.89
6	CH <sub>2</sub>	1.85/1.20	25.57
7	CH <sub>2</sub>	1.49/1.21	20.14
8	CH	2.06	32.74
9	CH	1.52	38.97
10	C	--	35.43
11	CH <sub>2</sub>	1.49/0.90	20.51
12	CH <sub>2</sub>	1.43/1.19	32.46
13	C	--	43.12
14	C	--	72.06
15	CH	3.51	60.18
16	CH	4.60	73.23
17	CH	2.36	57.44
18	CH <sub>3</sub>	1.24	18.39
19	CH <sub>3</sub>	0.97	23.70
20	C	--	172.88
OCH <sub>3</sub>	CH <sub>3</sub>	3.71	51.75

(3 $\beta$ ,5 $\beta$ ,14 $\beta$ ,15 $\alpha$ )-3-(Acetyloxy)-14,15-dihydroxy-androst-16-ene-17-carboxylic acid methyl ester, C<sub>23</sub>H<sub>34</sub>O<sub>6</sub>, CAS Registry Number: 113752-75-3



<b>29b</b>		<sup>1</sup> H	<sup>13</sup> C
1	CH <sub>2</sub>	1.55/1.34	30.37
2	CH <sub>2</sub>	1.56	25.13
3	CH	5.07	70.72
4	CH <sub>2</sub>	2.03/1.45	30.61
5	CH	1.67	37.03
6	CH <sub>2</sub>	1.91/1.31	26.49
7	CH <sub>2</sub>	1.86	19.76
8	CH	1.74	41.81
9	CH	2.23	34.70
10	C	--	35.26
11	CH <sub>2</sub>	1.47/1.18	20.89
12	CH <sub>2</sub>	2.24/1.48	39.36
13	C	--	50.66
14	C	--	82.69
15	CH	4.53	81.40
16	CH	6.70	138.99
17	C	-	148.60
18	CH <sub>3</sub>	1.23	16.61
19	CH <sub>3</sub>	0.95	22.64
20	C	--	165.35
OCH <sub>3</sub>	CH <sub>3</sub>	3.75	51.47
Ac COO	C	--	170.76
Ac CH <sub>3</sub>	CH <sub>3</sub>	2.05	21.52

(3 $\beta$ ,5 $\beta$ ,14 $\alpha$ ,16 $\beta$ )-3,16-Dihydroxy-15-oxo-bufanolide, C<sub>24</sub>H<sub>36</sub>O<sub>5</sub>, CAS Registry Number: none

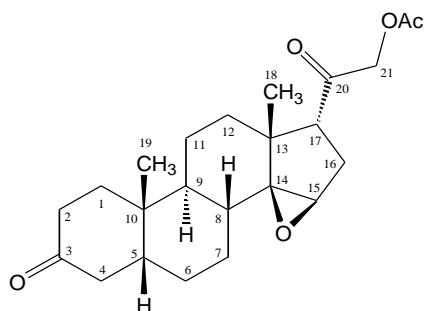


30M		<sup>1</sup> H	<sup>13</sup> C
1	CH <sub>2</sub>	1.47	31.00
2	CH <sub>2</sub>	1.55/1.48	28.41
3	CH	4.03	67.68
4	CH <sub>2</sub>	2.00/1.33	34.29
5	CH	1.76	37.52
6	CH <sub>2</sub>	1.98/1.17	27.45
7	CH <sub>2</sub>	2.29/1.06	25.74
8	CH	1.76	32.59
9	CH	1.45	40.35
10	C	--	36.22
11	CH <sub>2</sub>	1.47/1.26	21.45
12	CH <sub>2</sub>	1.85/1.45	40.42
13	C	--	43.08
14	CH	2.04	63.53
15	C	--	217.23
16	CH	4.12	72.19
17	CH	1.95	54.15
18	CH <sub>3</sub>	0.87	14.82
19	CH <sub>3</sub>	0.99	24.21
20	CH	2.37	32.06
21	CH <sub>2</sub>	4.60/4.24	74.14
22	CH <sub>2</sub>	2.24/1.71	26.11
23	CH <sub>2</sub>	2.65/2.51	29.83
24	C	--	174.83

(5 $\beta$ ,14 $\beta$ ,15 $\beta$ ,17 $\alpha$ )-21-(Acetyloxy)-14,15-epoxy-pregnane-3,20-dione,  
**Registry Number:** none

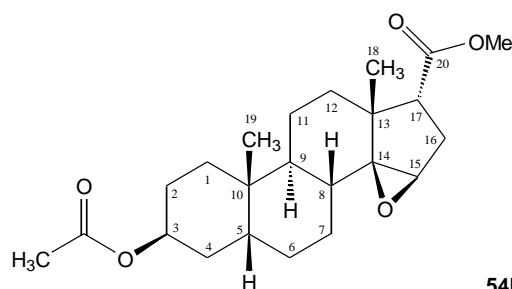
C<sub>23</sub>H<sub>32</sub>O<sub>5</sub>,

**CAS**



51D		<sup>1</sup> H	<sup>13</sup> C
1	CH <sub>2</sub>	2.05/1.47	36.47
2	CH <sub>2</sub>	2.32/2.20	37.07
3	C	--	212.40
4	CH <sub>2</sub>	2.61/2.04	42.03
5	CH	1.84	43.51
6	CH <sub>2</sub>	1.85/1.30	25.76
7	CH <sub>2</sub>	1.61/0.99	20.49
8	CH	2.11	33.03
9	CH	1.72	40.21
10	C	--	35.24
11	CH <sub>2</sub>	1.56/1.45	20.65
12	CH <sub>2</sub>	1.77/1.41	38.47
13	C	--	45.82
14	C	--	73.69
15	CH	3.58	59.36
16	CH <sub>2</sub>	2.41/2.11	27.35
17	CH	2.58	57.64
18	CH <sub>3</sub>	1.05	15.56
19	CH <sub>3</sub>	1.05	22.55
20	C	--	205.44
21	CH <sub>2</sub>	4.88	67.50
Ac COO	C	--	170.42
Ac CH <sub>3</sub>	CH <sub>3</sub>	2.15	20.56

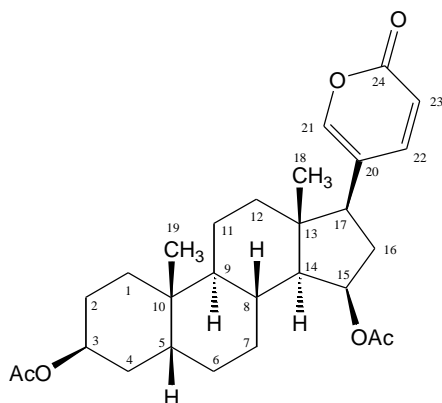
(3 $\beta$ ,5 $\beta$ ,14 $\beta$ ,15 $\beta$ ,17 $\alpha$ )-3-(Acetyloxy)-14,15-epoxy-androstane-17-carboxylic acid methyl ester, C<sub>23</sub>H<sub>34</sub>O<sub>5</sub>, CAS Registry Number: none



54E

54E		<sup>1</sup> H	<sup>13</sup> C
1	CH <sub>2</sub>	1.56/1.37	30.29
2	CH <sub>2</sub>	1.62/1.52	24.96
3	CH	5.07	70.35
4	CH <sub>2</sub>	1.85/1.43	30.38
5	CH	1.67	36.80
6	CH <sub>2</sub>	1.84/1.20	25.60
7	CH <sub>2</sub>	1.50/0.91	20.54
8	CH	2.06	33.04
9	CH	1.52	39.21
10	C	--	35.21
11	CH <sub>2</sub>	1.50/1.26	20.29
12	CH <sub>2</sub>	1.27	31.06
13	C	--	43.09
14	C	--	72.85
15	CH	3.44	58.40
16	CH <sub>2</sub>	2.12	28.02
17	CH	2.48	49.57
18	CH <sub>3</sub>	1.23	18.40
19	CH <sub>3</sub>	0.99	23.69
20	C	--	173.70
OCH <sub>3</sub>	CH <sub>3</sub>	3.66	51.42
Ac COO	C	--	170.64
Ac CH <sub>3</sub>	CH <sub>3</sub>	2.05	21.47

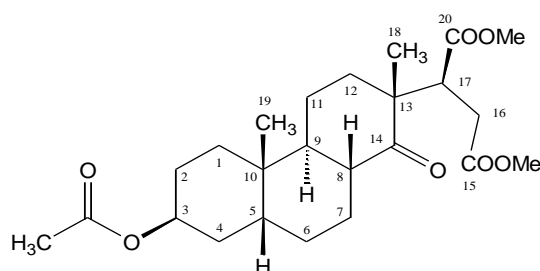
(3 $\beta$ ,5 $\beta$ ,14 $\alpha$ ,15 $\beta$ )-3,15-Bis(acetyloxy)-bufa-20,22-dienolide, C<sub>28</sub>H<sub>38</sub>O<sub>6</sub>, CAS Registry Number: 107204-41-1



54v		<sup>1</sup> H	<sup>13</sup> C
1	CH <sub>2</sub>	1.55/1.35	30.77
2	CH <sub>2</sub>	1.62/1.49	24.92
3	CH	5.08	70.43
4	CH <sub>2</sub>	1.93/1.45	30.54
5	CH	1.70	37.18
6	CH <sub>2</sub>	1.91/1.20	26.22
7	CH <sub>2</sub>	1.49/1.28	20.50
8	CH	1.79	32.09
9	CH	1.40	40.46
10	C	--	35.04
11	CH <sub>2</sub>	1.43/1.12	25.19
12	CH <sub>2</sub>	1.65/1.18	38.98
13	C	--	44.09
14	CH	1.26	58.53
15	CH	5.19	72.88
16	CH <sub>2</sub>	2.57/1.71	36.57
17	CH	2.28	50.82
18	CH <sub>3</sub>	0.75	14.74
19	CH <sub>3</sub>	1.02	23.77
20	C	--	117.20
21	CH	7.26	148.69
22	CH	7.27	144.91
23	CH	6.30	115.62
24	C	--	161.87

Ac COO at 3	C	--	170.75
Ac CH <sub>3</sub> at 3	CH <sub>3</sub>	2.05	21.50
Ac COO at 15	C	--	170.75
Ac CH <sub>3</sub> at 15	CH <sub>3</sub>	2.07	21.33

2-[7-(Acetyloxy)tetradecahydro-2,4b-dimethyl-1-oxo-2-phenanthrenyl]-succinic acid dimethyl ester, C<sub>24</sub>H<sub>36</sub>O<sub>7</sub>, CAS Registry Number: 119926-37-3

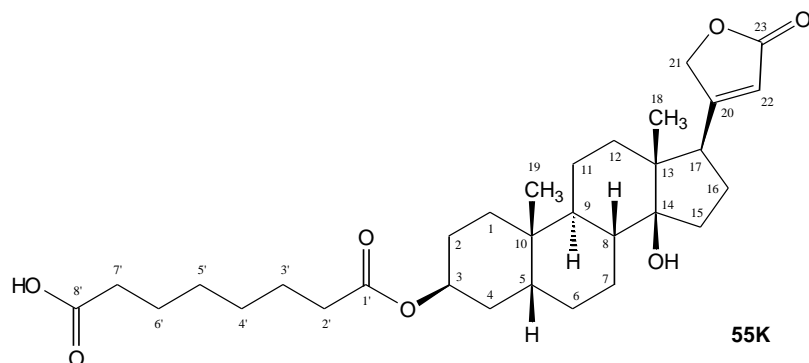


54Ee		<sup>1</sup> H	<sup>13</sup> C
1	CH <sub>2</sub>	1.56	30.34
2	CH <sub>2</sub>	1.63/1.48	24.94
3	CH	5.05	70.17
4	CH <sub>2</sub>	1.84/1.43	30.17
5	CH	1.67	36.48
6	CH <sub>2</sub>	1.83/1.27	25.22
7	CH <sub>2</sub>	1.54	20.08
8	CH	2.57	45.18
9	CH	1.81	41.24
10	C	--	35.65
11	CH <sub>2</sub>	1.63/1.57	20.41
12	CH <sub>2</sub>	1.79/1.62	36.38
13	C	--	48.62
14	C	--	214.92
15*	C	--	172.79
16	CH <sub>2</sub>	2.65	32.82
17	CH	3.30	46.74
18	CH <sub>3</sub>	1.22	18.42
19	CH <sub>3</sub>	1.02	23.18
20*	C	--	174.74
Ac COO	C	--	170.56

Ac CH <sub>3</sub>	CH <sub>3</sub>	2.04	21.46
OCH <sub>3</sub>	CH <sub>3</sub>	3.67	51.79
OCH <sub>3</sub>	CH <sub>3</sub>	3.67	51.62

\* assignement interchangeable

(3 $\beta$ ,5 $\beta$ )-3-[(7-carboxy-1-oxoheptyl)oxy]-14-hydroxy-card-20(22)-enolide, Digitoxigenin 3-suberate, C<sub>31</sub>H<sub>46</sub>O<sub>7</sub>, **CAS Registry Number:** 30219-07-9

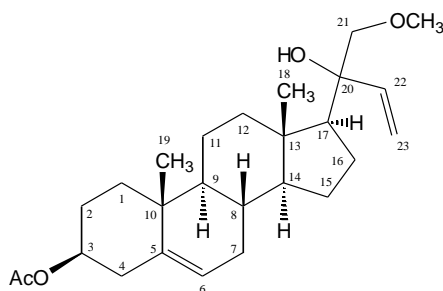


55K		<sup>1</sup> H	<sup>13</sup> C
1	CH <sub>2</sub>	1.44/1.34	30.44
2	CH <sub>2</sub>	1.60/1.54	25.03
3	CH	5.07	70.05
4	CH <sub>2</sub>	1.87/1.57	30.46
5	CH	1.67	36.84
6	CH <sub>2</sub>	1.88/1.28	26.30
7	CH <sub>2</sub>	1.69/1.24	21.24
8	CH	1.56	41.78
9	CH	1.60	35.60
10	C	--	35.12
11	CH <sub>2</sub>	1.42/1.24	21.11
12	CH <sub>2</sub>	1.51/1.40	39.93
13	C	--	49.55
14	C	--	85.55
15	CH <sub>2</sub>	2.14/1.70	33.16
16	CH <sub>2</sub>	2.17/1.86	26.82
17	CH	2.79	50.82
18	CH <sub>3</sub>	0.87	15.74
19	CH <sub>3</sub>	0.96	23.71
20*	C	--	174.50

21	CH <sub>2</sub>	5.01/4.81	73.41
22	CH	5.81	117.71
23*	C	--	174.4
1'	C	--	173.22
2'	CH <sub>2</sub>	2.30	34.64
3'	CH <sub>2</sub>	1.63	24.85
4'	CH <sub>2</sub>	1.36	28.72
5'	CH <sub>2</sub>	1.36	28.67
6'	CH <sub>2</sub>	1.64	24.48
7'	CH <sub>2</sub>	2.35	33.53
8'	C	--	177.60

\* assignement interchangeable

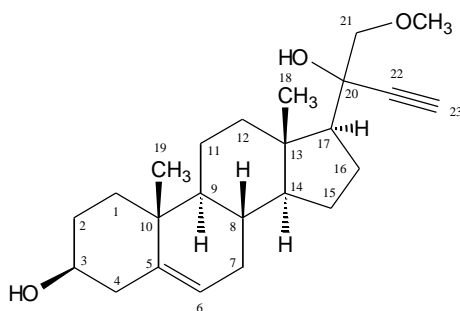
(3 $\beta$ )-3-(Acetyloxy)-20-ethenyl-20-hydroxy-21-methoxy-pregn-5-en, C<sub>26</sub>H<sub>40</sub>O<sub>4</sub>, **CAS Registry Number:** none



62A		<sup>1</sup> H	<sup>13</sup> C
1	CH <sub>2</sub>	1.86/1.14	36.96
2	CH <sub>2</sub>	1.86/1.58	27.73
3	CH	4.60	73.94
4	CH <sub>2</sub>	2.31	38.09
5	C	--	139.69
6	CH	5.37	122.49
7	CH <sub>2</sub>	1.96/1.52	31.74
8	CH	1.46	31.29
9	CH	0.93	49.98
10	C	--	36.59
11	CH <sub>2</sub>	1.49/1.46	20.77
12	CH <sub>2</sub>	2.07/1.23	39.70
13	C	--	42.82

14	CH	0.99	56.67
15	CH <sub>2</sub>	1.60/1.13	23.85
16	CH <sub>2</sub>	1.61	22.69
17	CH	1.63	55.27
18	CH <sub>3</sub>	0.82	14.05
19	CH <sub>3</sub>	1.01	19.30
20	C	--	77.59
21	CH <sub>2</sub>	3.42/3.28	78.94
22	CH	5.93	141.68
23	CH <sub>2</sub>	5.27/5.13	113.09
OCH <sub>3</sub>	CH <sub>3</sub>	3.37	59.34
Ac COO	C	--	170.57
Ac CH <sub>3</sub>	CH <sub>3</sub>	2.03	21.46

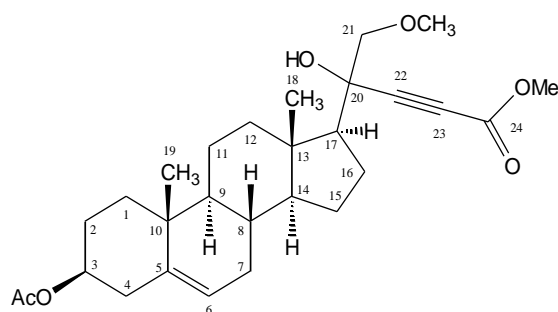
(3 $\beta$ )-20-Ethinyl-3,20-dihydroxy-21-methoxy-pregn-5-en, C<sub>24</sub>H<sub>36</sub>O<sub>3</sub>, CAS Registry Number:  
none



62F		<sup>1</sup> H	<sup>13</sup> C
1	CH <sub>2</sub>	1.84/1.08	37.22
2	CH <sub>2</sub>	1.84/1.51	31.63
3	CH	3.52	71.77
4	CH <sub>2</sub>	2.29/2.24	42.25
5	C	--	140.90
6	CH	5.35	121.48
7	CH <sub>2</sub>	1.98/1.55	31.86
8	CH	1.49	31.35
9	CH	0.93	50.09
10	C	--	36.52
11	CH <sub>2</sub>	1.51/1.48	20.74
12	CH <sub>2</sub>	2.21/1.19	39.83

13	C	--	43.54
14	CH	0.99	56.07
15	CH <sub>2</sub>	1.65/1.25	24.42
16	CH <sub>2</sub>	1.80/1.67	24.57
17	CH	1.71	54.63
18	CH <sub>3</sub>	1.00	13.48
19	CH <sub>3</sub>	1.02	19.40
20	C	--	73.58
21	CH <sub>2</sub>	3.44/3.31	80.17
22	C	--	84.72
23	CH	2.54	75.15
OCH <sub>3</sub>	CH <sub>3</sub>	3.45	59.57

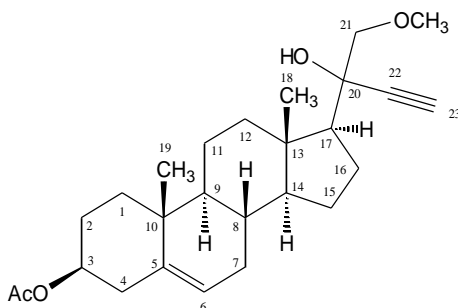
(3 $\beta$ )-3-(Acetyloxy)-20-hydroxy-21-methoxy-chol-5-en-22-yn-24-oic acid methyl ester, C<sub>28</sub>H<sub>40</sub>O<sub>6</sub>, CAS Registry Number: none



62I		<sup>1</sup> H	<sup>13</sup> C
1	CH <sub>2</sub>	1.85/1.12	36.96
2	CH <sub>2</sub>	1.85/1.58	27.72
3	CH	4.59	73.92
4	CH <sub>2</sub>	2.32	38.07
5	C	--	139.80
6	CH	5.37	122.36
7	CH <sub>2</sub>	1.97/1.54	31.82
8	CH	1.48	31.36
9	CH	0.95	49.96
10	C	--	36.62
11	CH <sub>2</sub>	1.51/1.48	20.67
12	CH <sub>2</sub>	2.21/1.19	39.62
13	C	--	43.65

14	CH	0.99	55.81
15	CH <sub>2</sub>	1.68/1.26	24.42
16	CH <sub>2</sub>	1.71/1.68	24.34
17	CH	1.71	54.98
18	CH <sub>3</sub>	0.99	13.50
19	CH <sub>3</sub>	1.02	19.29
20	C	--	73.75
21	CH <sub>2</sub>	3.47/3.33	79.50
22	C	--	88.62
23	C	--	78.51
24	C	--	153.73
OCH <sub>3</sub>	CH <sub>3</sub>	3.44	59.63
COOCH <sub>3</sub>	CH <sub>3</sub>	3.76	52.70
Ac COO	C	--	170.59
Ac CH <sub>3</sub>	CH <sub>3</sub>	2.03	21.46

(3 $\beta$ )-3-(Acetyloxy)-20-ethynyl-20-hydroxy-21-methoxy-pregn-5-en, C<sub>26</sub>H<sub>38</sub>O<sub>4</sub>, **CAS Registry Number:** none



62J		<sup>1</sup> H	<sup>13</sup> C
1	CH <sub>2</sub>	1.86/1.12	36.96
2	CH <sub>2</sub>	1.85/1.59	27.72
3	CH	4.60	73.94
4	CH <sub>2</sub>	2.32	38.07
5	C	--	139.79
6	CH	5.37	122.40
7	CH <sub>2</sub>	1.97/1.53	31.84
8	CH	1.48	31.31
9	CH	0.95	49.99
10	C	--	36.60

11	CH <sub>2</sub>	1.49	20.68
12	CH <sub>2</sub>	2.21/1.19	39.77
13	C	--	43.54
14	CH	1.00	55.98
15	CH <sub>2</sub>	1.67/1.25	24.42
16	CH <sub>2</sub>	1.79/1.69	24.57
17	CH	1.71	54.62
18	CH <sub>3</sub>	1.00	13.46
19	CH <sub>3</sub>	1.02	19.31
20	C	--	73.58
21	CH <sub>2</sub>	3.44/3.31	80.17
22	C	--	84.73
23	CH	2.54	75.14
OCH <sub>3</sub>	CH <sub>3</sub>	3.44	59.57
Ac COO	C	--	170.56
Ac CH <sub>3</sub>	CH <sub>3</sub>	2.03	21.44

## 8.2 Curriculum vitae

**CV is not available in the electronic version**